IRS Instrument Handbook

Spitzer Heritage Archive Documentation

IRS Instrument Team & Science User Support Team

Version 5.0, December 2011

S18.18

Table of Contents

Chapter 1. Introduction

1.1 Document Purpose and Scope

The IRS Instrument Handbook is one in a series of four documents that explain the operations of the Spitzer Space Telescope and its three instruments. The Spitzer Space Telescope Handbook gives an overview of the entire Spitzer mission and explains the operations of the observatory, while the other three handbooks document the operation of, and the data produced by, the individual instruments (IRAC, IRS, and MIPS).

The IRS Instrument Handbook is intended to provide all the information necessary to understand the IRS standard data products, as processed by version S18.18 of the data reduction pipeline, and which are retrievable from the Spitzer Heritage Archive. In addition to the detailed pipeline processing steps and data product details, background information is provided about the IRS instrument itself, its observational modes, and all aspects of IRS data calibration. While an introduction to data analysis is provided in this document, please refer to the additional documentation available on the Data Analysis and Tools section of the website.

For readers familiar with the Spitzer cryogenic mission documentation, this Handbook is based on information compiled from the IRS Data Handbook, the IRS Pipeline Description Document, and the Spitzer Observer's Manual.

This is version 4 of this document. Changes from previous versions are listed in Appendix A.

1.2 Basic Definitions

This section contains a description of the most commonly used terms in this handbook. A complete list of acronyms can be found in Appendix B.

The **InfraRed Spectrograph (IRS)** provided spectroscopic capabilities to the Spitzer Space Telescope. An **Astronomical Observing Template (AOT)** is the list of parameters for a distinct Spitzer observing mode. There are 3 possible IRS AOTs: Staring Mode, Mapping Mode, and Peak-Up Imaging (PUI). Each of these is described in Chapter 3. A fundamental unit of Spitzer observing is the **Astronomical Observation Request (AOR;** also referred to plainly as an **Observation)**, which is an AOT with all of the relevant parameters fully specified. We also refer to the data that results from such a request as an AOR. Each AOR is identified in the Spitzer Heritage Archive by a unique observation identification number known as an **AORKEY**. An AOR is composed of several **Data Collection Events (DCEs)**, or single-frame exposures. **Basic Calibrated Data (BCD)** products (also known as **Level 1** products) are data derived from DCEs pushed through the pipelines. See Chapter 5 for a description of the IRS pipelines. BCDs are designed to be the most reliable product produced by automated processing. **Post-BCD products** (also known as **PBCD** or **Level 2** products) are derived from a full AOR, e.g., a

combination of several BCDs. Automated Post-BCD products do not combine data from more than one AOR; users must perform this task themselves. Post-BCD data is meant to provide a quick look at the data. Users should always carefully examine Post-BCD products to determine if the standard reduction was optimal for their particular data set. See Chapter 6 for a more complete description of the BCD and Post-BCD data products.

The IRS has four modules which provided low- and medium-resolution spectroscopy: **Short-Low (SL), Long-Low (LL), Short-High (SH), and Long-High (LH)**. Spectroscopy could be obtained in either **Staring Mode** or **Mapping Mode**. In addition, the IRS provided imaging in two filters centered at 16 and 22 micron. This imaging capability was used for two purposes: 1) to identify point sources and accurately place them in any of the IRS slits (**Peak-Up Acquisition or PUA**); and 2) to perform photometry on science sources (**Peak-Up Imaging or PUI**). A full description of the IRS can be found in Chapter 2, and a description of the operating modes can be found in Chapter 3.

1.3 IRS Essentials

Most readers of this Handbook are interested in learning how to reduce their IRS data. Users can download IRS data from the Spitzer Heritage Archive, and they can familiarize themselves with the downloaded data files by reading Chapter 6. As users examine and reduce their data, they should keep in mind the common data features and caveats which are described in Chapter 7. An introduction to the analysis of IRS data is provided in Chapter 8. The Data Analysis and Tools section of the Spitzer website provides information on the software most commonly used to reduce IRS data, while the Data Analysis Cookbook provides examples of how to reduce specific IRS data sets. Below, we highlight some essentials that users should keep in mind as they approach data reduction.

Staring Mode: The single most important step in reducing IRS staring mode data is subtracting the background. This is easily accomplished either by starting with *bksub* products (see Chapter 6) for low resolution data, or by performing your own 2D background subraction with an offset sky for high-resolution data. In either case, 2D background subtraction should remove most bad pixels and clearly reveal the source. Many users will be able to proceed to spectral extraction using the tools **SPICE** or **SMART** after this step.

In some cases, users may wish to remove bad pixels prior to spectral extraction. This can happen if there are residual bad pixels remaining after 2D background subtraction, or if 2D background subtraction is problematic. The latter may occur, for example, if dedicated sky observations are unavailable for either high-resolution observations or for low-resolution observations of extended sources. **IRSCLEAN** is a convenient tool for removing bad pixels.

Users dealing with very long integrations or maps of faint sources, particularly in Long-Low, should consider removing latents prior to background subtraction or bad pixel removal. Latents are described in Chapter 7.

In some cases, users will find that their extracted spectra show fringing. Fringes in high-resolution data can be mitigated by the software tool **IRSFRINGE**. Scalloping or orders (particularly in LH, but also other modules) can be mitigated using the software tool **DARKSETTLE**.

Mapping Mode: If you are creating spectral maps, then **CUBISM** will be your primary software tool.

Peak-up Imaging: Most users will reduce imaging data using **MOPEX**.

All modes: In some cases, expert users will want to run their raw IRS data through the IRS pipeline using non-default parameters. These users may use the software tool **CUPID**.

1.4 Standard Acknoledgements for IRS Publications

Please see the Guidelines for Publication Acknowledgements for the appropriate acknowledgment to include in papers based on Spitzer data. Investigators using IRS data should also provide reference(s) to the seminal papers describing the Observatory, the seminal IRS paper (*Houck et al. 2004, ApJS 154, 18*), and any additional papers describing the IRS, as appropriate.

1.5 How to Contact Us

A broad collection of information about the IRS (http://irsa.ipac.caltech.edu/data/SPITZER/docs/irs/) and IRS Data Analysis (http://irsa.ipac.caltech.edu/data/SPITZER/docs/dataanalysistools) is available on the Spitzer website. In addition you may contact the helpdesk at http://irsa.ipac.caltech.edu/data/SPITZER/docs/spitzerhelpdesk.

Chapter 2. Instrument Description

2.1 Overview

The InfraRed Spectrograph (IRS) is one of three focal plane instruments on the Spitzer Space Telescope. It consists of four separate modules (Short-Low, Short-High, Long-Low, Long-High; see Figure 2.1) which provide low (R~60-130) and moderate (R~600) resolution spectroscopic capabilities from 5.2 to 38 microns. The low-resolution modules employ long-slit designs that allow both spectral and one-dimensional spatial information to be acquired simultaneously on the same detector array. Each spectroscopic aperture in the low-resolution modules is divided into two in-line sub-slits. These subslits provide spectroscopy in either the first or second order. The high-resolution modules use a cross-dispersed echelle design that allow broad spectral coverage in a single exposure. Each high-resolution module has a single slit. Spectra can be obtained in either Staring (Section 3.1) or Mapping (Section 3.2) mode.

In addition, the IRS provides imaging in two filters (13-18 and 18-26 microns) and onboard software to autonomously identify point sources and accurately place them (by offsetting the telescope) in any of the IRS slits. These peak-up arrays are also used to obtain calibrated images of the sky at 16 and 22 microns over an approximately 1x1 square arcminute field of view, providing the only direct imaging capability on Spitzer between 8 and 24 microns. See Figure 2.2 for an illustration of the relative sizes of the slits and Table 2.1 for a summary of the wavelength and resolution ranges of each module.
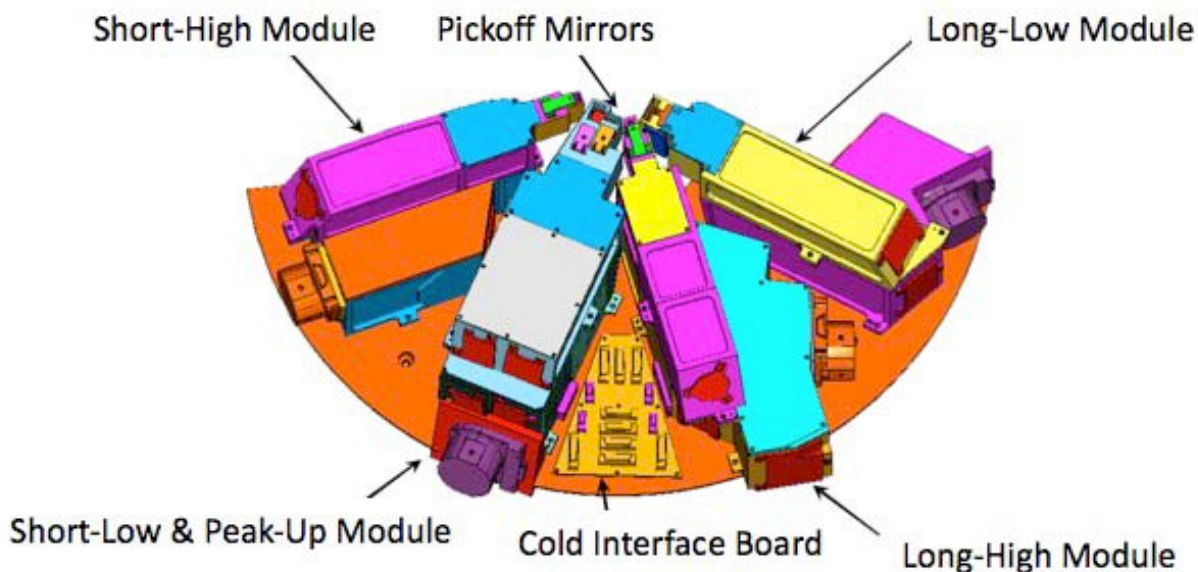
Figure 2.1: The IRS Cold Assembly.

Table 2.1: IRS module characteristics.

Module	Channel	Detector	Delivered Wavelength Range* (micron)	Resolving Power**	Plate Scale (arcsec/pix)	Slit width*** (arcsec)	Slit length (arcsec)
SL2 SL3 SL1	0	Si:As	5.13-7.60 7.33-8.66 7.46-14.29	60-127 61-120	1.8	3.6 3.7	57
PU-blue	0	Si:As	13.3-18.7	~3	1.8	80^	56^
PU-red	0	Si:As	18.5-26.0	~3	1.8	82^	54^
LL2 LL3 LL1	2	Si:Sb	13.90-21.27 19.23-21.61 19.91-39.90	57-126 58-112	5.1	10.5 10.7	168
SH	1	Si:As	9.89-19.51	600	2.3	4.7	11.3
LH	3	Si:Sb	18.83-37.14	600	4.5	11.1	22.3

*SL1 spectra may exhibit the "14 micron teardrop", which affects wavelengths beyond approximately 13.2 microns (see Chapter 7). LL1 spectra become very noisy beyond 38 microns.

**The resolving power is approximately constant as a function of wavelength within each low-resolution spectroscopic order.

***The width of each slit is constant to 1% over its length.

^ This represents the field of view for the peak-up arrays.
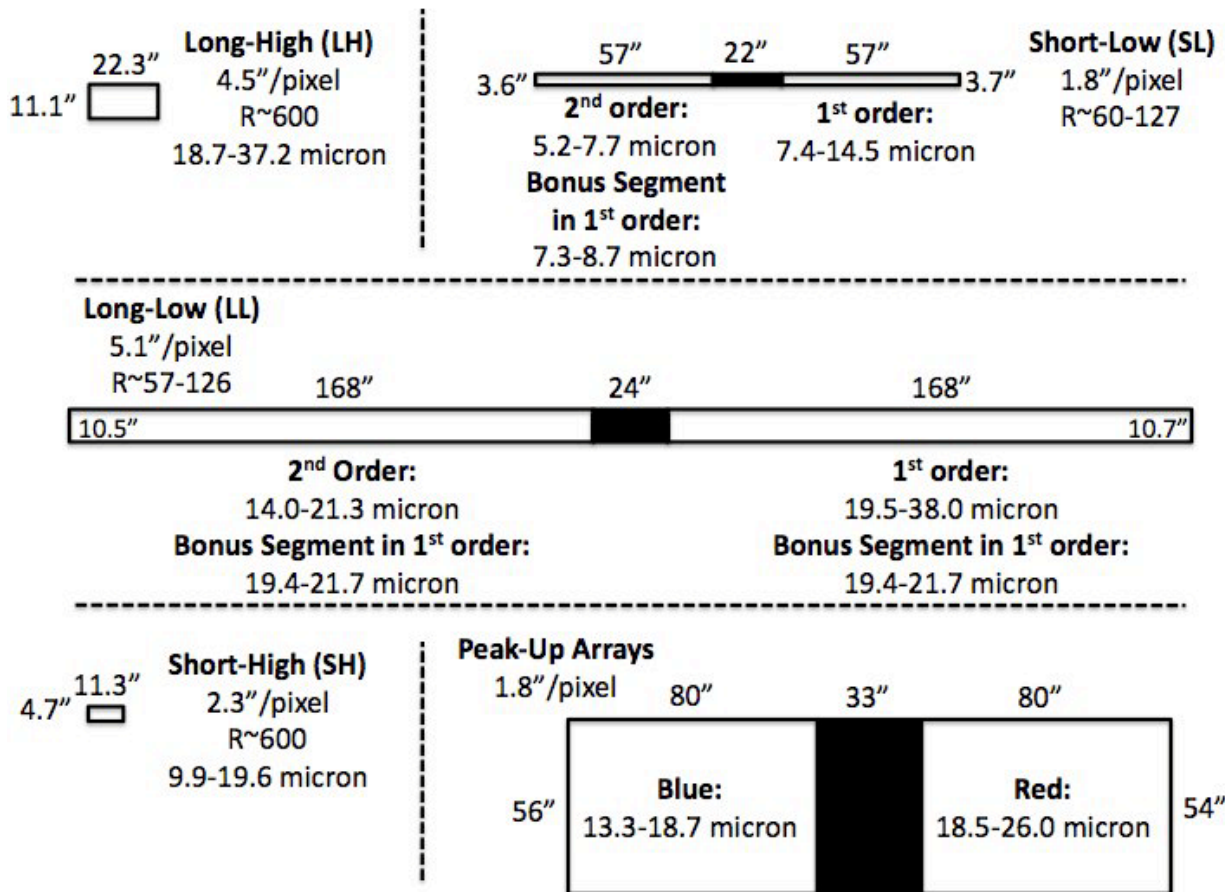
Figure 2.2 Schematic representation of the IRS slits and Peak-Up apertures. Note that the IRS slits are *not* parallel in the Spitzer focal plane.

2.2 PSF

The interaction of the light beam with the telescope surfaces resulted in the appearance of characteristic diffraction patterns at the telescope focal plane. As with other telescopes, these patterns consist primarily of Airy rings (due to the finite telescope aperture) and radial spikes (due to the secondary mirror supports). For bright sources, the power in these features may be significant. For example, the simulation software STINYTIM indicates that, for a source with a flux density of 1 Jy at 8 microns, the PSF will be detectable at the 1 mJy level up to 10 arcsec away from the source centroid. For a source that is 1 Jy at 25 microns, the 1 mJy level is reached at a distance of about 30 arcsec. As a rule of thumb, the flux will be smaller than 1/100 of the peak source flux density at distances larger than 1.5 to 2 slit widths from the source center (for the low-resolution modules). This rule of thumb is provided as a general guideline only and should not replace a detailed PSF analysis using STINYTIM. See Figure 2.3 for a simulation of the 8 micron PSF and Section 2.7 for more information about the PSF in the PUI mode.
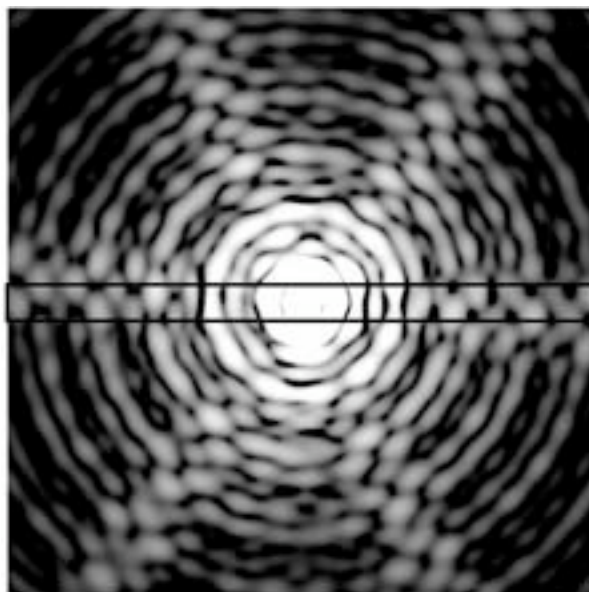
Figure 2.3: The PSF at 8 microns, centered in the SL slit (shown as a rectangle 3.6 arcsec wide). Simulated image using STINYTIM.

2.3 Short-Low (SL) Module

The Short-Low (SL) module is a grating spectrograph and imager that covers, in two orders, the nominal spectral range from 5.2 to 14.5 microns at $60 < R < 128$. The red coverage of the SL module extends to slightly longer wavelengths (15.4 microns) than indicated here, but SL spectra could not be calibrated redward of 14.5 microns. The plate scale for the SL 128x128 Si:As Blocked Impurity Band (BIB) array is 1.8 arcsec/pixel. When the source is on one half of the long slit, its light passes through a 7.5-15 micron bandpass filter and is diffracted by the grating in first order (SL1). When the source is moved to the other half of the same slit, its light passes through a 5-7.5 micron bandpass filter and is diffracted by the grating in second order (SL2). The module also produces a second, short spectral segment that covers the 7.3-8.7 micron spectral region in first order (R=60-72), when the source falls on the 2nd order (SL2) sub-slit. This overlap region, known as the "bonus segment," was intended to aid the user in normalizing the first- and second-order segments of the spectrum. Figure 2.4 shows the optical layout of the SL module.

- **Peak-Up Camera Optical Path**
- 1 **Pick-Off Mirror**
- 2 **Field Stop**
- 3 **Pass Filter Location**
- 4 **Pass Filter Location**
- 5 **Collimator**
- 6 **Fold Mirror**
- 7 **Lyot Stop**
- 8 **Schmidt Corrector**
- 9 **Schmidt Camera**
- 10 **Shared Focal Plane Array**

Short Low Optical Path
- 1' Pick-Off Mirror
- 2' Slit Assembly
- 3' Pass Filter Location
- 4' Pass Filter Location
- 5' Collimator
- 6' Grating
- 7' Schmidt Corrector
- 8' Schmidt Camera
- 9' Shared Focal Plane Array

Figure 2.4: Short-Low spectral (grey) & Peak-Up (black) optical components and light paths.

In addition to obtaining spectra, the SL module includes the IRS peak-up arrays. These arrays are used for both Peak-Up Acquisition (PUA; see Section 3.1) and for Peak-Up Imaging (PUI; see Section 3.3). Light passes through one of two bandpass filters and is imaged onto the SL detector array focal plane (in a different detector region from that used for the spectrum).

2.4 Long-Low (LL) Module

The Long-Low (LL) module is a grating spectrograph that covers, in two orders, the nominal spectral range from 14.0-38.0 micron at $57 < R < 126$. The red coverage of the LL module extends to slightly longer wavelengths (42.3 microns) than indicated here, but LL spectra could not be calibrated redward of 38.0 microns because of light leakage at the long wavelength end caused by pre-launch delamination of the order-sorting filter. The detector is a 128x128 Si:Sb BIB array with a plate scale of 5.1 arcsec/pixel. As with the SL module, the LL aperture consists of two in-line sub-slits with a small gap between them. When the source is in one sub-slit, light passes through a 14-21 micron bandpass filter and is diffracted by the grating in second order (LL2). When the source is moved to the other sub-slit, light passes through a 21-40 micron bandpass filter and is diffracted by the grating in first order (LL1). Long-Low also has a "bonus segment," similar to that in SL, which covers 19.4-21.7 micron (R=57-63). Figure 2.5 depicts the locations of the LL module components in the optical paths.
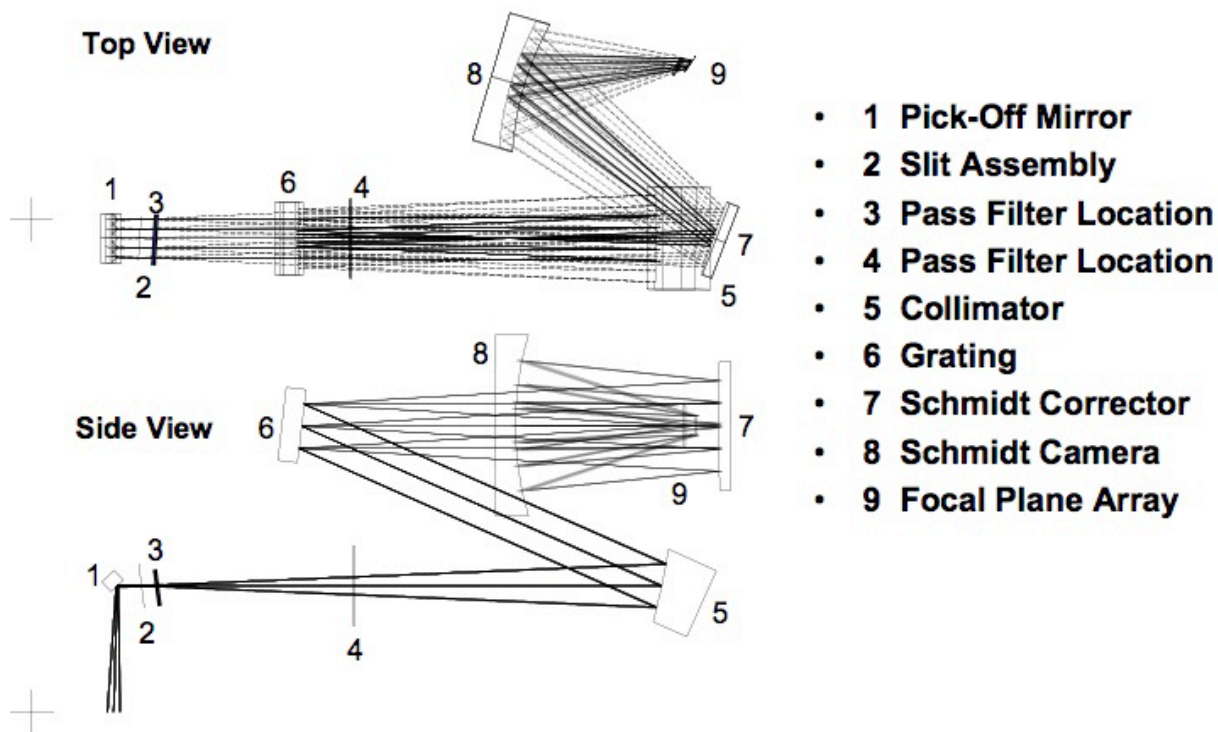
Figure 2.5: Long-Low module optical components and paths.

The IRS LL module displayed degraded sensitivity in 1st order during ground testing prior to launch due to delamination of the order-sorting filter. The LL1 filter survived launch to return useable science data. Based upon observations of hot stars, contamination of the LL1 spectrum from filter leakage is no more than 5% (shortward of about 38 microns). That is, the flux of the obtained spectrum deviates by less than 5% from the expected spectrum. This leakage is most pronounced beyond about 38 microns, where the spectrum can be severely contaminated by blue light.

2.5 Short-High (SH) Module

The Short-High (SH) module is a cross-dispersed echelle spectrograph that covers, in a single pointing, the nominal spectral range from 9.9-19.6 micron at R~600. It has a small wavelength overlap (18.7-19.6 micron) with the Long-High module. The detector is a 128x128 pixel Si:As BIB array with a plate scale of 2.3 arcsec/pixel. The SH aperture is a single slit of size 2x5 pixels. Its length was limited so that nearly an octave of a cross-dispersed echelle spectrum could fit onto the detector array without spatial overlap of orders. Figure 2.6 depicts the module components and optical paths.

- 1 Pick-Off Mirror
- 2 Slit Assembly
- 3 Pass Filter Location
- 4 Collimator
- 5 Cross Dispersion Grating
- 6 Echelle Grating
- 7 Camera Mirror
- 8 Focal Plane Array
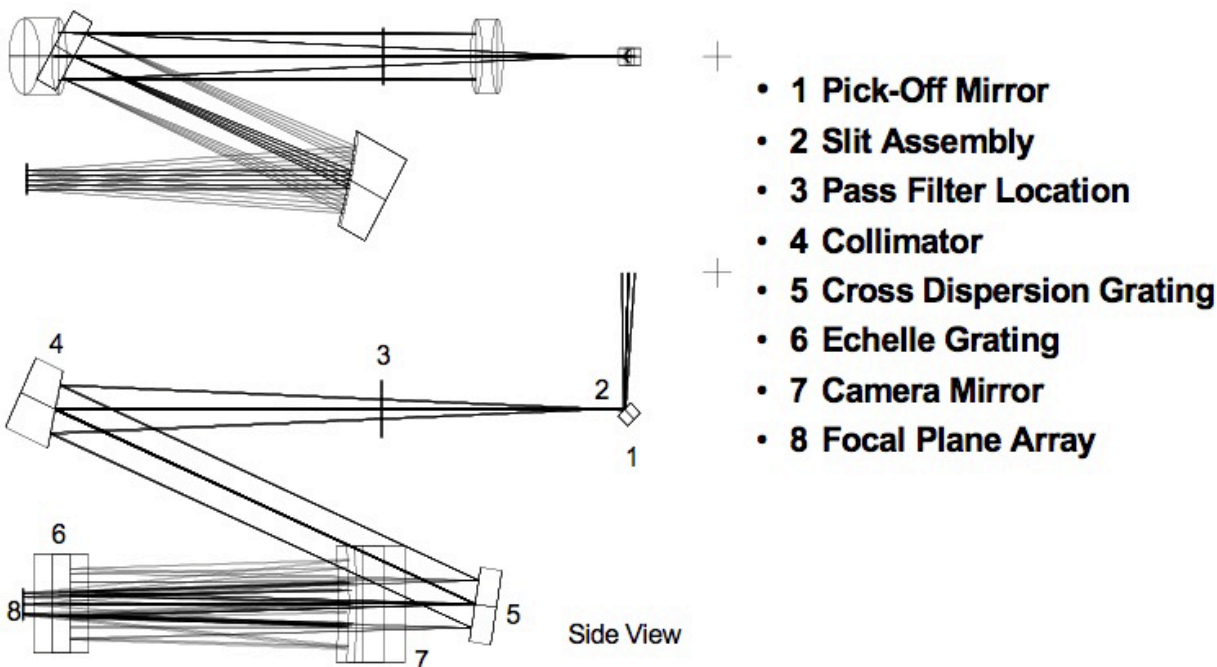
Figure 2.6: Short-High module optical components and paths.

2.6 Long-High (LH) Module

The Long-High module is a cross-dispersed echelle spectrograph which covered, in a single pointing, the nominal spectral range from 18.7-37.2 micron at R ≈ 600. It has a small wavelength overlap (18.7-19.6 micron) with the Short-High module. The detector is a 128×128 pixel^2 Si:As BIB array with a plate scale of 4.5 arcsec/pixel. As with the SH module, the LH aperture is a single slit. Its length was limited so that nearly an octave of a cross-dispersed echelle spectrum could fit onto the detector array without spatial overlap of orders. Figure 2.7 depicts the LH components and optical paths.

- 1 **Pick-Off Mirror**
- 2 **Slit Assembly**
- 3 **Pass Filter Location**
- 4 **Collimator**
- 5 **Cross Dispersion Grating**
- 6 **Echelle Grating**
- 7 **Camera Mirror 1**
- 8 **Field Stop**
- 9 **Camera Mirror 2**
- 10 **Fold Mirror**
- 11 **Focal Plane Array**
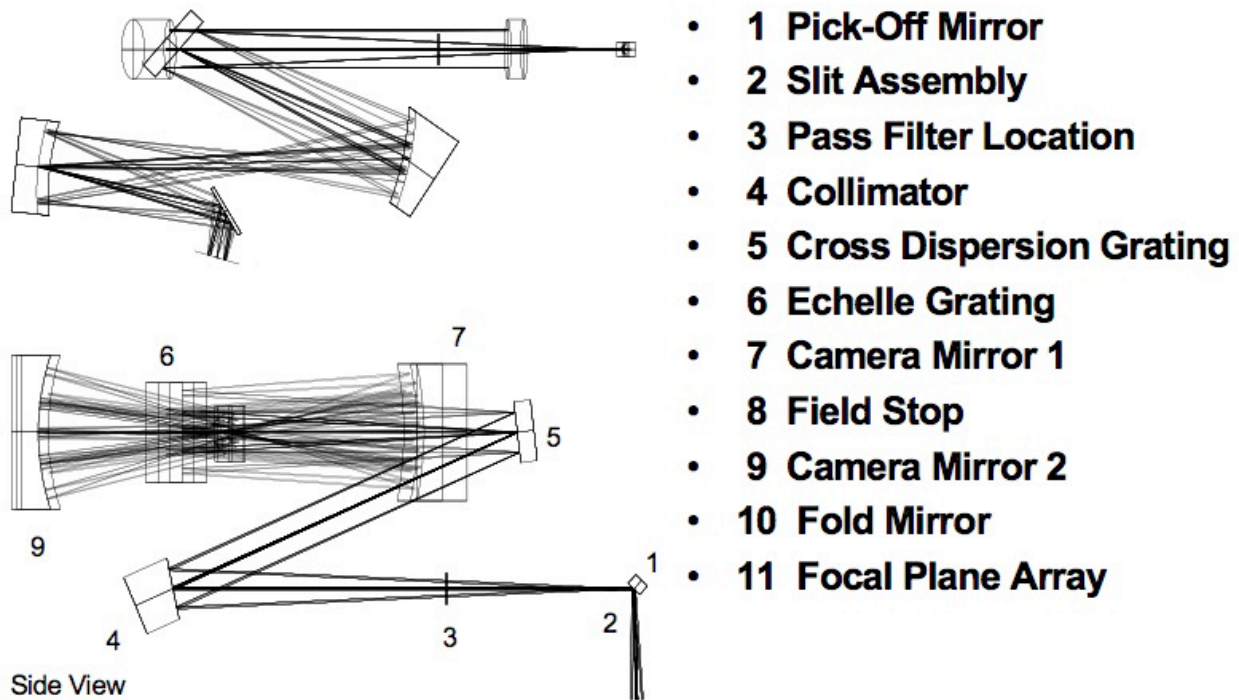
Figure 2.7: Long-High module optical components and paths.

2.7 Peak-Up Imaging

Red and blue peak-up images are obtained simultaneously on the SL detector. The field-of-view seen by each filter is 54x81 arcsec^2, and they are separated by a 33 arcsec wide vignetted zone (see Figure 2.2). The images are 35x45 pixels^2 in size and have a plate scale of 1.85 arcsec/pixel in the detector X direction, and 1.82 arcsec/pixel in the detector Y direction. The position of the two images on the SL detector is an accurate representation of their position on the sky; that is, the two fields-of-view together with the vignetted region see a contiguous 54x195 arcsec^2 area. A single WCS can be used to describe the combined red and blue regions within the 128x128 pixel detector. The geometric distortion has been accurately mapped and found to be small. The magnitude of the distortion causes no more than 1/2 pixel shift at the edge compared to the center of either peak-up array field-of-view. The distortion coefficients are applied to the astrometric solution in the World Coordinate System (WCS) provided in the FITS header of the pipeline-processed data. The system's response is shown in Figure 2.8.
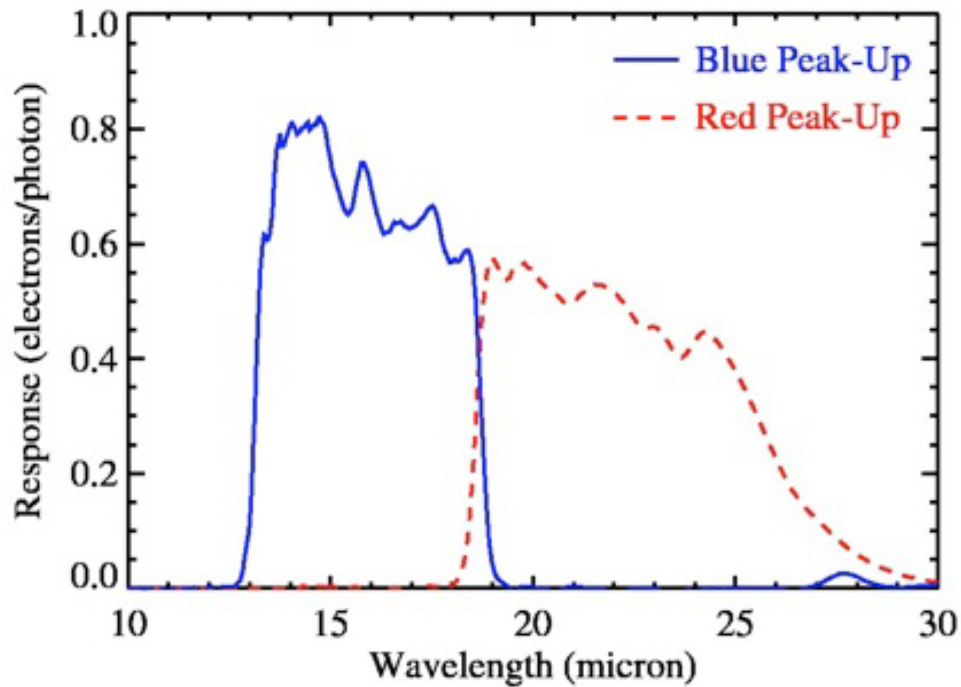
Figure 2.8: PUI response functions, in electrons/photon. This is the product of the detector's responsive quantum efficiency (QE times photoconductive gain) and the filter transmission.

The IRS provides diffraction-limited images through both peak-up filters (see Figure 2.9). The full-width-at-half-maximum (FWHM) of the PSF is approximately 2 pixels (3.8 arcsec) in the blue filter, and approximately 3 pixels (5.3 arcsec) in the red filter. The radius containing 50% of the encircled energy is 1.6 pixels (3.0 arcsec) in the blue filter, and 2.2 pixels (3.9 arcsec) in the red filter. These numbers were derived for stellar (blue) sources.
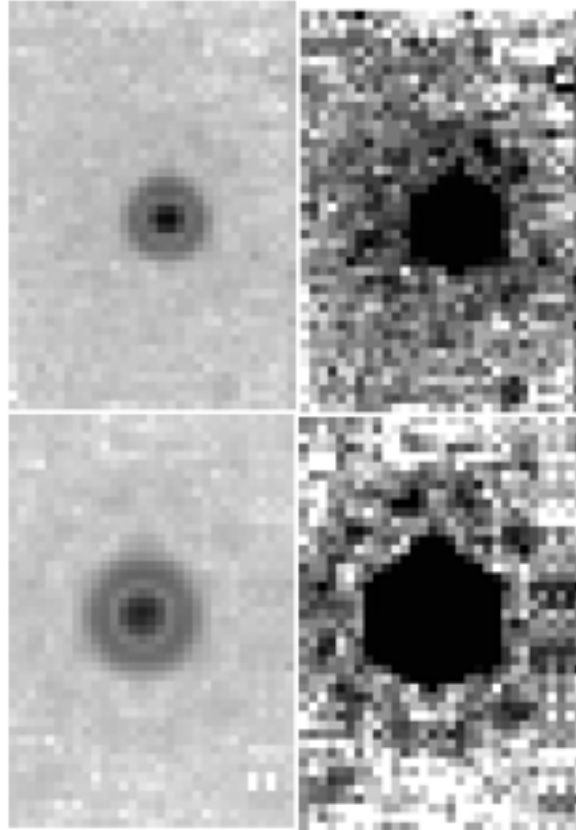
Figure 2.9: PUI PSFs for the blue (top) and red (bottom) apertures. These PSFs are co-additions of several high signal-to-noise stellar images placed within 0.1 pixels of one another on the array. The images on the left are stretched to show the central PSF and the first diffraction ring; the images on the right are stretched to show the second diffraction ring. These images show the full fields of view of the peak-up arrays.

2.8 Detectors

Each of the four IRS optical modules has a single 128x128 blocked impurity band focal plane array detector. Two (SL and SH) are arsenic-doped silicon (Si:As) arrays, and two (LL and LH) are antimony-doped silicon (Si:Sb) arrays. The Si:As arrays operate over a 5-26 micron wavelength window, while the Si:Sb arrays operate over a 14-40 micron window.

2.8.1   Bias and Detective Quantum Efficiency in LL and LH

The Detective Quantum Efficiency (DQE) is a function of wavelength (λ) and bias voltage. In Si:Sb arrays (LL and LH), an increase in bias voltage leads to a dramatic change in DQE at longer wavelengths (>36 microns); see Figure 2.10. However, it also exacerbates the dark current associated with radiation-damaged pixels. A performance optimization metric, developed from charged particle test data and infrared responsivity vs. wavelength measurements on Si:Sb detectors, was used to calculate the optimum bias voltage for a given cosmic ray dose.
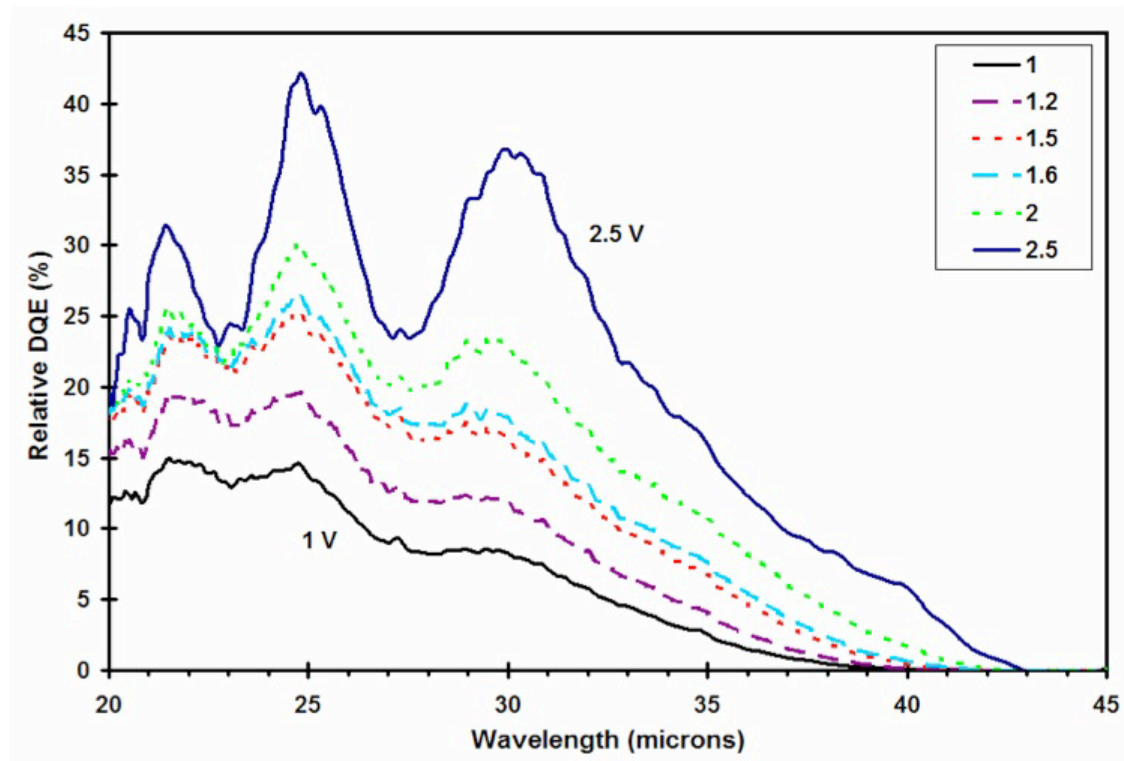
Figure 2.10: DQE for the Si:Sb arrays as a function of wavelength for different bias settings (1-2.5 V). The DQE declines linearly from 30 microns to 40 microns (reaching zero at approximately 40 microns) for the optimal bias voltage (1.6 V) that provides the best performance over the 14-36 micron interval.

In order to reduce the number of damaged pixels ("rogues") and to improve the signal-to-noise ratio nin observations of faint sources, the bias voltage on the Long High array was reduced from 2.0 to 1.6 volts at the start of IRS Campaign 25 (see Table 2.2). This change reduced the detector's quantum efficiency by a wavelength-dependent factor (by an average of ~30%). On the other hand, the change also reduced the number of bad pixels in the array by a factor of two to three, resulting in cleaner spectra.

For the same reason the bias was changed in Long High, in IRS Campaign 45 the bias voltage on the Long Low array was reduced from 1.8 to 1.6 volts and the array temperature was reduced from 4.4 to 4.1 K (see Table 2.2). As for LH, this reduced the dark current and photon sensitivity of the array. In the case of Long Low, the number of detected rogue pixels decreased to 1/3 of its previous value. This combination of effects increased the overall signal-to-noise ratio in the LL array by up to 60%, depending on wavelength.

2.8.2   *Array Temperature Control and Annealing*

In order to achieve optimum performance, the detector array temperature was closely controlled. Because charged particle radiation damage accumulation on the pixels causes an increase in baseline dark current, periodic annealing was required to re-establish this baseline. Raising the temperature (annealing) of the array to 25 K (±5 K) for a minimum time of 1 minute accomplished this. The IRS detectors were annealed as part of the detector check procedure that ran every three to four days of an IRS campaign,

including at the beginning after powering up the IRS and at the end just before shutting down. In addition, all IRS arrays were annealed once every 24 hours, prior to taking dark measurements at the start of each Period of Autonomous Operation (PAO).

2.8.3   IRS Detector Characteristics

1. *Photometric response* –The detector response stability was better than 1% over multiple cool-downs separated by months, and the responsivity of the detectors was unaffected by radiation. Overall repeatability depended upon the selected pointing (Peak-Up) accuracy but was as good as 2%.

2. *Effect of overexposures* – Collection of over 300,000 electrons/pixel before a reset caused a 1–2% reduction in responsivity in the affected pixels for a period of approximately one hour.

3. *Read noise* – The read noise was 30 electrons/pixel in SUR ("sample up the ramp") mode with 16 samples per ramp (see Figure 2.13).

4. *Dark current* – At a bias of 1.6 volts, the dark current was less than 10 electrons/sec per pixel for the SL/SH arrays and less than 40 electrons/sec per pixel for the LL/LH arrays.

5. *Gain* – The gain was 4.6 electrons/DN (data number).

6. *Pixel masks* – The pixel badness criteria are (1) having a dark current greater than 40 electrons/sec in SL/SH or greater than 160 electrons/sec in LL/LH, or (2) a responsivity less than 50% (or greater than 150%) of the median responsivity of the array.

7. *Cosmic ray transient effects* – Pre-launch proton irradiation tests showed no cosmic ray transient effects after the usual boost/reset sequence. However, there may be transient effects within a given ramp for a small number of reads before the next boost/reset. This is corrected in the science data processing pipeline.

8. *Bias* – As part of the normal maintenance plan for the IRS, the bias levels were occasionally adjusted. see Table 2.2 for a summary of these changes. This is corrected in the science data processing pipeline.

Table 2.2 Summary of changes in bias and temperature for all IRS modules.

IRS Campaign	SH bias / temp	LH bias / temp	SL bias / temp	LL bias / temp
IOC* campaign K2 - 24	2 V / 6.2 K	2 V / 4.4 K	2 V / 6.2 K	1.8 V / 4.4 K
25-44	2V / 6.2 K	1.6 V / 4.4 K	2 V / 6.2 K	1.8 V / 4.4 K
45-61	2V / 6.2 K	1.6 V / 4.4 K	2V / 6.2 K	1.6 V / 4.1 K

*In Orbit Checkout

9. **Droop –** Droop is a slope proportional to the photocurrent summed over all pixels, which is added to every pixel of the array when it is non-destructively read in SUR mode. Noise measurements show that this slope is a multiplexer (MUX) artifact, not a true current. The droop coupling constant (droop/[total array photocurrent]) is typically 3×10^{-5} for all arrays, which is equivalent to a ratio of droop to average dark current of 0.48. Droop is present in all IRS arrays.

10. **Well depth –** Well depth, defined as the point at which the differential responsivity has fallen to 90% of its small-signal value, exceeds 2×10^5 electrons/pixel for Si:As and exceeds 10^5 electrons/pixel for Si:Sb. The full well depth is a few times these values and irrelevant for the user, because digital saturation (301,466 electrons=65535 DN) is reached before electronic saturation.

2.9 Electronics

2.9.1   *Combined Electronics Sybsystem*

The architecture of the Combined Electronics (CE) subsystem incorporates two independent and redundant electronics boxes (A & B). The CE subsystem was used to operate both the IRS and MIPS cold instruments, although only one instrument could be used, or even powered up, at a time. While using the IRS, separate circuit boards in the CE handled detector array clocking, detector array signal conditioning, communication with the spacecraft, command and data processing, and engineering data collection functions. When the IRS was operating, all four detector arrays were clocked simultaneously. The on-chip output drivers were independently powered, so that any number of the IRS arrays could be powered on simultaneously. However, the array outputs were multiplexed to the analog signal conditioning circuit so that it was only possible to capture data from one array at a time.

The high-energy radiation environment for the IRS consisted primarily of (1) cosmic ray protons and heavy ions, and (2) solar protons and heavy ions. These particles range in energy from a few eV to over 1 GeV. The peak fluxes and total fluences of these particles vary with the level of solar activity and are on the order of 2-16 protons/cm^2/s. This environment caused a variety of effects in the IRS, manifesting as both long-term degradation and abrupt changes in the electronics and optics. The CE was designed to withstand the total radiation dose estimated over a 5-year mission. However, the largest contribution to the accumulated radiation dose damage occured during unusually large solar flares.

2.9.2   *Analog Signal Processing*

The Si Analog Signal Processing electronics selected and conditioned the signals from the science arrays in use. Figure 2.11 shows a block diagram of the signal path for the output from the Si detector(s). The Si Analog Signal Processing electronics provided signal output and processing for up to five (4 IRS plus 1 MIPS) Si arrays on a 5x4 channel multiplexer with four channels per array. There is no provision for accessing only a subset of an array. The output signal is 1.2 microV/electron. The voltage becomes more negative with increasing detector charge (see Figure 2.12 and Figure 2.13).
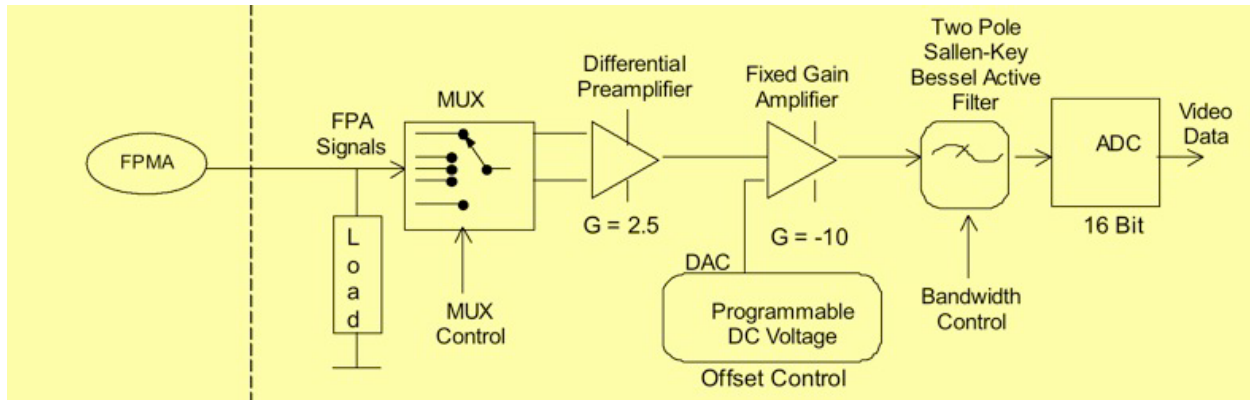
Figure 2.11: Si detector output signal path (one of four parallel paths).

2.9.3 Array Clock and Operation

The Si Analog Signal Processing electronics provide four Si clocks. Observation modes for the IRS require clocking the Si detectors using the Timing Pattern Generator (TPG) with specific timing patterns as defined below.

2.9.3.1 Basic Definitions

In order to discuss the IRS array clocking and data collection it is necessary to define several terms in addition to those defined in Section 1.2:

Sample: A 16-bit integer resulting from a single A/D conversion of a pixel signal.

Frame: A single clocking through a detector array, visiting every pixel. There are four frame types used in observations:

- *Sample Frame:* A frame in which each pixel is sampled (read).

- *Reset Frame:* A frame in which each pixel is reset.

- *Boost Frame:* A frame in which each pixel is reset with a boost voltage applied.

- *Spin Frame:* A frame in which each pixel is just addressed. No read or reset is applied. Spin frames allowed continuous clocking patterns without affecting the charge of a pixel.

Frame Count: The number of sample frames.

Two data collection techniques were used in general science data collection:

Spinning Double Correlated Sampling (DCS): Scheme in which the first frame after a reset frame and the frame just before the next reset were sampled, with spins in between. Peak-Up Acquisition (PUA) employed DCS mode.

IRS Raw or Sample-Up-the-Ramp (SUR): Scheme in which sample and spin frames were obtained between a reset frame and the next reset/boost frame; i.e., the ramp is sampled. Science data were collected in SUR mode.

In addition, we define different time amounts:

Frame Time: Time required to clock through one Si frame. IRS frame times are in standard seconds (derived from a 40 MHz oscillator on the CE I/O board).

Exposure Time: The time for which the Timing Pattern Generator was running during an IRS exposure ("wall clock time").

Effective Data Collection Event (DCE) Time, or Effective Exposure Time: The time for which the Timing Pattern Generator was actively collecting valid data, or the time between detector resets ("integration time").

DCE Time or Execution Time: The time between and including detector resets (= effective DCE time + reset time).

2.9.3.2 *Double Correlated Sampling (DCS)*

Figure 2.12 shows the parameters for the DCS data collection technique. This is the way in which the peak-up arrays were read for the purposes of IRS Peak-Up Acquisition (PUA). Following an initial series of bias boost and reset frames, each pixel was sampled. The total time required to sample every pixel in the array is the frame time. Several successive spins through the array were then carried out in which each pixel was accessed but not sampled. (Note that the frame time and the spin time are equal). After a specified number of spins, the pixels were again sampled, and the difference between the two samples at each pixel was saved and stored as an image. Each DCS mode sub-exposure generated a single 128x128 16-bit image.
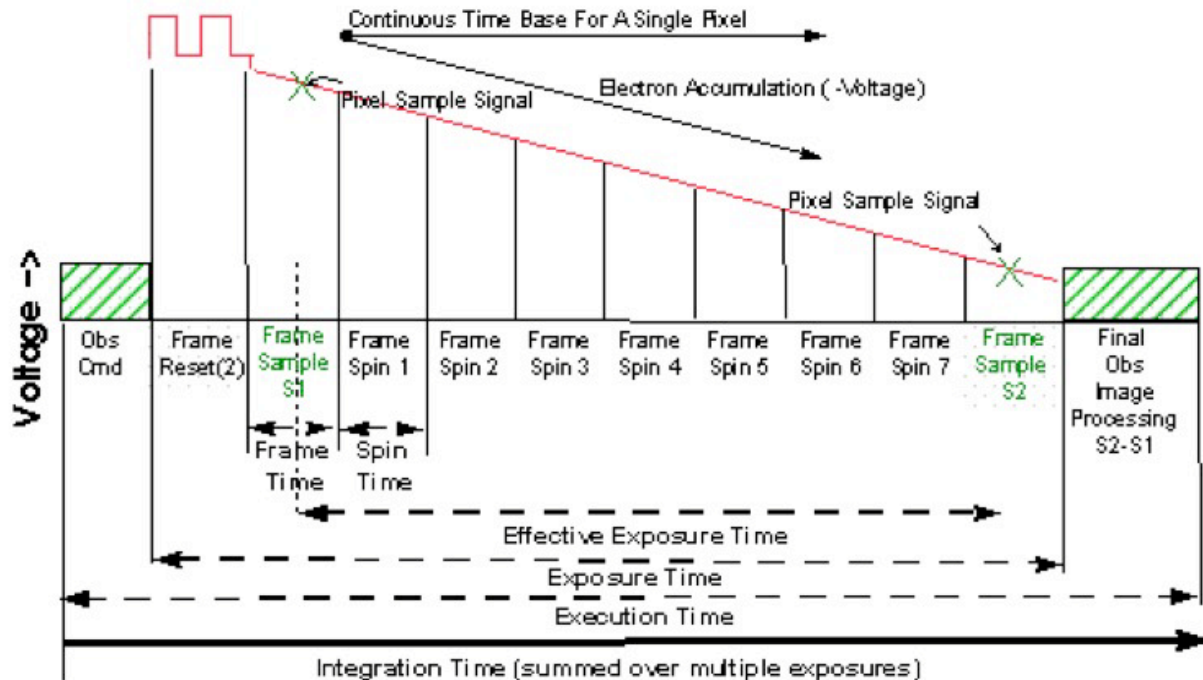
Figure 2.12: Double Correlated Sampling (DCS) data collection technique.

2.9.3.3   Sample-Up-the-Ramp (SUR) Data Collection

Figure 2.13 shows the parameters for the SUR data collection technique. This is how science exposures (peak-up imaging and spectroscopic exposures) were read. Following an initial series of bias boost and reset frames, each pixel was sampled. The total time required to sample each pixel in the array is the frame time. There may be spin frames in which each pixel was accessed but not sampled. Every time the pixel was sampled, the data from each sample were saved and stored as an image to be sent to the ground for processing. Each IRS SUR mode exposure generated N 128x128 16-bit images, where N is the number of commanded sample frames. Note that some combinations of clocking patterns and frame times were inefficient or otherwise undesirable; hence, only a subset of all possible combinations was available to observers.

Table 2.3 lists the number of samples ($N_{samples}$) used in SUR data collection mode for each available IRS integration time (t_{int}). The corresponding time interval between samples ($\Delta t_{samples}$) is found by dividing the integration time by the number of samples less one [$t_{\text{int}} /(N_{samples}-1)$]. The times given in the table are shorthand for the effective exposure times given in parentheses.
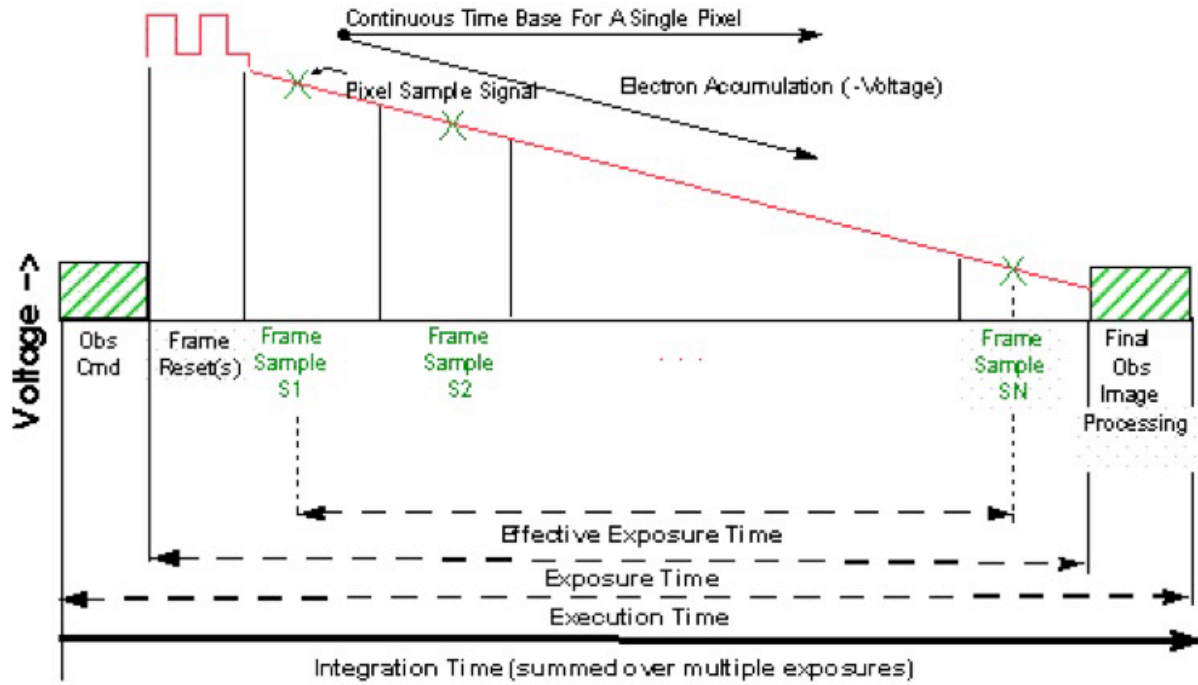
Figure 2.13: "Sample-Up-the-Ramp" data collection technique.

Table 2.3 SUR data collection mode sampling parameters.

t_{int}		$N_{samples}$	$\Delta t_{samples}$	
6	(6.27)	4	2	(2.095)
14	(14.63)	8	2	(2.095)
30	(31.35)	16	2	(2.095)
60	(60.90)	16	4	(4.065)
120	(121.80)	16	8	(8.125)
240	(241.80)	16	16	(16.125)
480	(481.65)	16	32	(32.115)

2.10   Sensitivity

The median 1-sigma continuum sensitivity for the IRS low-resolution modules is about 0.06 mJy from 6 to 15 microns and 0.4 mJy from 14 to 38 microns in 512 seconds of integration with low background. The median 1-sigma line sensitivity estimates for the short- and long-wavelength high-resolution modules are about 2.7×10^{-19} W/m^2 and 8.5×10^{-19} W/m^2, respectively, for 512 seconds of integration with low background (see Figure 2.14 through Figure 2.18).

2.10.1   Equations for Calculating Sensitivity and Signal-To-Noise for Point Sources

This section illustrates the procedure by which the expected instrumental sensitivity and signal-to-noise ratios were calculated.

The background photocurrent from sky and telescope is given by

$$i_{sky} = (\lambda B_\lambda / hc) A\Omega \Delta\lambda \tau \eta G \qquad \textbf{Equation 2.1}$$

where h is the Planck constant and

$$B_\lambda = f_{stray} 2hc^2 (1/\lambda)^5 10^8 \sum \varepsilon_i / e^{14387/\lambda T_i} -1 \quad [\text{Jy sr}^{-1}] \qquad \textbf{Equation 2.2}$$

where $2hc^2 = 1.19\times10^{-4}$ W micron^2, all lengths are in microns, f_{stray} is the ratio of total sky throughput to that of an ideal f/12 telescope, and ε_i are sky emissivities at temperatures T_i. We also define the following:

$A\Omega$= the telescope throughput in cm^2 sr.

$\Delta\lambda$ =the spectral bandpass falling on one pixel (= λ /R) in cm. Note: while there are 2 pixels per resolution element, the slit width is also two pixels. Hence, $\Delta\lambda$ is proportional to the slit width if the spectral plate scale is unchanged.

T_i = effective blackbody temperature of sky + telescope.

τ = the cold optical throughput for extended sources (i.e., omitting slit losses).

ηG = the detector responsivity (electrons/photon) [=$(\eta/\beta)\beta G$].

η =quantum efficiency of the detector at the desired wavelength.

βG = the dispersion-gain product.

In the faint source limit, the total noise in electrons/pixel is the sum of the photocurrent shot noise (i_{sky}), read noise, and dark current shot noise. It is given by:

$$N = \sqrt{i_{sky}\beta G t_{int} + (RN)^2 + i_d \beta_d G_d t_{int}} \quad \text{[electrons/pixel]}$$ **Equation 2.3**

where i_d is the dark current contribution, RN is the read noise in electrons, t_{int} is the integration time in seconds, and $\beta_d G_d$ is the dispersion-gain product for the dark observations.

The relationship between photocurrent/pixel and the incident flux density of a source in mJy is given by:

$$S_{mJy} = 1.511\pi(D^2/4)\tau_{tel}\tau_{align}\tau\tau_{slit}\eta G t_{int}/4R \quad \text{[electrons/pixel/mJy]}$$ **Equation 2.4**

where 1 mJy = 10^{-26} erg s^{-1} cm^{-2} Hz^{-1}, D is the telescope aperture (in cm^2), τ is the slit throughput of a point source with angular diameter λ_{max}/D (without considering losses), and $\tau_{tel}, \tau_{align}, \tau_{slit}$ are throughputs accounting for losses in the telescope, alignment effects, and slit, respectively. The second factor of 4 in Equation 2.4 comes from dividing the point source flux over 2 pixels per spectral resolution element and 2 pixels spatial extent. Again assuming the faint source limit, the 1σ staring point source continuum sensitivity (PSSC) in mJy at the full resolution of the spectrograph is:

$$PSSC = \alpha N / S_{mJy} \quad \text{[mJy]}$$ **Equation 2.5**

where the factor α accounts for the variation in PSF with wavelength and details of the point source extraction. Its value lies between 0.8 and 1.2. The 1σ staring point source continuum sensitivity (in mJy) smoothed at the required resolution of the spectrograph ($R_{req} = 50$) is referred to as the PSSCS, and is given by

$$PSSCS = PSSC\sqrt{R_{req}/R}$$ **Equation 2.6**

The spectra are smoothed from R to R_{req} and the S/N is assumed to increase as the square root of the number of pixels averaged. Suitable sub-pixel smoothing is assumed.

The 1σ staring point source sensitivity (in W m^{-2}) for unresolved lines is then

$$PSSL = 3 \times 10^{-15} PSSC/(R\lambda)$$ **Equation 2.7**

where the factor 3×10^{-15} = c (micron/s) (10^{-29} W m^{-2} Hz^{-1}/mJy), $PSSC$ is in units of mJy, and λ is in microns.

2.10.2 *Spectroscopic Sensitivity to Point Sources in the Faint-Source Limit*

This section provides sensitivity curves for all four IRS modules. These sensitivities are based on pre-launch models that were refined using in-orbit measurements of point source flux calibrators, and take into account the degradation of the LL1 module that was discovered during CTA ground-testing prior to launch. Figure 2.14 shows a comparison between the four modules. Plots of the point-source single pointing continuum sensitivity of the SL and LL modules are shown in Figure 2.15 and Figure 2.16, respectively. Plots of the point-source single pointing (unresolved) line sensitivity of the SH and LH modules are shown in Figure 2.17 and Figure 2.18, respectively. These plots also show the sensitivities

for the four observer-selectable integration times. Finally, Figure 2.19 shows the IRS digital saturation limits for bright point sources for the shortest ramp time (6 sec). Saturation is not necessarily fatal for an observation as the data processing pipeline reconstructs the ramp if at least two samples are available (albeit with a larger error than usual). However, very bright sources may leave latent imprints in the detectors that will compromise further observations until an anneal is performed.

In all of the figures shown in this section, it is assumed that the source is in the faint source limit (i.e., for a selected exposure time, the target flux is BELOW the relevant line shown in Figure 2.20. If the source is bright and lies above the line, then the curves shown in the following figures will significantly overestimate the expected signal-to-noise ratio. In Section 2.10.4 a simple scaling rule is given to convert the expected S/N ratio based on the (faint source) sensitivities to a more realistic value for bright sources.

In addition, all of the figures shown in this section assume that the source is a point source. If the source is actually extended, then the user should see Section 2.10.3 for information on how to correct the point-source sensitivies.
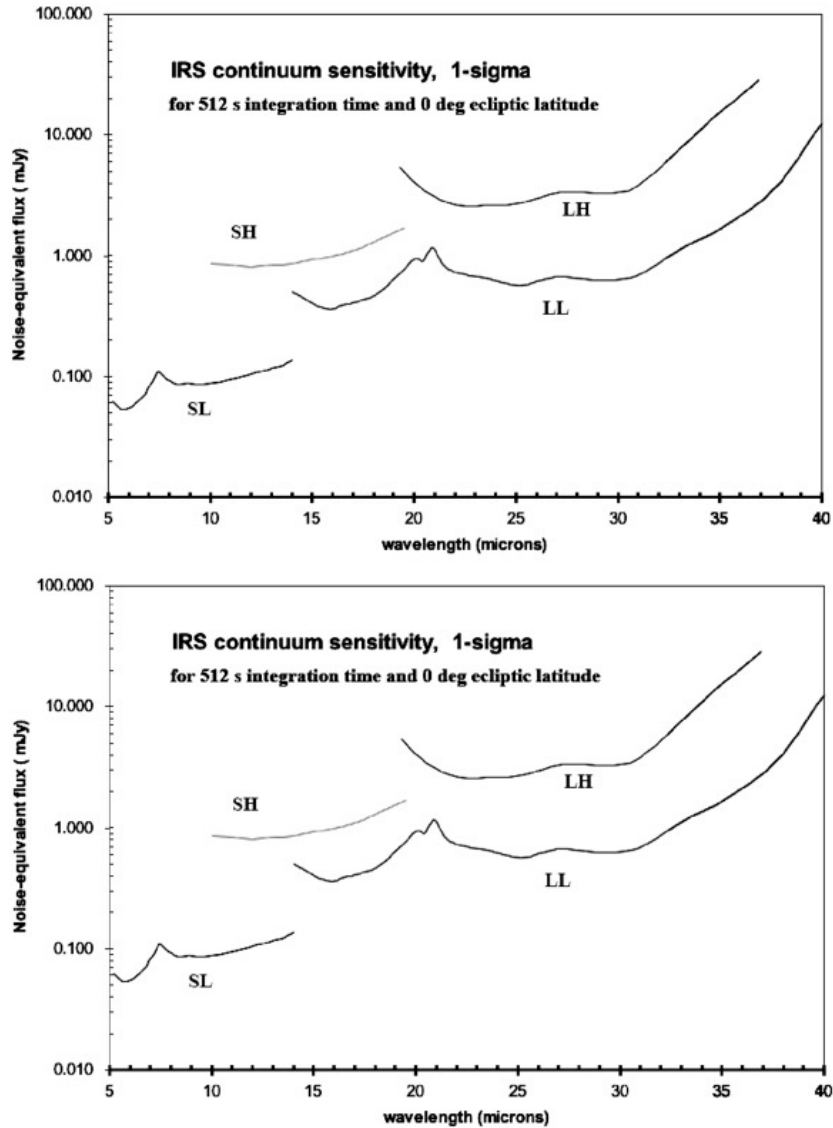
Figure 2.14: 1-sigma continuum sensitivity (in the faint source limit) of all four IRS modules in a 512 second integration with HIGH (top) and MEDIUM (bottom) backgrounds (the LOW background case, corresponding to an ecliptic latitude of 90°, is indistinguishable from the MEDIUM background case at the scale of these plots).
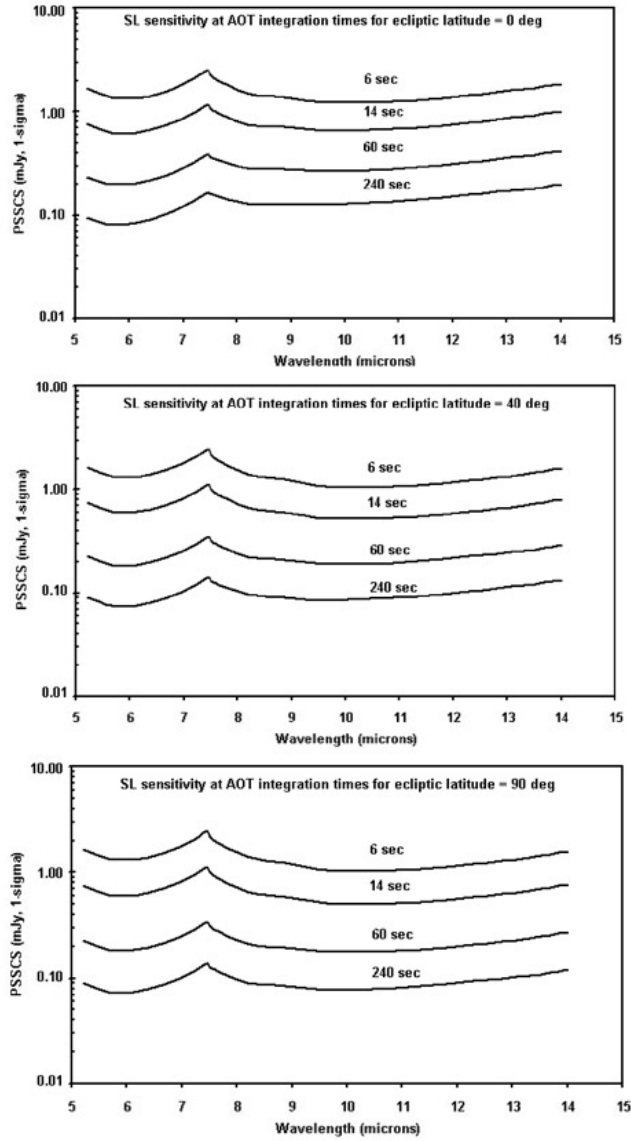
Figure 2.15: Short-Low 1-sigma point source staring continuum sensitivity (PSSCS) in the faint source limit after smoothing to a resolution of R = 50, with HIGH (top), MEDIUM (middle), and LOW (bottom) backgrounds.
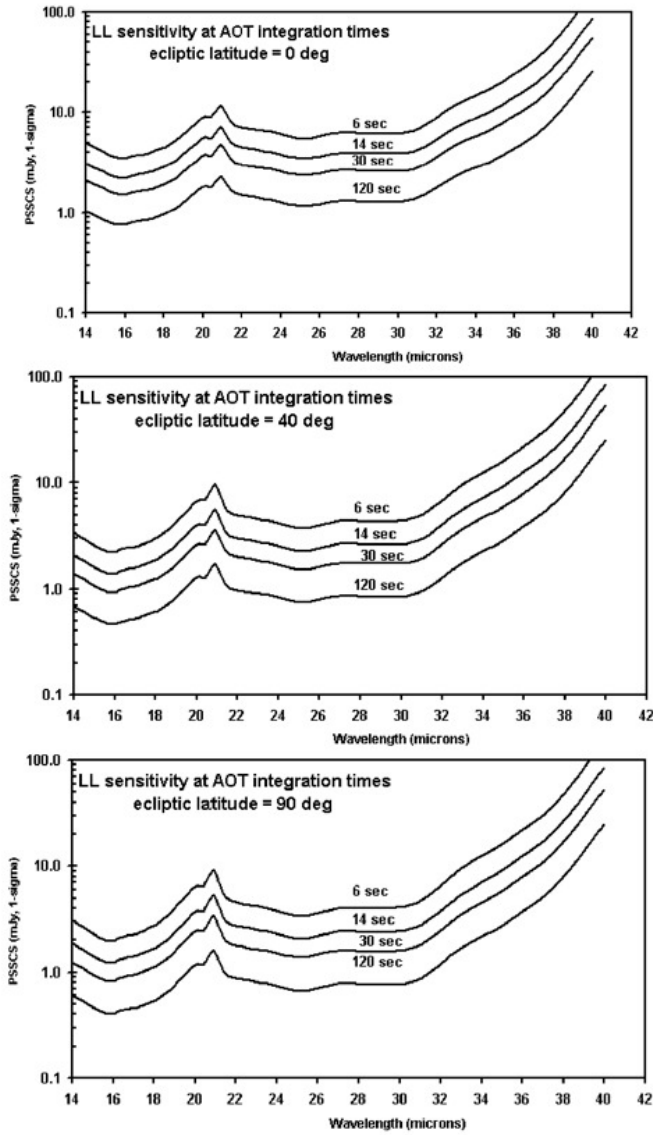
Figure 2.16: Long-Low 1-sigma point source staring continuum sensitivity (PSSCS) in the faint source limit after smoothing to a resolution of R = 50, with HIGH (top), MEDIUM (middle), and LOW (bottom) backgrounds. This figure includes the effects of the LL1 filter delamination discovered before launch.
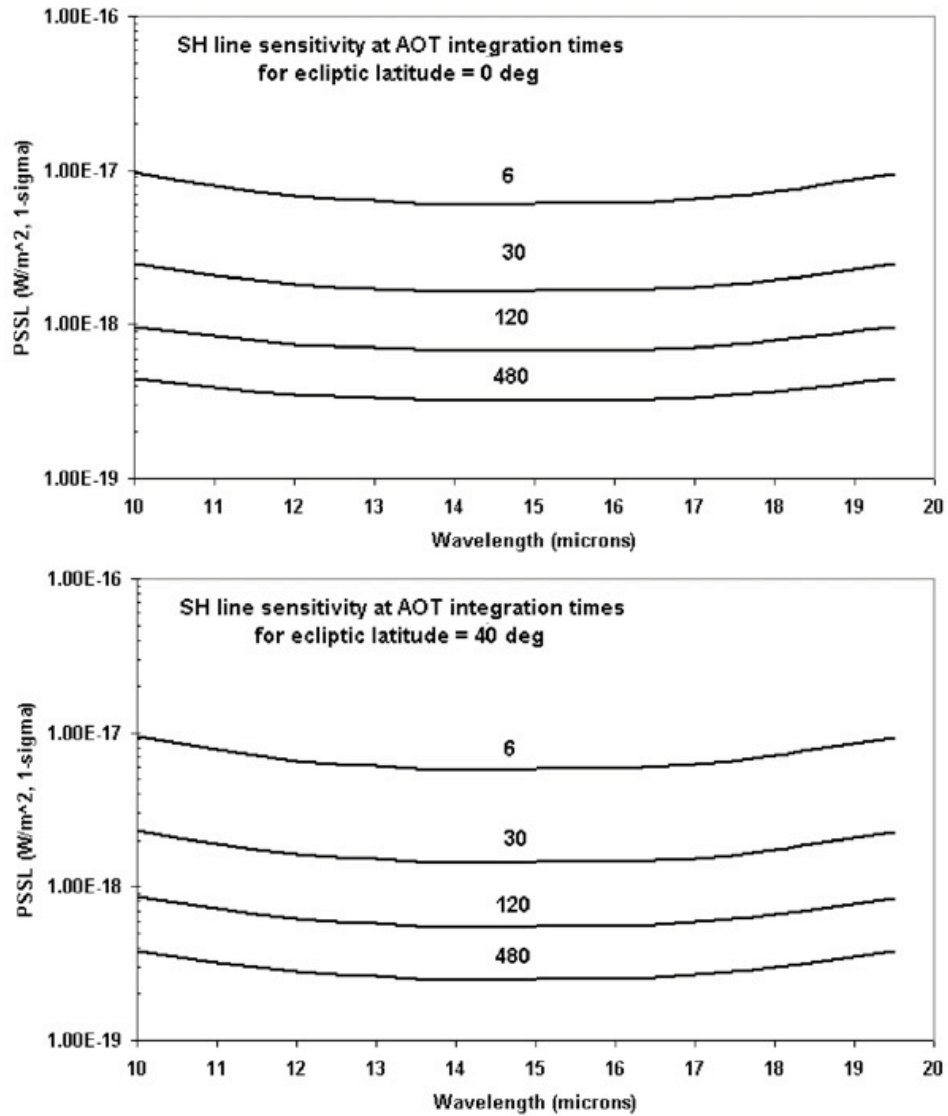
Figure 2.17: Short-High 1-sigma point source sensitivity (PSSL) to an unresolved emission line in the faint source limit, with HIGH (top) and MEDIUM (bottom) backgrounds (the LOW background case, corresponding to an ecliptic latitude of 90°, is indistinguishable from the MEDIUM background case at the scale of these plots).
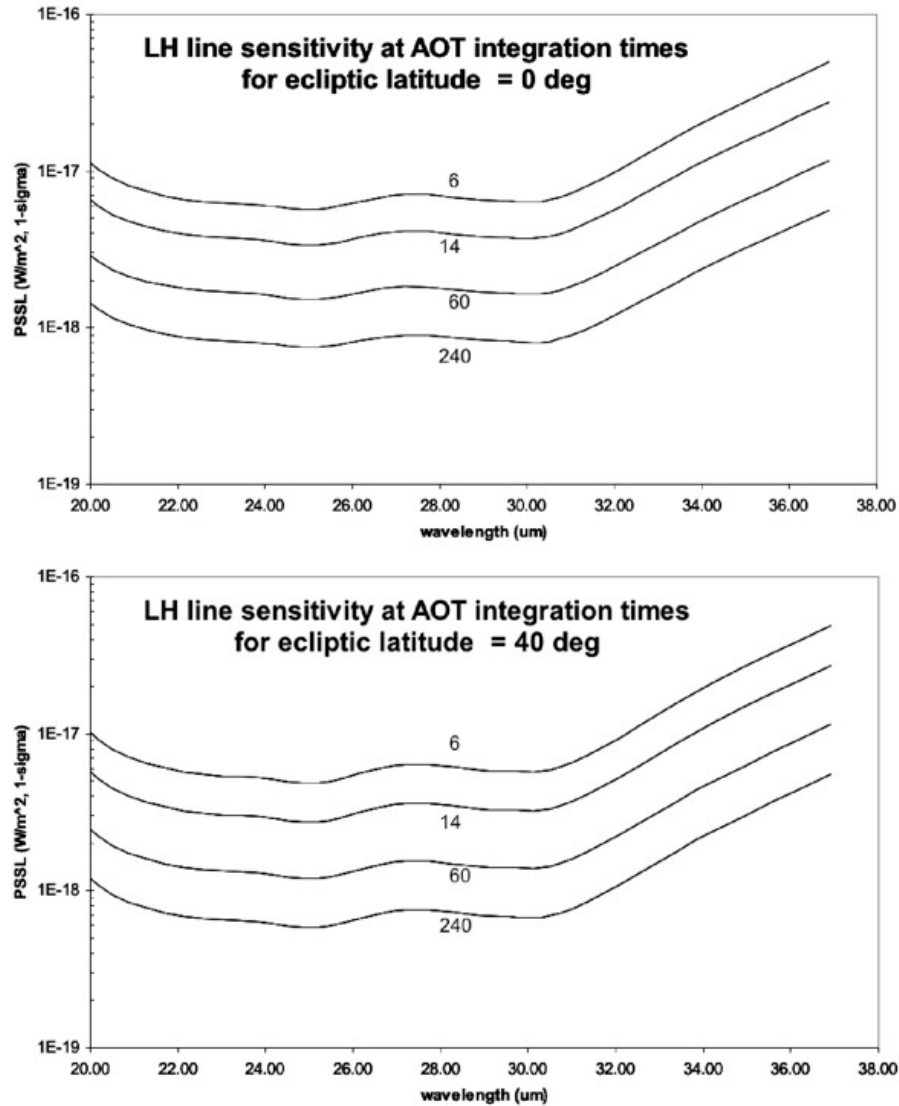
Figure 2.18: Long-High 1-sigma point source sensitivity (PSSL) to an unresolved emission line in the faint source limit with HIGH (top) and MEDIUM (bottom) backgrounds (the LOW background case, corresponding to an ecliptic latitude of 90°, is indistinguishable from the MEDIUM background case at the scale of these plots).
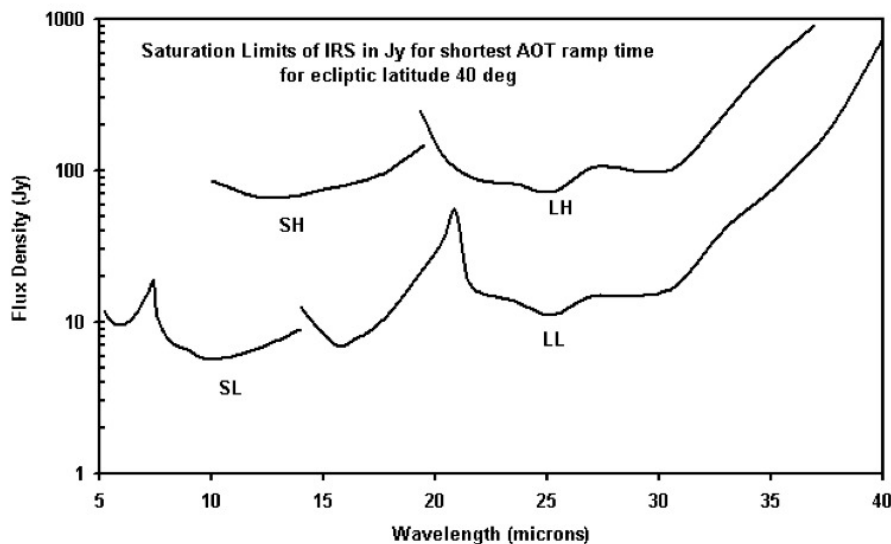
Figure 2.19: Saturation levels for the shortest ramp duration available in the IRS AOTs, with MEDIUM background (the HIGH and LOW background cases, corresponding to ecliptic latitudes of 0° and 90°, respectively, are indistinguishable from the MEDIUM background case at the scale of this plot). For flux densities at a given wavelength that exceed these limits, at least one of the samples will be saturated. Flux densities up to 3 times greater will have at least two unsaturated samples.

2.10.3   Spectroscopic Sensitivity Correction for Extended Sources

The calculations and sensitivity curves shown above apply only to observations of point sources. We provide a rough guide to the conversion from point- to extended-source sensitivities as follows. Note that the approximations used here are only good to about 20% because of wavelength dependence in the conversion factors that varies from module to module. The ESSC and ESSL are the 1σ staring extended source sensitivities per pixel for continuum and line, respectively. They are:

$$ESSC \sim 8 \times (PSSC)/\phi^2 [MJy \cdot sr^{-1}]$$

Equation 2.8

and

$$ESSL \sim 8 \times 10^9 (PSSL)/\phi^2 [Wm^{-2}sr^{-1}]$$

Equation 2.9

where ϕ is the linear edge size of a pixel projected onto the sky in arcseconds (Table 2.1, and different for each IRS module). The values of *PSSC* (or its smoothed equivalent for a variety of AOT integration times) and *PSSL* can be read from the sensitivity curves above.

For example, the 1-sigma point source sensitivity (*PSSC*) of the SL module at 8 microns is 1.05 mJy in 6 seconds (from the sensitivity curve in Figure 2.15). The pixel size for the SL module is 1.8 arcseconds. So, the corresponding extended source sensitivity for SL is given by

$$\text{ESSC(SL)} \sim 8 \times 1.05 / 1.8^2 = 2.6 \text{ MJy sr}^{-1} \text{ at 8 micron in 6 sec}$$ **Equation 2.10**

Similar calculations can be carried out for the other IRS modules and exposure times.

2.10.4 Spectroscopic Sensitivity Correction for Bright Sources

The PSSC and PSSCS as calculated above and shown in the sensitivity curves assume that the target is in the faint source limit. That is, the shot noise from the source is negligible compared with the other sources of noise described above. Conversely, Figure 2.20 shows the approximate flux density (the median flux density averaged over the whole wavelength response of each module) at which a target's shot noise dominates over the other sources of noise (sky background + dark current + read noise), as a function of exposure duration for each of the IRS modules. Thus, Figure 2.20 can be used to determine whether a target object of known infrared flux density corresponds more appropriately to the "Bright Source Limit" (BSL).

The low-resolution modules rapidly reach an asymptotic BSL in a few tens of seconds of integration time, whereas the high-resolution modules take longer to reach this plateau. Sources that have flux densities which lie below the curves plotted in Figure 2.20 for a given integration time are in the faint-source limit (i.e., they are background or read-noise limited), whereas sources that have flux densities which place them above the line for a given module have signal-to-noise ratios (S/N) that are dominated by the source flux density. Knowledge of the regime in which a source lies is crucial to calculating a realistic S/N estimate. Note that for all allowed AOT integration times of the low resolution modules, sources brighter than 130 mJy will always be source-dominated. For all allowed AOT integration times of the high resolution modules, sources brighter than 620 mJy will always be source-dominated.

In this section, we provide a simple scaling rule that allows the original estimate of the signal-to-noise ratio for faint sources obtained through the use of Figure 2.15 through Figure 2.18 to be corrected for the contribution of the shot noise from a bright source. Consider, for example, a continuum source with a known 8 micron flux density of 250 mJy. To estimate the S/N of this source in the SL module for an integration time of 14 sec, we first consider the *PSSC* for SL at this wavelength (i.e., the faint source limit case). Inspection of Figure 2.15 shows that at 8 microns, the 1σ *PSSC* is 0.7 mJy (in the LOW background case). If we were to (incorrectly) assume that the source itself contributed no noise, then we would estimate the signal-to-noise ratio $(S/N)_{faint} = (250/0.7) = 357$. However, we notice from Figure 2.20 that in SL for a 14 sec integration time, the Bright Source Limit (BSL) = 26.5 mJy. Thus, the 250 mJy target exceeds the BSL by a factor of ~9.4. We can now estimate a more realistic S/N for the source by using the simple scaling rule

$$(S/N)_{bright} = (S/N)_{faint} / (1 + [\text{SourceFlux} / \text{BSL}])^{0.5}$$ **Equation 2.11**

Where the source and BSL fluxes are given in the same units (e.g., mJy). In this example,

$$(S/N)_{bright} = 357 / (10.4)^{0.5} = 357 / 3.2 = 112$$ **Equation 2.12**

Hence, a more realistic value for the 8 micron S/N for a 250 mJy source observed for 14 sec in SL is ~110. This procedure can be generalized for use in estimating the S/N that was obtained for observations of bright sources (both point and extended) using any of the IRS modules.
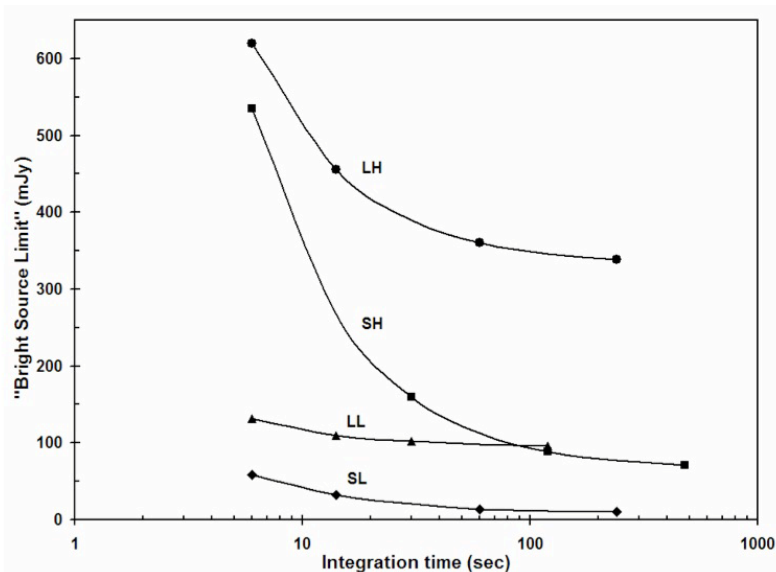
Figure 2.20: Bright Source Limit (BSL) as a function of integration time for each of the IRS modules. Targets with fluxes above the curves for a given integration time are source-dominated; targets with fluxes below the curves are read noise or background limited. The plotted points on the curve for each module indicate the allowed AOT durations for that module.

2.10.5   *Imaging Sensitivity to Point Sources*

We use the same basic calculations presented above to estimate the sensitivity and S/N for PUI observations. Table 2.4 summarizes the instrument sensitivity in the PUI mode. The flux density is the peak-up target flux density at 16 microns (blue) or 22 microns (red). The underlying procedure used to calculate the PUI sensitivities is presented for informative purposes here:

1. The background photocurrent from sky and telescope is given by Table 2.4, where, in the case of PUI, $\Delta \lambda \approx 5.4$ micron.

2. For faint sources, the total noise in electrons/pixel is the sum of the photocurrent shot noise, read noise, and dark current shot noise. It is given by:

$$N = \sqrt{i_{\mathrm{sky}} t_{\mathrm{int}} + (RN)^2 / N_{\mathrm{reads}} + i_{\mathrm{d}} t_{\mathrm{int}}} \ \text{[electrons/pixel]} \qquad \textbf{Equation 2.13}$$

where i_d is the dark current contribution, RN is the read noise in electrons, N_{reads} is the number of nondestructive samples up the ramp, and t_{int} is the ramp time in seconds.

3. The relationship between photocurrent per pixel and the incident flux density, S_{mJy}, is given by Equation 2.4, except that the slit losses, τ_{slit}, are replaced by the fraction of encircled energy in the assumed beam size, which, for PUI, is larger than the 4 pixels assumed in Equation 2.4. For the nominal

S/N calculations, we assumed a beam size equal to that of a circular aperture containing half the light of a point source.

4. The S/N for a point source is then the ratio of S_{mJy} to N.

Table 2.4 PUI 1σ sensitivity (microJy) for 6/14/30 second ramp times

Filter	LOW background	MEDIUM background	HIGH background
Blue	115 / 75 / 50	145 / 95 / 65	190 / 120 / 80
Red	180 / 115 / 75	220 / 140 / 95	280 / 180 / 120

Chapter 3. Operating Modes

3.1 Staring-Mode Spectroscopy

Staring Mode was the basic "point and shoot" operating mode of the IRS. In this mode, science targets were placed on one or more of the IRS slits for a specified integration time. The IRS Staring Mode AOT could be configured as either Standard (Section 3.1.1) or Peak-Up Only (Section 3.1.2).

The SPICE and SMART tools were designed to reduce data obtained in Staring Mode.

3.1.1   Standard Staring Mode

In Standard Staring Mode, the observer selected from one of four ramp durations, and also the number of cycles of that ramp duration to be performed. The ramp duration is the time between the first and last non-destructive reads of the array, and corresponds to the "effective exposure time." The shortest ramp duration for all of the slits was six seconds. The longest ramp duration for the slits varies from 120 seconds to 480 seconds, depending upon the module. The ramp durations were chosen to provide the highest dynamic range, while minimizing the number of routine calibrations required in orbit. The IRS SL and LL modules reach background-limited performance in about 40 seconds and about 10 seconds, respectively. Longer ramp durations have smaller overhead times but may have been affected more severely by cosmic ray hits. The "cycles" parameter is the number of times a given spectrum was repeated before moving on to the next slit position or the next target. Total "integration time" is determined by both ramp duration and number of cycles.

Standard Staring Mode successively placed the target at the two nominal slit locations for each requested slit, located 1/3 and 2/3 of the way along the length of the slit, to provide redundancy against cosmic rays and detector artifacts. The automatic "nodding" that occurred in Standard Staring Mode means that, for example, the choice of a 480 second ramp for one cycle in SH would produce two spectra, with each having an exposure time of 480 seconds, yielding a total on-source integration time of 960 seconds. The same exposure time with two cycles would produce four 480-second exposures, for a total on-source integration time of 1920 seconds.

Since the IRS slits are relatively narrow compared to the nominal pointing accuracy of the Observatory, it was often necessary to perform a peak-up acquisition (PUA) before starting a spectroscopic integration in order to achieve a given photometric accuracy (or even ensure that the target was in the slit). Furthermore, a peak-up allowed an observer to obtain a spectrum of a source even if its coordinates were not precisely known - as long as it is known to be bright enough for the peak-up to function properly.

There were three peak-up options available: IRS Peak-Up, PCRS Peak-Up, and No Peak-Up.

3.1.1.1 IRS Peak-Up

The IRS Peak-Up option used software resident in the Combined Electronics to accurately find a target on one of the two IRS peak-up fields-of-view (blue or red) that share the SL detector array. The position determined for the peak-up target was then used to offset the science target to one of the IRS slits. An IRS peak-up could be performed on either the spectroscopic target itself, or a nearby (< 30 arcmin) object whose offset from the science target is accurately known.

The onboard peak-up algorithm measures the centroid of the brightest source in the selected peak-up array field-of-view. It performs two measurements. First an "acquisition" centroid (ACQ) is measured at the "blind" pointing of Spitzer. After this, the brightest source is moved to the "sweet spot" (SS) of the selected peak-up array and the centroid (of the brightest source in the field) is measured again. Finally, the SS centroid position of the peak-up target is used to move the science target to the first commanded slit for spectroscopic observations. The exposure number is 0000 for ACQ and 0001 for SS. At each position, three images (DCE numbers 0, 1, 2) are taken and processed onboard to produce the frame that is used by the peak- up algorithm. This fourth, processed frame is always DCE number 3.

In the processed peak-up images, any source that is bright enough for centroiding will be clearly visible. In the ACQ frame, it should be at or near pixel (107,30) for the blue peak-up array and (105,92) for the red peak-up array; for SS, it will be at or near pixel (108,28) or (106,94) for blue or red, respectively. The onboard software considers the center of the lower left corner pixel of the array to be (0,0); that is, pixel centers are labeled with integers and pixel edges are labeled with half-integers. Beginning in IRS25 the PU window has been trimmed to 24x24 pixels.

The FITS headers of the peak-up images contain information about the operation of the telescope and the peak-up algorithm (see below). The data in each FITS file shows the combination of the three individual exposures. The onboard processing includes cosmic ray rejection, flat-fielding, and background subtraction. The data are in units of DN (Data Number).

The world coordinate system (WCS) for the peak-up images is provided in the FITS header. The red and blue peak-up arrays share a common WCS. The WCS is described in the system CTYPE1 = 'RA---TAN-SIP' and CTYPE2 = DEC—TAN-SIP', not 'RA—TAN' and 'DEC—TAN'. This system is the same as that used for IRAC and MIPS images, and includes non-linear distortion terms. In particular, image viewers like DS9, GAIA, and ATV used to display the full SL and peak-up images will give coordinates valid for the peak-up imaging fields of view.

If the peak-up algorithm does not find a valid centroid, then it will report a failure. In the peak-up images, particularly the processed DCE (see above), there will be no visible source. You can also identify these failures from the FITS header by looking at the value of the "PU centroid quality code," which is 0 for a failure and 1 for a success.

The peak-up algorithm can also result in a false positive. In this case, the peak-up software centroids on something other than the intended target and reports a success. You can look at the peak-up images to see if your intended source is at the centroid position reported in the header. The value of the centroid is given in the AXCNTRD1 and AYCNTRD1 keywords; note that these values are given in centipixels, so must

be divided by 100.0 in order to compare with pixel coordinates in the peak-up images. In addition, the value of the PTGDIFF keyword in the header gives the difference in arcseconds between the requested and reconstructed pointing. This value is almost always less than 1 arcsecond, which indicates that the intended coordinates were placed on either the acquisition or sweet spot.

3.1.1.2   PCRS Peak-Up

The second peak-up target acquisition option was PCRS Peak-Up. This choice selected the Pointing Calibration and Reference Sensor (PCRS) as the peak-up instrument. The PCRS operated in the visual part of the spectrum (from 5050-5950 Angstroms) and its main function was to calibrate and remove the drift between the star trackers and the telescope. The field-of-view for the PCRS is 40x40 arcsec^2, comprised of a 4x4 array of 10 arcsec pixels. Consequently, the PCRS functioned more like a "quad cell" centroiding device than a standard CCD that adequately samples the PSF. The PCRS could measure the centroid of stars in the 7.0 mag < V < 10 mag range to an accuracy of 0.14 pixels (1 sigma radial). The observer had the choice of peaking up on either the science target itself or an offset star.

The primary reference catalog for the PCRS was the PCRS Guide Star Catalog, which contains a carefully-selected subset of stars from the Tycho catalog.

3.1.1.3   No Peak-Up

The third peak-up target acquisition option is No Peak-Up. In this case, the telescope slewed to the observer-specified science target position without refining the pointing accuracy, waited for the nominal settling time, and began the spectroscopic observations. Positional uncertainty in this case is the nominal pointing accuracy of Spitzer, 1.0 arcsec.

3.1.2   Peak-Up Only Staring Mode

The Peak-Up Only observation type was intended to provide "early target acquisition" functionality to the IRS Standard Staring mode. In a Peak-Up Only observation, the peak-up algorithm was run in its normal fashion to acquire the science target but no spectroscopic data were taken. Peak-Up Only was intended to test the peak-up algorithm, not to obtain science images, which could be accomplished with the Peak-Up Imaging AOT (Section 3.3). Testing the algorithm was useful in cases where long spectroscopic observations were needed but no obvious peak-up target presented itself from other ground-based or space-based data, so it was desirable to confirm the success of the peak-up before exposing the spectrum. The peak-up images and the position of the target selected by the software were sent to the ground in this mode. Since the peak-up software ran its normal course, the overheads (including the initial slew overhead and the settling times within the peak-up process) were significant. In addition, the peak-up itself would have had to be repeated in conjunction with the actual spectroscopic exposure. The DCS images obtained during a Peak-Up Only observation were dark-current-subtracted, cleaned of cosmic rays, and flat-fielded on-board and these images are available in the Spitzer Heritage Archive (all of which was done for all Peak-Up data).

3.2 Mapping-Mode Spectroscopy

The Spectral Mapping AOT allowed an observer to configure a grid of map positions around a central target position and obtain spectra at each position. The observer specified the desired slits, each with different ramp durations and cycles, for single or cluster targets. The telescope was moved in a direction perpendicular to the long axis of the slit for the desired number of steps before moving parallel to the slit for the desired number of steps. By default, each map position produced a single ramp (unlike Staring Mode, described in Section 3.1, which automatically obtained spectra at two nod positions along the slit). However, the observer could set a larger number of ramp cycles to be obtained at each map position or repeat the entire mapping sequence multiple times. The individual pointings were arranged so that the science target defined the center of the map. The orientation of the map on the sky was determined by the date and time of observation.

The observer could choose any combination of IRS slits in Spectral Mapping Mode. For example, if the "Low 5.2-8.7" and "Low 7.4-14.5" options were selected, then you will get two maps, one centered on the 2nd order SL slit and one centered on the 1st order SL slit. In this case there would have been many extraneous spectra taken in both orders since there is only one physical SL slit (so spectra were always obtained in both orders - with one order offset from the target coordinates - even when only the 1st or 2nd order subslit was selected). In addition, for efficient mapping of extended sources, there were two more module choices in Spectral Mapping mode: Low Short Both and Low Long Both. These used the vignetted region between the subslits of the indicated modules as the reference point, rather than the center position along each subslit. If maps were desired in both 1st and 2nd orders, this option offered a significant savings in time over mapping in each subslit separately. Regardless of which module was selected, the observer must have specified the step size in arcseconds and the number of steps for each leg of the map. When observing a cluster with more than one slit in Spectral Mapping Mode, all targets were observed first in one slit, then all targets were observed in the second slit, and so on. This yielded better control of the pointing accuracy while observing in the narrow slits, and reduced the overhead necessary to switch from one IRS module to the next.

The observer could choose to map a given target (or cluster of targets) more than once using the "Number of Map Cycles" parameter. This invoked a peak-up (if requested), repositioned the telescope to the beginning of the first map leg of the first target, and repeated the entire map, starting with the narrowest slit requested. Mapping large areas did not typically require high pointing accuracy, but observers were reminded that the telescope pointing suffered random positional offsets of order 0.2 arcsec for every commanded movement of the telescope. Spectral mapping of multiple sources with multiple slits had the potential to generate a very large number of telescope movements, with significant associated AOR duration overheads if high positional accuracy was requested. When peak-up target acquisitions were requested, they were carried out only once per map cycle and, as noted above, only at the beginning of each map cycle of cluster targets. For example, a request for high-accuracy peak-ups for three multi-slit spectral maps of 20 cluster targets would have yielded a total of three peak-ups during the course of the AOR.

The CUBISM tool was designed to reconstruct and extract full spectral cubes from spectral mapping data sets.

3.3 Peak-up Imaging (PUI)

The IRS peak-up arrays provided science-quality imaging capability in the wavelength range that falls between that covered by IRAC and MIPS, and as such were of interest for imaging alone. For Cycle 2, a new AOT was made available to allow Peak-Up Imaging (PUI) observations. Both a red (18.5-26.0 micron) and a blue (13.3-18.7 micron) filter were available. The red filter provided images over a similar wavelength window as the MIPS 24 micron mode. Information regarding the field-of-view, distortion, and WCS for PUI are provided in Section 2.7.

The peak-up apertures were imaged onto the IRS SL detector array. A read-out of the array therefore also yielded SL1 and SL2 spectra at parallel locations on the sky. The locations of the slits were determined by the orientation of the telescope, which depended on the date of observation. Nonetheless, science quality spectra were obtained. The similarity in PUI and spectroscopic data reduction procedures ensured that the observer received fully calibrated 2D spectra along with the imaging data. Unlike peak-up images taken for the purpose of aligning objects in the slit for spectroscopy, the PUI mode produces science-quality data obtained in the sample-up-the-ramp (SUR) readout, as described in Section 2.9.3.3.

Chapter 4. Calibration

4.1 Spectroscopic Calibration

4.1.1   Dark frames

Since the IRS has no internal shutter, reference frames are not truly dark. Reference spectra were collected at the ecliptic poles, or near the target if the local background is significantly different from the high latitude zodiacal sky. However, each array has areas that are not directly illuminated by the optics. These areas were also used to monitor dark current performance.

4.1.2   Flat fields

Ideally, spectral flats should be constructed from observations of a spatially and spectrally flat source that is bright enough to achieve a good signal-to-noise ratio but not bright enough to saturate the arrays. In practice, this ideal source does not exist. Therefore, the IRS flats were created by stepping a standard star (with a smooth, well-known spectrum) through each slit to simulate an extended source. These observations were then combined to simulate an extended source. A model of this extended source was created by combining one-dimensional spectral models. A protoflat was produced by dividing the simulated extended source by the modeled extended source. Finally, the non-uniform spatial response of the protoflat was corrected using observations of the zodiacal light. The following subsections describe this process in more detail.

4.1.2.1 *Data Used for Spectroscopic Flats*

Table 4.1 Data used to create IRS flats

	SL	SH	LL pre-45*	LL post-44*	LH pre-25**	LH post-24**
standard star	HR 7341	HR 6688	HR6606	HR6606	HR6688	HR2491
standard star AORKEY(s)	19324416	13531136	LL1: 13364480 LL2: 13364736	LL1: 24399872 LL2: 24400128	13530368	16101888
steps parallel to slit	57	11	91	91	19	21
parallel step size (arcsec)	1.1	1.1	2.4	2.4	1.3	1.7
steps perpendicular to slit	0	5	0	0	3	15
perpendicular step size (arcsec)	N/A	1.8	N/A	N/A	3.5	1.7
ramp time (seconds)	6	30	14	14	60	6
num cycles	3	2	4	4	2	3
zodiacal background AORKEY(s)	19324928	12604416 13782528 16462848 13782272 13782784 9859072	8243968 9268992 9530880 10020352 10020608	24426240	11810304 11810816 9858560 9859072 11810560 12604416 9858816	16097792 16098048 16098304 16462848
Dedicated sky AORKEY(s)	N/A	13520384 13515776	N/A	N/A	13530880	16088320 16087296

*In campaign 45, there was a bias change to mitigate the increasing number of rogue pixels in the LL module, resulting in different flats for the pre- and post- bias change campaigns.

**In campaign 25, there was a bias change to mitigate the increasing number of rogue pixels in the LH module, resulting in different flats for the pre- and post- bias change campaigns.

4.1.2.2 *Combining Star Observations to Simulate an Extended Source*

In this section, we describe how the stepped standard star observations described in Table 4.1 were combined to simulate an observation of an extended source.

First, the *rsc.fits* (pre-flatfielded) data for the stepped standard star observations were combined. See Figure 4.1 for a LL example.
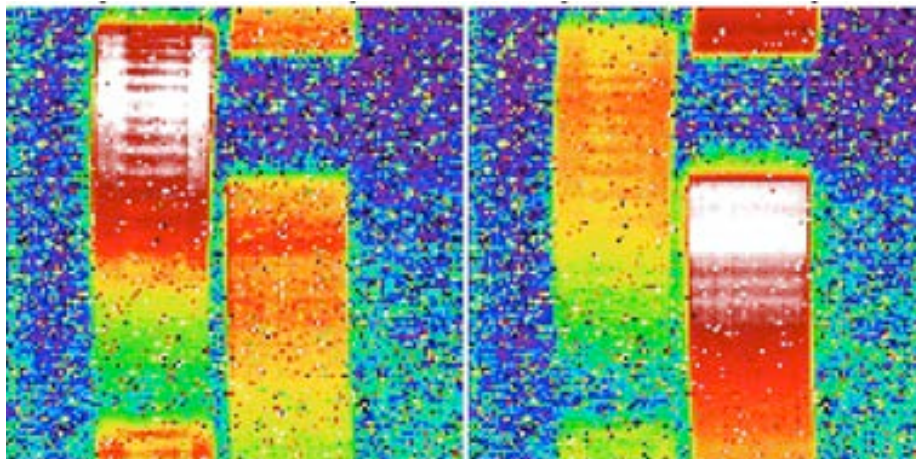
Figure 4.1: An example of the co-added pre-flatfielded data for a stepped standard star in LL1 (left panel) and LL2 & LL3 (right panel) modules.

Second, the background was subtracted from this co-added star data. For the SL and LL modules, the observations were carried out such that several of the slit positions were far from the star. These "edge"-steps in the map were used to estimate the background. The mean of these data was subtracted from the mean of the co-added star data. For the SH and LH modules, dedicated background AORs were used to estimate a mean and median background. Depending on the quality of the data, the mean or the median was adopted as a background image, which was then subtracted from the mean star-only data.

Third, if the star was stepped through the different orders separately (i.e. SL and LL), each of these orders was cut and pasted together to make a combined image. An example of the result of performing all of these steps for LL is shown in Figure 4.2.
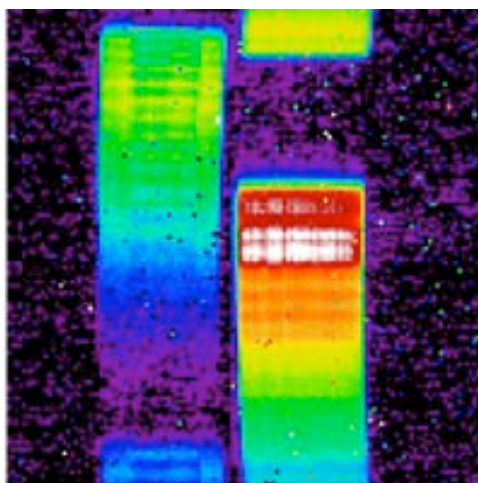
Figure 4.2: LL1 and LL2 co-added stellar data combined.

4.1.2.3   Create a model of the stepped-star observations

The next step was to take a one dimensional model spectrum of the star and create a two dimensional fits file as if the source were spatially extended and filled the slit. The wavsamp and omask were used to obtain the correct model. The wavsamp table contains the translation from the pixel coordinates to wavelength. A given wavelength for IRS is indicated by a tilted rectangle, often called a "pseudo"-rectangle. There is also a *wavsamp.fits* file which shows the two dimensional translation of the *wavsamp.tbl* file for the different modules. The omask file shows where the orders of a given module are present in the two dimensional data. It is usually used to mask out the inter-order regions. The two dimensional model file is illustrated in Figure 4.3.

Figure 4.3 The model of a stellar spectrum in 2D created by interpolating the 1D spectrum over the wavsamp file.

4.1.2.4   Protoflat

The protoflat (which is a flat that has not yet been corrected using zodiacal light observations) was created by the following procedure.

1. The simulated two dimensional extended source from Section 4.1.2.2 was divided by the modeled two dimensional extended source from Section 4.1.2.3.

2. This resulting file was normalized by dividing it by the median value calculated from all the finite data in the FITS file.

3. Rogue pixels were removed and replaced using IRSCLEAN.

Figure 4.4 illustrates the results for the LL module.

Figure 4.4 The LL protoflat.

4.1.2.5   Create an initial cmask.

The purpose of the cmask is to indicate where the flat is valid, uncertain, or invalid. All the regions outside the wavsamp are obviously invalid but in general the wavsamps are conservative. The actual spatial area that is imaged by the spectrograph is slightly larger, especially for the high-res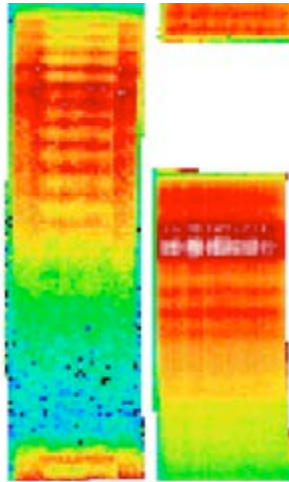olution modules. Of course, the sensitivity of the spectrograph falls off from the center of each order so the edges are highly uncertain. Since the area exposed to the sky by the array is larger (by ~5%) than the wavsamps, slightly larger wavsamps than the ones employed by SPICE were used. These were interpolated to be ~5-10% wider than the narrower wavsamps from which the spectra were extracted. As a first step in making the cmask, all the area outside this wavsamp was set to be invalid (bit 7). In other words, all the inter-order regions were set to 128. All the pixels within the order were set to 0.

To determine the "uncertain" flat pixels, the maximum value in each order was taken. All pixels less than 0.001 of the maximum in the flat were assumed to be regions where the flat is uncertain, and were set to bit 8, or a value of 256. This picked up most of the edges of the wavsamps. However, in the cases of LL and LH, the array efficiency drops sharply at the longer wavelengths and hence these modules have many more uncertain flat pixels towards longer wavelengths.

After an initial automated masking, the cmask was examined interactively to mask out pixels that the automated procedure missed. Narrowing the cmask too much reduced the signal and introduced tilts in the spectrum, especially for extended sources. However, keeping the cmask too broad, i.e. allowing many edge pixels to be counted as valid, led to noisier spectra. For the peculiar case of LL where the uncertain pixels form a band towards the long wavelengths, we usually declared most pixels longwards of 37 microns as uncertain. The interactive flagging of the cmask was done iteratively, based on experiments with real data of standard stars. If the derived flat introduced any spikes in the final spectrum, these pixels were flagged in the cmask. In addition, the width of the cmask was set to minimize the noise in the extracted spectra. For the high-resolution modules, this step was done carefully for each of the 10 orders. Figure 4.5 shows a typical cmask resulting from this iterative process.

Figure 4.5 A cmask for the LL-PRE25 data. The pixels marked white are the ones labeled uncertain by our process.

4.1.2.6   Correction for spatial variations

Since there are real (endemic to the array) and artificial (introduced by the discrete stepping of the star through the slit) spatial variations in the protoflat, we removed these variations by using a truly extended flat source, the zodiacal background. The basic process involved co-adding a large number of zodiacal background observations, cleaning this product with IRSCLEAN, and dividing the protoflat by the cleaned, co-added zodiacal background. The result provides a measure of the spatial variations in the protoflat, and is used to derive a correction for these variations. This spatial correction is then multiplied back into the protoflat to create the final flat. The LL spatial correction is shown in Figure 4.6. This spatial correction step does introduce a slight spectral slope (which was previously taken out by the model) but any residual slopes are removed in the fluxcon step later on in the pipeline. The final flat is shown in Figure 4.7. The right-hand panel shows a check to ensure a spatially flat image, which is done by again dividing the zodiacal background by the final flat.
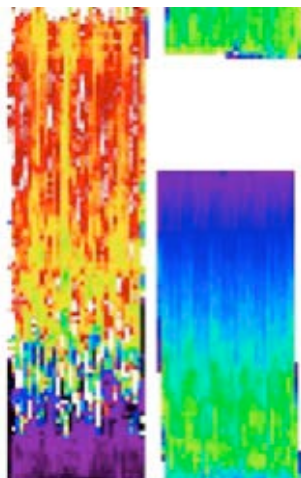
Figure 4.6 The spatial correction for the LL example, generated by taking a running 5-row average of the protoflat / zodiacal background file. Multiplying this back into the flat gives us the final flat.
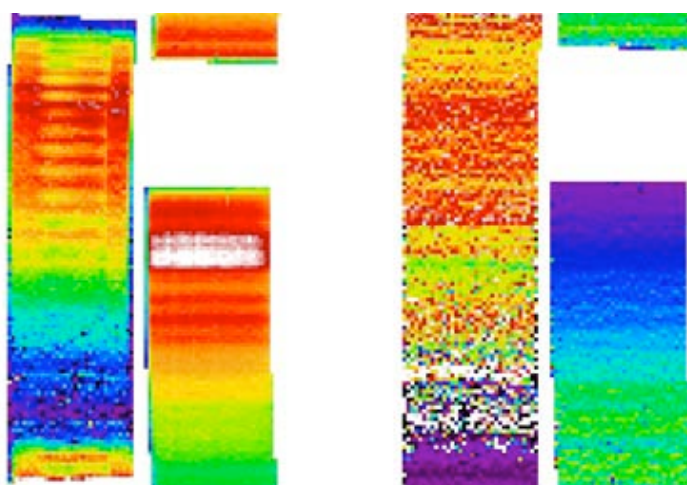
Figure 4.7 *Left*: **The final flat for LL.** *Right*: **The zodiacal background divided by the final flat, as a check to ensure a spatially flat image.**

4.1.3 Wavelength Calibration

Wavelength calibrations are built up primarily from observations of P Cyg, J900, PN M 1-42, NGC3242, NGC6720, NGC6781 for the high-resolution modules; and PN M 1-42, NGC7293, NGC6781, NGC7027, G333.9+00.6, and NGC6543 for the low-resolution modules. The lines used for each module are listed in Table 4.2.

Table 4.2 Lines used for Wavelength Calibration

SL	SH	LL	LH
[Mg V] 5.610 H_2 S(5) 6.910 [Ar II] 6.985 [Na III] 7.318 H I (6-5) 7.460 [Ar III] 8.991 H_2 S(3) 9.665 [S IV] 10.511 [Ne II] 12.814	[S IV] 10.510 [Ne II] 12.814 [Ar V] 13.102 [Ne V] 14.322 [Ne III] 15.555 [S III] 18.713	[Ne III] 15.555 H_2 S(1) 17.035 [Fe II] 17.936 [S III] 18.713 [Fe III] 22.925 [Ne V] 24.322 [O IV] 25.890 [S III] 33.481 [Si II] 34.815 [Ne III] 36.014	[Fe II] 19.058 [Cl IV] 20.311 [Ar III] 21.830 [Fe III] 22.925 H I (10-13) 22.331 [Ne V] 24.318 [Fe II] 24.519 [O IV] 25.890 [Fe II] 25.988 H I (9-8) 27.803 H I (10-12) 29.840 [Fe III] 33.038 [S III] 33.481 [Si II] 34.815 [Fe II] 35.349 [Ne III] 36.014

Bright extragalactic line measurements have also proven essential to adjusting the calibration in spectral regions that do not include bright Galactic lines. The SH calibration has been further refined by using observations of Titan.

The IRS wavelength calibration is generally good to approximately 1/5 of a resolution element. Table 4.3 lists the root mean square (RMS) wavelength residuals for the lines used in the calibration. For spectral regions that are not well-covered by calibration lines, larger errors are possible. The high-resolution RMS values are averaged over all orders. To transform to per-pixel values, users should remember that the unresolved line width is always assumed to be 2 pixels.

The spacecraft velocity ranged from ±30 km/s. Observers who care about this level of precision in their wavelength calibration can add the values of the keywords VHELCORR or VLSRCORR to the spectroscopically determined velocities, in order to obtain final velocities in the Heliocentric or LSR frames, respectively.

Table 4.3: IRS Wavelength Calibration.

Module	RMS residuals of wavelength calibration lines (micron)
SL1	0.013
SL2	0.008
SL3	0.007
LL1	0.024
LL2	0.009
LL3	0.028
SH	0.001
LH	0.002

Some orders were difficult to cover with spectral lines from calibration sources (e.g., SH order 14) and the wavelength solutions for these have been updated by referencing nearby galaxies with accurate recessional velocities and strong lines.

It should also be emphasized that a pointing offset could cause a shift in the wavelength of a line. For example, a 0.5 pixel offset (due to pointing error or incorrect coordinates) in the position of a source within the slit could shift the wavelengths of that observation by a few tenths of a pixel.

We have measured the variation of spectral resolution with wavelength for the different modules. For the SH and LH modules, the resolution is constant at R~600 with wavelength. For the SL and LL modules, the resolution varies from the blue end of the spectrum to the red end as shown in
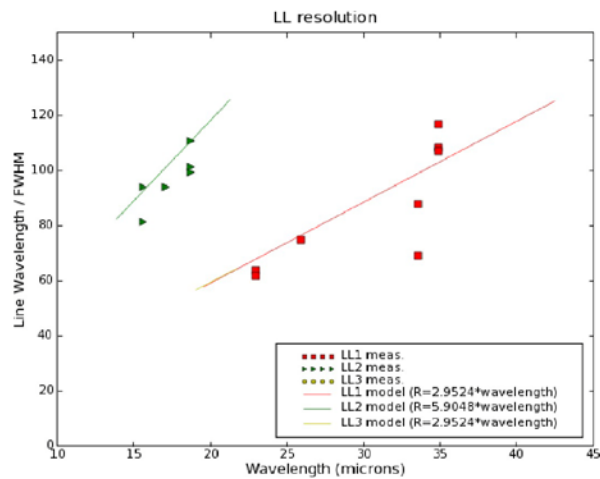
Figure 4.8 and Figure 4.9.

Figure 4.8 Measured LL resolution. The scatter is due to PSF undersampling and pointing errors.
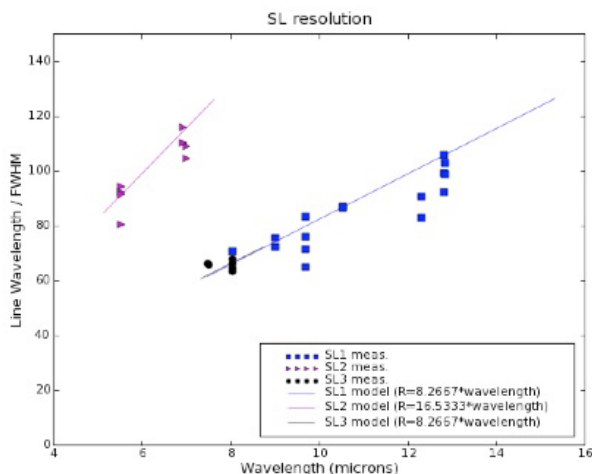
Figure 4.9 Measured SL resolution.

4.1.4 *Spectrophotometric Calibration for Point-Sources*

This section describes the basic steps used to derive the flux calibration for point sources. It also serves as a guide for deriving your own flux calibration. For example, if you want to extract a point-source spectrum with an aperture that is not the default one, the calibration provided in e.g. SPICE will not be valid. This means that the translation from instrumental units (electrons/sec) to Jy will be incorrect. The default aperture is the full-slit for the high-resolution modules and a tapered aperture for the low-resolution modules. To use a non-default aperture, you will need to perform your own spectrophotometric calibration. Here is how to do it:

1. Download Post-BCD products for staring observations of standard stars (from Campaign 18 onward). The primary calibrator for the low-resolution modules is HR 7341, while that for the high-resolution modules is HR 6688 (ksi Draconis). For every high-resolution observation of HR 6688 AOR there will be another AOR observing the nearby sky. You will need to download that too.

Be aware that the bias voltage for the LL module changed in Campaign 45, while the bias for the LH module changed in Campaign 25. To do your own calibration, use only stars that have been observed with the same bias as your target. For example, if you are interested in LH observations performed in Campaign 30, you will need to download all the observations of HR 6688 from Campaign 25 onwards.

The pointing scheme of the telescope was substantially improved after campaign 17 (3-15 Jan 05). Some observations performed before campaign 18, but calibrated with later pipeline versions, will show significant order mismatches.

Table 4.4 AORs used to calibrate S18.18 SL data, PRE-33 campaigns.

Campaign	AOR
21	13734400 13776384
22	15333376 15339520
24	15877120
25	16089856 16094464 16096768
26	16293888 16344064
27	16460800 16477184
31	17208832 17209856 17210368 17210880 17211392 17211904
32	19318528 19319808 19388416 19438080

Table 4.5 AORs used to calibrate S18.18 SL data, POST-32 campaigns.

Campaign	AOR
33	19507456 19508992
34	20075264 20138496 20139008 20139520 20140032 20140544
35	20566016 20592640 20593152 20593664
36	20694016 20702208
37	20926464 20957184
41	22161664 22165760
42	23727616
43	23997696
44	24236800 24240896

45	24378880
	24380416
	24381952
	24383488
	24385024
	24386560
	24388096
	24389632
	24391168
	24392704
	24394240
	24395776
	24399360
	24401664
46	24573184
	24573696
	24573952
	24574464
	24575488
	24576000
51	27383552
	27391488
	27392768
52	27752960
53	27954176
	27955712
54	28112896
55	28349440
	28418304
56	28576000
57	28709632
	28711424

Table 4.6 AORs used to calibrate S18.18 LL data, PRE-45 campaigns.

Campaign	AOR
21	13734400
	13776384
22	15333376
	15339520
24	15877120
25	16089856
	16094464
	16096768
26	16293888
	16344064
27	16460800
	16477184

31	17208832
	17209856
	17210368
	17210880
	17211392
	17211904
32	19318528
	19319808
	19388416
	19438080
33	19507456
	19508992
34	20075264
	20138496
	20139008
	20139520
	20140032
	2014054
35	20566016
	20592640
	20593152
	20593664
36	20694016
	20702208
37	20926464
	20957184
41	22161664
	22165760
42	23727616
43	23997696
44	24236800
	24240896

Table 4.7 AORs used to calibrate S18.18 LL data, POST-44 campaigns.

Campaign	AOR
45	24378880
	24380416
	24381952
	24383488
	24385024
	24386560
	24388096
	24389632
	24391168
	24392704
	24394240
	24395776
	24399360
	24401664
46	24573184
	24573696
	24573952
	24574464
	24575488
	24576000

51	27383552 27391488 27392768
52	27752960
53	27954176 27955712
54	28112896
55	28349440 28418304
56	28576000
57	28709632 28711424

Table 4.8 AORs used to calibrate S18.18 SH data, all campaigns.

Campaign	Object, Sky
18	13195008,13196544
19	13349632,13352192 13352960,13354496
20	13513984,13515776 13518592,13520384
21	13732864,13733120 13774848,13775104
22	15334144,15334400 15340288,15340544
23	15669504,15669760 15708160,15708416 15708928,15709184
24	15881216,15881472 15883008,15883264
25	16088832,16089088 16093440,16093696 16095744,16096000
26	16338432,16338688 16338944,16339200 16339456,16339712 16339968,16340224
29	16912128,16912384 16914432,16914688 16919040,16919296
30	17079040,17079296 17081088,17081344
31	17202176,17202432 17205760,17206016
32	19320320,19320576 19438592,19438848
33	19512320,19512576 19513088,19513344 19513856,19514112
34	20074240,20074496 20136448,20136704

35	20566528,20566784
36	20694528,20694784 20702720,20702976
39	21249536,21249792 21260288,21260544 21262592,21262848
40	21455616,21455872 21488896,21489152
41	22159616,22159872 22163712,22163968
42	23725056,23725312
43	23995392,23995648
44	24235264,24235520 24239360,24239616
45	24374272,24374528
46	24569856,24570112
49	25082368,25082624* 25085184,25085440*
50	27018240,27018496 27037440,27037696
51	27380736,27380992
52	27748864,27749120
53	27956224,27956480 27954688,27954944
54	28113408,28123904 28123648,28113664
55	28350976,28351232 28419840,28420096
56	28574976,28575232
57	28710400,28710656 28708608,28708864
60	32515072,32515328 33252864,33253120
61	33772800,33773056

(*) Not used in S18.18 calibration.

Table 4.9 AORs used to calibrate S18.18 LH data, PRE-25 campaigns.

Campaign	Object, Sky
18	13195008,13196544
19	13349632,13352192 13352960,13354496

20	13513984,13515776 13518592,13520384
21	13732864,13733120 13774848,13775104
22	15334144,15334400 15340288,15340544
23	15669504,15669760 15708160,15708416 15708928,15709184
24	15881216,15881472 15883008,15883264

Table 4.10 AORs used to calibrate S18.18 LH data, POST-24 campaigns.

Campaign	Object, Sky
25	16088832,16089088 16093440,16093696 16095744,16096000
26	16294400,16294656 16338432,16338688 16338944,16339200 16339456,16339712 16339968,16340224
29	16912128,16912384 16914432,16914688 16919040,16919296
30	17079040,17079296 17081088,17081344
31	17202176,17202432 17205760,17206016
32	19320320,19320576 19438592,19438848
33	19512320,19512576 19513088,19513344 19513856,19514112
34	20074240,20074496 20136448,20136704
35	20566528,20566784 20694528,20694784
36	20694528,20694784 20702720,20702976
39	21249536,21249792 21260288,21260544 21262592,21262848
40	21455616,21455872 21488896,21489152
41	22159616,22159872 22163712,22163968
42	23725056,23725312
43	23995392,23995648
44	24235264,24235520 24239360,24239616
45	24374272,24374528

46	24569856,24570112
49	25082368,25082624* 25085184,25085440*
50	27018240,27018496 27037440,27037696
51	27380736,27380992
52	27748864,27749120
53	27956224,27956480 27954688,27954944
54	28113408,28123904 28123648,28113664
55	28350976,28351232 28419840,28420096
56	28574976,28575232
57	28710400,28710656 28708608,28708864
60	32515072,32515328 33252864,33253120
61	33772800,33773056

(*) Campaign 49 data not used in S18.18 calibration.

2. Subtract the sky from the standard star observations. For the low-resolution modules, the pipeline provides ready-made sky-subtracted products. The files are called *bksub.fits*, *bmask.fits*, and *bkunc.fits*, and are the result of subtracting nod2 images from nod1 images and vice versa. (For an explanation of these names see Chapter 6). To do something different, start with *coa2d.fits*, *c2mask.fits*, and *c2unc.fits*. For the high-resolution observations, you will always need to subtract the sky by yourself. For each high-resolution AOR, subtract the sky products called *coa2d.fits* from the standard star products of the same name. Add the uncertainty images (*c2unc.fits*) of the sky to those of the standard in quadrature. Perform a logical 'OR' operation between the *c2msk.fits* from the sky and that from the star.

3. Extract your spectra. Start SPICE and run it in batch mode over the sky-subtracted images of your standard star. The setup should be **exactly the same** as in you intend to use for your science target. The SPICE products you will need for the calibration are called **extract.tbl*.

4. Combine all the individual **extract.tbl* files. These files contain the instrumental spectra, in units of electrons/sec. The pipeline uses a clipped median to combine all the spectra, with the uncertainties propagated accordingly. The bit flag values are OR-ed. There are other possibilities: a clipped average has better noise characteristics, for example. Alternatively, one may combine all 2D images for each nod, and then extract a single image.

5. Download a model for the standard star. These can be found at
http://irsa.ipac.caltech.edu/data/SPITZER/docs/irs/calibrationfiles/ .

6. Obtain the polynomial correction. To do so, divide the averaged *extract.tbl* by the model, and fit the result with the lowest-order polynomial possible. The pipeline uses polynomial fits of orders less than 3 for each individual order in each module. These are the 'fluxcons'.

7. Run SPICE on your science data, with the same setup as the calibrations. Obtain *extract.tbl* products.

8. Divide the *extract.tbl* products by the fluxcons. You can make SPICE use your calibrations to tune the spectra, in which case SPICE will take care of this step. Or you can do it in a separate script.

4.1.5 *Spectrophotometric Calibration for Extended Sources*

Extended sources need to be calibrated differently than point sources because the flux fills the slit. In principle, an extended source with a known surface brightness distribution and spectrum should be sufficient to derive the calibration. However such a source does not exist. Sources like the Moon are too bright for the IRS. The zodiacal background is another extended source which might be considered but it is weak and its spectrum and strength are not well known and vary from region to region. Thus an absolute calibration for extended sources is not possible. The best we can do is to derive an approximate calibration to give users an idea of the extent of the correction that may be required. To do this, we describe two correction factors in Sections 4.1.5.1 and 4.1.5.2 below: the Aperture Loss Correction Factor (ALCF) and the Slit Loss Correction Factor (SLCF). Both of these correction factors are built into the extended source capabilities of SPICE, SMART, and CUBISM.

4.1.5.1 *The Aperture Loss Correction Factor (ALCF)*

For an extended source we would like to extract light from the entire aperture. Hence FOR THE LOW RESOLUTION SLITS ONLY we first have to apply a correction for the aperture shape we adopted for point sources. This is called the aperture loss correction factor, or ALCF for short.

The first step in deriving the ALCF is to extract point sources using a flat-sided aperture with a width of 28 pixels. This is slightly smaller than the 32 or 33 pixels for the SL and LL modules and avoids the noise at the edges of the slits. The resulting extraction should be compared to the standard star models and a new fluxcon table should be derived. The ratio of the calibrated flat-aperture and standard extractions estimates the ALCF.

The differences between the flat-aperture and standard extractions are small, less than 10%. Figure 4.10 through Figure 4.17 show the comparison for a bright source in each of the SL and LL orders and at each of the nods. In these figures, the top panel shows the ratio of the extracted spectra in the 28-pixel flat aperture versus the standard expanding aperture. The second panel in each image shows the extracted spectrum with the open circles indicating the extracted signal from the flat-sided 28 pixel aperture. For SL2 and LL2, more light is being lost at the blue end of each order than at the red end. In other words, the change in the PSF is not linear and either the blue end PSF is wider or the red end PSF narrower than would have been expected. Secondly, note that the ratio for SL1 is nearly flat across the entire bandpass (except for the 14 micron bump). This means that the variation of the PSF from red to blue end is linear with wavelength for this slit in these orders. Beyond 35 microns, the signal to noise is extremely poor and therefore the calibration is highly uncertain.
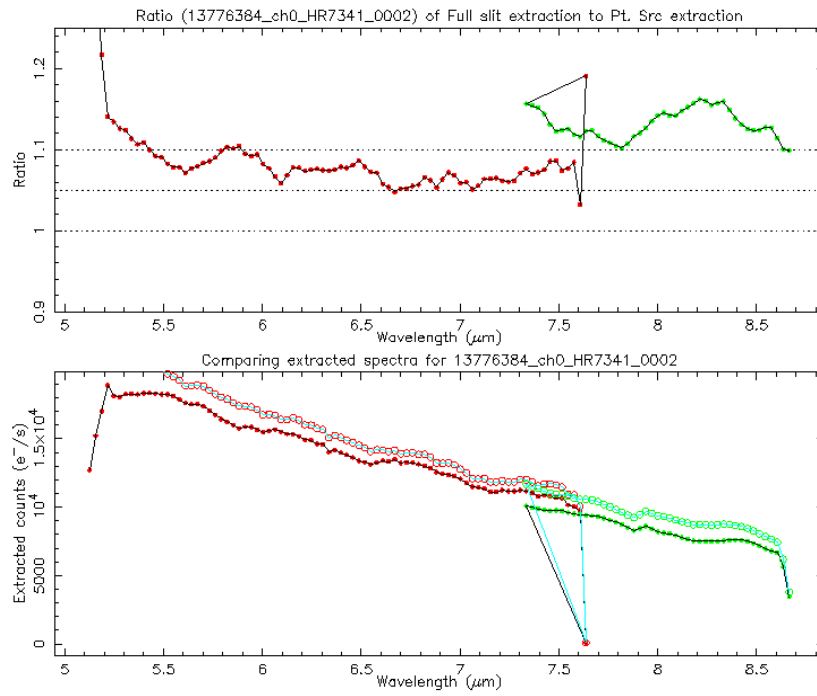
Figure 4.10: Comparison between standard and constant-width extractions for Short Low 2, nod 1.
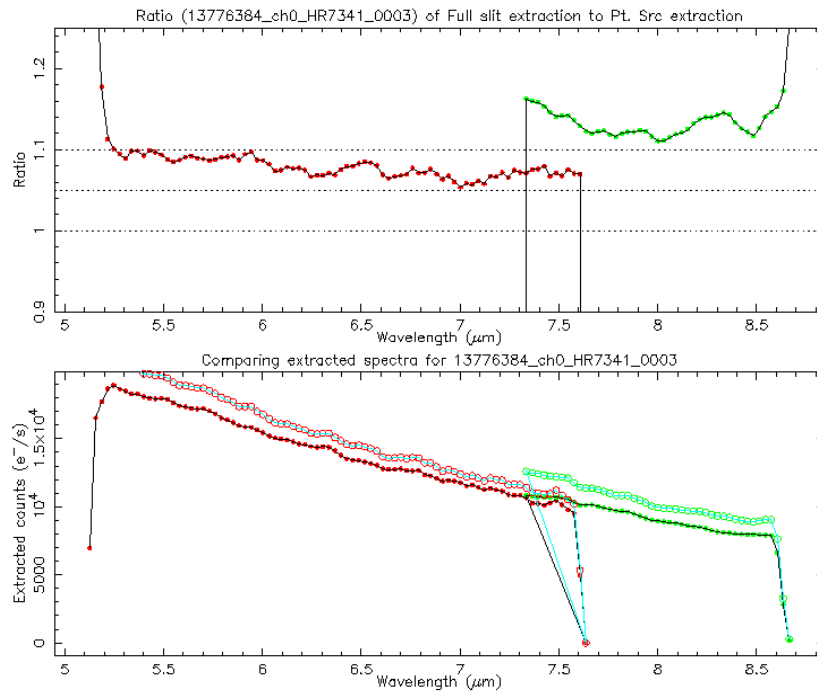
Figure 4.11: Comparison between standard and constant-width extractions for Short Low 2, nod 2.
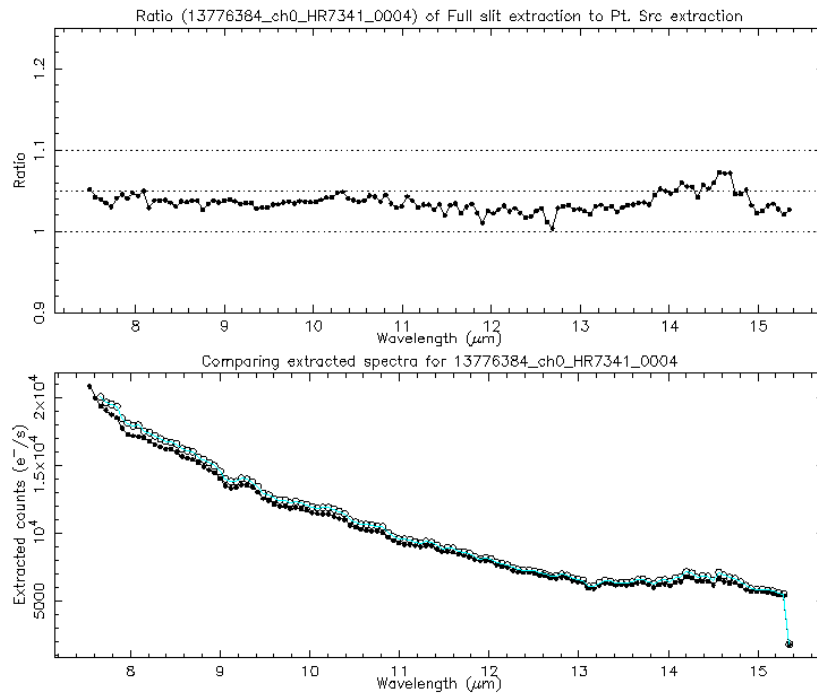

Figure 4.12 Comparison between standard and constant-width extractions for Short Low 1, nod 1.
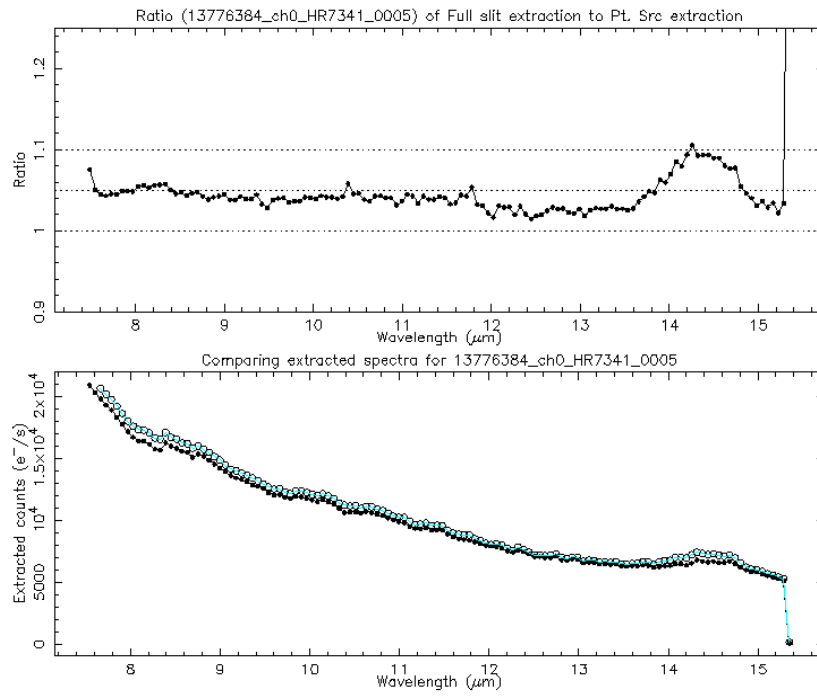
Figure 4.13 Comparison between standard and constant-width extractions for Short Low 1, nod 2.
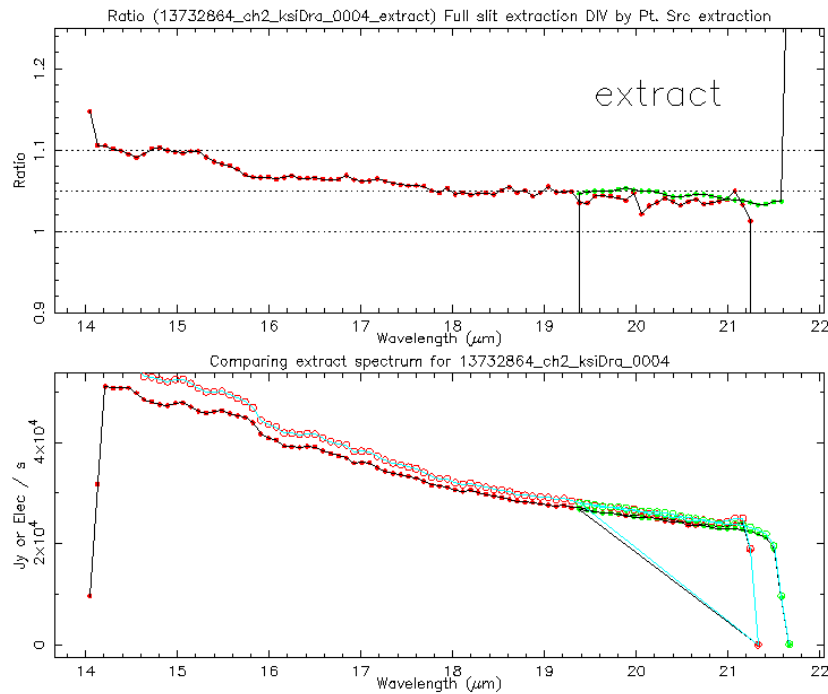

Figure 4.14: Comparison between standard and constant-width extractions for Long Low 2, nod 1.
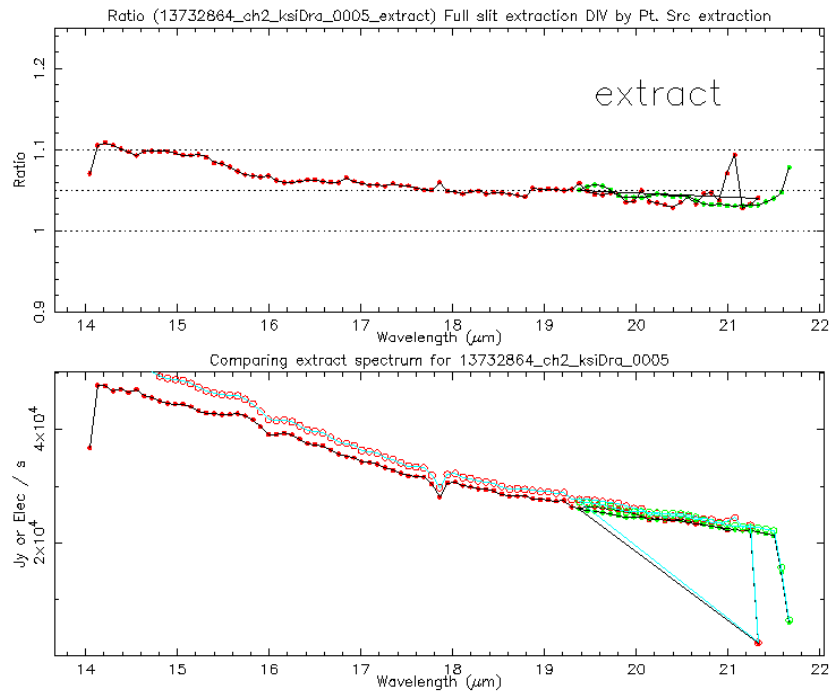
Figure 4.15: Comparison between standard and constant-width extractions for Long Low 2, nod 2.
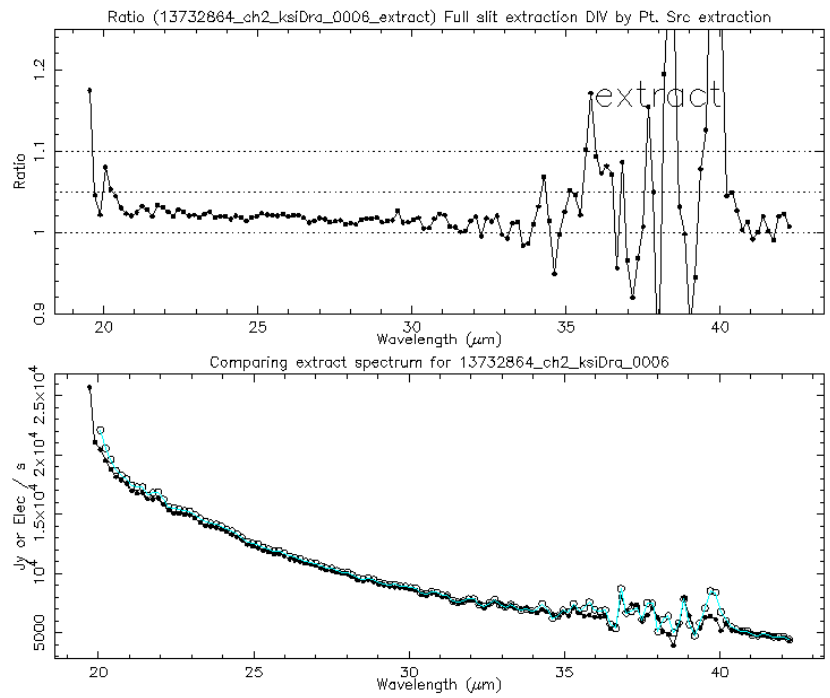

Figure 4.16: Comparison between standard and constant-width extractions for Long Low 1, nod 1.
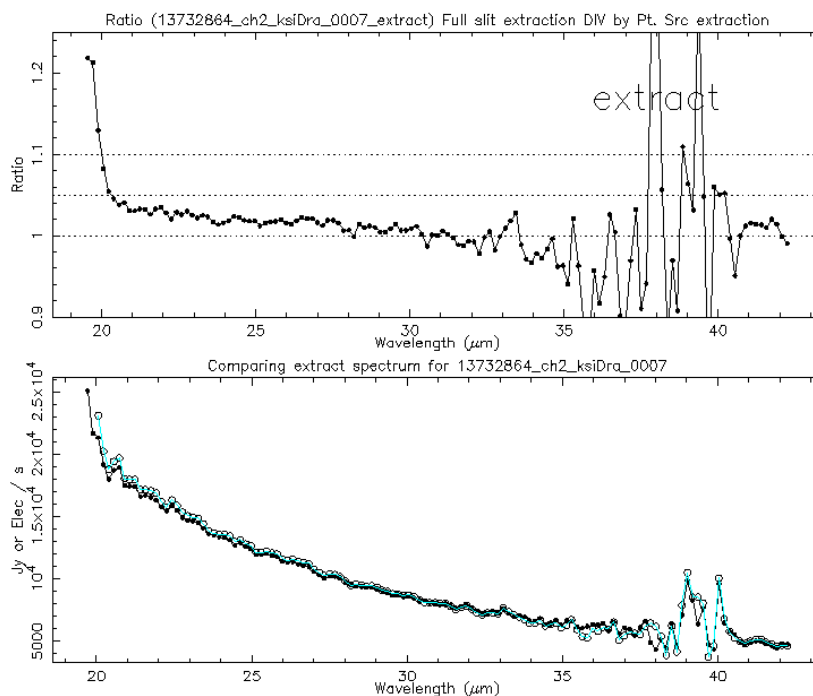
Figure 4.17: Comparison between standard and constant-width extractions for Long Low 1, nod 2.

4.1.5.2 The Slit Loss Correction Factor (SLCF)

The second correction that must be made is much more difficult. It is an estimate of how much light is lost or gained in the slit as a function of wavelength. For a star this correction is IMPLICIT in the calibration because the extracted spectrum is fixed to the model. Hence if we are losing 10% of the light at the blue end and 40% of the light at the red end, we already account for this. For an extended source, however, such corrections for light losses are meaningless because light also enters the slit from outside the slit. In the case of a spatially flat and spectrally flat source, the light losses from the slit should EXACTLY cancel the light GAINS into the slit and therefore there should be NO correction for slit loss. If one were to apply the standard fluxcon table that we have derived for stars, then the correction for the light loss must therefore be undone.

Note that the term "SLCF" is a misnomer because we are trying to reverse the correction already applied for light losses. But since the term has been in popular use, we continue its use here.

In principle the slit loss correction also depends on the brightness distribution of the source because the observations are a convolution of the beam profile and the source brightness distribution on the sky. But since the source brightness distribution for a given source is not known a priori, our correction can only be based on an approximation. The approximation we make is that the source is spectrally and spatially

flat and it fills the slit uniformly. To recover an unbiased flux, you must multiply by an SLCF which is simply the fraction of the PSF which the slit admits, as a function of wavelength.

4.2 Peak-Up Imaging (PUI) Calibration

The basic data processing steps for PUI are virtually identical to those for spectroscopy on the SL detector. These steps are described in Chapter 5. The sky darks and flatfields are created specifically for PUI but are applied together with the spectroscopy equivalents whenever the SL detector data are processed.

4.2.1 Sky Darks

As with spectroscopic observations, multiple observations of low background regions of the sky are combined into a calibration file to be subtracted, plane-by-plane in the SUR data, from the science observations. While this sky dark calibration is meant primarily to remove the detector bias voltage and the (relatively small) dark current that accumulates during the exposure, sky emission is also subtracted. Dark subtraction removes roughly 14 MJy/sr from the background - the value of the background where the SL darks are measured. However, the zodiacal background is a function of position on the sky and of the time when the data were taken. As a result, many calibrated observations will still have substantial residual sky background. Note that the variation of the zodiacal emission during the year may also result in observations in which the standard calibration will over-subtract the background.

Users whose science interests require accurate zodiacal measurements will need to add the zodiacal emission back into their data. For this purpose, we provide 2D dark images for each exposure time (6, 14, and 30 seconds; http://irsa.ipac.caltech.edu/data/SPITZER/docs/irs/calibrationfiles/peakupimagingdarks/). These dark images were run through the DARKDRIFT module (see Section 5.1.13) to remove jailbars and were flat fielded. Blue and red image cutouts were made, the image cutouts were multiplied by the appropriate zeropoint to convert from electrons/sec to MJy/sr, and the header keywords BUNIT and FLUXCONV were edited to match.

4.2.2 Sky Flats

Flat fields are generated from observations of regions of extended emission (e.g., high zodiacal light background). The flat fields are very uniform over the peak-up array fields of view, with a standard deviation in relative pixel response of about 1.2%.

4.2.3 Point Spread Function (PSF) and Point Response Function (PRF)

The IRS provided a 16 micron PSF FWHM of 3.8 arcseconds and a 22 micron PSF FWHM of 5.3 arcsec. Two dimensional images of the PSFs and their radial profiles are shown in Figure 4.18 and Figure 4.19.
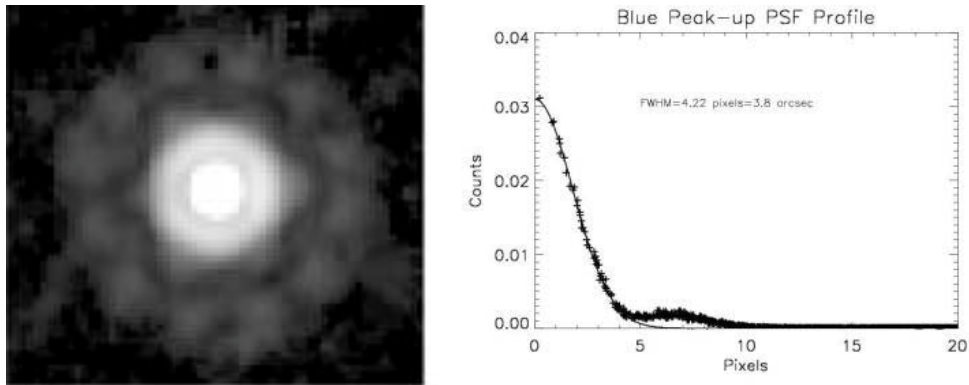
Figure 4.18 *Left*: **A 2D image of the 16 micron PSF, based on observations of the star HD 42525. The relevant data have AORKEYs 17080064 and 17082112, and were mosaicked using MOPEX. The image is approximately 54 arcsec on a side.** *Right*: **A radial profile of the Blue Peak-Up PSF.**
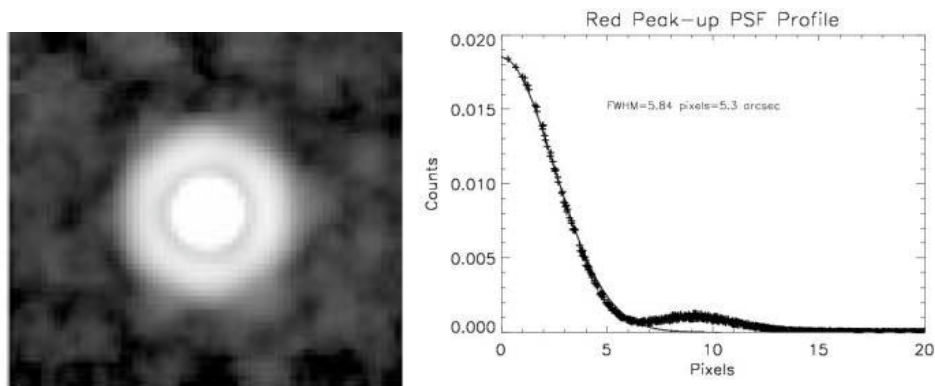

Figure 4.19 *Left*: **A 2D image of the 22 micron PSF, based on observations of the star HD 172728. The relevant data have AORKEYs 20552960 and 20678912, and were mosaicked using MOPEX. The image is approximately 54 arcsec on a side.** *Right*: **A radial profile of the Red Peak-Up PSF.**

A PRF is the convolution of an oversampled PSF with the pixel response function, and is required by the point source extraction module (APEX) within MOPEX to perform PSF fitting. An explanation of the difference between PRFs and PSFs is given in the document PRF vs PSF (PDF, 41 KB).

The SSC developed three different kinds of PRFs, with varying pixel scales and interpolation methods (see the MOPEX User's Guide). Users should choose the PRF that best matches the data reduction technique used to create their mosaics. The choices are:

1. standard pixel scale (1.8 arcsec) and default interpolation

2. resampled pixel scale (0.9 arcsec) and default interpolation

3. resampled pixel scale (0.9 arcsec) and drizzle interpolation

All are available in the IRS Calibration and Analysis Files section of the website, under PSF/PRF.

4.2.4 Photometric Calibration

The PUI calibration is set so that the flux of a point source on zero background measured through an infinite aperture will be correct. In practice, measurements are made with small apertures so these need to be corrected to infinite apertures. Standard star observations were processed by pipeline version S18.18. Aperture photometry was performed in a circular area of 12 and 13 pixel radius for blue and red PUI, respectively. A background value equal to the median in an annulus between 18 and 25 pixels was subtracted. Aperture corrections to infinite aperture were obtained using STinyTim 2.0 (see next section).

True fluxes of the standard stars were obtained from IRS spectra of the stars. An average spectrum was fit with a model and the model was integrated over the PUI bandpasses (to reduce the effect of noise). Thus the PUI magnitude zero-points are tied to that of the spectra. (See Figure 4.20).

A 2% uncertainty is seen between the zeropoints inferred from different standard stars. Observations of the same target are repeatable to 1-sigma 1-2% for both red and blue. A comparison between the MIPS 24 micron calibration and IRS calibration of extragalactic objects was found to be cross-consistent (see Teplitz et al. 2010, Sections 2.2 and 2.3.)

The flux conversion factor from electrons/sec to MJy/sr is 0.0114 (MJy/sr)/(electrons/sec) for blue PUI. For red PUI the factor is 0.0119 (MJy/sr)/(electrons/sec). These flux conversion factors were calculated assuming a source with the following spectral shape:

$$F_\nu \propto \nu^{-1}$$
Equation 4.1

They were pegged to a monochromatic wavelength, at the effective wavelength of each filter, defined as:

$$\nu_{eff} = \left(\int_{\nu_{min}}^{\nu_{max}} R(\nu) \frac{F_\nu(\nu)}{h\nu} \nu d\nu \right) \times \left(\int_{\nu_{min}}^{\nu_{max}} R(\nu) \frac{F_\nu(\nu)}{h\nu} d\nu \right)^{-1}$$
Equation 4.2

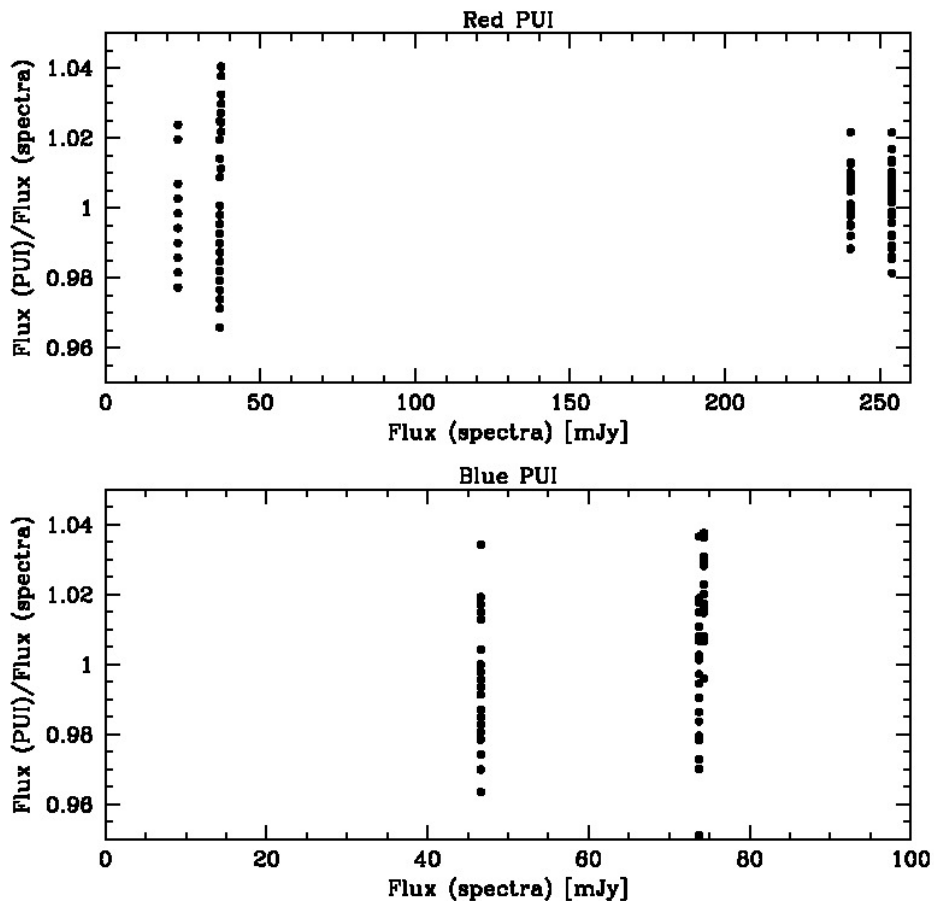Effective wavelength values were 15.8 microns for blue and 22.3 microns for red.

Figure 4.20 Photometric accuracy of the red (top) and blue (bottom) peak-up imaging. PUI fluxes are compared to the fluxes derived from spectra of each star, integrated over the PUI bandpasses. The red PUI calibrators are HD163466 (23.4 mJy), HD172728 (36.9 mJy), HR5467 (37.3 mJy), HD173511 (254 mJy), and HR6348 (240 mJy). The blue PUI calibrators are HD163466 (46.6 mJy), HD172728 (73.7 mJy), and HR5467 (74.3 mJy).

4.2.4.1   Aperture Correction

While PUI calibration assumes that the sources are measured within an infinite aperture, in practice it is often possible to measure them only within a small aperture. Multiplicative point source aperture corrections derived from STINYTIM are given below. PUI observations are diffraction-limited, so these corrections will be different for sources with different colors. In general, the user should derive his or her own aperture correction appropriate for the source of interest.

Table 4.11: Aperture Corrections to Infinity (1.8 arcsec/pix).

Blue			
Blackbody (K)	**3 pixel radius**	**6 pixel radius**	**12 pixel radius**
10000	1.560	1.150	1.077
8000	1.560	1.150	1.077
6000	1.560	1.150	1.077
4000	1.561	1.150	1.077
2000	1.562	1.150	1.077
$\nu F_\nu = \nu^\alpha$			
α	**3 pixel radius**	**6 pix radius**	**12 pix radius**
2	1.573	1.153	1.080
1	1.583	1.154	1.080
0	1.593	1.154	1.081
-1	1.602	1.155	1.081
-2	1.613	1.156	1.083
Red			
Blackbody (K)	**4 pixel radius**	**7 pixel radius**	**13 pixel radius**
10000	1.574	1.148	1.095
8000	1.574	1.148	1.095
6000	1.574	1.148	1.095
4000	1.574	1.148	1.096
2000	1.575	1.148	1.096
$\nu F_\nu = \nu^\alpha$			
α	**4 pix radius**	**7 pix radius**	**13 pix radius**
2	1.582	1.149	1.097
1	1.591	1.150	1.099
0	1.600	1.151	1.101
-1	1.608	1.152	1.102
-2	1.616	1.153	1.103

Derived from STINYTIM

4.2.4.2   Color Correction

For PUI observations, the Spitzer Heritage Archive provides photometrically calibrated data, assuming the source spectrum has the following spectral shape:

$$\nu F_\nu = \lambda F_\lambda = \text{constant} \qquad \textbf{Equation 4.3}$$

The calculations take into account the full spectral response of the instrument. Due to the so-called "Red Leak" (a small increase in response at about 28 microns) some emission will be detected in the Blue Peak-Up for very cold sources that would not have been detected in a system without the red leak. This translates into large correction factors for very cold (T<50 K) sources observed with the blue filter. While

these numbers are formally correct, observers should be very wary of blindly applying them to the data. Longer wavelength observations are advised in this case. To get the peak-up flux for a non-standard spectral shape, divide the flux by the appropriate color correction factor, as given in the tables below.

Table 4.12 Peak-up Imaging Color Corrections for Blackbodies.

T (K)	Blue Peak-Up Color Correction	Red Peak-Up Color Correction
50	6.845	1.558
60	2.800	1.284
70	1.796	1.150
80	1.421	1.078
100	1.145	1.011
120	1.049	0.987
160	0.988	0.976
200	0.976	0.980
240	0.976	0.986
320	0.984	0.997
640	1.010	1.018
1280	1.025	1.029
2560	1.032	1.034
5120	1.036	1.037
10240	1.038	1.038

Table 4.13 Peak-Up Imaging Color Corrections for $F_\nu \propto \nu^\alpha$ or $F_\lambda \propto \lambda^\beta$

α	Blue Color Correction	Red Color Correction	β
-3.0	1.051	1.041	1.0
-2.5	1.031	1.026	0.5
-2.0	1.016	1.013	0.0
-1.5	1.006	1.005	-0.5
-1.0	1.000	1.000	-2.0
-0.5	0.998	0.998	-1.5
0.0	1.000	1.000	-2.0
0.5	1.005	1.005	-2.5
1.0	1.013	1.013	-3.0
1.5	1.025	1.024	-3.5
2.0	1.039	1.039	-4.0
2.5	1.057	1.057	-4.5
3.0	1.078	1.078	-5.0

4.3 Peak-Up Acquisition (PUA) Calibration

Data in the peak-up array can be taken in two modes: as part of the target acquisition observations and as part of the imaging mode observations. These data are taken in Double Correlated Sampling (DCS) and

Sample-Up-the-Ramp (SUR) formats, respectively, and therefore have different calibration parameters. Here we give the approximate calibration for the acquisition mode.

The blue zeropoint calibration stars were HD163466 (47 mJy, 52 AORs), HD172728 (74 mJy, 32 AORs), and HR5467 (74 mJy, 44 AORs). Red zeropoint calibration stars were HD163466 (23 mJy, 26 AORs), HD172728 (37 mJy, 34 AORs), HR5467 (37 mJy, 16 AORs), and 29 Vul (89 mJy, 9 AORs). Each AOR consists of 3 images each at the acquisition position and the sweet spot position. All images have SAMPTIME=1.0486 sec, for a total exposure time of 8.32 sec. The bright PUI calibrators (20 Vul: blue; HD173511 and HR6348: red) were not usable because they were just under the saturation limit for 6 second peak-up imaging observations and thus saturated these 8.32 second peak-up acquisition images.

Four DCS mode darks, referred to as S1, S2, and S4, correspond to SAMPTIME=1.0486, 2.0972, and 4.1944, respectively. S1 was used for sources brighter than 1.4 mJy, S2 for sources between 1 and 1.4 mJy, and S4 for sources between 0.75 and 1 mJy. All calibration stars, and the majority of all peak-up acquisition data, use the S1 dark.

For each AOR, the appropriate DCS mode dark was subtracted from each of the six images. The images were then run through the DARKDRIFT pipeline module to remove jailbar artifacts (see Section 5.1.13). The DCS mode flat was then applied to the data. The three DCEs at the same position (acquisition of sweet spot) were coadded in order to mitigate the effects of cosmic rays. The calibration stars were measured using the same procedure as the PUI data (blue: 12 pixel radius aperture, red: 13 pixels). The aperture measurement was corrected ot infinite radius using the standard aperture corrections. The resulting zeropoints are 0.0115 +/- 0.0003 (MJy/sr)(electron/sec) (blue) and 0.0118 +/- 0.0005 (MJy/sr)(electron/sec) (red). This zeropoint is applied in the PUA pipeline.

The results of this pipeline are the *acqb.fits* and *acqr.fits* calibrated image cutouts in the S18.18 version of the IRS pipeline.

Chapter 5. Pipeline Processing

This chapter describes the basic operation of the IRS pipelines, illustrated as a flow chart in Figure 5.1. The following sections present descriptions of the modules comprising each pipeline: Sections 5.1 and 5.2 describe the BCD pipeline (Figure 5.2). Section 5.4 describes the Dark Calibration pipeline, which provides inputs to the BCD pipeline (Figure 5.9). Sections 5.5, 5.6, and 5.6 describe respectively the Peak-Up Cutouts, Two-Dimensional Coadder, and Background Subtraction pipelines. Section 5.7 describes the Spectral Extraction pipeline (Figure 5.10).

In what follows, an IRS data cube is a FITS file of dimensions $128 \times 128 \times n_{plane}$, where $n_{plane}=4$, 8, or 16 (depending on DCE integration time) for IRS Sample-Up-the-Ramp (SUR) data. The third axis in the cube can be interpreted as the time dimension. Each plane is a non-destructive read-out of the whole IRS array, and each pixel in a plane is referred to as a "sample." A "ramp" is the vector of the 4, 8, or 16 samples of a particular pixel. That is, a "ramp" consists of the non-destructive read-outs of one pixel, ordered by increasing time. The term "read-out channel" in IRS refers to a particular set of columns of the array, consisting of every fourth column. The starting column in this set determines its IRS read-out channel designation. There are four IRS read-out channels: columns 1, 5, 9, etc. comprise IRS read-out channel 1; columns 2, 6, 10, etc. comprise IRS read-out channel 2, and so on.

Figure 5.1 IRS Pipelines Flow chart. The BCD Pipeline is described in Sections 5.1 and 5.2, the Peak-Up Cutouts Pipeline is described in Section 5.4, the Two-Dimensional Coadder Pipeline is described in Section 5.5, the Background Subtraction Pipeline is described in Section 5.6, and the Spectral Extraction Pipeline is described in Section 5.7.

5.1 Description of Modules in the BCD Pipeline

Figure 5.2 shows the flowchart of the BCD pipeline, starting with the module CVTI2R4. The processing flow takes as input the file *raw.fits*, which was created from a MIPL ("Multi-Mission Image Processing Laboratory") file produced at JPL. MIPL files contain a complete telemetry record of the observation. The file *raw.fits* is a MIPL file whose header has been processed by the module TRANHEAD to a more compact, more readable format.
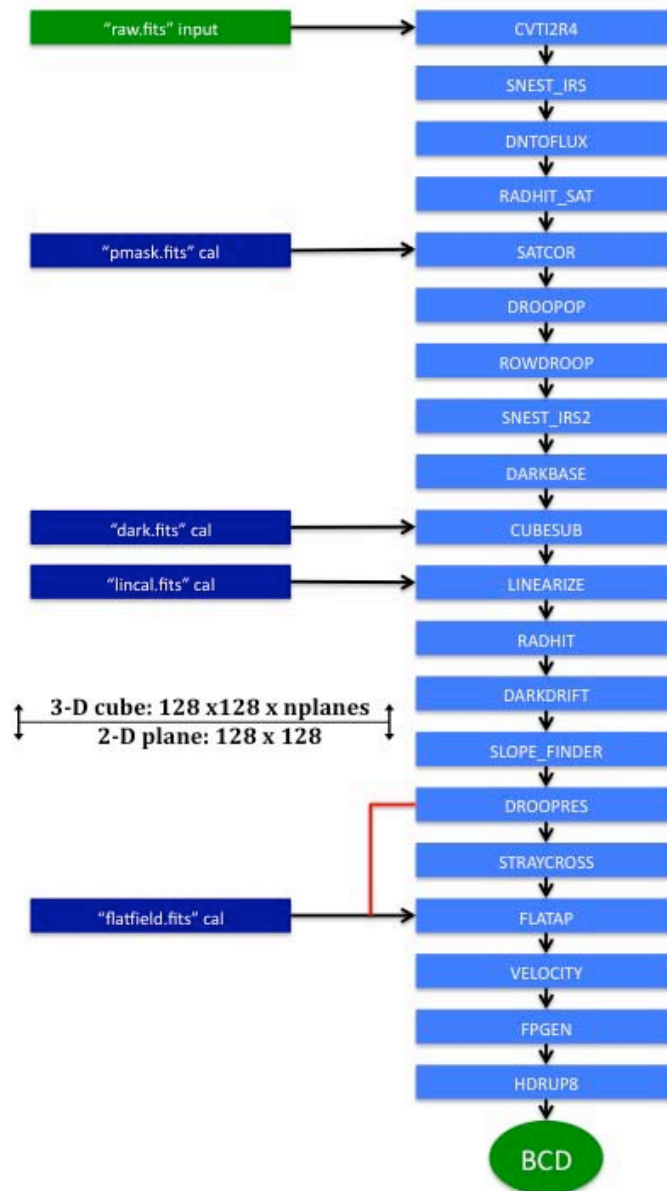
Figure 5.2 BCD Pipeline Flowchart. The red line indicates a pathway the archive takes, but that is not offered in CUPID. The calibration files shown in dark are produced manually offline. See Section 5.3 for a description of the creation of *dark.fits*.

5.1.1 CVTI2R4

CVTI2R4 ("Convert 2-byte Integer To 4-byte Real") is the first pipeline module that operates on FITS science data (pixels and samples, as opposed to the FITS headers only). The units of data samples are DN. The module converts FITS data from 16-bit signed integer to 32-bit real (float) format. All subsequent pipeline modules operate on 32-bit data. The files *cvti2r4.fits* and *dmask.fits* are the output of CVTI2R4. The *cvti2r4.fits* file is not available in the Spitzer Heritage Archive, but can be created by running CUPID. The data conversion process is as follows:

1. The 16-bit integer pixels and samples are converted to 32-bit real format.

2. Saturated samples are identified if they have the input value 32767.0 DN.

3. "Missing" data are samples whose values could not be read during telemetry. Usually missing data consist of whole rows in one or more planes of the data cube. The FITS header contains coded information on the location of these rows. Missing data samples have an input placeholder value of -1. The module sets missing data samples to an output value of NaN.

4. A value of 32768.0 DN is added to every sample of each plane, except for "missing data," in order to set the valid data range from 0 to 65535.0 DN .

5. A *dmask.fits* cube of 16-bit integer data type is initialized and has bit # 3 set for those samples identified as saturated in the data cube, and bit # 14 for those samples identified as "missing."

5.1.2 SNEST_IRS

This module ("Signal-To-Noise Estimate for IRS") generates, for the first time in the pipeline, the uncertainty of each sample of the data cube. The output file, *snest_irs.fits*, is a FITS cube of the same dimensions as the data cube. The units are DN. This file is not available from the Spitzer Heritage Archive, but can be created by running CUPID. The computation consists of adding Poisson noise and readnoise in quadrature. With I being the sample value in DN, $\sigma_{readnoise}$ the readnoise in electrons, and g the gain in electrons/DN , the uncertainty in the sample value is:

$$\sigma_{sample} = \sqrt{\frac{I}{g} + \frac{\sigma_{readnoise}^2}{g^2}} \qquad\qquad \textbf{Equation 5.1}$$

In deriving the above equation, the variance in electrons due to photon noise is just the sample value I times g. However, the units of this variance are actually electrons[2]. It should be noted that the parameters, $\sigma_{\square\square\square\square\square\square\square}$ (also denoted "Readnoise_Snest" with default value 40, 33, 67, and 55 electrons for SL, SH, LL, and LH, respectively) and g (also denoted "Gain_Snest" with default value 4.6 electrons/DN), affect the operation of only the current module. They do not affect the input values of readnoise and gain used elsewhere in the pipeline (in the modules DNTOFLUX, RADHIT_SAT, and RADHIT, described below in Sections 5.1.3, 5.1.4 and 5.1.12, respectively).

Before calculating Poisson noise, all samples of a given ramp are offset by adding a constant Δ (unique for each ramp). The purpose of adding Δ is to prevent negative samples or ramps with big offsets from affecting the noise estimation. This offsetting is an internal calculation for SNEST_IRS only and is not propagated. To obtain Δ, first the absolute values δ_i of pair-wise sample differences are computed. Denoting the signal at the i-th sample by p_i, and the number of samples in the ramp by N_{planes}:

$$\delta_i = \left| p_{i+1} - p_i \right| \qquad \qquad \textbf{Equation 5.2}$$

Here $i = 1...N_{planes} - 1$. Then the median of the δ_i values in the ramp is computed, denoted here by $\mathrm{median}(\delta)$.

Outlier samples p_j are identified if their corresponding $\delta_j > 3 \times \mathrm{median}(\delta)$. Excluding these outlier samples, the sample in the ramp with the smallest value is identified, and denoted here by P_{lowest}. See Figure 5.3. The offset to add to all samples of the ramp is:

$$\Delta = -\rho_{lowest} + \mathrm{median}(\delta) \qquad \qquad \textbf{Equation 5.3}$$

The minimum non-outlier sample in an offset ramp will thus be $\mathrm{median}(\delta)$, as illustrated in the lower panel of Figure 5.3.
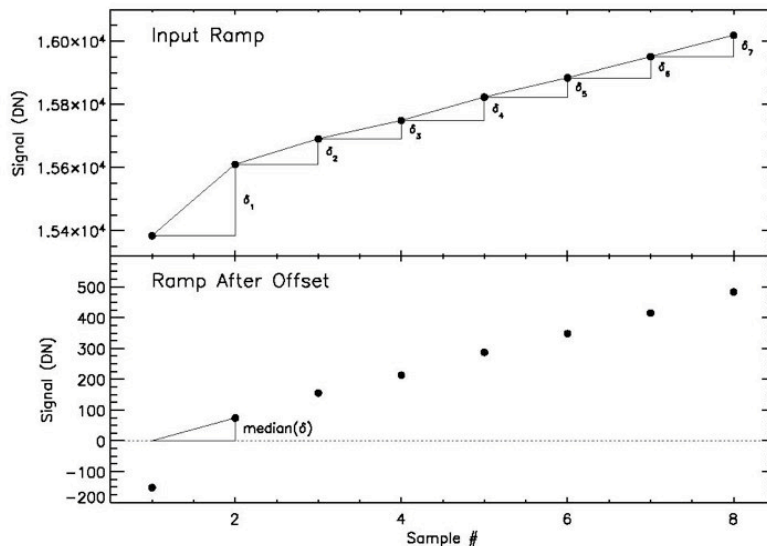
Figure 5.3 Before computing Poisson noise, the module SNEST_IRS applies an offset to each input ramp top panel. First, pair-wise differences δ_i for each sample are computed. Then the median of these (shown in the bottom panel) is used to exclude outlier samples, namely those whose $\delta_i > 3 \times \mathrm{median}(\delta)$. In this case, the first sample is an outlier. Finally, the ramp is offset (bottom panel such that the minimum non-outlier sample (in this case the second sample) has the value $\mathrm{median}(\delta)$. This calculation is internal to SNEST_IRS and is not propagated. Outlier samples get assigned an arbitrarily large Poisson noise value.

5.1.3 DNTOFLUX

The module DNTOFLUX converts the data cube DN values to electrons. The output files are *dntoflux.fits* and *dntoflux_unc.fits*. These are not available in the [Spitzer Heritage Archive](), but can be generated by running CUPID.

The data conversion process is as follows:

1. The data from the input files (sample values and their uncertainties) are multiplied by the gain, namely 4.6 electrons/DN. The gain is by default identical for all four IRS read-out channels.

2. The FITS header keyword BUNIT is set to the new unit (electrons) in the output files.

5.1.4 RADHIT_SAT

The RADHIT_SAT module ("Radiation Hit detection prior to Saturation Correction") detects and flags cosmic ray events in FITS data cubes and updates the status bits in the *dmask.fits* file. . The module looks for events in time series data (ramps) and works on a pixel by pixel basis; no spatial information is used. Cosmic ray hits are assumed to cause discontinuous signal jumps (either positive or negative) in the ramps. The samples with detected radhits are tracked by setting bit # 9 in the output updated dmask. RADHIT_SAT first finds the sample number in the ramp with the highest likelihood of having a radhit. This likelihood is computed from Bayesian statistics. In general, Bayesian statistics combine probabilities of events (such as the actual occurrence of a radhit), with other independent probabilities (such as how often false positives are detected by a measuring process). In determining whether a particular sample has suffered from a cosmic ray event, RADHIT_SAT compares the height of the jump (divided by the sample uncertainty) with an input radhit detection threshold. The signal-to-noise threshold is one of the controlling parameters of RADHIT_SAT, and is referred to as "NominalRHMag"; its default value is 80. The sample uncertainty is the quadrature combination of sample read noise and photon noise in electrons. The sample read noise is another controlling parameter of RADHIT_SAT, and is referred to as "Readnoise Radhit." From experience, its default value has been set to 26 electrons for SL and SH, and 46 electrons for LL and LH. If the Bayesian probability that the jump is a cosmic ray event exceeds a threshold probability ("RHPriorProb," another controlling parameter with default value 1%), the sample is declared a radhit, and its corresponding dmask sample is flagged as indicated above. Whenever a radhit is found, the remainder of the ramp is subdivided into segments before and after the radhit. The algorithm is run again on these segments to search for additional radhits. The process is repeated until either no radhits are found or there are no segments long enough (>3 samples) to run the algorithm.

In this invocation of RADHIT, strong radhits are detected and flagged to improve subsequent ramp fitting and droop correction (see SATCOR and DROOPOP in Sections 5.1.5 and 5.1.6 below). A second pass of RADHIT after data linearization is used to pick up the more subtle radhits prior to final slope computation; see Section 5.1.12.

5.1.5 SATCOR

SATCOR ("Saturation Correction") operates on the data by replacing saturated samples with extrapolations from the non-saturated samples in the ramp. By "saturation" we refer to A/D (analog-to-

digital) saturation, as identified by the CVTI2R4 module. The algorithm consists of fitting a slope to the non-saturated samples of a ramp and then using this slope to predict the values of saturated samples (see Figure 5.4). The outputs of this module (*satcor.fits* and *satcor_unc.fits*) are used only in the subsequent two modules, DROOPOP and ROWDROOP, to estimate the total charge on the array, using the saturation-corrected samples. Otherwise, the output of SATCOR is not propagated further downstream in the pipeline.

The first step in SATCOR consists of calculating the ramp slope of each pixel. This slope is the mean of slopes between pairs of consecutive samples, after excluding radhits.

In general (see below for some exceptions) SATCOR uses the last unsaturated sample and the calculated mean slope of the ramp up to that point to extrapolate the rest of the saturated ramp.

SATCOR requires as input the non-linearity coefficient α for each pixel, which is read from the *lincal.fits* calibration file. In practice, the same α is used for all pixels in a given module. The exception is the SL module, where the peak-up arrays may have a different coefficient than the rest of the array. The coefficients α are used by SATCOR to impart non-linearity (curvature) to the portions of the ramps that are saturation-corrected by the module. The first equation in the LINEARIZ module description (Section 5.1.11) expresses the observed (non-linear) signal in the ramp, S_{obs}, as an exponential function of ideally linear signal S_{lin}. The latter is a linear function of plane number n_p, so that the change in observed signal S_{obs} from plane $n_p - 1$ to n_p is given by the following equation, provided there were no radhits or saturation in planes n_p or n_p-1 for the given pixel.

$$\Delta S_{obs}(n_p) = \frac{e^{kn_p} - e^{k(n_p - 1)}}{2\alpha}$$

Equation 5.4

The constant

$$k = \ln(2\alpha S_{obs} + 1)/n_p$$

Equation 5.5

can be evaluated at the first plane ($n_p = 1$), by assigning to S_{obs} the value of the mean slope of the ramp.

In some special circumstances, SATCOR does not replace the saturated value with the computed linearized extrapolation. These are:

1) If the pixel is fatally flagged in the pmask, or if all samples of the ramp are saturated, or if the first non-skipped sample is saturated, then all samples of the SATCOR output ramp are set to NaN.

2) Samples which have previously been identified and flagged as radhits within a ramp will be passed to DROOPOP unchanged.

The output file of this module is *satcor.fits*. This file is not available in the Spitzer Heritage Archive, but it can be generated by running CUPID. For every sample that is saturation-corrected in *satcor.fits*, the *dmask.fits* corresponding sample is updated by setting bit # 4.
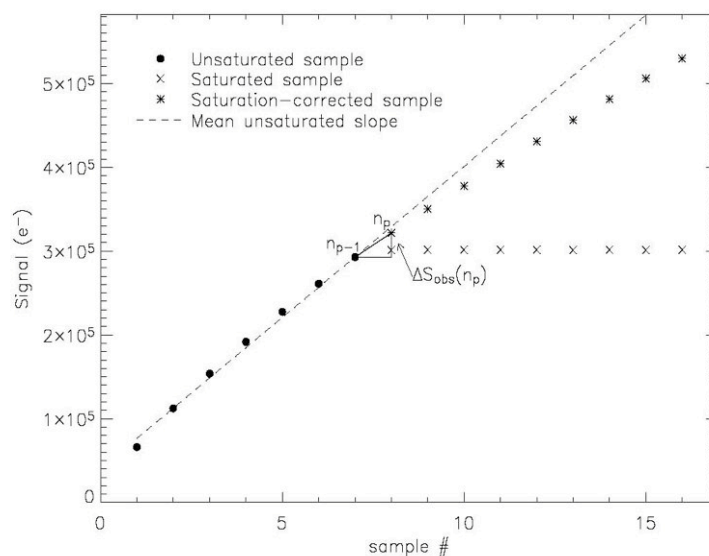
Figure 5.4 This ramp exhibits A/D saturation in samples 8-16 (x). SATCOR outputs saturation-corrected samples (asterisks). The operation consists of first obtaining the mean slope of the unsaturated portion of the ramp (dashed line). This slope is then used to extrapolate the signal from the last unsaturated sample (indexed as n_p-1), to the saturated sample immediately following (n_p). The calculation takes into account non-linearity of a realistic ramp, so that the extrapolated sample n_p will be smaller than if it were along the dashed line. The extrapolation is done in succession for higher samples up to the top of the ramp. The saturation-corrected samples are used only by the subsequent modules DROOP and ROWDROOP.

5.1.6   DROOPOP

Droop causes all samples across the array to have a larger signal value than they should. This phenomenon applies only to IRS SUR data, and not to Double Correlated Sampling (DCS) data (the data mode used during IRS Peak-Up Acquisition). Since we are measuring the accumulation of (negative) charge, ramps that become more negative appear to "droop", hence the origin of the term. The total charge on the array contributes to the droop for each pixel. A theoretical model of the droop effect does not exist. An empirical model indicates that an observed sample value, D^m_i (ith pixel in the array of N elements, N being 16384 for IRS), and the same sample value in the absence of the effect, D^t_i, are related by a so-called droop coupling constant R and the sum of remaining sample values in the array:

$$D^m_i = D^t_i + R\sum_{j \neq i}^{N} D^t_j$$ **Equation 5.6**

The above empirical relation applies to each plane of a 3-dimensional DCE. The relation can be algebraically manipulated to show that the droop effect can be corrected by subtracting a nearly constant offset from all samples in each plane of the DCE. The offset is unique to each plane of the DCE:

$$D_i^t = \frac{1}{1-R}\left(D_i^m - R\frac{\sum jD_j^m}{(N-1)R+1}\right)$$

Equation 5.7

In the IRS pipelines, the droop coupling constant R is assumed to be the same for all pixels. Each IRS instrument channel has its own droop coupling constant. In the IRS pipelines, the input droop "coefficient" is actually the quantity $(N\text{-}1)R$, and it is 0.45, 0.49, 0.20, and 0.19 for SL, SH, LL, and LH, respectively, with an uncertainty of 15%. Therefore, $1-R \approx 1$ since N is very large.

The algorithm for correcting for droop thus consists of these steps:

-Sum up all samples in a given DCE plane.

-Subtract a constant offset from all samples of the plane, which depends on the input droop coefficient and the sum of all samples of the plane.

-Re-scale samples by 1/(1-R), although the factor is nearly unity (to within 10^{-5}).

In the IRS pipelines, the input to DROOPOP ("Droop Operation" or correction) is the output of SATCOR (*satcor.fits*), where saturated input samples were saturation-corrected. The purpose of using saturation-corrected samples is to estimate, as accurately as possible, the sum of signal in the entire array. This is because droop occurs in either the detectors or multiplexer, before A/D conversion. After the execution of DROOPOP per the above algorithm, the samples that were saturation-corrected by SATCOR are reset to a constant arbitrary value (300,000 electrons). The particular value has no consequence since it is not used by any subsequent pipeline module.

The outputs of this module are *droopop.fits* and *droopop_unc.fits*. These files are not available in the Spitzer Heritage Archive, but can be generated by running CUPID.

5.1.7 ROWDROOP

The ROWDROOP module is designed to remove an apparent excess of photocharge generated only along the fast clock direction (detector rows). The effect manifests itself as an additional output signal in a given pixel, which increases in proportion to the total signal from all pixels in the same row. As opposed to the MUX-bleed effect seen in the IRAC detectors, there is no evidence that the signal produced by IRS row droop depends on distance from the source of the signal. In other words, the row droop is constant in the fast-clock direction. The strongest source of row droop in astronomical data occurs in the SL module when a bright source is situated on the peak-up array. This situation can induce measurable row droop across the SL spectral orders. In-orbit data have shown that row droop is negligible in the other instrument channels (SH, LL, and LH), so the pipelines do not correct for it in these channels.

The row droop correction consists of subtracting from each sample the product of the row droop coupling constant and the total row photo-charge:

$$D_{i,k}^{t} = D_{i,k}^{m} - c \sum_{i=0}^{128} D_{i,k}^{m}$$ **Equation 5.8**

where D_{i}^{m} is the observed value for the ith pixel of a row at sample k, and c is the row droop coupling constant.

The total row photo-charge must be measured on data that are not yet corrected for droop, or else we empirically find the row droop correction to be underestimated. This estimate should include any A/D saturation-corrected samples in the row, in analogy to DROOPOP for the entire array. The inputs for ROWDROOP are *satcor.fits* and *droopop.fits*. The total row photo-charge is estimated from *satcor.fits*, and the resulting row droop correction is subtracted from *droopop.fits*.

The coupling constant for row droop has been determined using in-orbit data to be c $=(4.5\pm0.68)\times10^{-5}$ for the SL array. It is independent of the coupling constant for array droop. There is no evidence for a dependency on read-out channel number.

The outputs of ROWDROOP are *rowdroop.fits* and *rowdroop_unc.fits*. In *rowdroop.fits*, the saturation-corrected samples are replaced with the arbitrary value 300,000 electrons, for the same reason as in DROOPOP. The output files are not available in the Spitzer Heritage Archive, but can be generated by running CUPID.

5.1.8   SNEST_IRS2

SNEST_IRS2 is the same as SNEST_IRS (see Section 5.1.2) with the following differences:

1. If a sample ends up with negative flux after pedestal subtraction, its flux is set to the median of all the other (pedestal adjusted) fluxes before the uncertainty calculation is made.

2. There is no longer any flagging or processing of "outliers".

3. All points after a rad hit are ignored when computing pedestal level.

5.1.9   DARKBASE

The DARKBASE ("Dark Baseline") module subtracts a constant offset from all samples of each read-out channel of its input file, *rowdroop.fits*. The purpose of this module is to take out a "pedestal" or baseline in the signal of all ramps, so that the output ramps extrapolate to zero signal at the start of the DCE. The module first fits a slope to the second and third samples of each ramp; the first sample is not used because we have empirically found it to often be "depressed" with respect to the rest of the ramp slope. The computed slope is then used to extrapolate to the signal at t=0 (the beginning of the DCE). In principle, such signal indicates the needed offset to apply to the ramps. In practice, such signals and resulting offsets are calculated statistically over the array, as follows:

For each read-out channel of the IRS arrays, the trimmed mean of the extrapolated t=0 signal (baseline) is calculated for all pixels (ramps) located within the un-illuminated region of the array. This region is specified by the *umask.fits* file, and is unique to each instrument channel. The trimmed mean uses an 80% trim fraction, meaning that, among all the values to average, a subset is constructed by first sorting the values in ascending order, and then discarding 10% of the values that are the lowest in the sorted set, and 10% of those that are the highest.

After computing the baseline for each of the four read-out channels, these baselines are respectively subtracted from all pixels (all samples of the ramps) of the corresponding read-out channels.

The computation of baselines excludes pixels masked in the pmask, and saturated samples masked in the dmask. No baseline subtraction is done for any such pixels or samples.

The output files of this module are *drk.fits* and *drku.fits*.

5.1.10 CUBESUB

The CUBESUB ("Cube Subtraction") module subtracts a 3-dimensional dark-current calibration FITS file (*dark.fits*), sample-by-sample, from the 3-dimensional *darkbase.fits* file. There is a dark-current calibration file for each IRS instrument channel and integration time, matched to those of the DCE. The dark-current calibration is campaign-dependent for LL and LH. Each *dark.fits* file is obtained by assembling in-orbit observations near the North Ecliptic Pole. These observations include a low-emission zodiacal background, in addition to instrument dark current. For more details on the generation of *dark.fits*, please see Section 5.3. In CUBESUB, no dark subtraction is done for fatally masked pixels in *pmask.fits*, or fatally masked samples in *dmask.fits* or the dark-calibrator mask *dark_cmask.fits*. The outputs of the module are *cubesub.fits* and *cubesub_unc.fits*.

5.1.11 LINEARIZ

The LINEARIZ ("Linearization") module corrects the ramps of IRS DCEs for the non-linear response of the detectors. In the absence of this effect, the signal of a given sample, in a particular pixel (ramp), would ideally be a linear function of time from the beginning of the DCE, or equivalently of plane (sample) number counting from the first sample of the ramp.

An empirical, one-parametric model of non-linearity relates the observed signal S_{obs} of a sample of a given ramp, to the ideal signal S_{lin} that would be observed in the absence of non-linearity:

$$S_{obs} = \frac{e^{2\alpha S_{lin}} - 1}{2\alpha} \qquad\qquad \textbf{Equation 5.9}$$

The parameter α is the so-called non-linearity coefficient. In the IRS pipelines, $\alpha < 0$, and its absolute value is $|\alpha| \sim 10^{-7}$ to 10^{-6}. Its units, 1/electron, are the reciprocal of the units of S_{lin} or S_{obs}.

The above exponential model is used in SATCOR. A series expansion of the exponential, keeping terms up to second order, leads to the so-called quadratic model of non-linearity that is used in LINEARIZ:

$$S_{obs} = S_{lin} + \alpha S_{lin}^2$$ **Equation 5.10**

The above can be solved for S_{lin} as a function of S_{obs}; only one of the two quadratic solutions is valid, given the requirement that S_{obs} should approach S_{lin} as α approaches 0:

$$S_{lin} = \frac{2S_{obs}}{1 + \sqrt{1 + 4\alpha S_{obs}}}$$ **Equation 5.11**

The application of the above expression, given the input signal S_{obs} of a sample, and the non-linearity coefficient α obtained from the *lincal.fits* calibration file, constitutes the main algorithm of the LINEARIZ module.

There are two conditions under which the module cannot correct a sample S_{obs}. In either case, a fatal bit is set in the output (updated) *dmask.fits* file for the corresponding sample.

-If S_{obs} is larger than a threshold for non-linearity read from the *lincal.fits* calibration file, the sample is deemed as "saturated beyond correctable non-linearity." The threshold in current IRS pipelines is 280,000 electrons. IRS observations typically do not reach this threshold without also being digitally saturated. Bit # 13 is set in the *dmask.fits* corresponding sample.

-If $S_{obs} > |1/4\alpha|$, the solution for S_{lin} is imaginary. In such case, it is deemed that linearity could not be applied for the particular sample. Bit # 12 is set in the corresponding *dmask.fits* sample.

The calibration file *lincal.fits* is a 3-plane cube. Its first plane contains the α coefficient for each of the 16,384 pixels in IRS arrays. The same value of α is used for all pixels of a given instrument channel. The second plane contains the threshold for saturation beyond correctable non-linearity, for each pixel. The third plane is the uncertainty in α, also for each pixel. This uncertainty is propagated in the BCD pipeline.

The outputs of this module are *lnz.fits* and *lnzu.fits*.
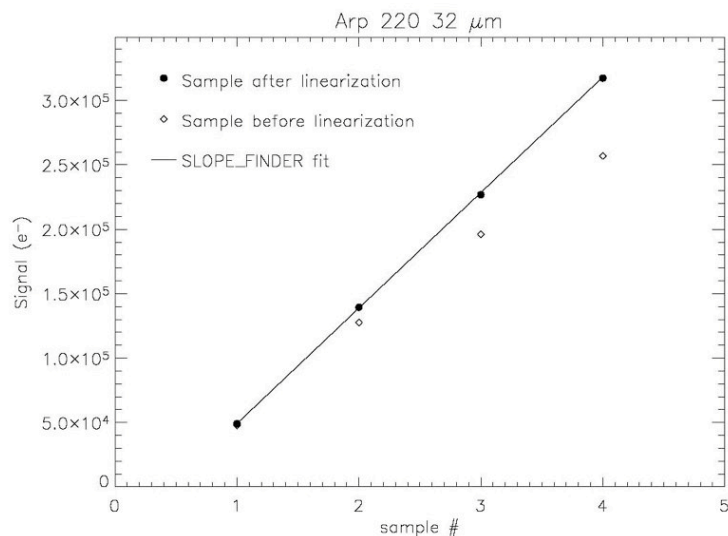
Figure 5.5 Illustration of non-linearity correction in a LL 6 second ramp for a bright source: the open rhombii are input samples, referred to as S_{obs} in the text; the filled circles are output samples, referred to as S_{lin}, after the operation of LINEARIZ. The solid line is the linear fit computed by the subsequent module SLOPE_FINDER.

5.1.12 RADHIT

This second invocation of the RADHIT module is used by the pipeline to detect and flag cosmic ray events in linearized droop-corrected FITS data cubes. The module and its controlling parameters are exactly as described under RADHIT_SAT. The only difference is that in this invocation of RADHIT, bit flags (bit # 9) in *dmask.fits* for previously detected radhits are "erased" and radhit detection is begun anew. The resulting updated *dmask.fits* is used by SLOPE_FINDER to disregard radhit samples in the computation of the final slope image.

5.1.13 DARKDRIFT

The DARKDRIFT module is known colloquially as the "jail-bar corrector." Its purpose is to correct additive offsets between the four read-out channels. When offsets are visible between the read-outs, the effect is a vertical striping or "jail bar" pattern. This pattern may result from drifts over time in the dark-current level that varies from read-out channel to channel. The module is consequently named "DARKDRIFT".

The darkdrift correction is computed and applied separately for each plane of the input data cube. First, the median is computed for all pixels belonging to each read-out channel, over the entire plane. Second, the average of the four medians (a constant offset) is subtracted from each median to form the correction for each read-out channel. Then, the correction for each read-out channel is subtracted from all pixels belonging to that read-out channel.

The effect is to "even out" the striping caused by the jail bars, while leaving the mean of each image plane unchanged.

In addition to the output FITS data and uncertainty cubes, DARKDRIFT outputs several values for each plane to the *darkdrift.tbl* file. For the input image the numbers of good and bad pixels, the median and trimmed standard deviation, and the data scale are output for each read-out. The final corrections and uncertainties computed by DARKDRIFT are also tabulated.

The main outputs of the module are the files *darkdrift.fits* and *darkdrift_unc.fits*. These files are not available in the Spitzer Heritage Archive, but can be generated by running CUPID.
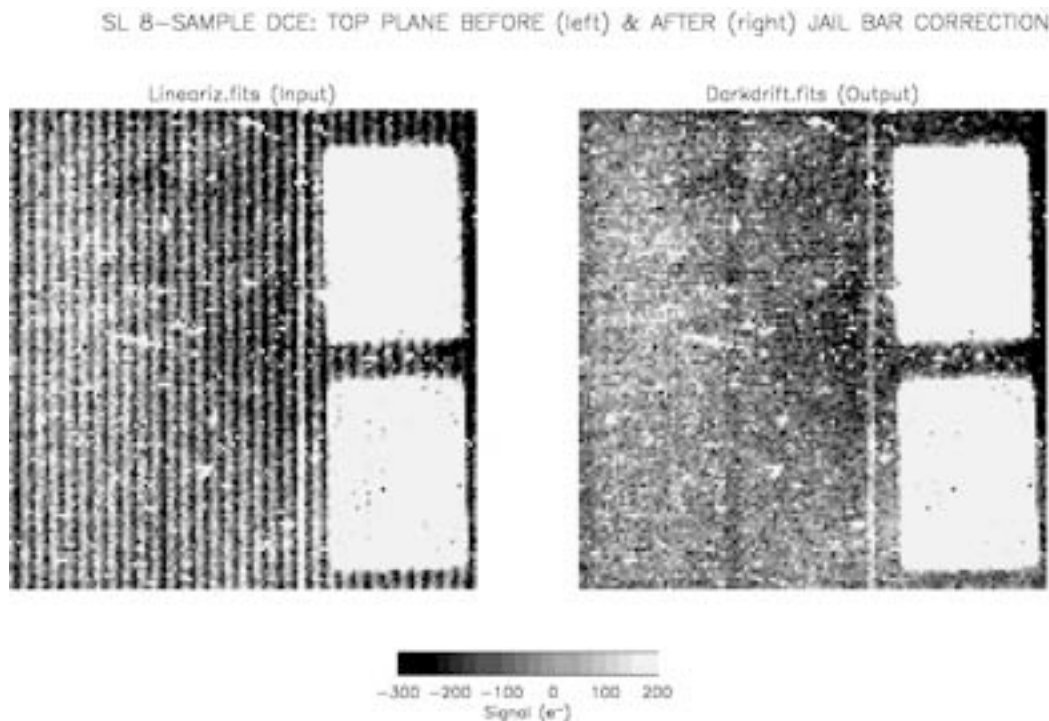
Figure 5.6 Illustration of darkdrift correction in the top plane of a SL 14 second DCE. The left frame is the input *lineariz.fits*, while the right frame is the output *darkdrift.fits*. Note that the prominent jail bars in the input practically disappear in the output. The correction is done on each plane of the DCE separately.

5.1.14   SLOPE_FINDER

The SLOPE_FINDER module converts a 3-dimensional data cube (ramp signal vs. time) to a 2-dimensional image containing slope-estimated signal intensities (electron/sec). The estimation of ramp slopes consists of the following algorithm. Note that all pixels are fit independently.

First, problematic samples are identified. These samples are excluded from the ramp fitting. In the IRS pipelines the first sample of every 8- or 16-sample ramp is excluded. Other excluded samples are: pixels masked in the pmask (the entire ramp is deemed unusable and the output slope is NaN); samples having

the following dmask bits: radhits (bit # 9), as well as all post-radhit samples in the same pixel; saturated samples, (bit # 3); samples with "data missing" (bit # 14); and samples that were uncorrectable for non-linearity (bit # 12 or 13).

After discarding problematic samples, arrays of the remaining samples are constructed: p_i and n_i are the sample value and plane number for the ith sample in these arrays, where $i = 1...N$ and $N \leq N_{planes}$. (N_{planes} is the original number of samples or planes in the DCE ramps, and N is the number of useful or non-problematic samples).

If $N < 2$, the output slope is NaN. Else, the slopes between consecutive useful samples and their average $\overline{D}$ are computed:

$$S_1 = \sum_{i=2}^{N} \frac{p_i - p_{i-1}}{n_i - n_{i-1}} \qquad \overline{D} = \frac{S_1}{N}$$

Equation 5.12

The standard deviation σ of this average slope is obtained from:

$$S_2 = \sum_{i=2}^{N} \left(\frac{p_i - p_{i-1}}{n_i - n_{i-1}} - \overline{D} \right)$$

$$\sigma = \sqrt{\frac{S_2}{N-1}}$$

Equation 5.13

Individual slopes $(p_i\text{-}p_{i-1})/(n_i\text{-}n_{i-1})$ are compared with $\overline{D}$, and if the worst one differs from it by more than $Z\sigma$, it is rejected. The parameter Z, also referred to as "Sigma Rejection Factor," has a value of 2.0. The slope averaging procedure, namely the computation of S_1, S_2, $\overline{D}$, and σ, may be repeated, this time excluding rejected slopes, and yielding in turn additional rejected slopes. However, the procedure is done only once. That is, the parameter "Maximum # Rejection Iterations," which is the number of times the slope averaging and rejection procedure is executed, has a default value of one.

After the above sequence, the ramp is broken into segments, each consisting of two or more consecutive non-problematic samples. Segment breaks are defined by rejected slopes in the slope-averaging sequence. The slope of each segment and its uncertainty is computed by a linear fit, using the procedure described in Appendix A of *Gordon et al. 2005, P.A.S.P., 117, 503–525,* "Reduction Algorithms for the Multi-band Imaging Photometer for Spitzer." The algorithm takes into account the correlation of uncertainties of the input samples, and it propagates them throughout.

The weighted mean of the various segment slopes (weighted by the inverse variance) is the final slope of the ramp. This slope and its uncertainty are multiplied by N_{planes} to obtain the "top-plane" signal and its σ, and divided by the integration time of the DCE. The resulting outputs are slopes in units of electron/sec.

The module creates, for the first time in the pipeline, a 2-dimensional mask called "BCD mask" or *bmask.fits*. This mask is created based on the 3-dimensional input DCE mask (dmask). For each of the dmask conditions (such as saturation, or radhit detection), a corresponding bit is set in the output bmask

pixel, whenever at least one sample in the corresponding input dmask ramp had the given condition flagged.

The outputs of the module are the 2-dimensional files *slope_finder.fits*, *slope_finder_unc.fits,* and *bmask.fits*. The files *slope_finder.fits* and *slope_finder_unc.fits* are not available in the Spitzer Heritage Archive, but they can be generated by running CUPID.
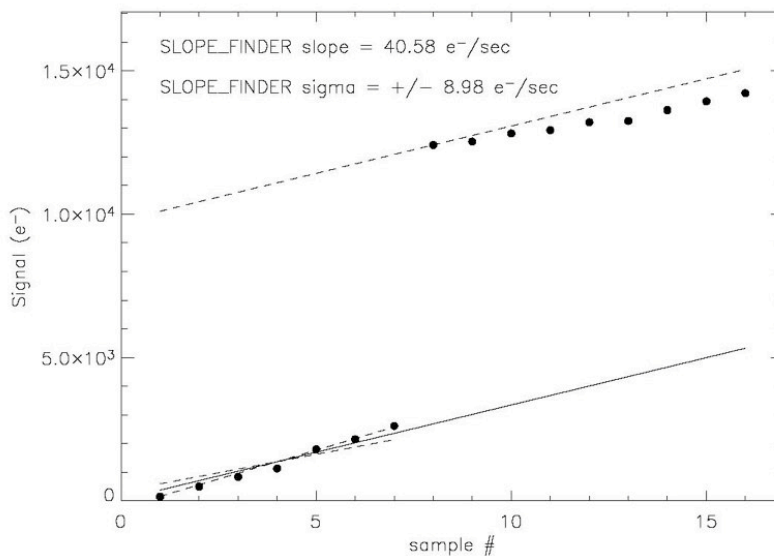
Figure 5.7 Slope in the presence of a radhit: the radhit shown occurs in sample # 8 of the ramp. SLOPE_FINDER excludes it and subsequent (top) samples, because the slope after a radhit is shallower than the slope extrapolated (dashed line) from the bottom of the ramp. The output slope (solid line) is computed from the bottom samples preceding the radhit. Sample # 1 is always excluded, and the slope between samples # 4 and 5 in this ramp is excluded as an outlier, during the outlier rejection iteration. Shown also are slopes $\pm 1\sigma$ from the mean slope, where σ is the output uncertainty for this ramp.

5.1.15 *DROOPRES*

The DROOPRES module is intended to correct residual droop (see Section 5.1.6 on DROOPOP). The residual droop is assumed to take the form of additive offsets in each of the four read-out channels. The DROOPRES module computes a trimmed average from the un-illuminated regions of the array for each read-out channel. This trimmed average is subtracted from all the pixels belonging to that read-out channel.

The un-illuminated regions of the array are specified by the umask. DROOPRES also ignores bad pixels specified by the pmask.

In the IRS pipelines, the trimmed average is computed for the central 80% of data values in the un-illuminated regions. The outputs of this module are the 2-dimensional files *droop.fits* and *drunc.fits*.

5.1.16 REMOVSTRAYCROSS

The REMOVSTRAYCROSS module ("Remove Stray light or Crosstalk") is comprised of two separate programs, depending on the IRS channel. The program SLREMOV corrects SL data for stray light falling onto the spectral orders from the peak-up subarrays. The program CROSSTALK corrects SH and LH data for interorder optical crosstalk, i.e., light leakage from one order to another. The programs assume a functional form for the light fall-off and subtract a fit to the data. REMOVSTRAYCROSS does not operate on LL data. The file *rsc.fits* is the output of REMOVSTRAYCROSS, with error plane *rscu.fits*.

5.1.16.1 SLREMOV

The SL stray light signature is found to be well-described by an exponential decay from the edge of the peakup arrays leftward. The function

$$Z_{ij} = b_{ij} \exp\left[\left(i - a_j\right)/n_j\right]$$

Equation 5.14

is fit to the data in row *j* in an interorder mask region. Here *i* is the column number, and constants a_j (the normalization point) and n_j (the decay length) describe the decaying behavior of the stray light along row *j* starting at the left edge of the peak-up sub-array. These $\{a_j, n_j\}$ pairs are found to be relatively stable row-specific constants.

To improve signal to noise and ameliorate the effects of bad pixels, a median of five rows (rows *j*-2 to *j*+2) is used in the fit that is applied to row *j*. The stray light image Z_{ij} is built from the fits to these "combined" rows and subtracted from the data. In the event that there is little useful stray light signal in a given row (the stray light fit derives a signature with maximum level smaller than a specified multiple of the noise RMS), no stray light correction is done for that row. The peak-up subarrays are not affected by stray light correction.
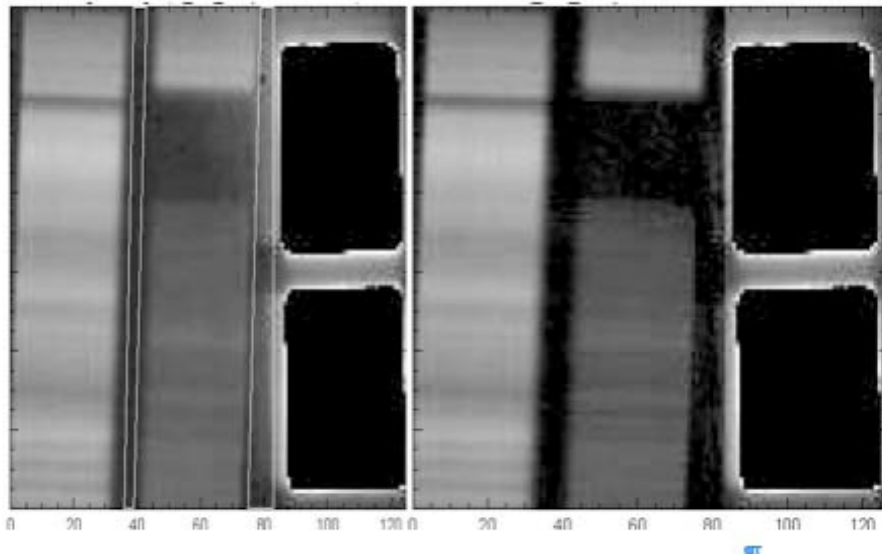
Figure 5.8 Correcting the stray light. The frame on the left displays a SL ground-based laboratory image. The peak-ups are saturated and have been blacked out for maximum contrast. The white

lines drawn on the image delineate the areas in the stray light mask used to determine the parameters b_{ij}. The frame on the right shows the same image, corrected for stray light.

5.1.16.2 CROSSTALK

The IRS SH and LH modules provide the high-resolution complement to the low-resolution modules through the use of echelle gratings. For each of these modules, the orders are projected on to the detectors in such a way that the short-wavelength ends of the orders are closer together on the detector than the long wavelength ends. This leads to optical leakage or cross-talk between the orders which is greatest at the short-wavelength end. The final design of the optics and the detector geometry is a compromise between obtaining good spectral coverage and minimizing cross-talk. For the IRS, the effect of cross-talk is minimal because the orders are not severely overlapping. However, in cases where the illuminating source is blue and bright the cross-talk can be as large as 10-15% at the edges of the short-wavelength orders, although only 2-3% near the center. Since we want to be able to recover the total emission in these blue orders, we provide a module (CROSSTALK) which automatically corrects for this effect.

The basic assumption of the crosstalk correction algorithm is that the intensity distribution of each order in the cross-dispersion direction can be fit with a simple function similar to a Lorentzian (see below). Experiments with laboratory test data have found that such a function is a good approximation to within a few percent of the shape of the cross-dispersed signal and moreover can adapt its basic shape to various forms of input structure, from a nearly perfect point-spread-function, to an extended source which fills the slit. The two main shape parameters are determined by fitting to the order least contaminated by cross-talk (hereafter the "uncontaminated order" or the m=11 order), and the results of this fit are used to constrain subsequent fits to all the bluer orders simultaneously in the same horizontal row across the image. In some cases the m=11 order is not bright enough to allow a reliable determination of the fitting parameters, and in these cases pre-determined "preferred" parameters are used to constrain the fits to the various orders. Although there is an implied assumption that line-tilt is small, the largest effects of crosstalk occur in the orders which are close together, where the assumption of zero line-tilt is almost valid.

The functional form found to best represent the shape of the uncontaminated order (based on ground-test data) is of the form:

$$f(x) = A_0/(1+z^{\alpha}); z = (x-x_{\alpha})/w \qquad \textbf{Equation 5.15}$$

Here A_0 is the maximum amplitude of the order at $x=x_0 2w$, 2w is the FWHM of the order shape, and α is the slope of the Lorentzian-like function. Indeed when α=2 the function $f(x)$ is exactly Lorentzian. We found for a wide range of fits to various uncontaminated orders, that α ranges from 3 to 5 depending on the source.

The algorithm depends upon getting a good measurement of the shape-parameter for the reddest uncontaminated order (m=11). The FWHM of each order shape is scaled according to wavelength. Based on an initial pass through the input data, the algorithm will decide to apply the crosstalk correction to the whole array, or to just the places where the emission is strong enough to justify correction. In some cases no correction will be made if the astronomical source is weak.

5.1.17 FLATAP

The module FLATAP ("FlatField Apply") takes the results from REMOVSTRAYCROSS or DROOPRES and divides by the flat-field. The flat-field image (a 2-plane cube containing the flat-field itself in layer 1 and the uncertainty plane in layer 2) is divided into the input image to correct for spatial and spectral responsivity variations, thus "flattening" the data. The areas in the input image that are flattened are only those specified in the associated flat-field *cmask.fits*. This is a slightly enlarged area covering the regions defined by the *wavsamp.tbl* file. (For SL, the peak-up arrays are also flattened and have their own valid region within the flat-field cmask.) Regions that are not flat-fielded are left in the output data unchanged; their corresponding pixels in *bmask.fits* have bit # 8 set. Regions that are flat-fielded, but where the flat-field is of questionable quality (e.g. portions of the edges of the orders), have bit # 7 set in their corresponding pixels in *bmask.fits*. Currently FLATAP operates on both the stray light- or cross-talk-corrected and uncorrected images, producing two output files (*bcd.fits* and *f2ap.fits* respectively). Input uncertainty files are combined (in quadrature) with the flat-field uncertainty and propagated. However, the flatfield uncertainty has been set to zero. The output uncertainties are *func.fits* and *f2unc.fits*, respectively. If the observer chooses to make his/her own correction, or to skip it, instead of using SLREMOV or CROSSTALK, the uncorrected versions of the image and its uncertainty are *droop.fits* and *drunc.fits*.

5.1.18 VELOCITY

The module VELOCITY computes Spitzer spacecraft (S/C) velocity components along the line of sight to the observed target. The components it separately computes are: (i) the S/C heliocentric velocity, and (ii) the S/C velocity relative to the Local Standard of Rest (LSR). These components are written to the header keywords VHELCORR and VLSRCORR, respectively. The values of these keywords can be directly added to Spitzer-measured velocities of astronomical targets, to express them in either heliocentric or LSR reference frames.

The module first computes, at the given Modified Julian Date (read from the keyword MJD_OBS), the S/C velocity components in the S/C coordinate system: V_X, V_Y, and V_Z.

Then it computes the quantities X, Y, Z defined as follows:

$$X = \cos(RA\_FOV) \times \cos(DEC\_FOV)$$
$$Y = \sin(RA\_FOV) \times \cos(DEC\_FOV)$$
$$Z = \sin(DEC\_FOV)$$

Equation 5.16

where *RA_FOV* and *DEC_FOV* are header keywords.

The value of VHELCORR is then the dot product of [*X, Y, Z*] and [V_X, V_Y, V_Z]. The value of *VLSRCORR* is given by:

$$VLSRCORR = VHELCORR + 0.145 \times X - 17.320 + 10.000 \times Z$$

Equation 5.17

5.1.19   FPGEN

The FPGEN module ("Final Product Generator") updates the FITS header keywords of *bcd.fits* to make them more human readable. It does the following: (1) modifies comments in the comments field of individual keywords, (2) reorders keywords, (3) renames keywords, and (4) adds new keywords with information from the database. The following are examples of this processing:

-In the header keyword, `INSTRUME= 'IRSX '`, the comment field "`/ Spitzer Space Telescope instrument ID`" is deleted by FPGEN.

-The header keywords APERTURE and APERNAME are renamed to FOVID and FOVNAME.

-The keywords PKUPRA (RA peakup position in degrees) and PKUPDEC (Dec peakup position in degrees) are read from the database.

Many header keywords are simply "passed through" (copied directly) from the original *bcd.fits* header. These keywords may be re-ordered by FPGEN. Examples of keywords that are passed through are those for World Coordinate System (WCS) information; see Section 5.4 on the Peak-Up Cut-Outs pipeline.

5.1.20   HDRUPD8

The HDRUPD8 ("Header Update, version 8") module adds or deletes header keywords from a *bcd.fits* file. The text of the header lines to be added or deleted is contained in a file that is passed to HDRUPD8. This module operates in conjunction with FPGEN.

5.2 Notes on Uncertainty Propagation in the BCD Pipeline

The modules that propagate uncertainties are SNEST_IRS, DNTOFLUX, LINEARIZ, SLOPE_FINDER, and FLATAP, as described above. No other modules propagate uncertainties, and for them the output **unc.fits* are identical to the input ones. The uncertainties are correlated among pixels in the operations of DROOPOP, ROWDROOP, DARKBASE, DARKDRIFT, DROOPRES, and REMOVSTRAYCROSS. The correlated uncertainties in these modules are unrealistically large. Since they are the same for all pixels in the array, or in entire read-out channels, or in entire rows, they do not reflect the actual statistical noise from pixel to pixel. Uncertainties are not propagated in CUBESUB, because the darks include significant zodiacal background signal; the uncertainties from the latter are instead propagated during the background subtraction ("bksub") pipeline for low-resolution IRS data.

5.3 Description of Modules in the Dark Calibration Pipeline (Creation of *dark.fits*)

This pipeline consists of two parts. First, individual input files *raw.fits* are processed through a pipeline that is a subset of the BCD one. This pipeline is denoted as Dark Calibration Pre-processing. Second, multiple pre-processed products are combined through an ensemble pipeline, to yield one output dark calibration file. See Figure 5.9. The selection of files to be combined in the ensemble is done manually;

the names of these files are contained in lists in text format. The products described in this section are not available in the Spitzer Heritage Archive, but can be generated by running CUPID.
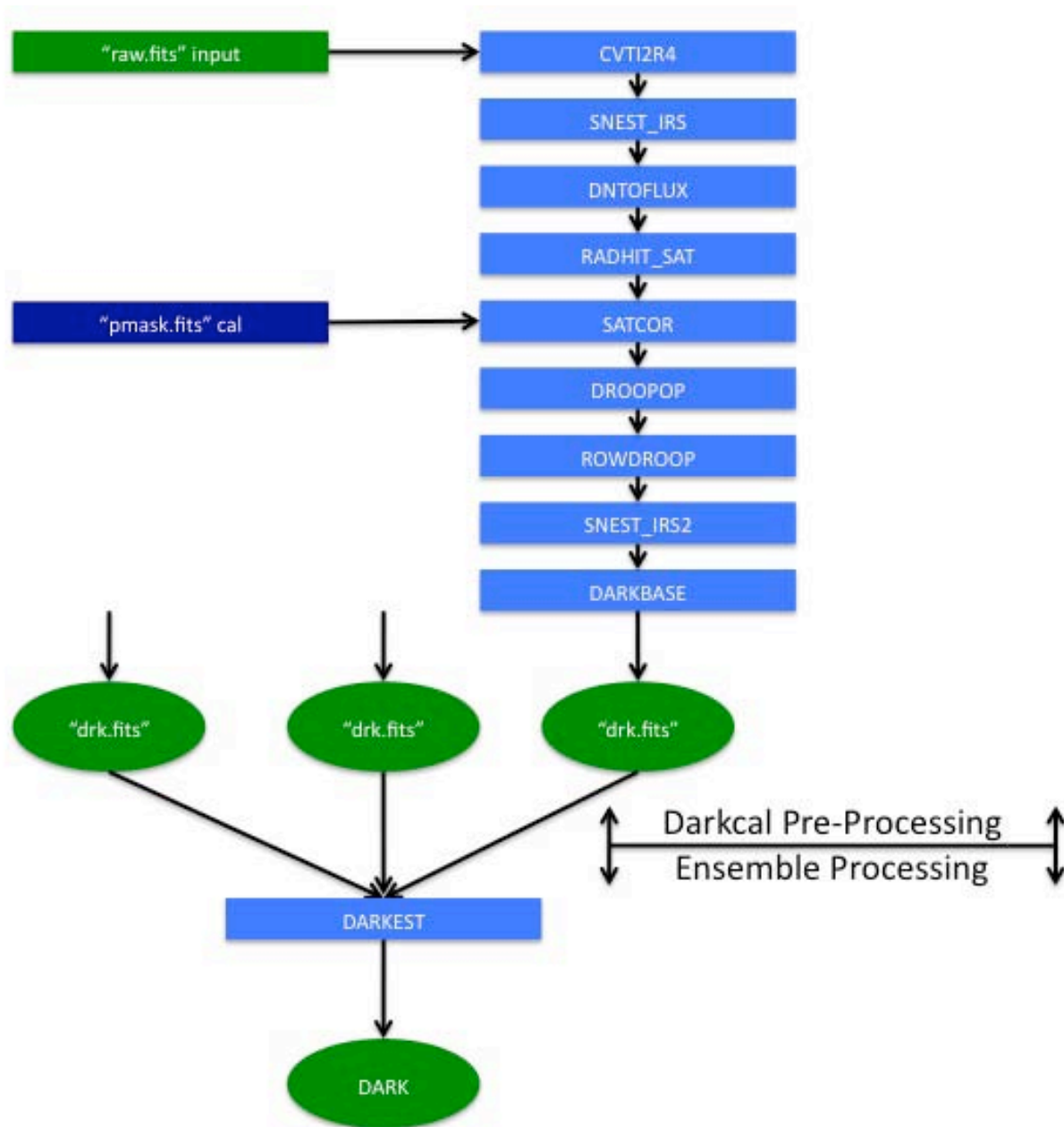
Figure 5.9 Dark Calibration Pipeline Flow Chart. This pipeline consists of two steps: Pre-processing, up to DARKBASE, and ensemble processing, which combines several DARKBASE outputs (*drk.fits*). The figure above illustrates the case of three *drk.fits* that are combined to produce the output *dark.fits*.

5.3.1 Dark Calibration Pre-Processing Pipeline

The input file *raw.fits* is processed through the modules CVTI2R4, SNEST_IRS, DNTOFLUX, RADHIT_SAT, SATCOR, DROOPOP, ROWDROOP, and DARKBASE. The modules and their execution are exactly as described in Section 5.1. The outputs of this pipeline are *drk.fits*, *drku.fits,* and *dmask.fits*

5.3.2 Dark Calibration Ensemble Pipeline

This ensemble pipeline consists of only one module, DARKEST. Multiple input *drk.fits* files are combined.

5.3.2.1 DARKEST

The module DARKEST ("Dark Estimator") computes the median of several input files *drk.fits*, whose names are listed in the text file *filelist_flux.txt*. Other inputs to the module are the corresponding uncertainty files *drku.fits* and DCE masks *dmask.fits*, respectively listed in the text files *filelist_unc.txt*, and *filelist_dmask.txt*. These input lists are made manually by the user.

The processing of each pixel is done independently of other pixels. The module computes the median of the input files *drk.fits*. The output is *dark_flux.fits*. This file can be used in subsequent BCD pipelines, as shown in Figure 5.2, during the operation of the module CUBESUB.

The output dark calibration mask, *dark_cmask.fits*, has bit # 10 set if the spatial standard deviation in a 2×2 pixel^2 boxcar exceeds a threshold. Bit # 13 is set whenever a pixel is fatally masked in the *pmask.fits* of the corresponding instrument channel.

5.4 Description of Modules in the Peak-Up Cutouts Pipeline

This pipeline consists of two modules: CROPFITS and DNTOFLUX.

5.4.1 CROPFITS

The module CROPFITS ("Crop a FITS file") creates a FITS file that is a rectangular subset of the original one. This module is used to create images of the blue and red IRS Peak-Up images contained in SL input files *bcd.fits*. The rectangular area to be included is defined by four parameters: "*h*," "*w*," "*i1*," and "*j1*," which are, in units of pixels, the height, width, and lower-left x-and y-coordinate of the lower-left corner of the rectangle, respectively. The coordinates are 1-indexed, meaning they are counted starting from 1.

WCS information is handled properly by this module, and the resulting files may be used in MOPEX.

This module produces the following output files:

- *cropfits_b.fits* and *cropfits_r.fits* (from *bcd.fits*)

- *cropfits_unc_b.fits* and *cropfits_unc_r.fits* (from *func.fits*); and

- *mskb.fits* and *mskr.fits* (from *bmask.fits*)

The files *cropfits_b.fits*, *cropfits_r.fits*, *cropfits_unc_b.fits*, and *cropfits_unc_r.fits* are not available in the Spitzer Heritage Archive, but they can be generated by running CUPID.

5.4.2   DNTOFLUX

The module DNTOFLUX is the same module referred to in the BCD pipeline (Section 5.1.3). It multiplies the input file *b0_cropfits_b.fits* by 0.0114 MJy/sr/electron/sec, and the input file *b0_cropfits_r.fits* by 0.0119 MJy/sr/electron/sec. The BUNIT header keyword is set to the new unit (MJy/sr) in the output files *bcdb.fits* and *bcdr.fits*. The uncertainty files are also processed to produce the files *uncb.fits* and *uncr.fits*.

5.5 Description of Modules in the 2-Dimensional Coadder Pipeline

This pipeline consists of only one module, COADD2D, and is considered an ensemble pipeline, because multiple input *bcd.fits* files are combined. The pipeline selects all BCDs of the same exposure (EXPID) within an AORKEY, to form the list of files to be combined.

5.5.1   COADD2D

The module COADD2D ("2-Dimensional Coadder") computes the asymmetric trim mean of several input files *bcd.fits*, whose names are listed in the text file *inputlist-coadd*. Other inputs to the module are the corresponding uncertainty files *func.fits* and BCD masks *bmask.fits*, respectively listed in the text files *inputlist_unc_coadd*, and *inputlist_bmask_coadd*.

The "asymmetric trim mean" algorithm is carried out for each pixel, independently of other pixels. Asymmetric trimming consists of successively discarding pixel values at the upper or lower extremes of the set that will be averaged. The algorithm details are as follows:

Denote by pix_i ($i=1...N$) the set of N pixels to be trim-averaged, where N is the number of BCDs being co-added. The asymmetric trim fraction parameter f_{asym}, also denoted as "Cut-off Fraction" (with default value 0.2) determines the maximum number N_{asym} of pixel values pix_i that are discarded at the extremes of the set: $N_{asym} = N_{pix} f_{asym}$. That is, using the default for f_{asym} up to 20% of pixel values may be discarded. The iterative process for discarding extreme pix_i consists of four steps:

1. Compute median(pix) of the set pix_i, where $i = 1...N$.

2. Determine which of the two extreme values (the highest or the lowest) of the set pix_i deviates more from median(pix); denote it as P_{ext}, and its absolute deviation from median(pix) as D_{ext}.

3. Excluding P_{ext}, compute the median absolute deviation D_{med} of the set pix_i from median(pix).

4. If $D_{ext} < m_{cut} D_{med}$, where the parameter m_{cut} also known as "Cut-off Multiple," has a default value of 5.0, then terminate the iteration and compute the mean of the remaining set pix_i. Otherwise, discard P_{ext}

from the set pix_i; if fewer than N_{asym} pixels have been discarded through these iterations, go back to step 1 and continue. Else, if N_{asym} pixels have been discarded from the set, terminate the iteration and compute the mean of the remaining set.

In the main output of the module, *coa2d.fits*, pixels are set to NaN whenever there are no non-NaN values in the trimmed set pix_i. Equivalently, output NaN values result whenever all pixels in the trimmed set are fatally masked in their respective *bmask.fits* or *pmask.fits* files. The inter-order regions are NaN in *coa2d.fits*.

The output uncertainties in *c2unc.fits* are the sum in quadrature of the input uncertainties in *func.fits* for the trimmed set, divided by the number of pixels in the trimmed set. Weights are not used in this procedure.

The output mask file *c2msk.fits* has bits # 12 and 13 set whenever there are no values in the trimmed set pix_i that are not NaN. Bit # 7 is set for pixels tagged in the input *bmask.fits* as "questionable flatfield applied."

5.6 Description of Modules in the Background Subtraction Pipeline

This pipeline consists of only one module, IMSUBTRACT. It operates on only SL and LL, and only on IRS Staring Mode observations. Its inputs are co-added files *coa2d.fits*. It mutually subtracts the observations in a pair of nod positions, in order to suppress the sky background signal. Sky-subtracted images produced in this way should only be used for point source observations.

5.6.1   IMSUBTRACT

This module subtracts two FITS files, and also operates on the corresponding uncertainty and mask files. All FITS files must have identical dimensions. In this case, all FITS files are 128×128 2-dimensional images. The header from the first input image is copied to the output image.

The output primary image *bksub.fits* is computed by subtracting the second image from the first. An output pixel will be NaN if either of the corresponding input pixels is NaN.

The output uncertainty image *bkunc.fits* is computed by combining the two input uncertainty images in quadrature. An output pixel will be NaN if either of the corresponding input pixels is NaN.

The output mask file *bkmsk.fits* will have a bit set if either or both of the input files *bmask.fits* has it set at the corresponding pixel.

5.7 Description of Modules in the Spectral Extraction Pipeline

This pipeline consists of four modules: PROFILE, RIDGE, EXTRACT, and IRS_TUNE. See Figure 5.10. It may operate on the outputs of: (i) the BCD pipeline; (ii) the 2-dimensional coadder pipeline; or (iii) the background-subtraction pipeline. In the following description, reference is made to the BCD pipeline file names when listing input files (BCD, uncertainty, and mask files) for extraction pipeline modules. The equivalent files from the 2-dimensional coadder or the background subtraction pipelines may be substituted as inputs to the modules in this section.
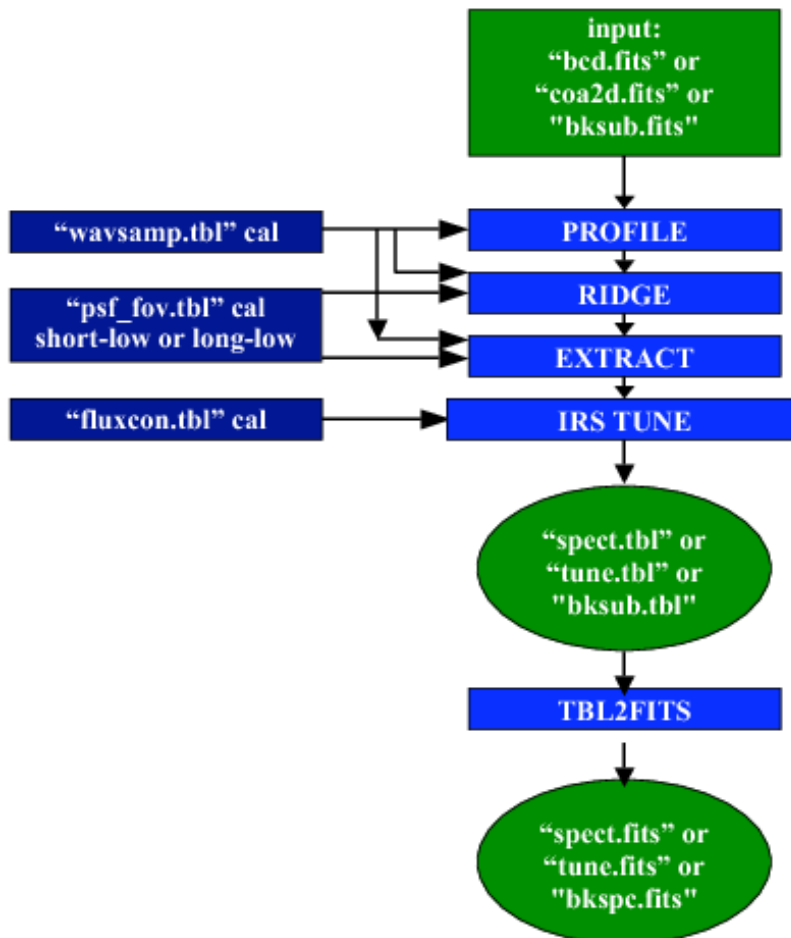
Figure 5.10 Extraction Pipeline flowchart. The Extraction Pipeline runs after the BCD Pipeline and extracts one-dimensional spectra from two-dimensional slope images. The input of the thread is a two-dimensional BCD image in FITS format. The output from the thread is a table file containing the extracted spectrum. The thread also takes mask and uncertainty files as input, and propagates uncertainties and status flags into the output table.

5.7.1 PROFILE

The PROFILE ("Spatial Profile") module computes the median spatial flux profile across all user-selected orders in the same slit. The inputs to the module are *bcd.fits* and the input calibration file *wavsamp.tbl*, which specifies the location of the selected spectral orders.

The selection of spectral orders to use in measuring the spatial profile depends upon the information in the BCD FITS header keyword FOVID, which defines a field-of-view. In SH and LH, all orders (11-20) are used by default. In SL and LL, the default order depends upon the commanded field of view (e.g. an observation in LL2 will default to orders 2 and 3). Alternately, the orders to be used by PROFILE may be chosen by means of the parameter *ord*: the orders are specified as comma-separated integers, without intervening spaces; for SL and LL, the orders are 1, 2, or 3; for SH and LH, the orders are 11 through 20.

This module computes a wavelength-collapsed median spatial profile of all orders in the dispersed IRS image. It takes the median of all orders at a given spatial position and produces a table of the flux distribution and the corresponding standard deviation for each of a number *N_cut* positions across the orders, where *N_cut* is a parameter (see below). The module uses the *wavsamp.tbl* file to specify the location of the orders.

The input *wavsamp.tbl* file specifies the location of the spectral orders on the array in x-y coordinates. It consists of "pseudo-rectangles" which describe the fractional pixels that comprise each wavelength in the spectrum (see Figure 5.11). These pseudo-rectangles are specified by their four vertices. Each line of the *wavsamp.tbl* file consists of an order number, coordinates of the center of the pseudo-rectangle (x center, y center), wavelength, tilt angle, and four vertices (x0, y0, x1, y1, x2, y2, x3, y3). Table 5.1 shows an example of *wavsamp.tbl*.

The PROFILE module divides each pseudo-rectangle in each order into *N_cut* parts and integrates (sums) the signal within each part. The parameter *N_cut* has default values of 1,000 for SL and LL, and 200 for SH and LH. It is not recommended to adjust *N_cut* from these defaults. The integral (sum) of the *n*th part (*n* running from 1 to *N_cut*) is divided by its area to yield a flux. Then the median of the fluxes of all corresponding *n*th parts in all pseudo-rectangles (all wavelengths) is calculated, to yield the median flux at that particular *n*th spatial position. The module uses a running window of 7 parts along the pseudo-rectangles, centered on the *n*th part, to compute the median at the *n*th position. The standard deviations are calculated from the fluxes at each part.

NOTE: The profile is calculated as a function of left-to-right percentage along the spatial direction of the slit.

The output of PROFILE is a table describing the median signal and standard deviation in each of the *N_cut* parts or sub-rectangles. The default name of this file is *profile.tbl*. Figure 5.12 shows an example of the profile calculated from a SL observation of a faint source on a complex background. An excerpt from a *profile.tbl* table for the same module is shown in Table 5.2.

Table 5.1: Sample *wavsamp.tbl* file.

```
\wavsamp version 5.0 (Thu May 9 10:19:35 PDT 2002)
\processing time 17:05:26 PST 03/12/2003
```

```
\comment WAVSAMP SL, generated from b0_ordfind.tbl 03/12/03
\character channelID = 0
| order |x_center |y_center | wavelength | angle    | x0       | y0
| x1       | y1       | x2       | y2       | x3       | y3       |
| int    | real    | real    | real      | real     | real    | real
| real     | real     | real     | real     | real     | real     |
        2  60.75172  78.86935     5.27230  -1.880000  76.65864
78.83240  44.87576  79.87564  44.84472  78.90629  76.62761  77.86305
        2  60.72052  77.89996     5.30254  -1.880000  76.62761
77.86305  44.84472  78.90629  44.81336  77.93686  76.59624  76.89362
        2  60.68900  76.93050     5.33278  -1.880000  76.59624
76.89362  44.81336  77.93686  44.78167  76.96736  76.56455  75.92412
        2  60.65714  75.96097     5.36303  -1.880000  76.56455
75.92412  44.78167  76.96736  44.74964  75.99780  76.53253  74.95456
        2  60.62495  74.99137     5.39327  -1.880000  76.53253
74.95456  44.74964  75.99780  44.71729  75.02817  76.50017  73.98493
        2  60.59243  74.02171     5.42351  -1.880000  76.50017
73.98493  44.71729  75.02817  44.68461  74.05847  76.46749  73.01523
```

Table 5.2: Sample *profile.tbl* file (excerpt).

```
\int CHNLNUM = 0
\int FOVID = 27
\int ORDER1 = 1
| pct  | dn         | stdev      | n    | region |
| real | real       | real       | int  | int    |
   0.50  2.5838E+01  4.1910E+01   108        0
   1.50  3.1066E+01  4.0129E+01   108        0
   2.50  3.0284E+01  3.7313E+01   109        0
   3.50  2.8732E+01  2.2572E+01   113        0
   4.50  2.8311E+01  2.0112E+01   121        0
   5.50  2.6560E+01  1.8742E+01   129        0
```
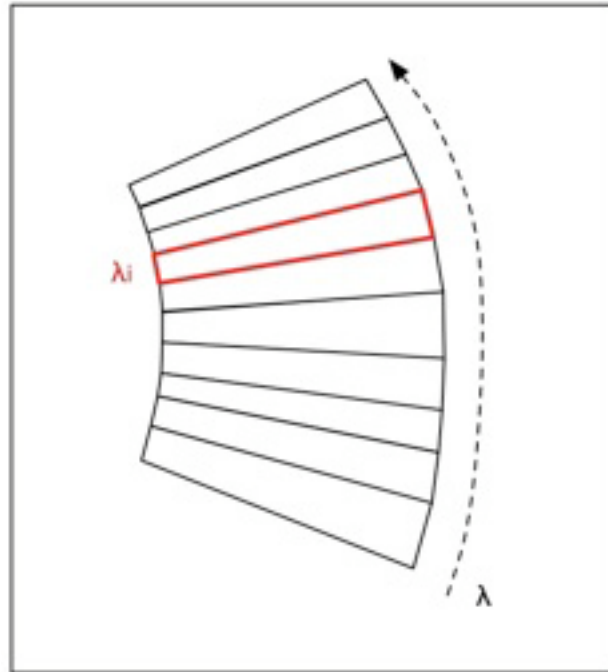
Figure 5.11 One spectral order defined by the *wavsamp.tbl* file is illustrated, with a single pseudo-rectangle highlighted. Order curvature is highly exaggerated here for illustration.
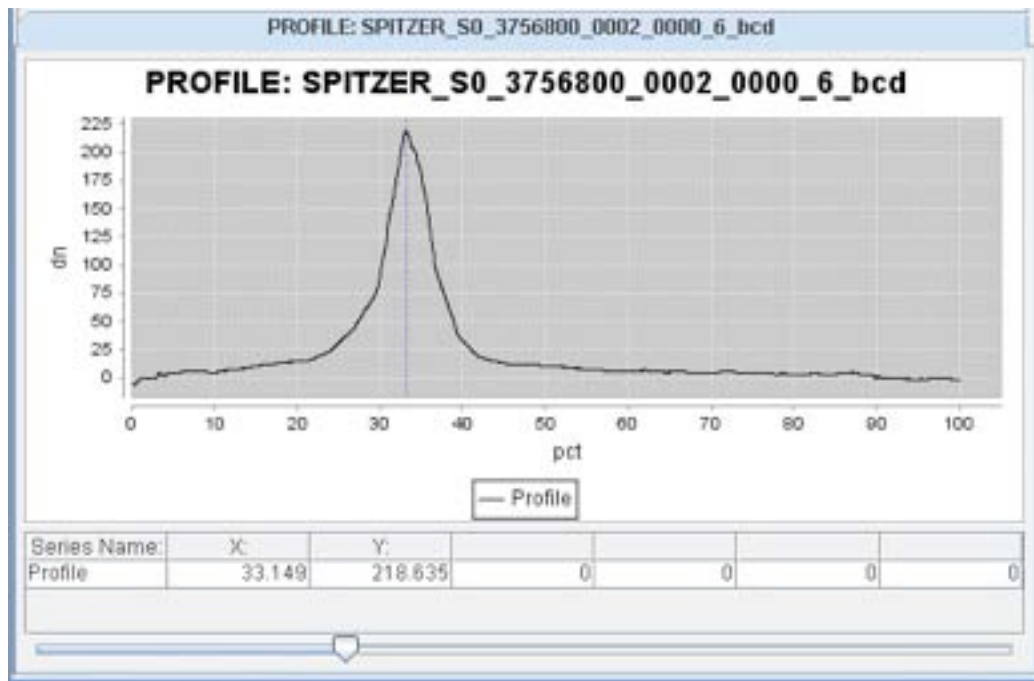
Figure 5.12 An example of the plotted output of the PROFILE module.

5.7.2   RIDGE

The RIDGE module finds the peak in the spatial profile that was produced by the PROFILE module. In other words, it defines the spectral trace of the source to be extracted. The peak is represented as a percent value (from 0.0 to 100.0) of the slit length. By default the module computes this peak position. Alternatively, the peak position can be forced to have a specified value, set by the input parameter *Cut Percentage*, also denoted *c*. The module takes as input the file *profile.tbl*, and the two calibration files *wavsamp.tbl* and *psf_fov.tbl*.

The search for the peak position (if *Cut Percentage* is not given) is performed within plus or minus *Percent Range* (a parameter, also denoted as *g*) of the position expected based on the selected field-of-view. In the pipeline, *Percent Range* = 25% for SL and LL, meaning that, for low-resolution data, the search for a peak is performed within a spatial window of width 50% of the slit length, centered on the commanded nod position. For SH and LH, instead of the parameter *g*, the parameters *Percent Low* = 25% and *Percent High* = 75% (also denoted *glo* and *ghi*, respectively) are used in the pipeline. They supersede *g* and as a result RIDGE searches for a peak in a window of width 50% of the slit length, centered on the slit.

The search algorithm is as follows:

- Read in the data in *profile.tbl* (as a function of percent length along the slit): y_0
- Calculate a linear fit to y_0, and subtract it from the data to obtain y_h
- Perform median filtering of this flattened y_h data, using a number of points *Median_Pts* to get y_f. In the pipeline, the parameter *Median_Pts* (also denoted as *m*) has value 5.
- Calculate the new mean, μ_f and sigma, σ_f, for the median-filtered data y_f
- Find the peak value m_h in the unfiltered, flattened data, y_h
- The profile has a candidate peak if

$$m_h \geq \mu_f + NUM\_SIGMA \times \sigma_f$$ **Equation 5.18**

In the pipeline, the parameter *Num_Sigma* (also denoted *s*) has value 5.0.

The final cut percentage *P* is then set to the position of the candidate peak found above. But if no candidate peak is found, *P* is set to the expected position of the field-of-view as defined by the DFRAC column of the *psf_fov.tbl* file.

Once *P* is determined, the RIDGE module computes the ridge line, defined to be the locus of the cut percentage *P* at each of the pseudo-rectangles (measured from the leftmost edge of each). It outputs the ASCII table *ridge.tbl*, containing the ridge line, in the form of IRS array coordinates (x,y) of the peak for each order and each wavelength. In actuality, two sets of coordinates (x,y) are output at each wavelength; they are the left and right edges of the nominal extraction window used by EXTRACT, centered at *P*.

5.7.3   EXTRACT

The EXTRACT module takes as one of its inputs the file *bcd.fits*, and extracts the 1-D spectrum along the trace defined in the input file *ridge.tbl*. It also takes as input the associated uncertainty *func.fits*, and

bmask.fits. The corresponding inputs from the 2-dimensional coadder are *c2unc.fits* and *c2msk.fits*, and from background subtraction they are *bkunc.fits* and *bkmsk.fits*.

In the high-resolution slits, this module extracts a one-dimensional spectrum from the full slit. In the low-resolution slits, the spectrum is extracted along the RIDGE location in accordance with the wavelength-dependent Point Spread Function (PSF) and the spectral trace. The width of the extraction is defined in the *psf_fov.tbl* calibration file, which gives the width to employ at a fiducial wavelength for each order. The width and fiducial wavelength may be overridden if specified in the parameters *w* and *l*, in units of pixels and microns, respectively. The width of the extraction scales with wavelength in all low-resolution slits, under the assumption that the spectrum is diffraction limited. However, the width does not scale between subslits. Rather, the extraction width has been empirically determined for each subslit, and wavelength scaling is performed within each order individually. The exception to the wavelength-dependent window width in low resolution is the case of mapping observations taken in the "Both" fields of view, namely "Long-Low-Both" or "Short-Low-Both." In that case, the default is to perform a full-slit extraction. The module may use a non-scaling width by setting the parameter *l* to 0 while also setting the extraction width to *w*.

The source spectrum incident on the array is not rectilinear in either the spectral or cross-dispersed direction. As a result, the EXTRACT module does not extract whole pixels, but rather subdivides the array into a network of polygon-shaped sampling elements referred to as "pseudo-pixels" (see Figure 5.13), which lie within the "pseudo-rectangle" that defines each wavelength in each order (specified in the *wavsamp.tbl* calibration file). Pseudo-pixels do not necessarily overlap the rectangular pixel grid. These elements allow Nyquist sampling of spectra in the dispersion direction. Extraction is performed by calculating the signal that falls within the boundary of the "pseudo-rectangles" which lie within the extraction window. Light is assumed to be evenly distributed within a pixel for purposes of calculating fractional contribution. The file *bmask.fits* identifies fatally masked pixels that will be excluded from the average of the pseudo-rectangle.
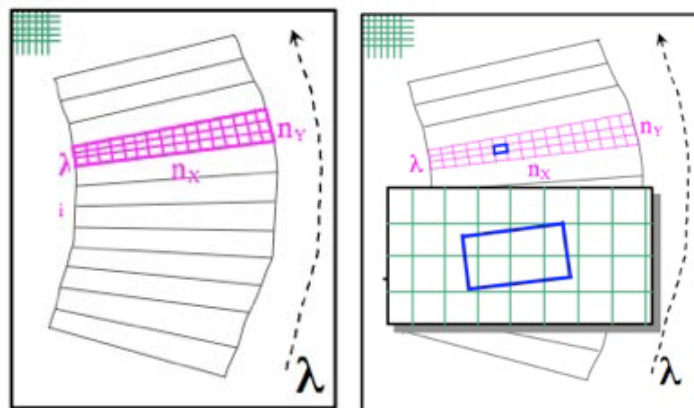
Figure 5.13 (Left) A pseudo-rectangle is divided into pseudo-pixels. The pixels form the FITS image for a rectangular grid, as illustrated in the upper left corner. (Right) A pseudopixel is shown overlaid on the pixels of the original FITS image. The pseudo pixel contains partial detector pixels, so each partial pixel must be carefully accounted for to perform the extraction.

For SL, LL, and LH data, the extraction is the sum of signal in the non-fatally masked pixels at each wavelength divided by the height (measured along the spectrum in pixels) of the extraction window, as set by the *wavsamp.tbl* wavelength calibration file. For SH, the extraction is the sum of signal in the non-fatally masked pixels at each wavelength.

The module interpolates by default over NaN pixels in the data. NaNs can be present in IRS BCDs when there is no good data available for that pixel. The NaN pixels may or may not be fatally masked. EXTRACT averages the 2 rows above the NaN pixel, and the 2 rows below, column by column within the same order. It then fits a line to those column averages to interpolate over the NaN pixel. To disable this feature, the parameter *fix* can be set to 0.

The output of the module is the one-dimensional extracted spectrum, in units of electron/sec, written to the table *extract.tbl*.

The uncertainty defined in the input uncertainty plane is propagated into the extracted output spectrum. The output spectrum table includes the order, wavelength, flux (in electron/sec), propagated error, and cumulative pixel status for each wavelength. The cumulative pixel flag is a bit-wise OR of the flags of contributing pixels.

5.7.4   IRS_TUNE

The IRS_TUNE module converts the extracted spectrum from units of electron/sec to flux density (Jy). This module is for point source extractions. The conversion is only valid for the standard extraction width (specified in *psf_fov.tbl* for low resolution, or the full width used in EXTRACT for high resolution). The module takes as input *extract.tbl*.

This module applies absolute flux calibration to the 1-dimensional spectral output file from EXTRACT. For each separate spectral order in SL and LL and each Echelle order in SH and LH, POINT SOURCE TUNE applies adjustments to the shape of the order and corrects by a scaling constant, in units of electrons/sec/Jy, to convert the spectrum to units of Jy. The scaling and shape adjustments are contained in an input calibration file, *fluxcon.tbl*. This file contains the coefficients calculated by fitting an nth-order polynomial, where $1 \leq n \leq 5$, to the EXTRACT output of one or more calibration stars so that their observed IRS spectra are forced to match a model spectrum taken as truth. The ASCII table *spect.tbl* is the output from IRS_TUNE. It contains five columns listing the order number, wavelength in microns, flux in units of Jy, uncertainty in the flux density measurement in Jy (not suited to derive signal-to-noise ratios), and cumulative pixel status flag (copied from the output of EXTRACT). The corresponding output in the case of 2-dimensional coadder input is *tune.tbl*, and in the case of background subtraction input is *bksub.tbl*, as shown in Figure 5.1.

5.7.5   TBL2FITS

The TBL2FITS ("Table To FITS") module converts the input *spect.tbl* from IPAC ACSCII table format into a FITS binary table file. The FITS binary table is written as an "extension" in the FITS file. All header keywords including COMMENT and HISTORY are copied over. The data values from the IPAC table are all written to the FITS table as either integer (16-bit) or float (32-bit) values. The output is *spect.fits*.

Chapter 6. Data Products

6.1 Classes of Spitzer Data Products

Spitzer data can be downloaded from the Spitzer Heritage Archive. Table 6.1 lists the classes of data products that are available. After downloading the data from the archive, the user will end up with a directory tree, the top level of which will have the AORKEY number, prefixed by an "r". The AORKEY uniquely identifies a single Spitzer observation sequence, which is called an Astronomical Observation Request, or AOR. Within this directory, there will be one subdirectory for each module used in the AOR. The possible subdirectory names are *ch0/*, *ch1/*, *ch2/* and *ch3/*, which correspond to the Short-Low (SL), Short-High (SH), Long-Low (LL) and Long-High (LH) modules, respectively. Peak-Up Acquisition or Imaging data, if taken, will also be found in the *ch0/* subdirectory. Within each module subdirectory there may be *bcd/*, *pbcd/*, *cal/*, and/or *raw/* subdirectories, depending on which classes of data were selected for download.

Table 6.1 Classes of Spitzer data products.

Name	Alternate Name	Alternate Name	Description	Download Directory	Event for which files are provided
Raw			The raw three dimensional data files.	*raw/*	spec:DCE PUA:DCE PUI:DCE
Calibration			Files that were used to calibrate the data.	*cal/*	spec:AOR PUA:AOR PUI:AOR
Level 1	Basic Calibrated Data	BCD	The primary calibrated data frames that emerge from the Spitzer pipeline.	*bcd/*	spec:DCE PUA:DCE PUI:DCE
Ancillary Level 1	Ancillary Basic Calibrated Data	Ancillary BCD	Additional calibrated data frames that emerge from the Spitzer pipeline.	*bcd/*	spec:DCE PUA:DCE PUI:DCE
Level 2	Post-BCD	PBCD	The primary products that come from combining individual BCDs.	*pbcd/*	spec:nod PUA:N/A PUI:AOR
Ancillary Level 2	Ancillary Post-BCD	Ancillary PBCD	Additional products that come from combining individual BCDs.	*pbcd/*	spec:DCE PUA:DCE PUI:DCE

6.2 File Naming Convention

6.2.1   Raw and Level 1 (BCD) Data

The Raw and Level 1 (BCD) files within the *raw/* and *bcd/* download directories (see Table 6.1) adhere to the following naming convention:

SPITZER_S+module_aorkey_expid_dcenum_version_type.suffix

where

- *S+module* = S0, S1, S2, or S3. These correspond to Short-Low (SL), Short-High (SH), Long-Low (LL), or Long-High (LH), respectively. S0 also corresponds to peak-up data.

- *aorkey* = Unique ID number for each AOR.

- *expid* = Exposure ID number. This denotes a distinct array exposure command. The value of *expid* depends on how many FOV positions (see Section 6.6.4) are used. For example, with all 4 modules exercised in staring mode, there would be the following values of *expid*:

    SL2 nod 1: *expid*=1
    SL2 nod 2: *expid*=2
    SH nod 1: *expid*=3
    SH nod 2: *expid*=4
    LL2 nod 1: *expid*=5
    LL2 nod 2: *expid*=6
    LL1 nod 1: *expid*=7
    LL1 nod 2: *expid*=8
    LH nod 1:   *expid*=9
    LH nod 2: *expid*=10

    If only LL2 and LH are exercised:

    LL2 nod 1: *expid*=1
    LL2 nod 2: *expid*=2
    LH nod 1: *expid*=3
    LH nod 2: *expid*=4

    For a 2x2 map in SL1:

    SL1 center, posn 1: *expid*=1
    SL1 center, posn 2: *expid*=2
    SL1 center, posn 3: *expid*=3
    SL1 center, posn 4: *expid*=4

- *dcenum* = The nth exposure in a sequence, at a given spatial position.

- *version* = A counter that is incremented each time a data set is re-processed, starting at 1 for the first processing.

- *type* = The type of pipeline product, e.g. *bcd*, *coa2d*.

- *suffix* = The file format, e.g. *fits*, *tbl*.

For example, one might find the following file in the archive:

SPITZER_S0_21247232_0005_0002_7_bcd.fits

In this case,

S+module = S0, indicating that this is a SL or peak-up observation.

aorkey = 21247232

expid = 0005.

dcenum = 0002.

version = 7, meaning that these data have been reprocessed 7 times, though various versions of the Spitzer pipeline (see Chapter 5).

type = bcd, meaning that this is a Basic Calibrated Data file.

suffix = fits, meaning that this is a FITS format file.

6.2.2   *Level 2 (PBCD) Data*

The Level 2 (PBCD) files within the *pbcd/* download directory (see Table 6.1) adhere to a naming convention similar to that used for Level 1 (BCD) data (see 6.2.1). The parameters *aorkey*, *expid*, and *version* are still used to identify the observation. However, *dcenum* is not used. Instead, an additional "ensemble number" ("E" for ensemble product, or "A" for ancillary ensemble product, followed by the ensemble product ID) is inserted. An example of a Level 2 (PBCD) file is:

SPITZER_S0_21247232_0005_7_E5138813_coa2d.fits

S+module = S0

aorkey = 21247232

expid = 0005.

version = 7, meaning that these data have been reprocessed 7 times, though various versions of the Spitzer pipeline (see Chapter 5).

ensemble product ID = 5138813

type = coa2d, meaning that this is a co-added data file (see Chapter 5).

suffix = fits, meaning that this is a FITS format file.

6.2.3   Calibration Data

Because the calibration files used to produce the data products are the same for many different AORs they appear without any reference to AOR, cycle number, etc.

6.3 Spectroscopic Data Products

6.3.1   Raw Data

The IRS Raw Data consist of one or more Data Collection Events (DCEs) that have been converted to FITS format files. Each individual DCE corresponds to a separate file. These files are presented as three-dimensional data cubes, consisting of a number of non-destructive reads (samples) at fixed time intervals of the 128×128 pixel^2 detector plane, where the number of reads N is determined by integration time and corresponds to the number of layers of the FITS data cube. Thus, the imaged spectra have dimensions of $128 \times 128 \times N$ in the DCE FITS file. Each data plane represents one readout of the array. All IRS spectra will contain either 4, 8, or 16 reads of the array between resets. Any ramp duration (exposure time) longer than 14 seconds results in a sixteen plane raw FITS data product.

Table 6.2 lists the number of reads per ramptime availble for each module, and Table 6.3 lists all the raw files which may be delivered for an AOR that includes spectroscopic observations.

Table 6.2 Number of reads (samples) per ramptime available for each module.

Ramptime	Number of Reads (Samples)
SH	
6	4
30	16
120	16
480	16
LH	
6	4
14	8
60	16
240	16
SL	
6	4
14	8
60	16
240	16
LL	
6	4
14	8
30	16
120	16

Table 6.3 Raw Files Delivered.

Name	Description	Format (a)	Channels (b)	Size (kb)
raw.fits	Raw data cube in units of DN.	$128 \times 128 \times N$ 16-bit int	0,1,2,3	<600
rawb.fits	Raw data cube in units of DN for blue peak-up array. For a spectroscopic AOR, these correspond to Peak-Up Acquisition images.	$128 \times 128 \times N$ 16-bit int	0	200
rawr.fits	Raw data cube in units of DN for red peak-up array. For a spectroscopic AOR, these correspond to Peak-Up Acquisition images.	$128 \times 128 \times N$ 16-bit int	0	200

(a) N = number of samples per ramp
(b) 0=Short-Low (SL), 1=Short-High (SH), 2 = Long-Low (LL), 3 = Long-High (LH)

6.3.2   Calibration Data

In this section we describe the data files that have to do with spectroscopic calibration, including dark subtraction, wavelength calibration, non-linearity corrections, flat-fielding, wavelength calibration, and flux conversion. Table 6.4 lists all of the calibration files delivered by the Spitzer Heritage Archive for a spectroscopic AOR.

Table 6.4: Calibration Files Delivered.

Name	Description	Format (d)	Channels	Size (kb)
b*flatfield.fits	The first data plane contains a 2D flat-field image. NaNs are fatally flagged or unreliable pixels. The second plane stores the uncertainty image (nominally set to 0.001). See Sections 4.1.2 and 5.1.17. See tablenote (a).	$128 \times 128 \times 2$ 32-bit real	0,1,2,3	150
b*flatfield_cmask.fits	Mask of regions to flat-field. The region of the image which will have the flat-field applied contains the value zero. Regions in the flat-field which are deemed "uncertain" have values 256 (bit 8). Regions which are not to be flat-fielded (as determined by wavsamp_omask) are set to 128 (bit 7). See tablenote (a).	128×128 16-bit int	0,1,2,3	37
b*fluxcon.tbl	Conversion from electrons/sec to Jy. Of the 20 columns, the most useful are: Col 1 = spectral order; Col 2 = reference wavelength in microns; Col 8 = flux conversion factor in (electron/sec)/Jy; Col 9 = uncertainty in the flux conversion factor; Col 10 = a_o, Col 12 = a_1, Col 14 = a_2, Col 16 = a_3, Col 18 = a_4, Col 20 = a_5, where a_0, a_1, … a_5 are the coefficients in the polynomial fit described in Section 5.7.4. Also see Section 4.1.4 and Table 6.5 and tablenote (a).	ASCII	0,1,2,3	5
b*fovmask.fits	Maps FOV values to the image. See tablenote (c).	128×128 16-bit int	0,1,2,3	37

b*lincal.fits	Non-linearity model cube. The first plane gives the α coefficients of each pixel. The second plane gives the signal threshold in electrons for applicability of the non-linearity model. Samples exceeding this threshold are not corrected. The third plane contains the uncertainties of each α coefficient. See also Section 5.1.11 and tablenote (a).	$128 \times 128 \times 3$ 32-bit real	0,1,2,3	200
b*lincal_cmask.fits	Masks pixels not to be corrected for non-linearity. Pixels whose linearity is not corrected are set to have values of 4096. See tablenote (a).	128×128 16-bit int	0,1,2,3	37
b*lincal_satcor.fits	Linearity model used during "satcor" (saturation correction) process.	128 x 128 x 3 32-bit int	0,1,2,3	200
b*lincal_satcor_cmask.fits	Pixel mask bits for b*lincal_satcor.fits file. It uses the same bits as the b*lincal_cmask.fits file.	128 x 128 16-bit int	0,1,2,3	37
b*linecorr.tbl	Reference file.	ASCII	0,1,2,3	1
b*omask.fits	Gives locations of the orders for use in stray light removal.	128 x 128 16-bit int	0,1,2,3	37
b*pmask.fits	Mask of semi-permanent bad pixels in the array.	$128 \times 128 \times N$ 16-bit int	0,1,2,3	37
b*r#dark.fits	Dark subtraction cube, in electrons. See tablenote (b).	$128 \times 128 \times N$ 32-bit real	0,1,2,3	281
b*r#dark_cmask.fits	Masks unilluminated pixels to prevent division by flat. See tablenote (b).	$128 \times 128 \times N$ 16-bit int	0,1,2,3	132
b*r#dark_unc.fits	Dark uncertainties. See tablenote (b).	$128 \times 128 \times N$ 32-bit real	0,1,2,3	281
b*umask.fits	Unilluminated region mask.	128×128 16-bit int	0,1,2,3	37
b*wavsamp.tbl	This file is the fundamental element of the wavelength calibration. It defines the parameters of the pseudo-rectangles in array pixel coordinates. The columns of the table are: Column 1 = spectral order, Columns 2 and 3 = x and y coordinates of the center of a given pseudo-rectangle, Column 4 = wavelength (microns) associated with that rectangle. Subsequent columns define the corners of the rectangles. See Sections 4.1.3 and 5.7.3	ASCII	0,1,2,3	32
b*wavsamp_offset.fits	This FITS file gives the distance on the sky in arcseconds from a given pixel to the field-of-view center.	128×128 32-bit real	0,1,2,3	67

*b*wavsamp_omask.fits*	This FITS file shows the order number associated with a given region in an image. For the low-resolution modules (LL and SL), the first and second order spectral regions are denoted by 1 and 2 respectively. The bonus order is denoted by the number 3 (although it is really a first order spectrum). For the high-resolution modules (SH and LH), the echelle orders range from *m*=11 (reddest) to *m*=20 (bluest).	128×128 16-bit int	0,1,2,3	37
*b*wavsamp_wave.fits*	This FITS file shows the wavelength associated with a given pixel. The extraction procedure involves interpolation, so this association is for informational purposes only, and is not appropriate for science quality extractions. The exact wavelength and cross-dispersion solution is provided in the *wavesamp.tbl* file.	128×128 32-bit real	0,1,2,3	67
b0_lmask.fits	Short Low Stray Light Correction Mask.	128×128 16-bit int	0	37
b0_pkumask.fits	Mask unilluminated areas of the Peak-Up arrays.	128×128 16-bit int	0	37
b0_psf_fov.tbl	Slit FOV and PSF information. See tablenote (c).	ASCII	0	2
b0_slt_coeffs.tbl	Stray light coefficients.	ASCII	0	2
b2_psf_fov.tbl	Slit FOV and PSF information. See tablenote (c).	ASCII	2	2
*cal_set*txt*	Identifies what set of CAL files was used in the processing.	ASCII	0,1,2,3	1
cdelt12_distort_blue.tbl	Astrometric distortion coefficients.	ASCII	0	2
cdelt12_distort_blue.tbl	Astrometric distortion coefficients.	ASCII	0	2
cdelt12_distort_full.tbl*	Astrometric distortion coefficients.	ASCII	0	2
cdelt12_distort_red.tbl	Astrometric distortion coefficients.	ASCII	0	2
instrument_FOV.tbl	Gives locations of the FOVs on the focal plane. See tablenote (c).	ASCII	0,1,2,3	5
slit_pa_offsets.tbl	Gives twist angle offsets (north through east) of the FOVs on the focal plane. See tablenote (c).	ASCII	0,1,2,3	1

(a) For the LH module, the calibration files are different for campaigns pre25/post24. For the SL module, the calibration files are different for campaigns pre33/post32, and for the LL module, the calibration files are different for campaigns pre45/post44.

(b) The darks for LH and LL are campaign-dependent.

(c) See Section 6.6.4 for more information on FOV.

(d) N = number of samples per ramp.

Table 6.5: Wavelength ranges used to derive *fluxcon.tbl*.

Order	λ_0 (µm)	λ_1 (µm)
SL2	5.25	7.55
SL3	7.39	8.42
SL1	7.58	13.81**
LL2	14.24	20.84
LL3	19.91	21.10
LL1	20.42	37.86
SH20	9.89	10.6113
SH19	10.39	11.23
SH18	10.96	11.90
SH17	11.59	12.60
SH16	12.30	13.33
SH15	13.11	14.30
SH14	14.03	15.23
SH13	15.14	16.39
SH12	16.32	17.89
SH11	17.75	19.50
LH20	19.05	20.55
LH19	19.81	21.66
LH18	20.90	22.90
LH17	22.10	24.28
LH16	23.48	25.74
LH15	25.02	27.42
LH14	26.76	29.38
LH13	28.80	31.57
LH12	31.04	34.11
LH11	33.74	36.83

**excludes part of teardrop, which starts at 13.44 microns. See Section 7.3.8.

6.3.3   Level 1, Basic Calibrated Data, or BCDs

The individual data frames that emerge, calibrated, from the Spitzer pipeline are Level 1 Data, or Basic Calibrated Data, or BCDs. Table 6.6 is a list of the BCD files delivered by the Spitzer Heritage Archive for a spectrosopic AOR. Figure 6.1 is a cartoon illustrating the relationship between these files.

Table 6.6 BCD Files Delivered.

Name	Description	Format (a)	Channels (b) Type (c)	Size (kb)
bcd.fits	A BCD is either (1) a 2-D echellogram for the high-resolution data (modules S1 and S3); (2) a long-slit 2-D spectrum for the low-resolution data (modules S0 and S2); or (3) an image for the peak-up modes (module S0).	128×128 32-bit real	0,1,2,3 P	< 87

bcdb.fits	If SL spectra were obtained, the peak-up module was also exposing on an adjacent part of the sky. *bcdb.fits* is the cropped, calibrated blue peak-up image.	41x56 32-bit real	0 P	31
bcdr.fits	If SL spectra were obtained, the peak-up imaging arrays were also exposing on an adjacent part of the sky. *bcdr.fits* is the cropped, calibrated red peak-up image.	41x56 32-bit real	0 P	31
bmask.fits	Mask file for *bcd.fits*.	128×128 16-bit int	0,1,2,3 P	37
dmask.fits	Mask file for *lnz.fits*.	$128 \times 128 \times N$ 16-bit int	0,1,2,3 A	<520
drk.fits	Flux image computed in the DARKBASE step (section 5.1.9), just before dark subtraction. If the target is a blank field, these files can be used as to create a dark.	$128 \times 128 \times N$ 32-bit real	0,1,2,3 A	<300
drku.fits	Uncertainty file for *drk.fits*.	$128 \times 128 \times N$ 32-bit real	0,1,2,3 A	<300
droop.fits	2D data with "droop" correction: a constant number is subtracted from all the pixels. See tablenote (a).	128×128 32-bit real	0,1,2,3 A	98
drunc.fits	Uncertainty file for *droop.fits*.	128×128 32-bit real	0,1,2,3 A	67
f2ap.fits	Alternate BCD data without stray light removal or cross-talk correction.	128×128 32-bit real	0,1,2,3 A	98
f2unc.fits	Uncertainty file for *f2ap.fits*.	128×128 32-bit real	0,1,2,3 A	67
full.fits	Red and blue peak-up acquisition image.	128×128 32-bit real	0 P	100
func.fits	Uncertainty file for *bcd.fits*.	128×128 32-bit real	0,1,2,3 P	67
lnz.fits	3D data cube with linearized ramps, in units of electrons.	$128 \times 128 \times N$ 32-bit real	0,1,2,3 A	< 1000
lnzu.fits	Uncertainty file for *lnz.fits*.	$128 \times 128 \times N$ 32-bit real	0,1,2,3 A	< 1000
mskb.fits	BMASK for *bcdb.fits*.	41x56 16-bit int	0 P	8.4
mskr.fits	BMASK for *bcdr.fits*.	41x56 16-bit int	0 P	8.4
out.pline	Output log.	ASCII	0,1,2,3 A	<27
out0.pline	Log file for creation of *full.fits* and initial cutouts of *bcdb.fits* and *bcdr.fits*.	ASCII	0 A	100
outb.pline	Log file for final header updates of *bcdb.fits*.	ASCII	0 A	30
outr.pline	Log file for final header updates of *bcdr.fits*.	ASCII	0 A	30
ridge.tbl	Extraction position table from *bcd.fits*.	ASCII	0,1,2,3 A	< 57

rsc.fits	Data stray light and cross-talk corrected.	128 × 128 32-bit real	0,1,2,3 A	98
rscu.fits	Uncertainty file for *rsc.fits*.	128 × 128 32-bit real	0,1,2,3 A	67
spec2.tbl	Spectrum extracted from *f2ap.fits*.	ASCII	0,1,2,3 A	< 132
spect.fits	Spectrum extracted from *bcd.fits*. Contains the same data as *spect.tbl*, in a different format.	32-bit real	0,1,2,3 A	25
spect.tbl	Spectrum extracted from *bcd.fits*. Contains the same data as *spect.fits*, in a different format.	ASCII	0,1,2,3 P	< 132
uncb.fits	Uncertainty file for *bcdb.fits*.	51x56 32-bit real	0 P	48
uncr.fits	Uncertainty file for *bcdr.fits*.	51x56 32-bit real	0 P	48
xout.pline	Log files output from the extraction pipeline processing.	ASCII	0,1,2,3 A	22

(a) N = number of samples per ramp
(b) 0=Short-Low (SL), 1=Short-High (SH), 2 = Long-Low (LL), 3 = Long-High (LH)
(c) P = Primary, A = Ancillary
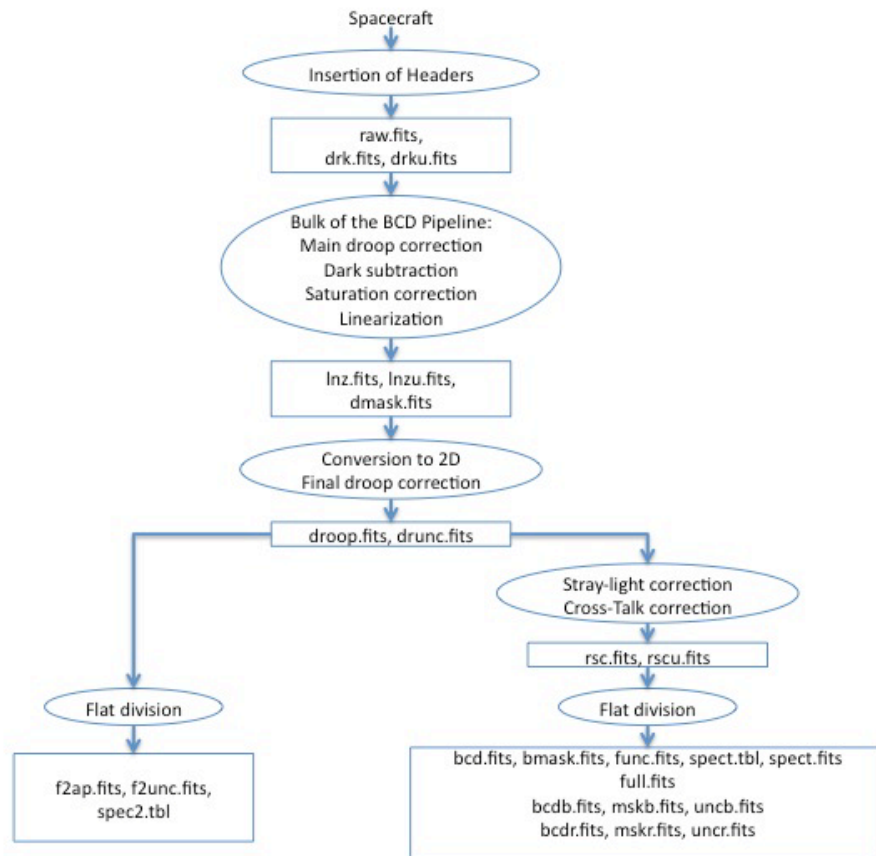
Figure 6.1: Schematic relationship between BCD files.

6.3.4   *Level 2 (Post-BCD) Data*

The products that come from combining Level 1 data are called Level 2, or post-BCD, or PBCD data. Table 6.7 is a list of the PBCD files delivered by the Spitzer Heritage Archive. Figure 6.2 is a cartoon illustrating the relationship between these files.

Table 6.7 PBCD Files Delivered.

Name	Description	Format	Channel (b) Type (c)	Size (kb)
2dcoad.txt	List of coadd weights.	ASCII	0,1,2,3 A	< 1
bkmsk.fits	Mask file for *bksub.fits*.	128 × 128 16-bit int	0,2 P	< 37
bkspc.fits	Coadded, nod-subtracted spectrum, in Jy. See tablenote (a).	32-bit real	0,2 A	25
bksub.fits	For the low-resolution modules in Staring Mode, the co-added products of one nod are subtracted from those of the other to produce a sky-subtracted image (*bksub.fits*). This file (and *bksub.tbl*) should be treated with caution if the area is crowded or contains extended emission around the science target.	128 × 128 32-bit real	0,2 A	< 90
bksub.tbl	Coadded, nod-subtracted spectrum in Jy. This file (and *bksub.fits*) should be treated with caution if the area is crowded or contains extended emission around the science target. See tablenote (a).	ASCII	0,2 P	< 30
bkunc.fits	Uncertainty file for *bksub.fits*.	128 × 128 32-bit real	0,2 P	< 67
c2msk.fits	Mask file *for coa2d.fits*.	128 × 128 16-bit int	1,2,3,4 P	37
c2unc.fits	Uncertainty file for *coa2d.fits*.	128 × 128 32-bit real	0,1,2,3 P	67
coa2d.fits	In AORs with multiple cycles, DCEs at each telescope pointing are averaged to produce the *coa2d.fits*. The DCEs that contribute to each averaged product are listed in **inlist.txt*.	128 × 128 32-bit real	0,1,2,3 P	< 90
ibsmk.txt	List of bmask files for *coa2d.fits*.	ASCII	0,1,2,3 A	< 1
inlst.txt	List of input files for *coa2d.fits*.	ASCII	0,1,2,3 A	< 1
out.pline	Output log.	ASCII	0,1,2,3 A	< 27

ridge.tbl	Extraction position table from *bcd.fits* or *bksub.fits*.	ASCII	0,2 A	< 57
tune.fits	Extracted spectrum from coa2d, in Jy. See tablenote (a).	32-bit real	0,1,2,3 A	25
tune.tbl	Extracted spectrum from coa2d, in Jy. See tablenote (a).	ASCII	0,1,2,3 P	< 134
xout.pline	Log files output from the extraction pipeline processing.	ASCII	0,1,2,3 A	< 15

(a) The data columns are: (1) spectral order, (2) wavelength in microns, (3) flux density in Janskys, (4) flux density uncertainty in Janskys, and (5) pixel status flag.

(b) 0=Short-Low (SL), 1=Short-High (SH), 2 = Long-Low (LL), 3 = Long-High (LH)

(c) P = Primary, A = Ancillary
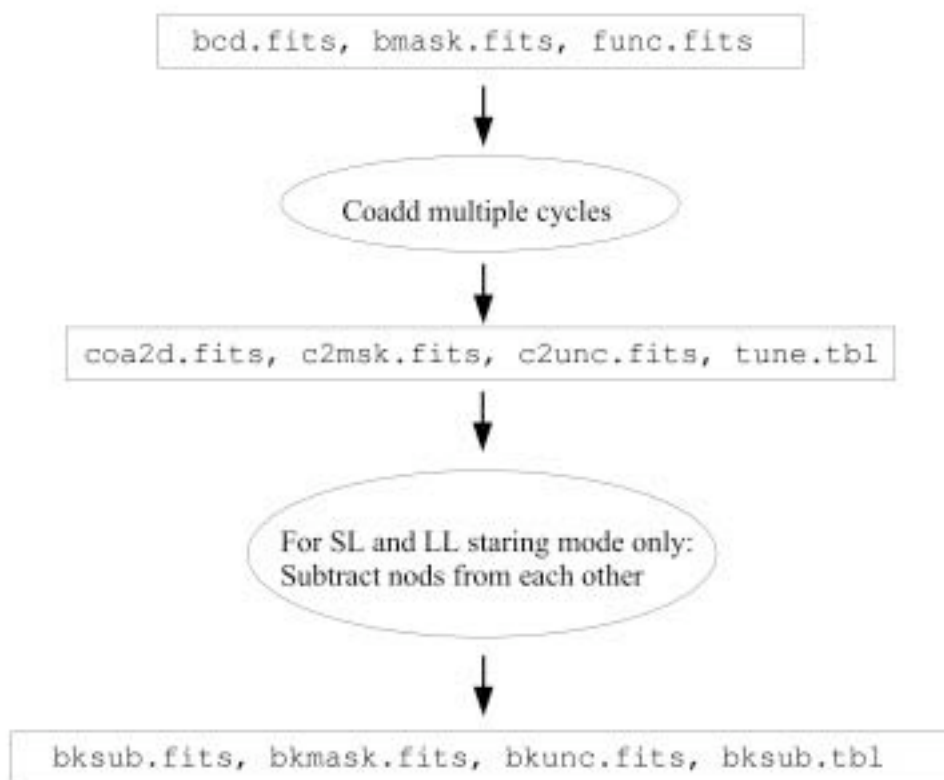
Figure 6.2 Schematic relationship among PBCD files.

6.4 Peak-Up Acquisition (PUA) Products

If your AOR included an IRS peak-up acquisition or was a Peak-up Only observation, then those peak-up data are also available in the archive. Peak-up images are not delivered for PCRS peak-ups. Table 6.8 is a list of Peak-Up Acquisition products available in the archive.

Table 6.8 Peak-Up Acquisition (PUA) Files Delivered.

Raw Files				
Name	**Description**	**Format (a)**	**Channel (b)**	**Size (kb)**
rawb.fits	Raw data file for blue peak-up acquisition image.	$128 \times 128 \times N$ 16-bit int	0	200
rawr.fits	Raw data file for red peak-up acquisition image.	$128 \times 128 \times N$ 16-bit int	0	200
BCD Files				
Name	**Description**	**Format**	**Channel (b) Type (c)**	**Size (kb)**
acqb.fits	Blue peak-up acquisition image.	41×56 32-bit real	0 P	30
acqr.fits	Red peak-up acquisition image.	41×56 32-bit real	0 P	30
full.fits	Red and blue peak-up acquisition image.	128×128 32-bit real	0 P	100
mskb.fits	BMASK for *acqb.fits*.	41×56 16-bit int	0 P	50
mskr.fits	BMASK for *acqr.fits*.	41×56 16-bit int	0 P	50
out0.pline	Log file for creation of *full.fits* and initial cutouts of *bcdb.fits* and *bcdr.fits*.	ASCII	0 A	100
outb.pline	Log file for final header updates of *bcdb.fits*.	ASCII	0 A	30
outr.pline	Log file for final header updates of *bcdr.fits*.	ASCII	0 A	30

(a) N = number of samples per ramp

(b) 0=Short-Low (SL), 1=Short-High (SH), 2 = Long-Low (LL), 3 = Long-High (LH)

(c) P = Primary, A = Ancillary

Peak-Up Imaging (PUI) Products

Table 6.9 lists the data products associated with observations taken in Peak-Up Imaging (PUI) mode.

Table 6.9: PUI Files Delivered.

Raw Files				
Name	**Description**	**Format (a)**	**Channel (b)**	**Size (kb)**
rawb.fits	Raw blue peak-up array data.	$128 \times 128 \times N$ 16-bit int	0	200
rawr.fits	Raw red peak-up array data.	$128 \times 128 \times N$ 16-bit int	0	200
Calibration Files				
Name	**Description**	**Format**	**Channel (b)**	**Size (kb)**
b0_prf_blue.fits	PRF for blue peak-up images.	125×127 32-bit real	0	67
b0_prf_red.fits	PRF for red peak-up images.	125×127 32-bit real	0	67
Basic-Calibrated Data (BCD) Files				
Name	**Description**	**Format**	**Channel (b) Type (c)**	**Size (kb)**
b_msk.fits	RMASK for *bcdb.fits*.	41×56 8-bit int	0 A	22
bcdb.fits	Cropped, calibrated blue image. The pixels are rectangular.	41×56 32-bit real	0 P	31
bcdr.fits	Cropped, calibrated red image. The pixels are rectangular.	41×56 32-bit real	0 P	31
full.fits	2D data before cropping or fluxcal.	128×128 32-bit real	0 A	107
mskb.fits	BMASK file for *bcdb.fits*.	41×56 16-bit int	0 P	8.4
mskr.fits	BMASK file for *bcdr.fits*.	41×56 16-bit int	0 P	8.4
outb.pline	Log file for final header updates of *bcdb.fits*.	ASCII	0 A	30
outr.pline	Log file for final header updates of *bcdr.fits*.	ASCII	0 A	30
r_msk.fits	MOPEX RMASK file for *bcdr.fits*.	41×56 8-bit int	0 A	22
uncb.fits	Uncertainty file for *bcdb.fits*.	41×56 32-bit real	0 P	48
uncr.fits	Uncertainty file for *bcdr.fits*.	41×56 32-bit real	0 P	48
Post-BCD Files				
Name	**Description**	**Format**	**Channel (b) Type (c)**	**Size (kb)**
b_cov.fits	Coverage map for *b_mos.fits*.	63×201 32-bit real	0 A	59

b_mos.fits	MOPEX blue peak-up imaging mosaic. The images have been re-sampled to square pixels.	63 × 201 32-bit real	0 P	59
b_unc.fits	Uncertainty file for *b_mos.fits*.	63 × 201 32-bit real	0 P	59
cdf.log	List of post-BCD namelist files.	ASCII	0 A	0.3
mopex.log	Log of MOPEX processing.	ASCII	0 A	91
mopex.nl	MOPEX namelist file.	ASCII	0 A	4
r_cov.fits	Coverage map for *r_mos.fits*.	63 × 201 32-bit real	0 A	59
r_mos.fits	MOPEX red peak-up imaging mosaic. The images have been re-sampled to square pixels.	63 × 201 32-bit real	0 P	59
r_unc.fits	Uncertainty file for *r_mos.fits*.	63 × 201 32-bit real	0 P	59

(a) N = number of samples per ramp

(b) 0=Short-Low (SL), 1=Short-High (SH), 2 = Long-Low (LL), 3 = Long-High (LH)

(c) P = Primary, A = Ancillary

6.5 Bit Masks

Pixel status is tracked in the pipeline with several masks. In each mask, individual bits are set for each pixel that meets a particular condition. Some conditions are permanent, while others are peculiar to the current DCE (such as cosmic ray hits). Several steps in the pipeline update the current pixel status. Ultimately, each wavelength in the extracted spectrum has a status flag that is derived from all pixels that contribute to that wavelength. In this section, we describe the masks that are of most interest to the user. WARNING: Different masks do not always use the same bit to indicate the same condition.

6.5.1   Pixel Mask - *pmask.fits*

The two-dimensional "pixel mask" *pmask.fits* tracks semi-permanent bad pixel conditions. This file is the same for many different AORs. Table 6.10 describes the bit flags set in the pmask. More information can be found in the header of the *pmask.fits* files, available in the *cal/* directory.

Table 6.10: pmask Bit Settings.

Bit #	Condition
0	Not used
1	Not used
2	Not used
3	Not used
4	Not used
5	Not used
6	Non-linear "rogue" pixels

7	Dark current is too variable (dark calibration accuracy will be unacceptably low)
8	Not used
9	Not used
10	Dark current is too high (pixel is hot)
11	Not used
12	Not used
13	Not used
14	The pixel does not respond to light (pixel is dead)
15	Reserved: sign bit

6.5.2   DCE Mask - dmask.fits

The three-dimensional "DCE mask" *dmask.fits* stores pixel conditions encountered during a pipeline run. It is created by CVTI2R4 (Section 5.1.1) module very early in the pipeline, and updated up to the last step in the pipeline that operates on the 3D data cube, LINEARIZE (Section 5.1.11). Typical conditions masked are saturation (298,000 electrons), radiation hits, data "missing" in downlink, uncorrectable non-linearity, etc. Each of these conditions are identified sample-by-sample in the 3-D FITS file. Table 6.11 describes the conditions that cause each bit to be set. Note that bit 12 will be set if bits 7, 10, or 14 are set in the pmask, if there is digital saturation, of if data are missing in telemetry. Samples with bit 13 set cannot be linearized either, and they will be ignored. This mask may be useful in the case of a solar storm which resulted in an unusually high number of cosmic rays. In this case, bit 9 will be set in each sample that received a hit. If more than one sample per pixel has bit 9 set, the data from that pixel should be regarded with suspicion.

Table 6.11: dmask Bit Settings.

Bit #	Condition
0	Incomplete or questionable mux bleed correction (MUXBLEED-CORR)
1	No row droop correction applied (ROWDROOP)
2	Radhit detection was done (RADHIT)
3	Digital saturation detected (CVTI2R4)
4	Saturation corrected by IMAGEST mode 2
5	Latent-image flag
6	Droop removed using questionable value (DROOPOP)
7	Not used
8	Not used
9	RADHIT detection
10	Baseline adjustment failed (reserved for BASECAL)
11	Data bad (initial dmask; RADHIT checks this bit)
12	Non-linearity correction could not be computed (LINEARIZ)
13	Sample exceeds 280000 e−. (LINEARIZ)
14	Data missing in downlink (CVTI2R4)
15	Reserved: sign bit

6.5.3   BCD Mask - bmask.fits

The two-dimensional "BCD mask" *bmask.fits* is the pixel status mask associated with the fully processed two-dimensional BCD product. The bmask is used to describe the status of both the *bcd.fits* data and the *f2ap.fits* data. It stores pixel conditions encountered during the entire pipeline run. The bmask uses the dmask as input, masking some of the same conditions. However, sample-to-sample information is not retained. Instead, if one or more samples along a ramp are flagged in the dmask, then the corresponding pixel is flagged in the bmask. Additional conditions flagged in the bmask (on a pixel-by-pixel basis) are:

- Only one or zero samples were used to compute a slope (bits 12 or 13)

- Flat-field was not applied or was questionable (bits 7 or 8).

- Stray light removal or cross-talk correction was not applied (bit 9).

- Pixels 7, 10, and/or 14 masked in the pmask (bit 14).

Table 6.12 describes the conditions that cause each bit to be set. The extraction pipeline considers bits 7, 12, 13, and 14 as fatal and interpolates over them. Bit 7 is considered fatal because it is used to signal the region in which the flat changes very rapidly (at the edges of the slit). Although the setting of bit 8 ("no flat applied") also marks a "fatal" condition, it is used on un-illuminated regions of the slit, and is irrelevant for the extraction pipeline.

Table 6.12: bmask Bit Settings.

Bit #	Condition
0	Not used
1	Latent-image flag
2	Digital saturation detected along the ramp (bit 3 in dmask).
3	RADHIT detection along ramp (bit 9 in dmask).
4	Non-linearity correction could not be computed (bit 12 in dmask).
5	Not used
6	Droop removed using questionable value (bit 6 in dmask).
7	Flat-field applied using questionable value (FLATAP)
8	Flat-field could not be applied (FLATAP)
9	Stray-light removal or cross-talk correction not applied
10	At least one sample exceeds 280000 e−. (bit 13 in dmask).
11	Data missing in downlink (bit 14 in dmask).
12	Only one usable plane
13	No usable planes
14	Pixel masked in pmask
15	Reserved: sign bit

6.5.4   Co-added Masks - c2msk.fits and bkmsk.fits

The two-dimensional "Coadd 2D mask" *c2msk.fits* is produced by the 2D co-adder. The coadd module generates an average of multiple DCEs and performs outlier rejection; it omits pixels that are fatally flagged in the bmask. The output mask, the c2msk, does not preserve information on which fatal bit

condition was set. The only conditions masked are: too few values were co-added for the pixel (currently < 1), and pixel fatally masked in bmask.

The *bkmsk.fits* is the mask corresponding to the *bksub.fits* product. It is the result of performing the "OR" operation between the two masks of the images used in the subtraction.

Table 6.13: c2msk/bkmsk Bit Settings.

Bit #	Condition
0	Not used
1	Not used
2	Not used
3	Not used
4	Not used
5	Not used
6	Not used
7	Flat-field applied using questionable value
8	Not used
9	Not used
10	Not used
11	Not used
12	Not used
13	No valid planes are available to coadd
14	Not used
15	Reserved: sign bit

6.5.5   *Masked Pixels in the Extracted Spectra - spect.tbl, spec2.tbl, tune.tbl, bksub.tbl*

Extracted spectrum tables include a status flag for each wavelength. Multiple pixels contribute to each wavelength, and some wavelengths include fractions of some pixels. The status flag is the result of a bit-wise "OR" operation on the pixel status flags in the 2D mask file for all contributing pixels. That is, each bit in the spectrum flag is set if it was set in any of the contributing pixels, even those that contribute only fractionally to the wavelength. No information is retained about which of the contributing pixels had which status.

The definition of the bits in the status flag is the same as in the mask corresponding to the data from which the spectrum was extracted. Thus, the *spect.tbl* and *spect2.tbl* tables have flags with the same definition as the *bmask.fits*; *tune.tbl* tables have flags with the same definition as the *c2msk.fits*. Some status flags in the bmask are "fatal," meaning that no usable information was contained in the flagged pixel. For example, bit 13 ("no usable planes") is fatal. Other flags suggest that the pixel is highly suspect, but may still be of interest for some programs.

6.6 Header Keywords

The FITS header keywords in an IRS BCD data file provide detailed information about the observation. The header is updated late in the pipeline as part of the creation of the BCD file. Thus, the *bcd.fits* file contains the updated header, while partially-processed products from earlier in the pipeline may have different keywords. In addition, a history of the pipeline processing is provided at the end of the FITS header. In this chapter, we review the keywords in the spectroscopic *bcd.fits* header. Many keywords are self-explanatory, so we highlight only those of greatest interest to the observer. An example FITS header is given as an appendix to this handbook. The meaning of most keywords is the same for Peak-Up Imaging observations.

6.6.1 Basic Keywords

CALSET indicates the version of the calibration files used to produce the data product.

CREATOR indicates the latest pipeline version used to reprocess the files.

AORKEY is a unique 7-digit identification number for each Astronomical Observation Request. It is part of the file name for each BCD.

PROGID gives the program ID under which the current data were obtained.

FOVNAME is the name of the field-of-view used for the observation. For example, a Staring Mode observation using SL1 will result in DCEs acquired with the target (given by header keywords RA RQST and DEC RQST) positioned first at "IRS Short-Lo 1st Order 1st Position", and then at "IRS Short-Lo 1st Order 2nd Position", corresponding to each of the designated nod positions. See also Section 6.6.4.

BUNIT gives the units of the data; e.g., "electrons/sec".

 FLUXCON gives the conversion factors from electrons/sec to Janskys. This keyword is given for each spectral order, but pertains only to the module associated with the BCD.

VHELCORR and VLSRCORR allow correction of the spectra for the orbital velocity of Spitzer. The values of these keywords should be added to velocities derived from IRS spectra, to obtain final velocities in the Heliocentric or LSR frames respectively. These keywords will be of interest only to observers measuring velocities with high precision from Short-High or Long-High spectra.

For bookkeeping, it may be useful to search for particular targets by looking at OBJECT = Target Name.

The IRS peak-up keywords are mostly relevant to the peak-up DCEs. In spectral DCEs the only peak-up keyword of interest is APKUPCEN. If the value of this keyword is 1, then the corresponding peak-up was successful, meaning that the centroid of the brightest source in the peak-up array field-of-view was returned.

6.6.2 *Exposure Time*

There are several integration-time-related keywords. Of greatest interest to the observer is the "effective integration time", which is the time on-chip between the first and last non-destructive reads for each pixel. It is called

$$\text{RAMPTIME} = \text{Total integration time for the current DCE.}$$

The value of RAMPTIME gives the usable portion of the integration ramp, occurring between the beginning of the first read and the end of the last read. It excludes detector array pre-conditioning time. It may also be of interest to know the exposure time at other points along the ramp. The SUR sequence consists of the time taken at the beginning of a SUR sequence to condition the array (header keyword DEADTIME), the time taken to complete one read and one spin through the array (GRPTIME), and the non-destructive reads separated by uniform wait times. The wait consists of "clocking" through the array without reading or resetting. The time it takes to clock through the array once is given by the SAMPTIME keyword. So, for an N-read ramp:

$$\text{RAMPTIME} = 2 \times (N-1) \times \text{SAMPTIME} \qquad \textbf{Equation 6.1}$$

and

$$\text{DCE duration} = \text{DEADTIME} + \text{GRPTIME} + \text{RAMPTIME} \qquad \textbf{Equation 6.2}$$

Note that peak-up data is not obtained in SUR mode. It is obtained in Double Correlated Sampling (DCS) mode. In that case, RAMPTIME gives the time interval between the 2nd sample and the preceeding reset. The on-source exposure time is given by GRPTIME:

$$\text{GRPTIME} = [\text{spincount} + 1] \times \text{SAMPTIME} \qquad \textbf{Equation 6.3}$$

where the spincount is 7 for all peak-up acquisition observations.

6.6.3 *Reconstructed Pointing*

The RA, DEC, and position angle of the observation are recorded in several ways. The FITS header includes information on both the requested pointing and the actual position of the telescope, as measured during the time of the observation and corrected for proper motion, as entered in SPOT. All reconstructed values are averaged over the time interval of the DCE. The pointing-related keywords include:

RA_RQST, DEC_RQST, PA_RQST, and UNCRTPA give the requested values for the current DCE. Here the position angle is given for the +Z axis of the telescope, measured East of North. Its uncertainty can be found in the keyword UNCRTPA.

RA_REF and DEC_REF give the original target position. If the observation is part of a group (e.g., cluster target type or Spectral Mapping mode), then the central target position may be different from the requested position of the current DCE.

RA_FOV, DEC_FOV, and PA_FOV give the field-of-view pointing, while RA_SLT, DEC_SLT, and PA_SLT give the center of the slit pointing. The reconstructed pointing of the telescope is recorded for both the re-quested field-of-view and the center of the slit. So, in a Staring Mode observation of a single target, the pointing on the center of the slit will change at the two nod positions, but the two fields-of-view will each be pointed at the same position (with some small pointing uncertainty). Field-of-view and center of the slit positions will be the same for Spectral Mapping mode in which the slit centers have been requested.

PTGDIFF is the difference between the reconstructed pointing (for the field-of-view) and the requested pointing. The requested and reconstructed pointings are computed with double-precision, but the reconstructed pointing and, therefore, the value of PTGDIFF is accurate only to 0.2 arcsec (1σ radial). This uncertainty applies equally to the above FOV and SLT keywords. For data taken before December 2004, pointing control was based on gyros, resulting in relatively large values of PTGDIFF. Since December 2004, pointing control has been based on the star tracker. If an IRS or PCRS peak-up operation failed, then the telescope could not make a correction to the attitude, and by default assumed the correction to be zero. In this case, the value of PTGDIFF may be misleadingly small. This is also the result if no peak-up is requested. A false positive peak-up, on the other hand, may lead to large PTGDIFF values by virtue of differences between the reference (commanded) positioning and the attitude measured from the star tracker.

6.6.4   FOVID and FOVNAME

The IRS BCD headers include the keywords "FOVID" and "FOVNAME", both of which describe the field of view of the observation. The difference is that FOVID takes on integer values, while FOVNAME is a character string. The table below provides a translation between these FOVID and FOVNAME.

Table 6.14 Translation between header keyword values for FOVID and FOVNAME.

FOVID	FOVNAME
18	IRS_Red_Peak-Up_FOV_Center
19	IRS_Red_Peak-Up_FOV_Sweet_Spot
22	IRS_Blue_Peak-Up_FOV_Center
23	IRS_Blue_Peak-Up_FOV_Sweet_Spot
26	IRS_Short-Lo_1st_Order_1st_Position
27	IRS_Short-Lo_1st_Order_2nd_Position
28	IRS_Short-Lo_1st_Order_Center_Position
29	IRS_Short-Lo_Module_Center
32	IRS_Short-Lo_2nd_Order_1st_Position
33	IRS_Short-Lo_2nd_Order_2nd_Position
34	IRS_Short-Lo_2nd_Order_Center_Position
38	IRS_Long-Lo_1st_Order_1st_Position
39	IRS_Long-Lo_1st_Order_2nd_Position
40	IRS_Long-Lo_1st_Order_Center_Position
41	IRS_Long-Lo_Module_Center
44	IRS_Long-Lo_2nd_Order_1st_Position
45	IRS_Long-Lo_2nd_Order_2nd_Position
46	IRS_Long-Lo_2nd_Order_Center_Position
50	IRS_Short-Hi_1st_Position

51	IRS_Short-Hi_2nd_Position
52	IRS_Short-Hi_Center_Position
56	IRS_Long-Hi_1st_Position
57	IRS_Long-Hi_2nd_Position
58	IRS_Long-Hi_Center_Position

6.6.5　Example IRS Data
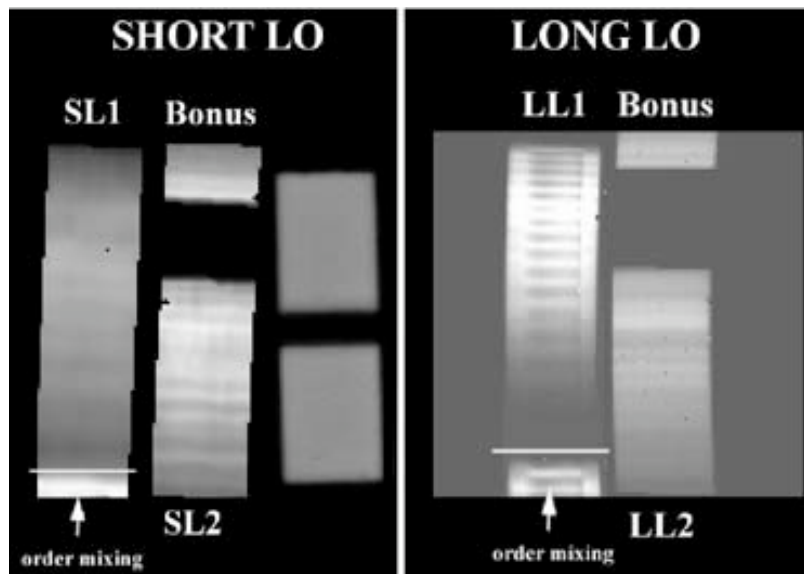
Figure 6.3: Flat field images for the Short-Low (left) and Long-Low (right) modules. These images illustrate the full areas of the detector arrays dedicated to each spectral order. For both modules, the 1st order (longer wavelength) spectrum is on the left and the 2nd order (shorter wavelength) spectrum is on the right; wavelength increases from top to bottom within each order. The short bonus segment is visible above the 2nd order spectrum for both modules. The SL image also shows the two peak-up arrays. Spectral fringing is visible in the LL1 spectrum.
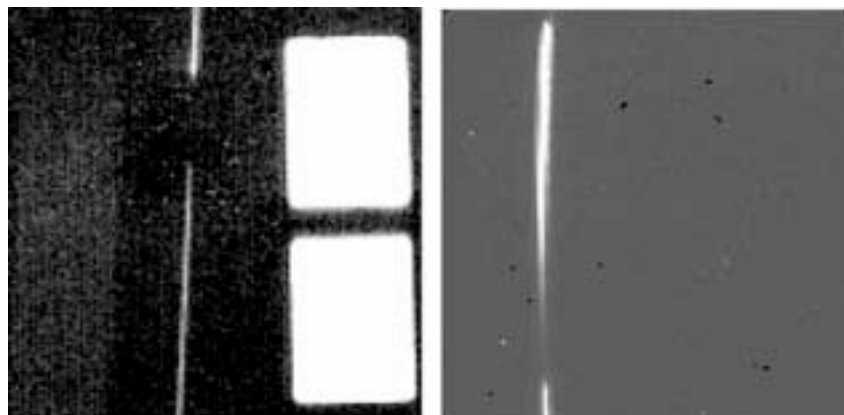
Figure 6.4: Unprocessed point-source data from the SL (left) and LL (right) modules. The SL image shows a spectrum obtained in 2nd order (along with the 1st order bonus segment at the top and the saturated IRS peak-up arrays on the right), while the LL image shows a spectrum obtained in 1st order.
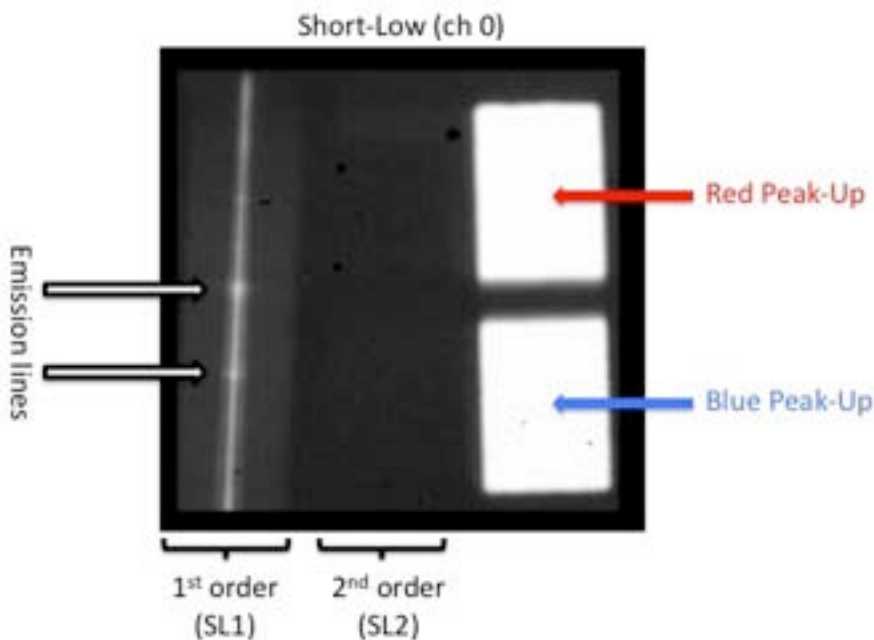
Figure 6.5: Example *bcd.fits* image of a galactic nucleus. In this case the galaxy was observed using the 1st order Short-Low sub-slit (SL1). The bright continuum can be seen running vertically down the image on the left. Two bright (and several faint) emission lines/bands are clearly detected as features of increased intensity superimposed on the continuum. The square regions to the right are the well-exposed peak-up apertures. Note that light from the 2nd order SL sub-slit (SL2) is also deposited on the detector array to the right of SL1; however, SL2 is off-target (i.e., SL2 is looking at blank sky). This is because the SL2 sub-slit is located more than 1 arcminute away from the SL1 target position on the Spitzer focal plane. Consequently, there is no apparent SL2 spectrum.
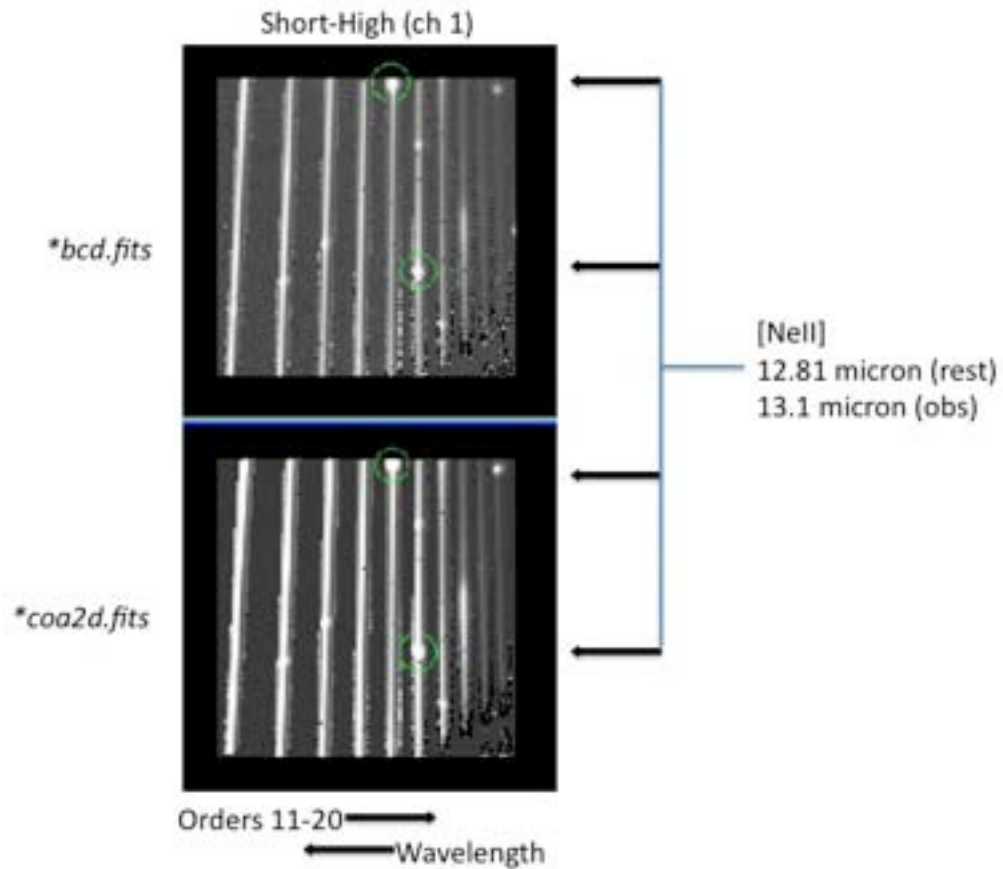
Figure 6.6: Example *bcd.fits* and *coa2d.fits* IRS data products for a bright (~0.5 Jy at 15 microns) galaxy with strong emission lines observed using the Short-High (SH) module of the IRS. The rest frame 12.81 micron [NeII] line, appearing at an observed wavelength of ~13.1 microns, is circled in both images. Due to the overlap between orders in SH, the [NeII] emission line appears in both orders 15 and 16 in these data. The *bcd.fits* and *coa2d.fits* files are from the first nod position. Six individual nod frames were combined to produce the *coa2d.fits* image.
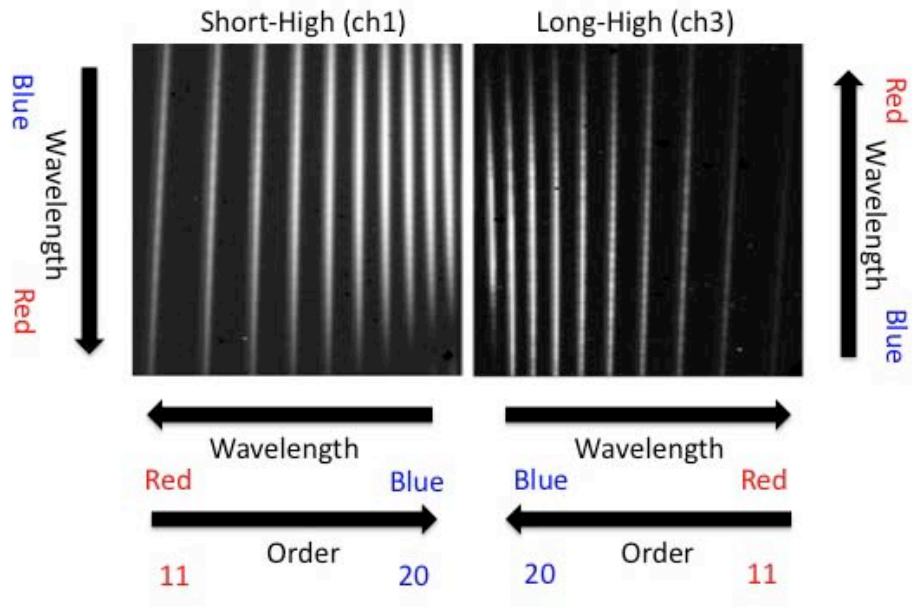
Figure 6.7: Unprocessed point-source data from the SH and LH modules. Both images show the typical layout of a cross-dispersed echellogram.
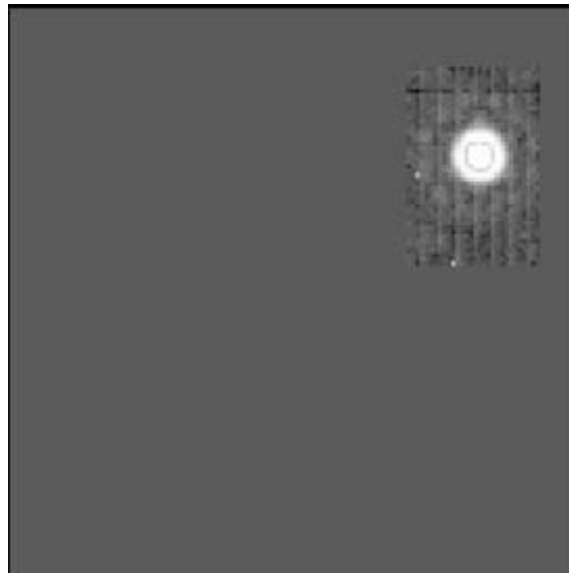
Figure 6.8 Example image of a star in the red IRS peak-up array. This image shows the onboard-processed DCE #3, with the rest of the image masked.
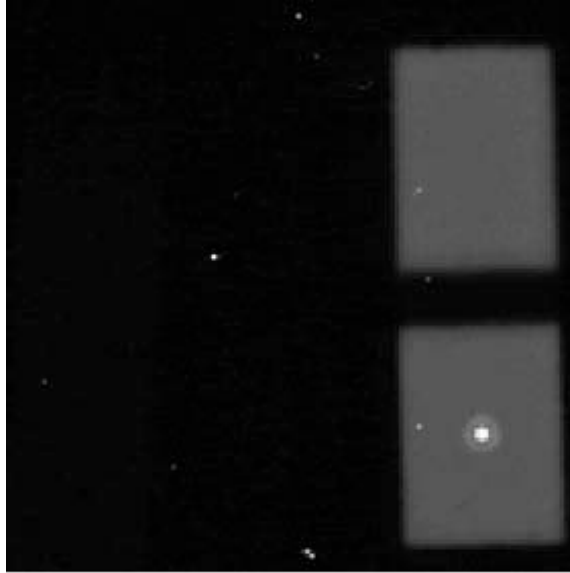
Figure 6.9: **In-orbit image of a point source on the blue IRS peak-up sub-array. The first diffraction ring of the point source is clearly visible. Bright pixels in the image are cosmic ray hits. The illuminated red peak-up sub-array is visible in the figure above the blue sub-array, but does not contain any stars.**

Chapter 7. Data Features and Artifacts

This chapter summarizes the most common features and artifacts seen in IRS Peak-Up and spectroscopic data. We describe these features, show images with representative examples, and recommend methods for their removal from the data.

7.1 Peak-Up Imaging (PUI)

7.1.1   Saturated Data

Saturated samples in the data can be identified in raw DCEs or in intermediate BCD products (*lnz.fits* or *dmask.fits*). The IRS uses a signed 16-bit A-to-D converter, resulting in a DN range for science observations of -32747 DN to 32767 DN. Therefore, in raw DCEs, saturated samples have values of 32767 DN. For data taken in DCS mode, like peak-up acquisition data, the range is 0 to 65535 DN.

Because the gain is 4.6 electrons/DN, saturated samples in *lnz.fits* have values typically above 298,000 electrons. This is slightly less than 4.6×2^{16} because of dark current subtraction. Saturated samples have mask values in *dmask.fits* with bit #3 set. That is, the bit-by-bit logical "OR" operation of the sample mask value with the value 8 is non-zero.

The presence of saturated samples does not necessarily invalidate the data of the corresponding *bcd.fits* pixel because saturated samples in a ramp are excluded from slope calculations. Therefore, the reduction in the signal-to-noise ratio due to saturation depends on how many samples are saturated in the ramp. Bit #2 is set in *bmask.fits* for BCD pixels in which at least one sample of the ramp was saturated. Bit #13 is set if all samples of the ramp are saturated, and bit #12 is set if all but the first sample are saturated.

7.1.2   Latent Images

Bright objects falling on the IRS SL detector can result in persistent charge that appears as a latent image of the object in subsequent exposures. For exposures with $(1-5) \times 10^4$ electrons pix^{-1} in the last sample, 0.04 to 0.1% will remain behind as latent images in the subsequent exposure. These latents decay rather slowly, with an e-folding time of ~1100 sec. For many successive exposures source flux can appear to increase by several percent. Given the parallel position of the peak-up fields-of-view to the SL slits, it is not uncommon for a bright object to fall on the peak-up arrays during science operations. Proper dithering strategies can mitigate the latent image problem, although with some loss of signal-to-noise on the affected pixels.

A second source of latent charge on the detector is simply the background. As a result, during very long Peak-Up Imaging AORs or those in very high background regions, the background level may be seen to rise slowly over time. This effect is stable and varies smoothly, so users may fit the (small) rise in the background and subtract it.

7.1.3   Rogue Pixels

A rogue pixel is a pixel with abnormally high dark current and/or photon responsivity (a "hot" pixel) that manifests as pattern noise in an IRS BCD image. The term "rogue" was used originally to distinguish pixels whose hotness was unpredictable, but now rogue pixel masks include those that are permanently as well as temporarily hot. Proper dithering will mitigate the effect of rogue pixels, but they should be masked before mosaicking. See also Section 7.2.2.

7.2 All Spectral Modules

7.2.1   Saturated Data

Please see Section 7.1.1.

7.2.2   Rogue Pixels and NaNs

Rogue pixels are warm/unstable pixels. Early in the mission, all four IRS arrays were subjected to powerful solar proton events that deposited the equivalent dose of protons expected over 2.5 years in only two days. This damaged 1% of the SL and SH pixels, and 4% of the LL and LH pixels. See also Section 7.1.3. The greatest science impact is to the LH module because the illuminated portion of the orders subtends only a few pixels in the spatial direction, making it more difficult to recover lost information by nodding the source along the slit. As the Spitzer cold mission progressed, the number of rogues and permanently damaged pixels increased. The bias for LH was lowered in IRS Campaign 25 in order to slow down the rate of rogue production at the expense of a decrease in sensitivity. Similarly, the bias and temperature were changed for LL in Campaign 45.

The damaged pixels are masked from data processing by assigning NaN status to them. This prevents numerical operations from being affected by their presence. Assigning any other real number would lead to improper processing of the surrounding signal information, such as during the extraction process. By default, the post-BCD EXTRACT module (see Section 5.7.3) interpolates over the NaN pixels when adding flux within an aperture. The affected pixels are marked in the corresponding pmask and bmask.

Occasionally, it is possible for rogue pixels to propagate through the pipeline without being flagged as NaNs. In this case, these spurious pixel values will be extracted and appear as sharp spikes in the final spectrum. Such features should be readily recognizable as spectral features which are too sharp to be real. The IRSCLEAN_MASK package enables observers to visually inspect such pixels and interpolate over them. If there is any doubt about the reality of a given spectral feature seen in an extracted spectrum, we recommend that the observer always examine the 2D BCD images to cofirm that the feature shows the expected spatial and spectral dispersion on the array.

7.2.3   Radhits on rogue pixels

Low and high resolution spectra may show large spikes when cosmic radiation hits (radhits) fall on highly-nonlinear (rogue) pixels. This effect is made more evident by the pipeline's (S15 and onward) rejection of samples following a radhit event. The early samples in nonlinear (rogue) pixels generally have a steeper slope than the samples rejected after the radhit, increasing the flux after radhit rejection.

Rogue pixel data have incorrect values and should generally be filtered out before or during spectral extraction. Two methods can be used to remove the offending pixels:

1. Use SPICE to re-extract the spectrum (using *bcd.fits* files as a starting point). Within SPICE you can use the EXTRACT 'Mask' pulldown menu to mark bit #3. This will cause SPICE to ignore pixels with radhits. Then run EXTRACT.

2. Use the IRSCLEAN_MASK routine to filter and replace the offending pixels.

7.2.4 Severe Jailbars

Very strong vertical stripes (jailbars) are sometimes seen in a single BCD image of an AOR. This may lead to very noisy or corrupted spectra.

A few rows of data in one plane of the corresponding cube will be seen to have anomalously high values (can be several tens of thousands of DN). These rows are not tagged as missing data, and in cubes of 4 samples, they are not recognized as outliers. Even before slope estimation, these rows affect the entire array because droop is impacted for all pixels of that plane, leading to severe jailbars.

The severe jailbars discussed here occur very infrequently (~1/700 DCEs). The root cause of the corrupted rows in the cube leading to severe jailbars is unknown. More mild jailbars may observed as a result of other causes.

There is currently no fix for this problem in the pipeline. It would have to be fixed at the raw datacube level. If multiple DCEs are available, throw out the offending DCE and recompute the spectrum.

7.2.5 Latent Charge

Despite the resetting of the detector after every integration, a small fraction of charge on the detector persists between frames. This latent charge is thought to be small, (~1−2% of the charge on the pixels) and decays slowly over time. It is removed by the annealing process which occurs every three to four days of an IRS campaign.

In the case of very faint sources, the source of latent charge is the zodiacal background. This charge can build up to significant levels over long integrations, sometimes as much as 30−50% of the true background in ~4 hour integrations. The slope of the latent build up is a function of wavelength and sky background but does not appear to be constant from AOR to AOR. The latent signal can be removed by fitting the slope of the background in each row (i.e. wavelength) as a function of frame number and subtracting that amount row-by-row from each frame. The slope can be fit by 1D or 2D polynomials and the fits should be visually checked to ensure that anomalous values for the sky have not been obtained. Figure 7.1 shows an example of the charge build-up in a long integration in a field with low (~18 MJy/sr) background as well as a 2D polynomial fit which was removed from each BCD at each wavelength.

This effect should not be confused with the build up of charge and stabilization of signal discussed in Grillmair et al. (2007, ApJ 658, L115), when observations of a bright source are undertaken.
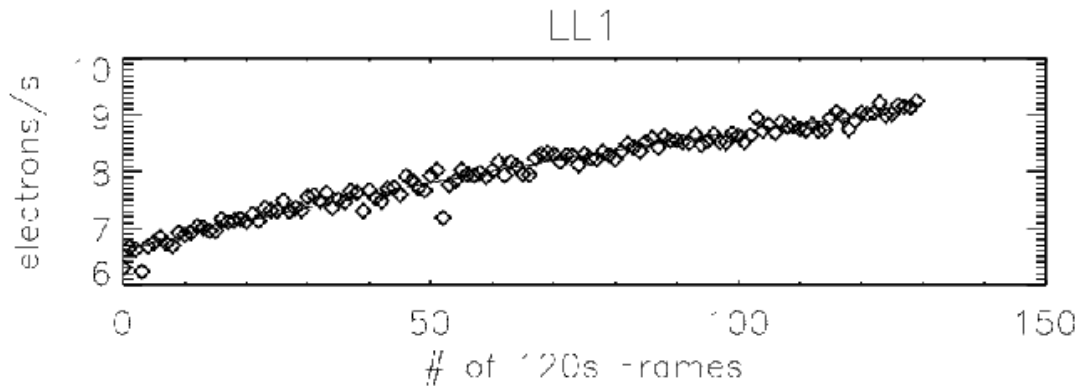
Figure 7.1: Latent charge build-up in electron/s on the LL array in a long (120 s) integration.

7.3 Low Resolution (SL and LL) Spectral Modules

7.3.1   *Low-Resolution Nonrepeatability*

The one standard deviation repeatabilities of standard star flux measurements are: 4.6% for SL1, 2.2% for SL2, 3.1% for LL1, and 2.3% for LL2. These are for observations (AORs) that use high accuracy self-peakup. This is based on 129 observations of the standard star HD 173511 (see Figure 7.2). Note that the distributions of flux values are non-Gaussian and that the SL1 distribution in particular has a tail of low flux values. The variations in measured flux are attributed to a combination of inaccuracies in telescope pointing (which can place the source away from the center of the slit) and flat field errors.

All spectrographs are susceptible to pointing errors. Flux calibrations are based on the median of all HR 7341 observations, so individual observations may give fluxes above or below the "truth" value.
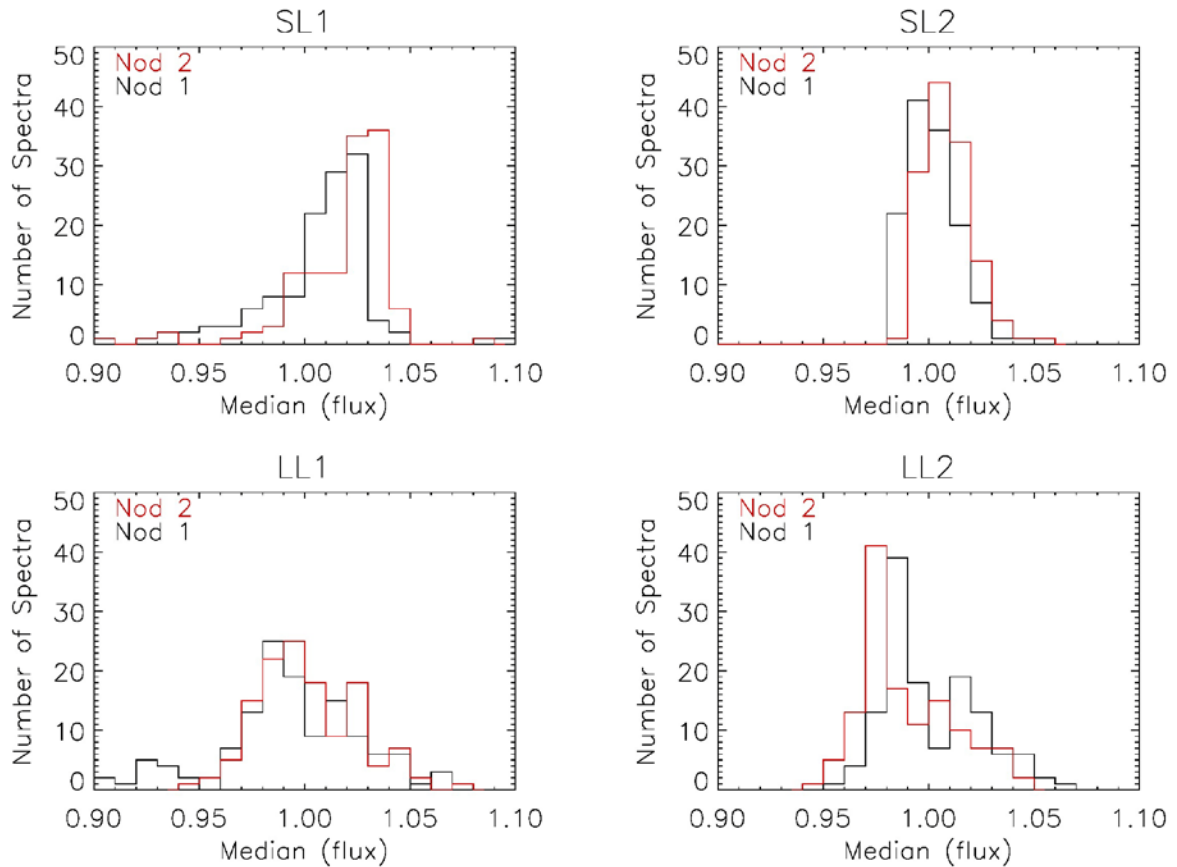
Figure 7.2: 129 observations of the standard star HD 173511, processed using the S18.18 pipeline. The observations used high accuracy self-peakup. In each case the spectra have been normalized to the median of all fluxes at nod 1.

7.3.2   Order Mismatches

Depending on telescope pointing accuracy (see Section 7.3.1), there can be mismatch between SL2/SL1, SL1/LL2, or LL2/LL1. See Figure 7.3 for an example of an SL1/LL2 mismatch. Such a mismatch could be mistaken as a broad spectral feature.
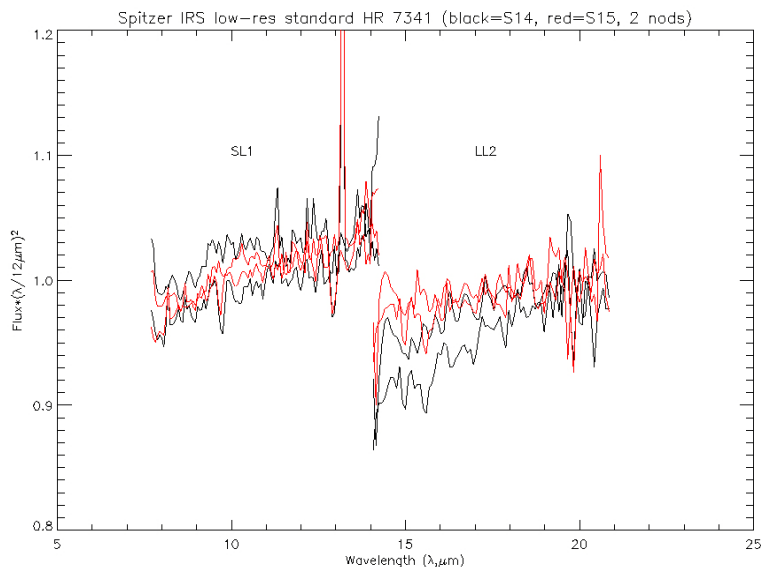
Figure 7.3 Order mismatch between SL1 and LL2, which might be mistaken as a broad absorption feature. For each order the two nods are shown.

Mitigation: Critically inspect all order matching. Individual orders that are low may be scaled up to match. Imaging photometry from IRAC, MIPS24, and IRS Peak-Up may be used to derive more accurate order matching corrections. However, see Section 7.3.3 on SL1 curvature induced by wavelength-dependent slitloss.

7.3.3   Curvature in SL1

Spectral curvature (concave upward) may be induced in SL1 when the source is not centered in the slit, due to chromatic PSF losses. The curvature increases with apparent flux deficit. See Figure 7.4.

Observers should be very wary of broad spectral features at levels <5%, especially at the order boundaries. The effects of the spectral curvature and order mismatch may be mistaken as broad absorption features.
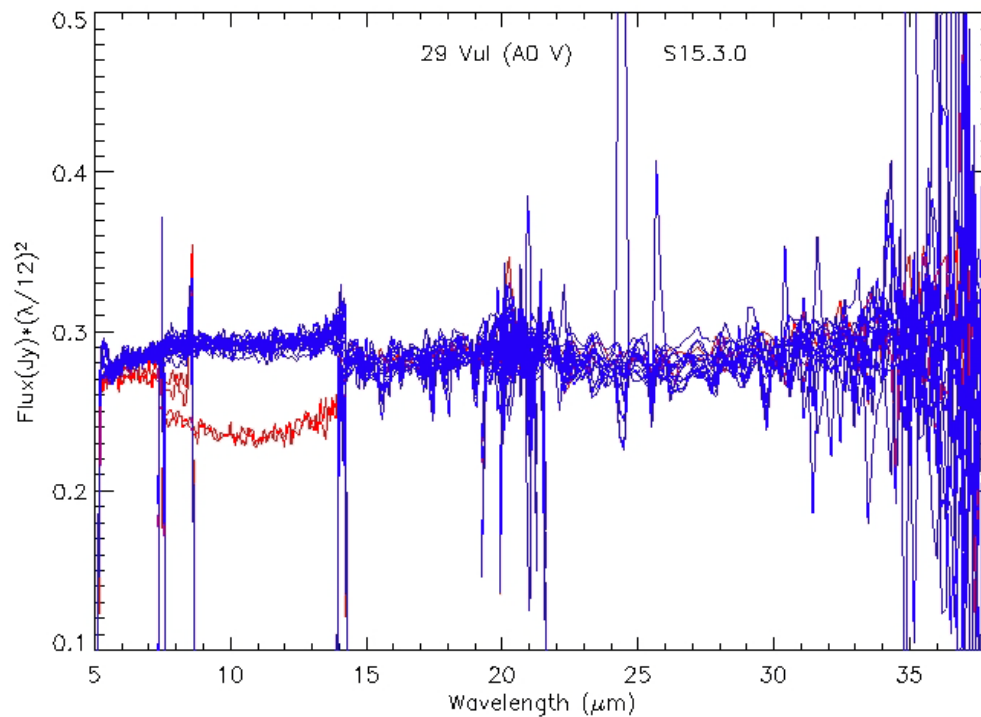
Figure 7.4 IRS Staring observations of 29 Vul, processed with S15 (bksub products). The red traces correspond to IRS observation campaign 7, while the blue correspond to five other campaigns.

7.3.4 *LL1 24 micron Deficit*

LL1 spectra of faint sources show a dip at 22-28 microns relative to standard models (see Figure 7.5. and Figure 7.6 for examples.) The amplitude of the effect is 2-3% for faint (<80 mJy) sources. Some sources which show the deficit apparently have nonlinear ramps.
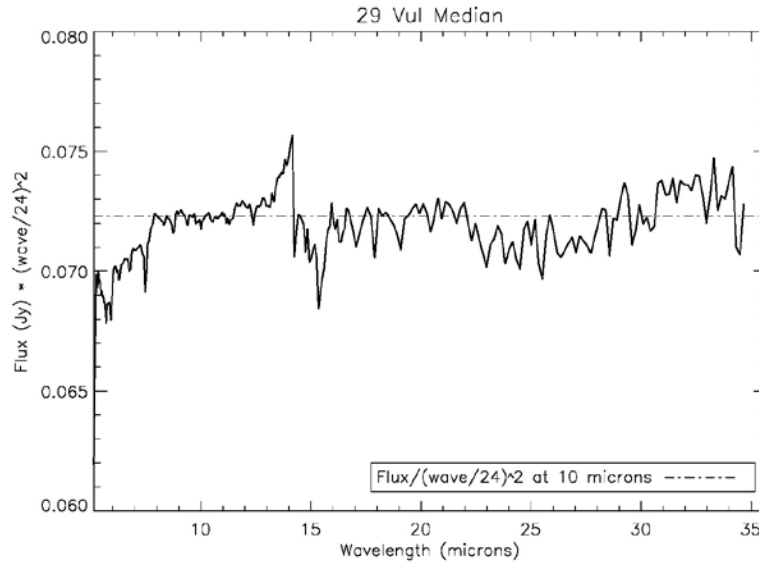
Figure 7.5 Illustration of the 24 micron deficit. The 14 micron teardrop is also visible.
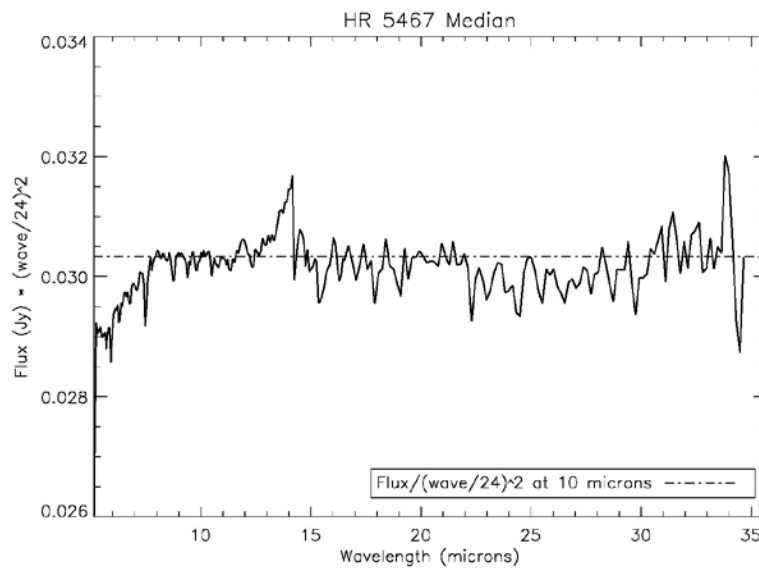
Figure 7.6 Another illustration of the 24 micron deficit. The 14 micron teardrop is also visible.

7.3.5 *Incorrect Droop and Rowdroop corrections following peakup saturation*

Spurious broad absorption or emission features or incorrect spectral slopes or curvature are seen in some SL1 or SL2 spectra. This may be due to saturation of the peak-up arrays. SL exposures with long exposure times may saturate in the peak-up arrays. In cases of strong saturation, the droop and rowdroop corrections will be incorrect because the total charge on the chip (which determines the droop correction) and on each row (which determines the rowdroop correction) cannot be measured. The effect becomes worse as more pixels are saturated for a greater portion of the ramp. It may not be obvious from the image that the peak-up arrays are saturated.

7.3.6   Wiggles in Optimally Extracted SL spectra

Sinusoidal oscillations are seen in some high signal-to-noise SL spectra extracted using SPICE's "Optimal" extraction option.

This effect is caused by a mismatch between the source and the standard star spatial profile (*rectempl*) file. The mismatch may be due to an incorrect "Ridge" percentage or to undersampling of the PSF. The undersampling of the PSF in SL is evident in the BCD images as the source jumps from one column of pixels to the next, along the spectral trace. The location of these jumps must match between source and template to get a clean optimal extraction. SL is the module most affected by undersampling.

To mitigate this effect,

1. Use Regular extraction for high signal-to-noise data. Generally, if the S/N is high enough to see the wiggles there is little or no gain from using Optimal extraction.

2. Compare Regular and Optimal SPICE extractions to verify the source of the wiggles.

3. Manually change the percentage in "Ridge" to minimize the wiggles. In general, automatic ridge finding is preferred for accurate ridge determination. However, it is possible for the automatic procedure to miss the correct peak.

4. Generate and use a standard star template (*rectempl*) that is a better match to the source. The template will match best if the position along the slit is the same (within 0.1 to 0.2 pixels) as the source position, modulo one pixel. For example, if the template is shifted by exactly one pixel, optimal extraction will work well, while if it is off by 0.5 pixel, the match will be poor.

5. Try using the optimal extraction algorithm in SMART.

7.3.7   Residual Fringes in SL and LL

SL and LL spectra show residual (non-sinusoidal) wiggles after flat fielding, at the 1-2% level. The detector fringing pattern is sensitive to source location relative to the slit, which can be affected by pointing inaccuracies. In particular, the phase of the fringes changes with source distance from the slit center. The flat field has been constructed to accurately remove the fringes for the mean pointing at the standard nod positions. The residual fringes are non-sinusoidal, so IRSFRINGE does not do a good job at fitting and removing them. Users should critically assess the reality of spectral features at the 1-2% level.

7.3.8   SL 14 micron Teardrop

Excess emission is found in the two-dimensional SL1 spectral images, to the left of the spectral trace, at 13.5-15.0 microns. We refer to this feature as the "14 micron teardrop", and it is illustrated in Figure 7.7.
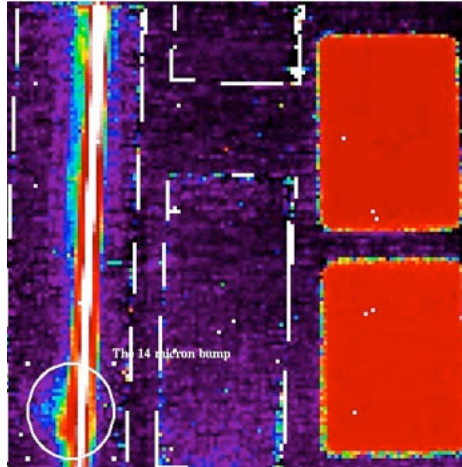
Figure 7.7 Example *bcd.fits* image illustrating the 14 micron teardrop. The source was observed using SL1. The bright continuum can be seen running vertically down the image on the left. The white circle indicates the teardrop, which appears as a region of excess flux to the left of the continuum.

The following three spectra show what the teardrop looks like in the extracted spectra.
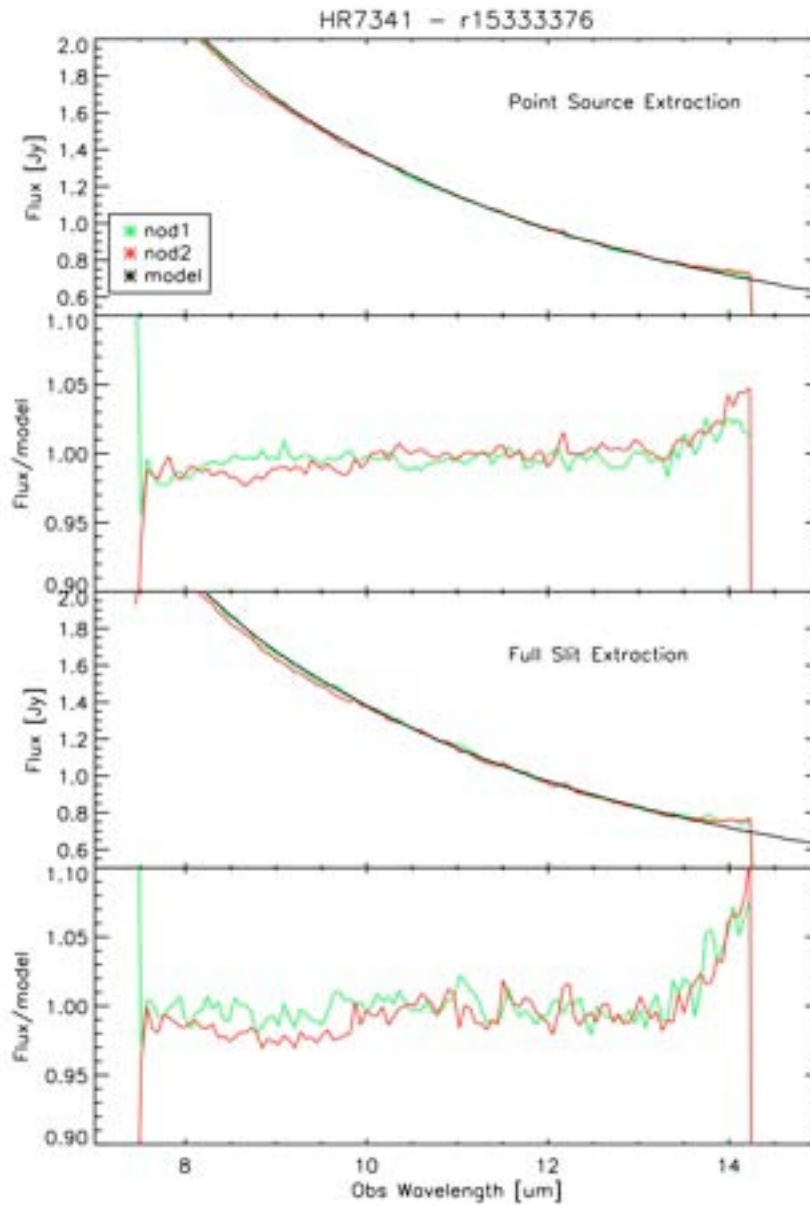
Figure 7.8 Illustration of 14 micron teardrop in the extracted spectra of HR 7341. The top two panels show the results for Regular Point Source extraction and the bottom two panels show the results for Full Width extraction. The teardrop is most clearly seen in panels 2 and 4, where it appears as an upturn kicking in at around 13.5 microns.
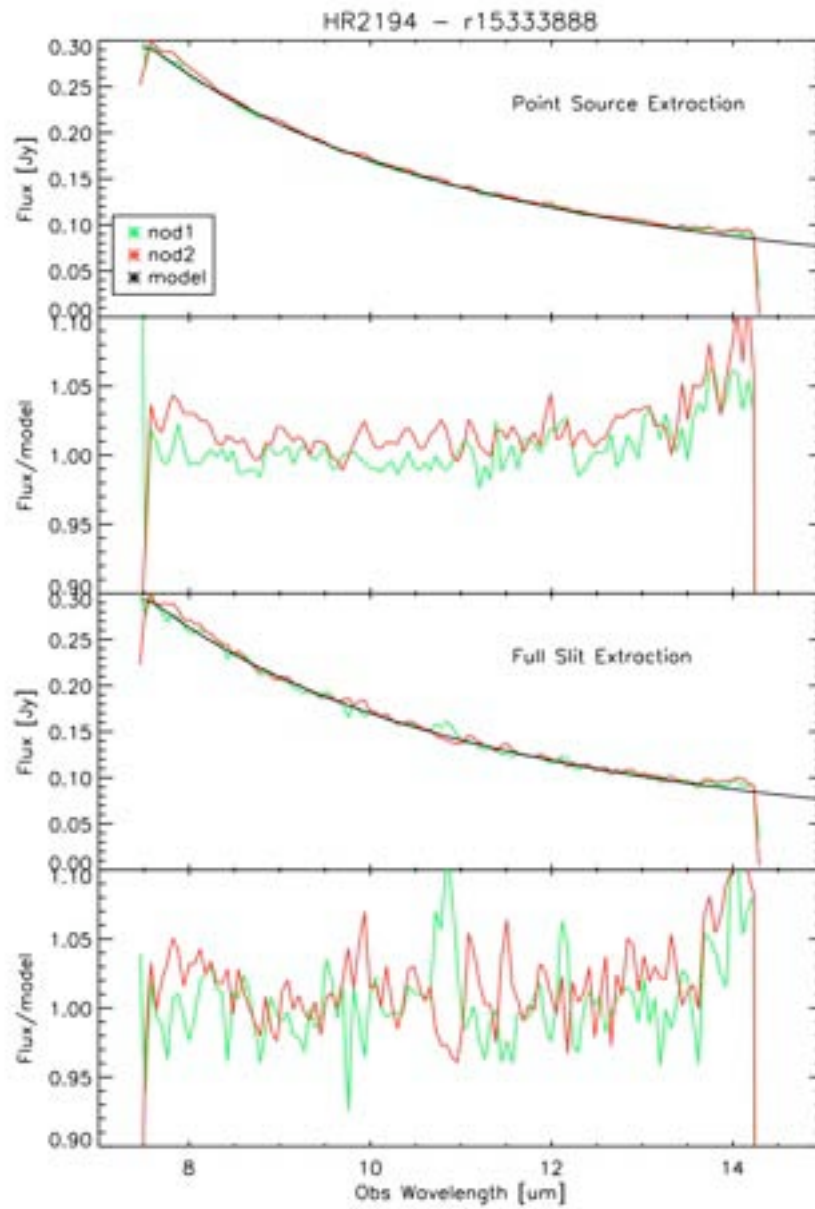
Figure 7.9 Same as Figure 7.8, but for HR 2194.
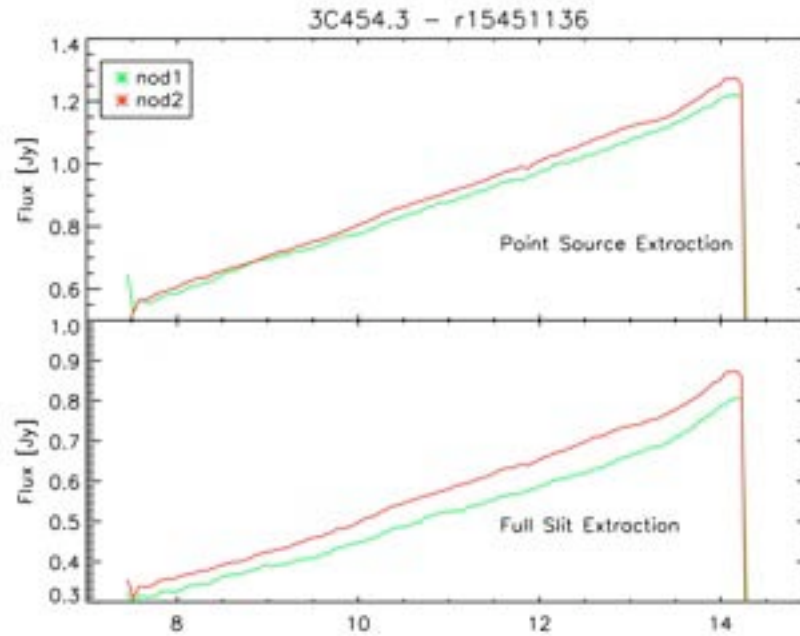
Figure 7.10 Similar to Figure 7.8, but for 3C 454.3, a red source. Comparisons to models have been omitted due to unavailability of models.

The teardrop is due to light leakage, optics, or detector response. It has not been introduced by pipeline processing. To illustrate this, the figures below show the various products from the pipeline for one observation of the standard star HR 7341. The teardrop is present in all of the pipeline products beginning as early as the Linearize cube.
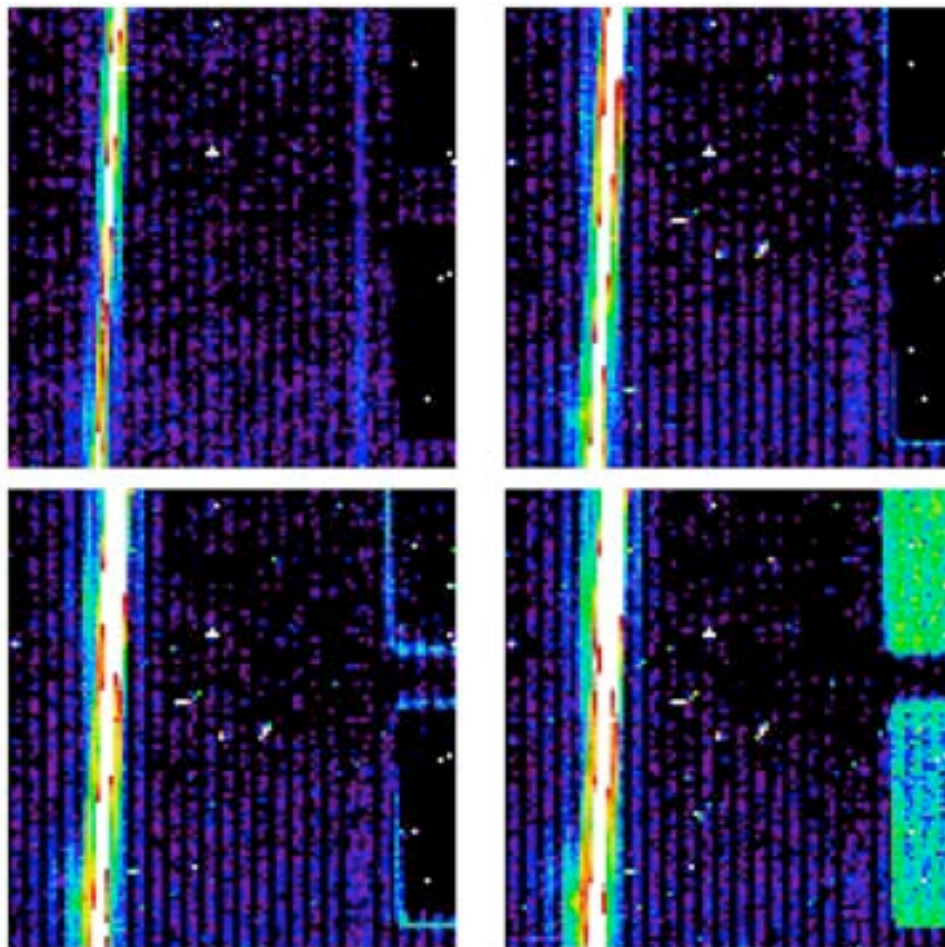
Figure 7.11 LNZ Cube: Output of linearize – Frames 1-4.

After collapsing the cube above, the pipeline produces the following products:
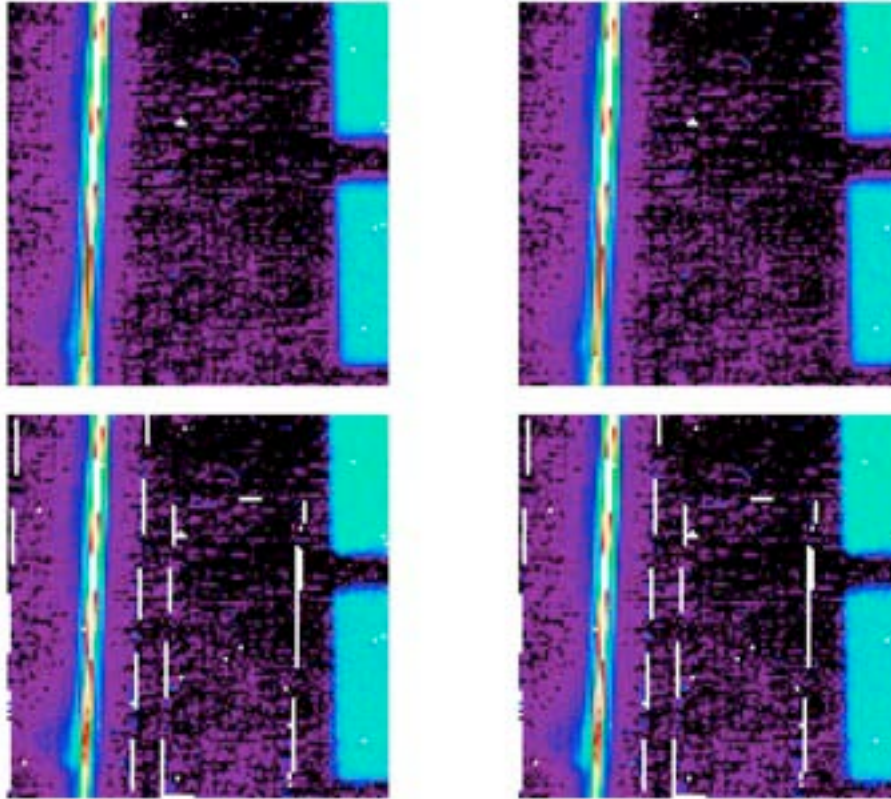
Figure 7.12 Various pipeline products which all show the 14 micron teardrop: After the various droop corrections (top left); after stray light correction but before flat fielding (top right); after flat fielding (lower left); flat fielded but NOT stray light corrected (lower right).

As illustrated the next three figure, the teardrop shape changes slightly with slit position, indicating that it is most likely correlated with the angle at which the light enters the slit, consistent with an internal reflection.
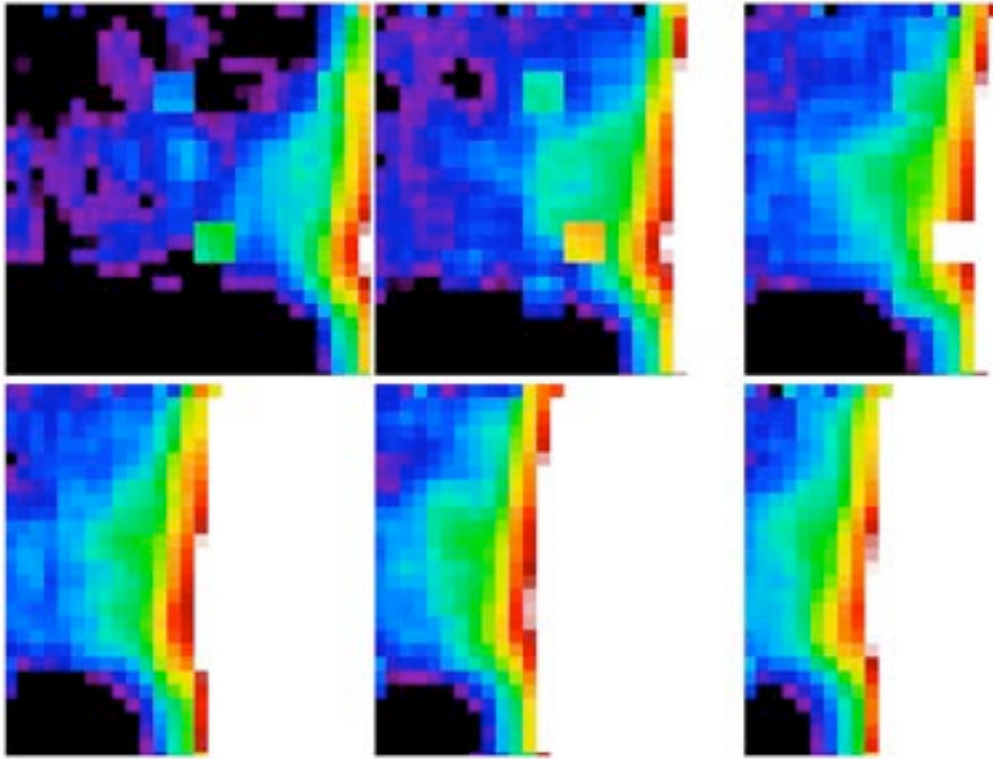
Figure 7.13 Nine mapping positions (2, 12, 22, 27, 32, 37, 42, 52, and 62) of the flat fielding data for eta1 Dor, zoomed in on the teardrop. The teardrop shape changes slightly with slit position, consistent with an internal reflection origin.
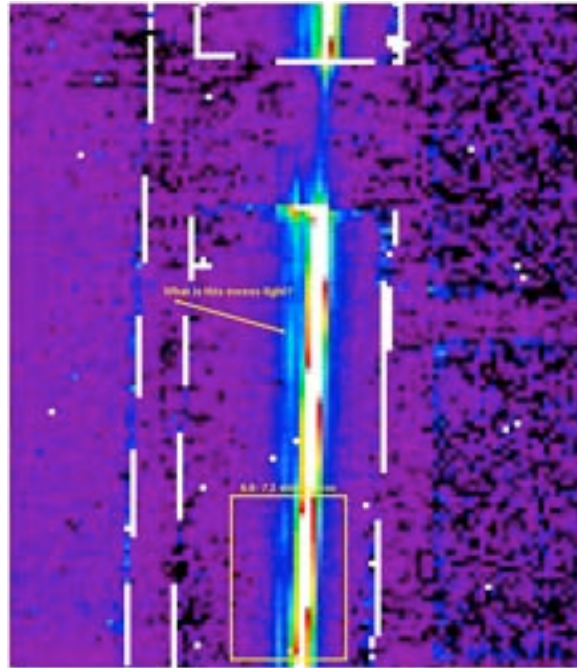
Figure 7.14 Two dimensional SL2 spectral image showing an observation of HR 7341. The wavelength region spanning 6.6-7.5 microns is highlighted with a box. We do not see any excess emission similar to the teardrop between 6.6 and 7.5 microns in SL2. This suggests the feature in SL2 at 6.5-7.6 microns is different in nature from the SL1 teardrop, and likely does not depend on extraction aperture.

In the figure below, we examine the strength of the teardrop versus the source flux density. We find that 1) the strength of the teardrop does not correlate with source flux density; and 2) for point-source extractions, the teardrop tends to be stronger for nod 2 compared to nod 1.
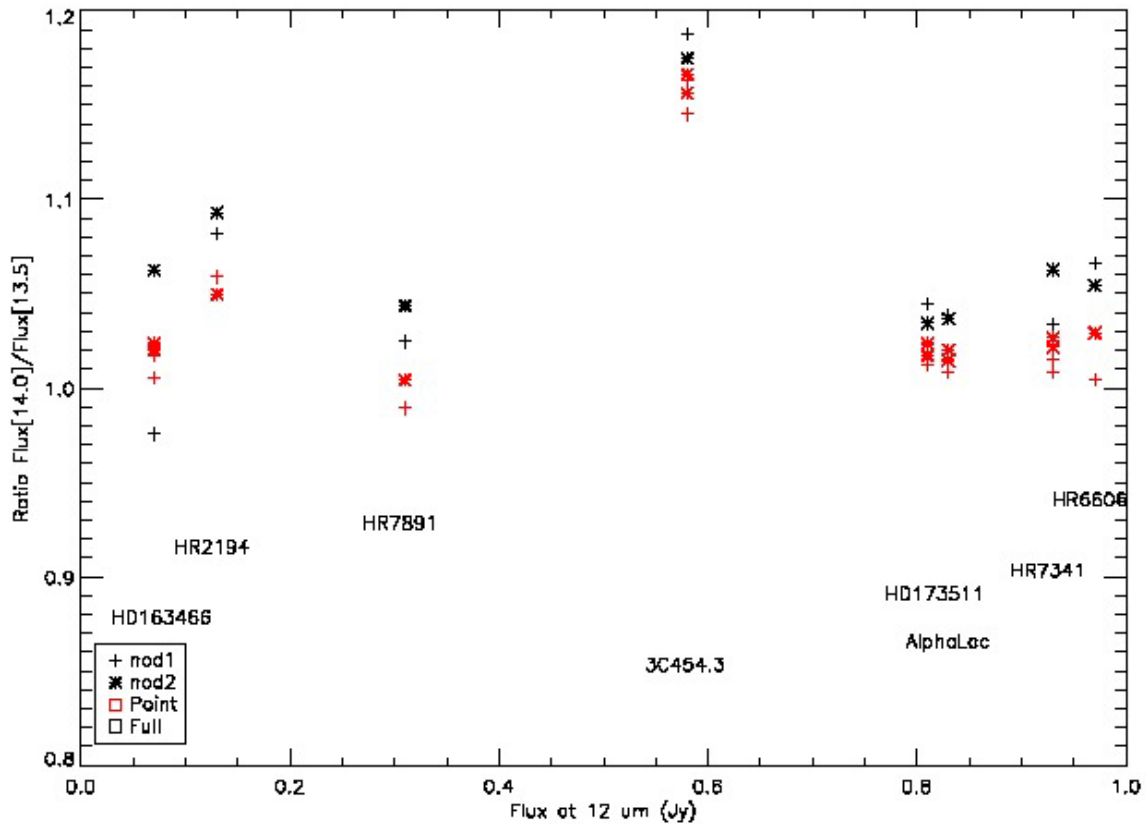
Figure 7.15 The strength of the teardop (quantified as the ratio of flux densities at 14.0 and 13.5 microns) versus the source flux density (measured at 12 microns) for 8 sources. For each source, black symbols represent full-slit extractions and red symbols represent point-source extractions. Plus signs represent nod 1 and asterisks represent nod 2. There is no correlation between the strength of the teardrop and the flux of the source. However, the teardrop is almost always stronger at nod 1 than nod 1 for point source extraction.

Mitigation: The behavior of the teardrop excess depends in a complicated way on source position in the slit and extraction aperture. There is no good way to correct for this feature. Users should use extreme caution before interpreting features between 13.2-15.0 microns.

7.4 High Resolution (SH and LH) Spectral Modules

7.4.1   LH Tilts from Residual Dark

During observations with the Long-High (LH) module, the dark current may have anomalously high values in the first 100-200 seconds of a series of exposures. Depending on the integration time and the number of cycles selected, data in the first exposure (or first nod position) may be affected. The "excess flux" is not evenly distributed over the LH array, being brightest on the blue end of each echelle order. The faint excess flux is seen as a bright band stretching across the bottom of the array, both on and between the orders, as illustrated in Figure 7.16.
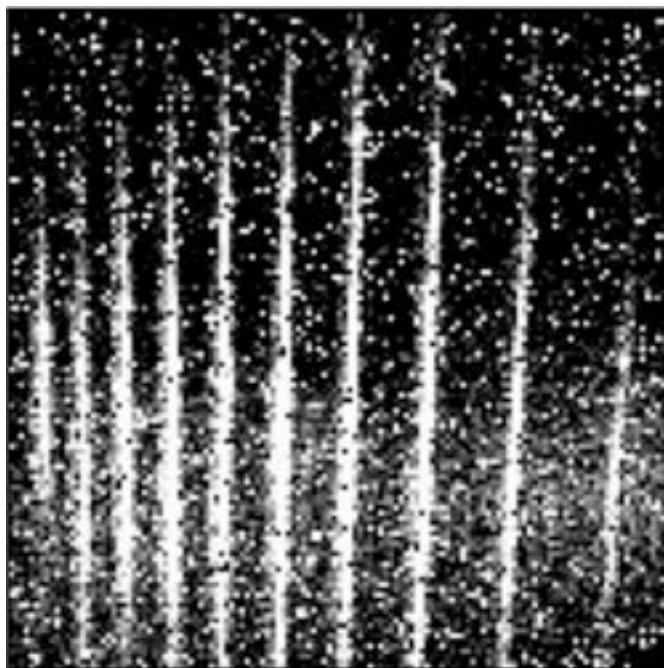
Figure 7.16 Illustration of excess LH dark current, which is distributed unevenly over the array with the brightest region towards the blue end (bottom) of the array.

This phenomenon manifests itself in extracted spectra of relatively faint sources as a "scalloping" or order tilting, wherein the slopes of affected orders are made bluer (flatter), inducing order-to-order discontinuities. The order-to-order discontinuities are typically 30-50 mJy. The magnitude of the effect does not seem to be related to source brightness. In Figure 7.17 we show two extracted LH spectra of a faint point source. The top spectrum has the source at the nod 1 position, while the bottom spectrum has the source at the nod 2 position. A background sky spectrum has not been subtracted in either case, but

the edges of the (color-coded) orders have been trimmed. The order mismatches are obvious in the nod 1 data, but vanish in the nod 2 data.
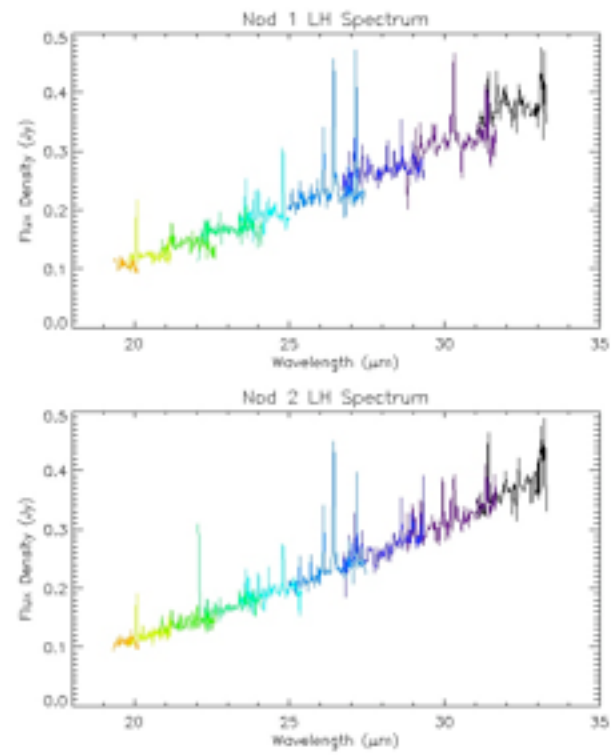
Figure 7.17 Nod 1 and nod 2 spectra. Notice the blue tilts in the nod 1 spectrum.

If you have observations of faint point sources with LH, and you are seeing these order tilts in your spectra, we recommend that you check your LH BCDs in the first nod position (or during the first few hundred seconds of a series of exposures), to see if this effect is more apparent. If order discontinuities such as described above are evident in the first few exposures or the first nod position, observers should consider not including these data during co-addition. If your LH data do not show this effect, you can include all the data in your final co-added spectrum.

Alternatively, users may wish to correct the effect using the DARKSETTLE software. An example is given in the DARKSETTLE recipe in the Spitzer Data Analysis Cookbook.

No similar effect has been conclusively identified in SL, LL, or SH modules. RED tilts of up to 10% have been seen in the longest wavelength LH orders 11 and 12, for bright red sources. This effect appears to be unrelated to dark current variations.

7.4.2   LH Orders 1-3 Red Tilts

LH orders 1-3 (at 29-37 micron) are sometimes mismatched and show red tilts with respect to shorter wavelength orders. The mismatch increases from 2% (order 3-4) to 10% (order 1-2). This effect appears to be most prominent for bright red sources (e.g., Mrk 231 in Figure 7.18). It does not appear for bright blue stars, such as the primary LH calibration standard star ksiDra. The cause of these LH red tilts is unknown.
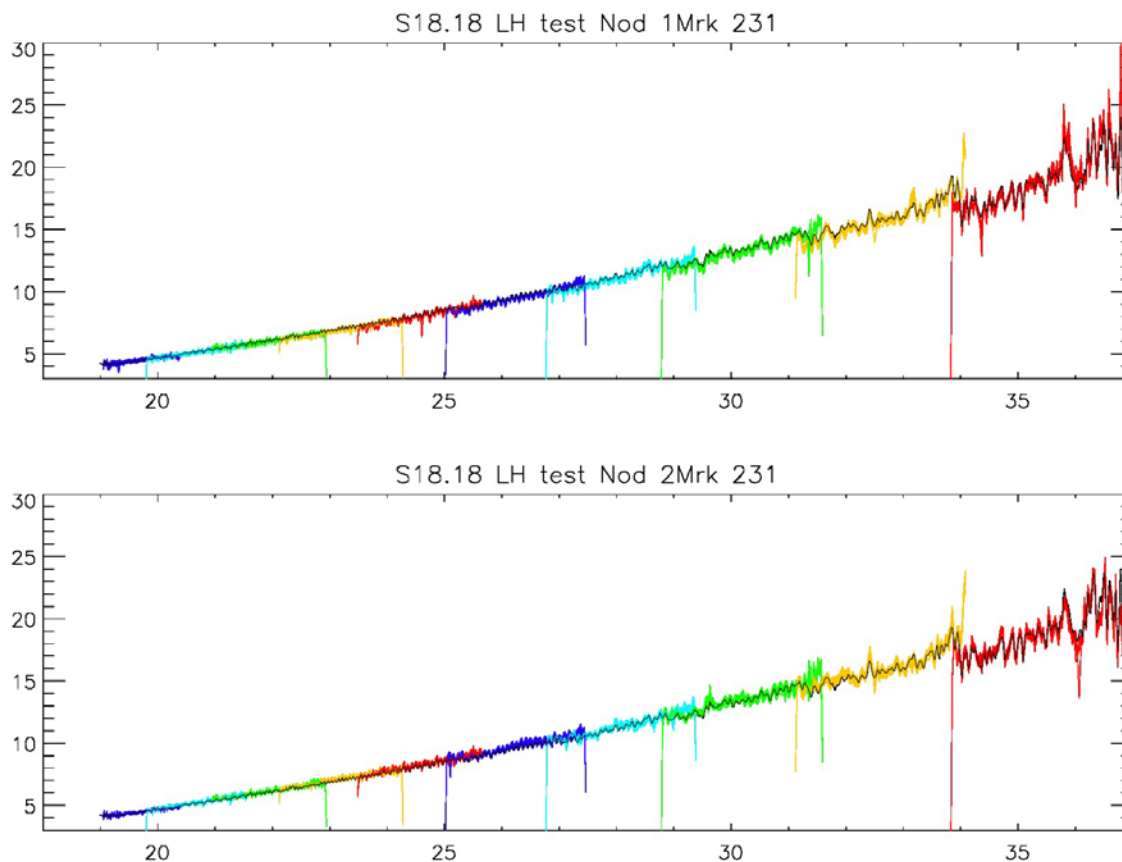
Figure 7.18 The LH spectrum of Mrk 231 shows red tilts in orders 1-3 (29-37 micron).

7.4.3   *High-res vs. Low-res spectral slope difference*

There is a small tilt of 2% over the 9-35 micron range of high-resolution spectra, relative to low-resolution spectra. Spectra match at 9 micron but LH is 2% higher at 35 micron than LL. Different standard stars and Decin models are used to calibrate LL and LH. HR 7341 (0.97 Jy at 12.0 microns) is used to calibrate LL. Ksi Dra (11.2 Jy at 12.0 microns) is used to calibrate LH. The 2% difference may be attributed to uncertainties in the fluxes of these two standard stars, which are of this order. Users may want to use broad band photometry to scale their spectra to the correct level.

7.4.4   *SH Spectral Ghosts*

"Ghosts" of extremely bright spectral lines can sometimes be seen in SH data, as illustrated in Figure 7.19. These ghosts have an integrated flux of about 0.5% of the primary line in spectra extracted over the full slit. In the 2D spectra, the ghosts can have peak pixels that are about 1% of that seen in the primary feature. The ghost lines are off center to the left in the blue direction and to the right in the red direction, and partially overlap the slit edges. The separation of the ghosts from the line of origin increases with wavelength should not be mistaken for physical velocity structure in the target (the implied velocity if the ghosts were a physical structure ranges from 1800 km/s in order 20 to 2900 km/s in order 13 in the

example shown in the figure). The ghosts are easiest to see in the 2D spectra, because they have a "tell-tale" spatial offset along the slit bracketing strong emission lines. Users who see very faint satellite lines around their emission features should inspect the sky-subtracted 2D spectra to determine if they are ghosts.

Ghost features are not seen in LH, and would be detectable if they had peak pixel values a few tenths of a percent of that in the primary feature.
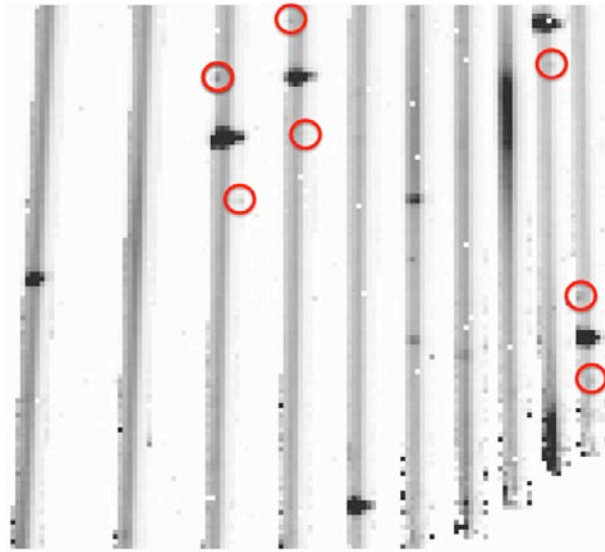
Figure 7.19 A bcd from AOR 16921344 of the planetary nebula J900. Red circles highlight the locations of the spectral ghost features.

Mitigation: Users concerned about removing these ghosts from their spectrum can easily do so by masking the pixels in the 2D image before extracting the spectrum.

7.5 Solved Issues

We include here issues that may be relevant for users that have data processed with older pipeline versions.

7.5.1   Bug in S18.7 High-resolution IRS Post-BCD products (Solved in S18.18)

As part of the standard IRS post-BCD data processing, all the BCDs associated with a given pointing are co-added. A bug in the pipeline sometimes causes incorrect weights to be used in the co-addition for S18.7 and earlier IRS high-resolution data. The problem occurs most frequently for SH data.

The affected files are all found in the *pbcd/* directory of data sets downloaded from the Spitzer Heritage Archive. Any of the co-added files (*coa2d.fits*, *c2msk.fits*, *c2unc.fits*) may be incorrect. If a *coa2d.fits* file

is found to be incorrect, any files generated from it will be also. The affected files have the following suffixes: *tune.fits*, *tune.tbl*. The BCDs are unaffected by this problem, so these files can be used to extract spectra and/or assemble spectral maps without cause for concern. To determine if your data are affected, please examine the *2dcoad.txt* files in the *pbcd/* directory of your data set. The first column of this file contains the weights used in the co-addition. The weights should all be close to unity. If you see low and/or negative weights, then your co-added files may be corrupted.

The IRS team plans to reprocess all data in mid 2010, and this will rectify the problem. In the meantime, if desired, users can create their own *coa2d.fits* files by combining the appropriate *bcd.fits* files. The associated 1D spectra can then be extracted using SPICE. While it is possible to use a variety of software packages to create the co-added images, we are providing an IDL procedure for this purpose. This procedure, *coad.pro*, can be found on the Data Analysis & Tools portion of the [Spitzer Heritage Archive](). Alternatively, users may co-add 1D spectra which have been extracted from the BCDs, which are unaffected by the bug.

7.5.2   *Low-Res Nod 1 vs. Nod 2 Flux Offset (solved in S15)*

SL Nod 2 fluxes are consistently 4% lower than Nod 1. This is the result of a spatial tilt in the flat field. LL2 Nod 1 fluxes are 4% lower than Nod 2 at 14-18 microns, decreasing to 1% at 21 microns. As a result, Nod 2 and Nod 1 are tilted relative to one another.

Users should average the nods to compute the source flux and determine the flux calibration. After S15, the flat field has been adjusted to remove the Nod1-Nod2 difference.

7.5.3   *LL Nonlinearity Correction Too Large (solved in S14)*

Slopes are overestimated at high count levels in LL. The effect is >5% for a 1 Jy source, and >20% for a 2 Jy source. The effect is worst for long exposure-times. The SL nonlinearity correction appears to be OK.

Red sources appear redder and blue sources appear bluer due to this effect. However, curvature and other high order effects can also appear, reflecting the detector response. For example, fringes in the flat-field may be amplified, leading to extra 'noise' in LL spectra. The primary LL calibration source, HR 7341 (0.97 Jy at 12 microns) is affected by this problem at a low level. Reducing the nonlinearity coefficient causes a 5% drop in flux at 14-17 microns (LL2). The effect is <2% at 17-21 microns (LL2) and <1% at 26-36 microns (LL1).

To mitigate this problem, the non-linearity coefficient was adjusted for S14, resulting in a 5% drop in flux at 17-21 microns (LL2). This last effect was corrected by revised flux calibration in S15.

7.5.4   *Tilted SH and LH Flatfields (solved in S14)*

Before applying the fluxcon, the SH and LH orders appear tilted to the red. This is due to a difference between the standard extraction, which forces the *wavsamp* rectangle height to 1.0 pixels, and the custom extraction used to make the flatfield, which uses a variable height rectangle as defined by the *wavsamp*.

Pre-S15, the tilts were removed by applying the *fluxcon* table. From S15 onward, the variable height rectangles defined via the *wavsamp* are used for all extractions. This has the added benefit of matching the instrumental resolution.

7.5.5   *Bumps in LH Near 20 Microns (solved in S15)*

Bumps are seen in LH orders 19 and 20, at ~19, 20, and 21 microns (see Figure 7.20). They are attributable to bright features at the order edges which are accentuated by the S13-S14 LH flatfield. Features were not present pre-S13, and were fixed in the S15 flatfield. The pipeline S13.2 reduction shows three new peaks around 20 microns that are spurious. The features show in a full slit extraction but when the extraction aperture is shrunk to 2 pixels, the feature vanishes in one nod position but remains in the other. This is due to pixels X=13, Y=12 to 22 which all look unusually bright in the 2D frame even when the source is off on the other side of the slit.

To mitigate this problem, a new LH flat field was created for S15, with bad regions suppressed. For S13, trimming the orders can remove the strongest of the three peaks but not its two weaker neighbors.
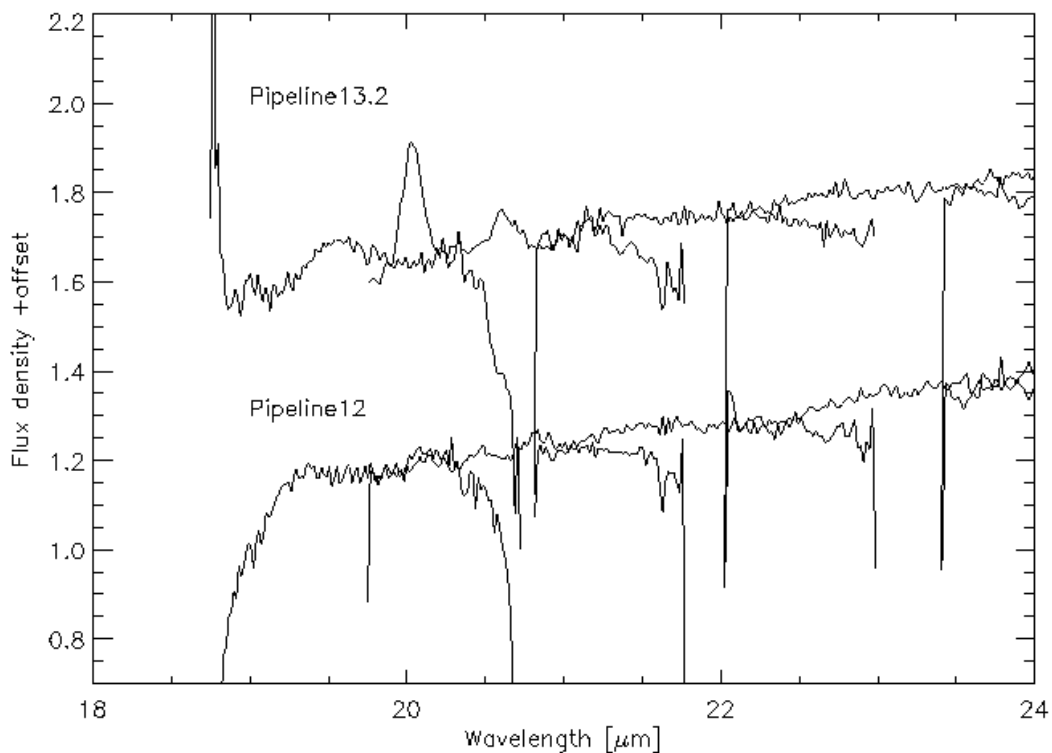
Figure 7.20 LH spectrum. Notice the peaks at 19, 20, and 21 microns in the S13.2 spectrum.

7.5.6 *Mismatched LH Orders (solved in S17)*

For pipeline version S15.0, before flux calibration (in *extract.tbl* spectra), LH orders are mismatched and appear tilted to the red. This is caused by the increasing *wavsamp* height with wavelength in each order to accommodate the spectrograph resolution. The effect is not apparent in the flux calibrated (*spect.tbl*) spectra, as it is corrected by the *fluxcon* polynomial.

For S17 onward, this effect is corrected at the spectral extraction stage. The flux in each wavelength bin is normalized to a *wavsamp* height of 1 pixel.

Note that this issue should not be confused with the LH blue tilts and red tilts discussed in Section 7.4.1, which still may be seen in some spectra.

7.5.7 *LL Salt and Pepper Rogues (solved in S17)*

In S15, LL 'Super Darks' averaged over many campaigns were used to subtract off the instrumental bias signature. Due to the variable nature of rogue pixels, this introduced salt (new rogues not in the super dark), and pepper (rogues in the super dark, but not in the current campaign) into the data.

From S17 onward, campaign-dependent 'moving window darks' are used to better match the rogues in each campaign and to track the changing minimum zodiacal light level. The salt and pepper in S15 BCDs can be very effectively removed by subtracting an appropriate background observation.

Chapter 8. Introduction to Data Analysis

This chapter provides an overview of the data reduction procedures that a typical user should follow for both spectroscopic and imaging observations made with the IRS. Please see the Data Analysis & Tools page for further information and examples.

8.1 Summary of Data Reduction Software

Several software tools are available for the reduction of Spitzer IRS data. These include CUPID, SPICE, SMART, CUBISM, IRSCLEAN, DARKSETTLE, IRSFRINGE, PAHFIT, and MOPEX. Each of these tools is described in detail on the Data Analysis & Tools page. Briefly, CUPID allows users to run the Spitzer IRS pipelines to re-create BCD files from the archived raw files. SPICE is an interface to the extraction pipeline and it executes the pipeline modules in order, allowing the user to select the source and type of extraction for IRS staring mode data. SMART can also be used for staring mode spectral extraction and additionally allows the user to fit spectral lines. CUBISM is a tool for creating and analyzing spectral cubes from observations made in IRS Mapping Mode. IRSCLEAN removes bad pixels from 2D spectral images (see Section 7.2.2). DARKSETTLE allows users to remove time-dependent charge (see Section 7.4.1). IRSFRINGE allows users to remove spectral fringing (see Section 7.3.7). PAHFIT is a tool for fitting PAH spectral features in IRS spectra. Finally, MOPEX is a tool for mosaicking and performing photometry on Spitzer imaging data, including IRS red and blue peak-up images.

8.2 Data Reduction Steps for IRS Spectroscopic Modules

The detailed procedure you should follow for reducing your data depends on the module used and on the type of source you are looking at. However, the most basic reduction consists of five basic steps, described in Section 8.2.1 and shown schematically in Figure 8.1. After examining the results of a basic reduction, you may find that further steps are necessary due to, for example, bad pixels (see Section 7.2.2) or latents (see Section 7.2.5). We therefore provide a set of optional steps that you may add to your procedure to optimize your results. Throughout this section, Mapping Mode refers to maps designed to recover spatial information on extended sources. Users dealing with Mapping Mode observations designed to perform very deep observations of point sources may want to follow the guidelines for Staring Mode observations.
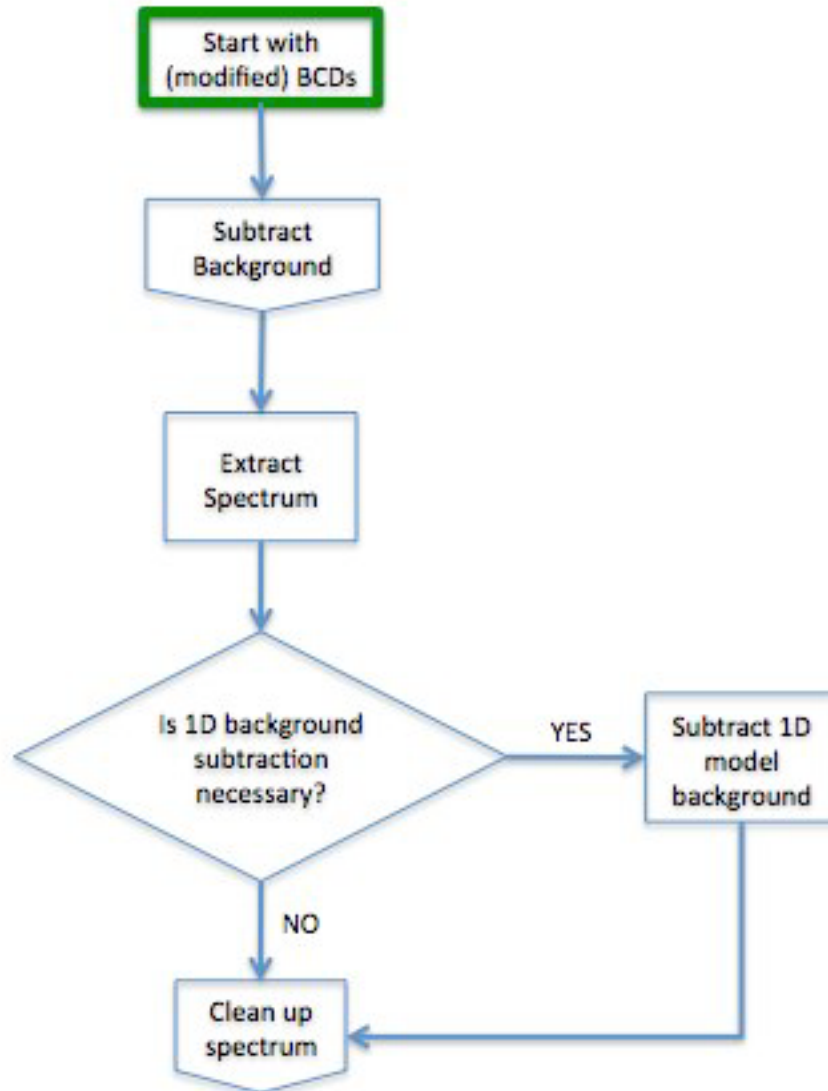
Figure 8.1 This flowchart describes the basic steps necessary to reduce IRS low-resolution spectra. Additional flowcharts illustrating the 2D background subtraction procedure and how to clean up the 1D spectrum are provided in Figure 8.2 and Figure 8.3.
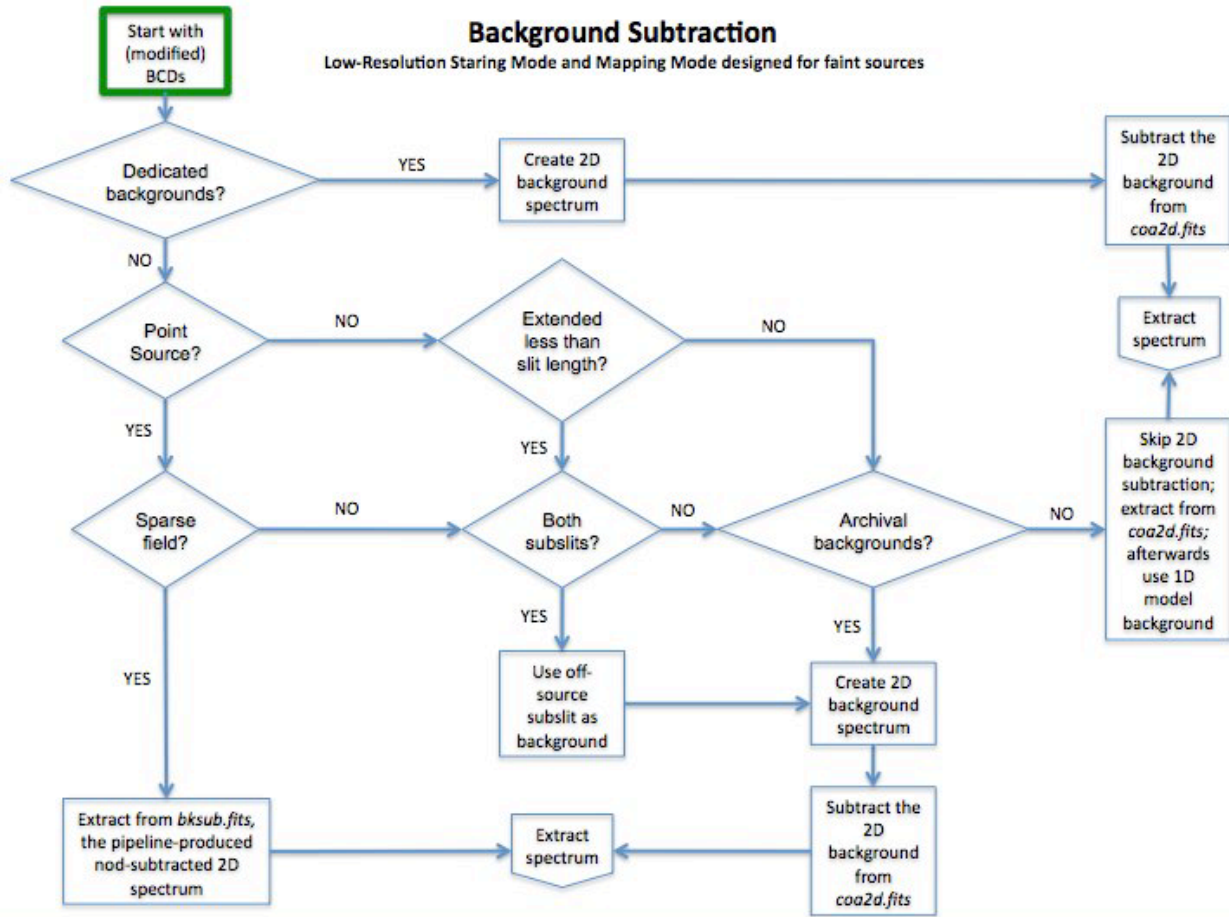
Figure 8.2 This flowchart illustrates how to subtract the background from your low-resolution 2D IRS spectrum.

Clean up spectrum
All IRS Modules
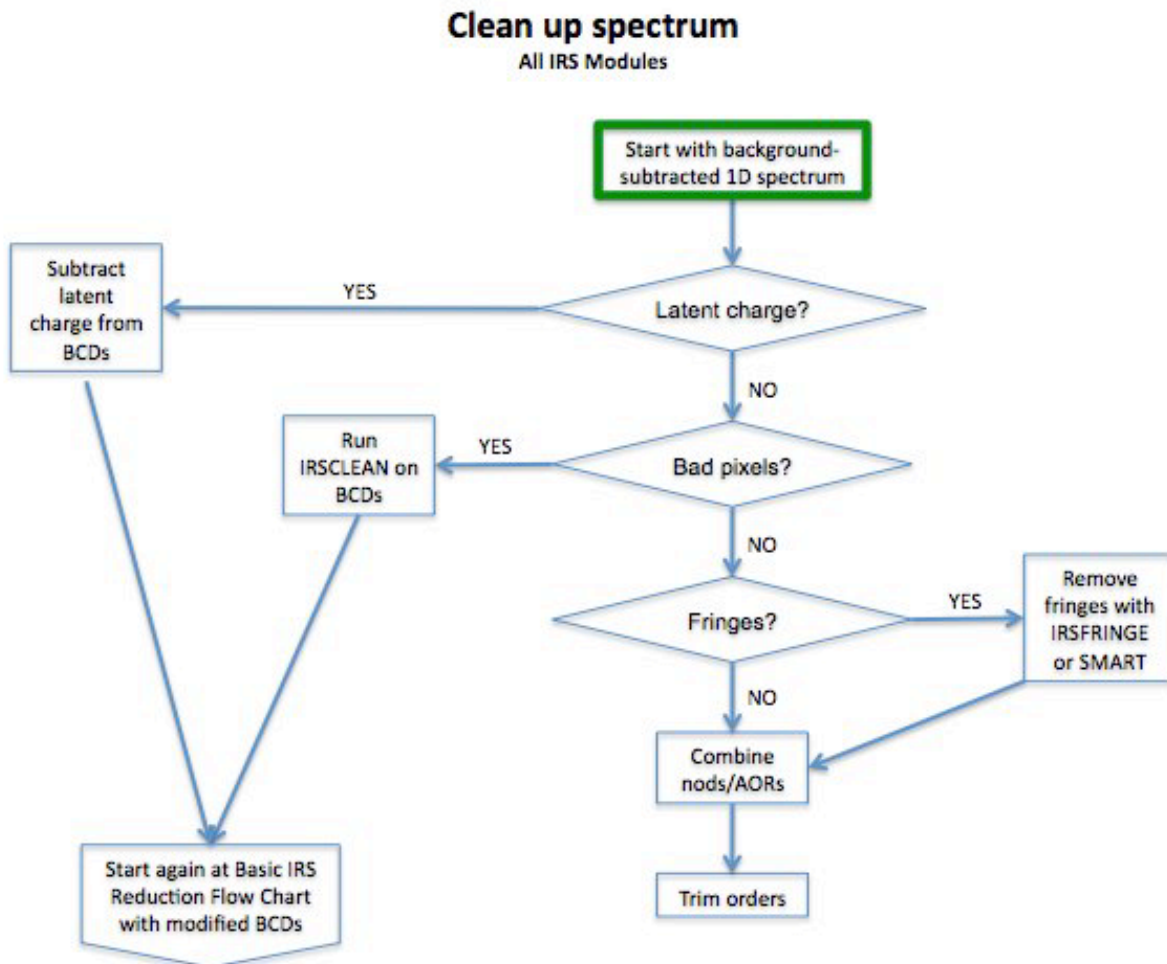
Figure 8.3 This flowchart illustrates the main issues found with low-resolution IRS spectra. These include latent charge (see Section 7.2.5), residual bad pixels (which can be corrected using IRSCLEAN; see Section 7.2.2), and fringes (which can be corrected using IRSFRINGE or SMART; see Section 7.3.7).

8.2.1   Basic Steps

1. <u>Examine the data</u>. Identify the pipeline product that you should start with, and examine the data before proceeding with any custom reduction. For example, if you are interested in low resolution spectroscopy of point sources in relatively empty fields, the sky-subtracted extracted spectrum *bksub.tbl* may be sufficient for your purposes. However, many users interested in IRS spectroscopic data will need to re-extract the spectra. In particular, the default pipeline does not perform optimal extraction of faint point sources or extended source extraction. Users who wish to use these extraction algorithms will need to start with one of the 2D products, such as *bksub.fits*. Other users will need to create new 2D products before extracting 1D spectra. For instance, the pipeline does not automatically perform sky subtraction for the high resolution modules. Therefore, users interested in high-resolution data should start with *coa2d.fits* files. In some cases, users will observe one object over several AORs. The pipeline will not co-add BCDs across AORs, so these users should start with the *bcd.fits* files. Users interested in spectral maps should also start with the *bcd.fits* files. Regardless of which pipeline product you start with, you

should examine the 2D spectral products for a better understanding of your data. For completeness, the following steps assume that you have decided to start with the *bcd.fits* files.

2. <u>Co-add 2D on-source spectra.</u> Create sigma-clipped averages or medians of all of the 2D files taken at the same position. Be sure to combine the associated uncertainty (by adding in quadrature) and mask (by using the bitwise OR operator) frames. When combining any images, it is important to retain header information from the original BCDs, or they will not be usable in the spectral extraction software. For Staring Mode observations you can use the software of your choice (e.g. IDL, IRAF). You may wish to examine the software [COAD](#) for an example in IDL. For Mapping Mode observations, this is done automatically in CUBISM when you build a cube.

3. <u>Co-add 2D background spectra.</u> Create sigma-clipped medians of all 2D background files. As with the on-source spectra, be sure to combine the associated uncertainty and mask files, and to retain the original header information. The result will be subtracted from the on-source spectrum in the next step. The sky observations help to mitigate the effects of rogue pixels, which are especially numerous in Long-High data. (See Section 7.2.2.) If you are interested in line emission only you may not need to subtract the sky, as the general background does not have strong line features.

> **Low-Resolution Point-Source Staring Mode:** If you have low-resolution observations taken in IRS Staring mode, you have observations of each target in two nods. Calling one nod position A and the other position B, you can co-add all nod B images to obtain a 2D background spectrum for nod A. Similarly, you can co-add all nod A images to obtain a background spectrum for nod B. This is an option for point sources if the slit does not have other sources in it. It is the method used in the pipeline to create the *bksub.fits* files. Alternately, you can construct a background frame from the off-source subslit. This method works for both point sources and extended sources on scales less than about 60 arcseconds. For example, if you are observing a source with both SL1 and SL2 in your AOR, when the source is in SL2, you can construct a sky from SL1 and vice-versa. Be sure to check that the off-source subslit does not contain serendipitous sources before using it to estimate the background. The selected background frames may be co-added using the software of your choice (e.g. IDL, IRAF).

> **Low-Resolution Extended Source Staring Mode:** For extended sources observed with the low resolution modules, there would ideally be sky observations taken close in time to the science observations. If dedicated sky observations do not exist, search the archive for blank sky observations taken within 24 hours of your target data. Sky measurements taken several days before or after your source observations may introduce artifacts into your spectra due to (for example) changing darks and onset of rogue pixels (see Section 7.2.2.) For these and other reasons (e.g. changing pointing modes, aperture positions, bias voltages), it is highly recommended that appropriate sky measurements are selected from the same IRS campaign as the source observations. If these sky observations are not at similar ecliptic coordinates as your targets, you will have to apply a background scaling factor to be able to use these as a sky for your data. Also, to avoid adding noise to your data in the sky subtraction phase, choose archival data which have comparable or longer integration times than your data frames. If your source is extended on scales less than 60 arcseconds, you should consider using the off-source subslit (see the description in the preceding

paragraph). The selected background frames may be co-added using the software of your choice (e.g. IDL, IRAF).

High Resolution Staring Mode: For high-resolutions observations, there would ideally be sky observations taken close in time to the science observations. If dedicated sky observations do not exist, search the archive for blank sky observations taken within 24 hours of your target data. If these sky observations are not at similar ecliptic coordinates as your targets, you will have to apply a background scaling factor to be able to use these as a sky for your data. Also, to avoid adding noise to your data in the sky subtraction phase, choose archival data which have comparable or longer integration times than your data frames.

Mapping Mode: The primary and recommended technique for assembling a background frame is to use dedicated background observations that were scheduled along with the mapping AOR, or to use data obtained as part of the mapping observations which went far enough off the source to remove all source flux from the slit. Once identified, the background observations may be co-added within CUBISM.

4. Subtract the background. The co-added 2D sky frame should be subtracted from the co-added 2D on-source frame using the software of your choice (e.g. IDL, IRAF). Be sure to combine the uncertainty and mask files and retain the original header information.

5. Extract 1D spectra. Run SPICE on your 2D spectral files, performing the basic steps of Profile, Ridge, Extract and Tune. Users may choose from three templates. "Point Source with Regular Extract" should be used for bright point sources where the trace is clearly visible in the 2D image. "Point Source with Optimal Extract" may improve the signal-to-noise ratio for faint point sources. "Extended Source with Regular Extract" should be used for extended sources. The SPICE extended source calibration assumes that the source has a uniform surface brightness. It calculates the slit loss correction factor based on that assumption. The user also has the option to manually select the extraction width. Please note that if you choose a custom width, your flux calibration will need to be redone as described in Section 8.2.2.

6. Examine your results. After completing a basic extraction as described in the previous four steps, examine the results. If you see spikes in your data, away from the order edges, you may wish to clean out rogue pixels (see Section 7.2.2). If you see mismatches between the orders or scalloping of the orders, you might investigate the presence of time-dependent dark current (see Section 7.4.1). If you see fringes, you will likely want to remove them using IRSFRINGE (which is recommended for high-resolution data only). Please see Chapter 7 and Section 8.2.2 for a list of additional steps you may wish to incorporate into your procedure. We highly recommend going through the basic procedure first, and only performing the optional steps if they are indicated by an examination of the results.

8.2.2   *Optional Steps*

The following steps are not necessary for all users, but may be applicable to your data set. You should follow the basic procedure outlined in Section 8.2 and review Chapter 7 before deciding if any of the following steps are necessary.

1. <u>Remove bad pixels</u>. Background subtraction should have removed many bad pixels. If your spectrum still contains significant numbers of bad pixels, which may manifest themselves as sharp features away from the order edges in your extraction spectrum, you may wish to remove them (see Section 7.2.2). For data taken in Mapping Mode, you can use CUBISM to remove known rogue pixels and flag any other pixels that look bad. For data taken in Staring Mode, you can use IRSCLEAN to perform the same task. These tools operate on the 2D spectra, so you will have to re-extract your spectrum after cleaning.

2. <u>Remove latent charge</u>. A small fraction (e.g. 1-2% for LL) of charge on the detector persists between frames despite the resetting of the detector that occurs prior to every integration. (See Section 7.2.5.) This latent charge decays slowly over time and is removed only by the annealing process. In the case of very faint sources, the source of latent charge is the zodiacal background. For long duration (>1 hour) integrations on very faint (<1-3 mJy) sources, this charge can build up to a significant level. The user may search for any charge accumulation (especially for high background and long integrations) by monitoring the signal as a function of time. One way of doing this is to take the median of each row (or 2-3 rows) within an order in each BCD and see if the median of the same group of pixels increases with time. If so, you can fit a (first-order) polynomial to these median values and subtract the trend. The user can do this with the software of their choice (e.g. IDL, IRAF) and then proceed with background subtraction and spectral extraction.

3. <u>Remove time-dependent dark current</u>. During observations with the Long-High (LH) module, the dark current may have anomalous values in the first 100-200 seconds of a series of exposures. (See Section 7.4.1.) Depending on the integration time and the number of cycles selected, data in the first exposure (or first nod position) may be affected. The flux is not evenly distributed over the LH array, being brightest on the blue end of each echelle order. The faint excess flux is seen as a bright band stretching across the bottom of the array, both on and between the orders. This phenomenon manifests itself in extracted spectra of relatively faint sources as a "scalloping" or order tilting, wherein the slopes of affected orders are made bluer (flatter), inducing order-to-order discontinuities. If your spectra show evidence of time-dependent darks, you may wish to run DARKSETTLE to ameliorate the effects.

4. <u>Combine 1D spectra from a given AOR</u>. If you have low-resolution observations taken in Staring Mode, you now have two 1D spectra, one for each nod position, which you can average together. The co-addition can be performed with the software of your choice (e.g. IDL, IRAF).

5. <u>Co-add 1D spectra from different AORs</u>. Some users may be dealing with very deep observations of faint sources. In some cases, observations of a single source will span multiple AORs. In these cases, the extracted 1D spectra will need to be co-added before spectral features are measured. The co-addition can be performed with the software of your choice (e.g. IDL, IRAF).

6. <u>Trim the edges of the orders</u>. The edges of the orders are noisy and you need to reject the first few and last few pixels. The trim ranges used to calibrate the data are given in Table 6.5. Notice that in the high-resolution arrays, the short-wavelength edge of each order is generally noisier than the long-wavelength edge. This is due to the blaze of the gratings. In general, the long-wavelength side of each high resolution order is more trustworthy than the short-wavelength side, and you may be able to disregard the latter.

7. <u>Subtract the background in 1D</u>. If you have high-resolution data or low-resolution observations of extended sources, and no dedicated sky backgrounds, you have two options. If you have low resolution

observations taken close in time, you can interpolate the sky values extracted from the low resolution data to derive the background at high resolution wavelengths.

8. <u>Remove fringes</u>. If your extracted spectra exhibit fringing, you may use <u>IRSFRINGE</u> to remove the effect. See Section 7.3.7.

9. <u>Apply a flux calibration correction</u>. If you have changed the extraction width from the default, you will have to apply a flux calibration correction. For a point source, this is essentially a ratio of the flux from a calibration star using the default extraction width to the flux from the same star using your extraction width. You may wish to fit a polynomial or low-order function to the calibration correction in order to reduce noise. Multiply the 1D spectrum by this ratio (which is wavelength dependent). Be sure that you have done exactly the same steps of rogue pixel masking, background subtraction and <u>SPICE</u> extraction on the calibration star as you have done for your target, before you estimate the flux calibration correction. See Section 4.1.4 for more details.

10. <u>Check the flux calibration</u>. Compare the flux in the spectrum with broadband imaging observations, perhaps using SPITZER_SYNTHPHOT (see the <u>Data Analysis Cookbook</u> for access to the software and a recipe for using it). It is also useful to extract a spectrum from a blank part of the slit in your reduced 2D spectrum to check if there is any residual sky or latent charge (see Section 7.2.5) remaining.

11. <u>Fit spectral features</u>. You may use <u>PAHFIT</u>, <u>SMART</u>, IRAF, IDL, or the software tool of your choice to fit spectral features in your extracted spectra. Be careful not to confuse rogue pixels/cosmic rays with emission/absorption lines. When doing full slit extraction for SH/LH, the rogue pixels (since they only decay slowly with time) can appear in both nod positions in the spectrum while cosmic rays will appear only in one nod. In addition, check that the line is not the 14 micron teardrop known to exist in SL1 data (see Chapter 7). Finally, check that the full width at half maximums (FWHMs) of the lines are reasonable i.e at least the spectral resolution of the instrument.

8.2.3   *Transit or Eclipse Spectra*

Spectra of transiting or eclipsing exoplanets were taken using the low resolution modules in either Staring or Mapping mode, but typically in such a way as to minimize telescope movement.
Relying as they did on comparing spectra taken during different parts of an exoplanet's orbit (e.g. (star+planet)-star=planet emission, or (star+planet-atmosphere)-(star+planet)=atmospheric absorption), it was important to keep the system stable, reducing as much as possible variable slit losses and movement of the source on the detector. Exposures were typically taken continuously over a period of 4-6 hours, bracketing the time of transit or eclipse by one to two hours on either side. Since the parent stars are quite bright, latent charge buildup is rapid and obvious. However, normal latent charge removal was found to be insufficiently precise for measurements at the 100-1000 ppm level. Consequently the first 10-20 minutes of each 4-6 hour observation sequence (after which a steady state is reached) were usually discarded. Due to telescope pointing oscillations at the 0.05 arcsec level, corrections to the measured flux vs time per wavelength bin were made using a derived pointing model or some functional approximation. Background subtraction is defined somewhat differently than usual, with the "background" being measured at the same point on the sky either during secondary eclipse (for an exoplanet emission spectrum) or during primary transit (atmospheric absorption spectrum). While a "stabilizing adjustment" might be made to each exposure by measuring and subtracting a median of pixels in the off order (to

remove any small offsets due to droop or other electronic effects) the actual background was typically measured and subtracted in the 1D spectra by generating a light curve for each wavelength bin and measuring the depth of eclipse. More details concerning the reduction process of transit spectra can be found in Richardson et al. (2007, Nature 445, 892), Grillmair et al. (2007, ApJ, 658, L115), Swain et al. (2008, ApJ, 674, 482), and Grillmair et al. (2008, Nature 456, 767).

8.3 Data Reduction Steps for IRS Peak-Up Imaging (PUI)

1. Examine the data. The Post-BCD mosaics (*b_mos.fits* and *r_mos.fits*) will often be adequate for doing photometry. However, if visual inspection reveals bad pixels near the science target or in the desired background annulus region of the image, creating your own mosaic using MOPEX may help to mitigate such artifacts. MOPEX also allows you to create a mosaic with a north up and east left orientiation rather than a detector x-y orientation. Photometry on Post-BCD mosaics and MOPEX mosaics are consistent to within 0.1% on average, with a maximum deviation of around 2%.

2. Create a mosaic. In the BCD directory, your data will have suffixes *bcdb.fits* (16 microns) and *bcdr.fits* (22 microns). You can use MOPEX to create a mosaic from these individual images.

3. Extract photometry. You can extract photometric information from your mosaics using APEX (distributed as part of MOPEX). PRFs are provided to use within APEX. The units of photometry from APEX are automatically given in microJy. If you are using another package, e.g. IRAF, the fluxes will be output in the BCD units of MJy/sr. In order to correct to microJy, you should convert to steradian per arcsecond, and then multiply by the pixel area. The default pixels in the mosaics are 1.8" x 1.8" = 3.24 square arcseconds per pixel (the BCDs have a pixel area of 3.367 square arcseconds per pixel). The conversion factor for the default mosaics is therefore:

1 MJy/sr = (1E12 microJy)/(4.254517E10 arcsec^2) x 3.24 arcsec^2 = 76.1544 microJy.

4. Apply a color correction. For Peak-Up Imaging observations, the photometric calibration assumes the source spectrum has the spectral shape νF_ν = constant. The calculations take into account the full spectral response of the instrument. Due to the so-called "Red Leak" (a small increase in response at about 28 microns) some emission will be detected in the Blue Peak-Up camera for very cold sources that would not have been detected in a system without the red leak. This translates into large correction factors for very cold sources (T<50 K) observed with the Blue Peak-Up camera. While these numbers are formally correct, the observers should be very wary of blindly applying them to the data. Longer wavelength observations are advised in this case.

To get the peak-up flux for a non νF_ν = constant shape, divide the flux by the appropriate color correction factor. See Table 4.12 and Table 4.13.

5. Apply an aperture correction. Photometry measured within a given aperture must be corrected to obtain the total flux within an infinite aperture. Section 4.2.4.1 provides aperture corrections to infinity for a variety of spectral types and aperture radii.

Chapter 9. IRS Enhanced Spectrophotometric Products

9.1 Introduction

This document describes the IRS Enhanced Spectrophotometric Products. The Enhanced Products consist of two elements:

(1) A collection of 16,986 low-resolution, Merged Spectra

(2) A Catalog of extracted source positions, synthetic photometry in several bands, PSF profile widths, and other useful quantities. See Table 9.5 in Section 9.4 for a listing and brief description of all data columns in the Catalog.

These products were produced starting with the final SSC pipeline (ver. 18.18) bksub.tbl SL and LL spectra. The bksub.tbl spectra (see Table 6.7 in the IRS Instrument Handbook) were extracted from the nod two minus nod one and nod one minus nod two background-subtracted basic calibrated data, using an aperture that expands linearly with wavelength (see Section 5.7.3 of the IRS Instrument Handbook). The calibrated fluxes are consequently strictly valid only for point sources.

9.2 Merged Spectra

All low-resolution spectra of a given target in an AOR were combined to give a single low- resolution spectrum. For AORs with spectra from all 4 low-resolution slits (SL2, SL1, LL2, LL1), the resultant spectra span the wavelength range 5.21-38 microns.

The median spectrum was created for all exposures at a given nod position. The two nod spectra were then averaged to give a single spectrum per spectral order (Fig. 9.1). The available orders were then concatenated with the wavelength clipping ranges shown in Table 9.1. The standard flux calibration for each order was maintained. No additional scaling was applied to the flux densities of the orders to make them match. The flux uncertainty ('error') was computed by adding the flux uncertainty from the two nod spectra in quadrature.

Each Merged Spectrum is an ASCII IPAC table, containing a header followed by a number of data rows, one for each spectral sample. The meaning of data rows and columns is identical to that in the bksub.tbl files except for the values in the "order" column. See Table 9.2 for details.

Table 9.1 – Orders and wavelengths in a Merged Spectrum file

Order Number	Module Name	Minimum Wavelength	Maximum Wavelength

1	SL2	5.21	7.56
2	SL1	7.57	14.28
3	LL2	14.29	20.66
4	LL1	20.67	38.00
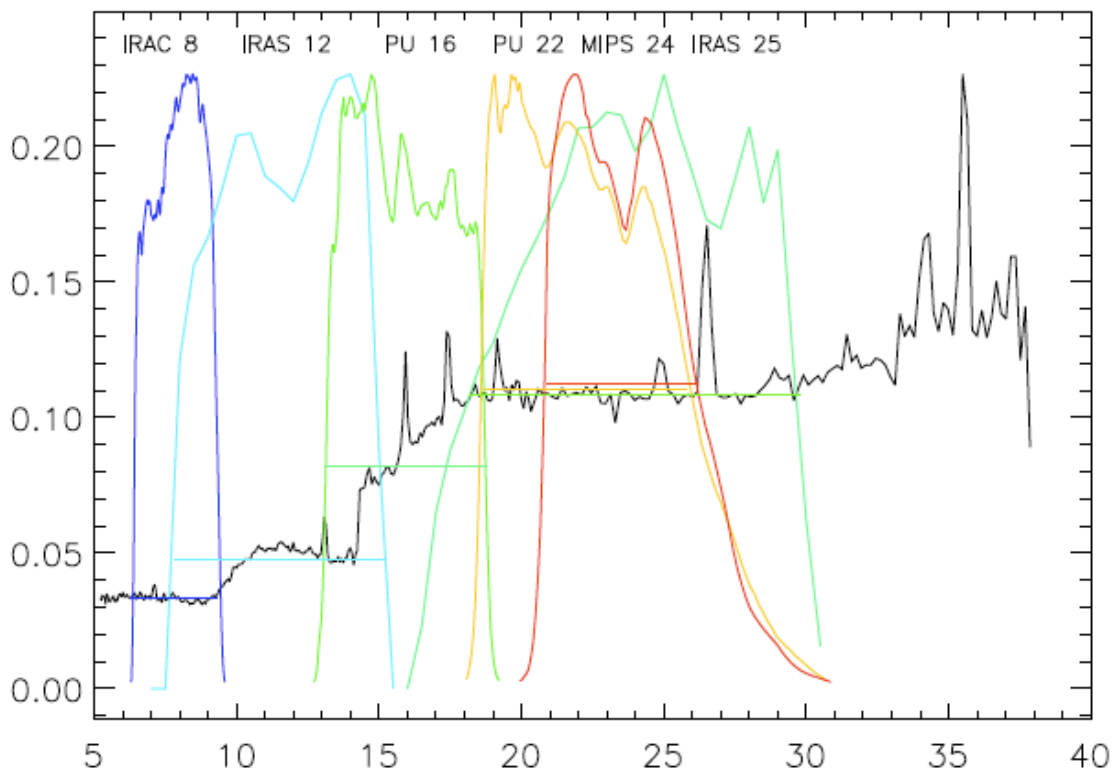
Figure 9.1 - Example IRS Merged Spectrum (black line). The IRAC 8 (blue), IRAS 12 (cyan), IRS PU 16 (green), IRS PU 22 (orange), MIPS 24 (red), and IRAS 25 (blue-green) transmission curves are superimposed on the merged spectrum. The synthetic flux in each band is indicated by a colored horizontal line. For clarity, the MIPS 24 and IRAS 25 photometry have been shifted up or down by 0.002 Jy, respectively.

Table 9.2 - Data columns in a Merged Spectrum table file:

Column Name	Units	Description
Order	Integer	1 for SL2; 2 for SL1; 3 for LL2; 4 for LL1
Wavelength	microns	Wavelength of spectral sample. The data rows are in strict order of ascending wavelength and there is no order overlap.
flux_density	Jy	Flux density at a wavelength sample in the Merged Spectrum.
error	Jy	Estimated uncertainty of the flux density. This is computed by adding the two nod "error" values in quadrature. When doing this computation, if any nod "error" value is less than 0.0001, it is assumed to be 0.0001 .
bit-flag	Integer representation of binary number	Status bit-flags for this sample -- This is computed as the logical "OR" of bit-flags from the two input nods. Section 6.5.5 of the IRS Data Handbook gives the meanings of the individual bits.

NOTE: There are never any NaN values in the table. If a value is not available for a data row, that data row will simply be left out of the table.

9.3 Calculated Values for Merged Spectra

9.3.1   SNR Estimates (keywords: SNR_SL2, SNR_SL1, SNR_LL2, SNR_LL1)

An SNR estimate is given for each order in the merged spectrum. It is computed as the mean of all "flux density" values divided by the mean of all "error" values. These values are only in the product headers, not in the Catalog.

9.3.2 Spectrophotometry (keywords: IRAC8, IRAS12, IRS16, IRS22, MIPS24, IRAS25)

Source photometry was synthesized from the merged spectra in 6 standard filters:

IRAC 8, IRAS 12, IRS blue peak-up (PU 16), IRS red peak-up (PU 22), MIPS 24, and IRAS 25 (Fig. 9.1). The merged IRS spectra were convolved with the band-pass transmission curves to compute the flux at the effective central wavelength in each filter (Section 9.5).

The uncertainty values for the IRS Enhanced spectrophotometric fluxes were computed by propagating the uncertainties from the merged spectra. An additional uncertainty factor of 1.1-1.8% was added in quadrature with the pipeline uncertainties to account for additional sources of photometric noise, such as slit-loss or flat field noise (Section 9.5). This 'repeatability' uncertainty factor was measured for each order from the fractional standard deviation of the ensemble of HR 7341 primary standard star flux measurements.

IRS Enhanced spectrophotometry was checked against actual IRAC 8, PU 16, PU 22, and MIPS 24 observations of IRS calibration stars (Fig. 9.2). These calibration stars were observed many times by IRS, so median flux values and their 1σ errors are shown for each band . The synthetic IRS photometry for these stars matches the IRAC 8, PU16, PU 21, and MIPS 24 photometry to better than 5%.
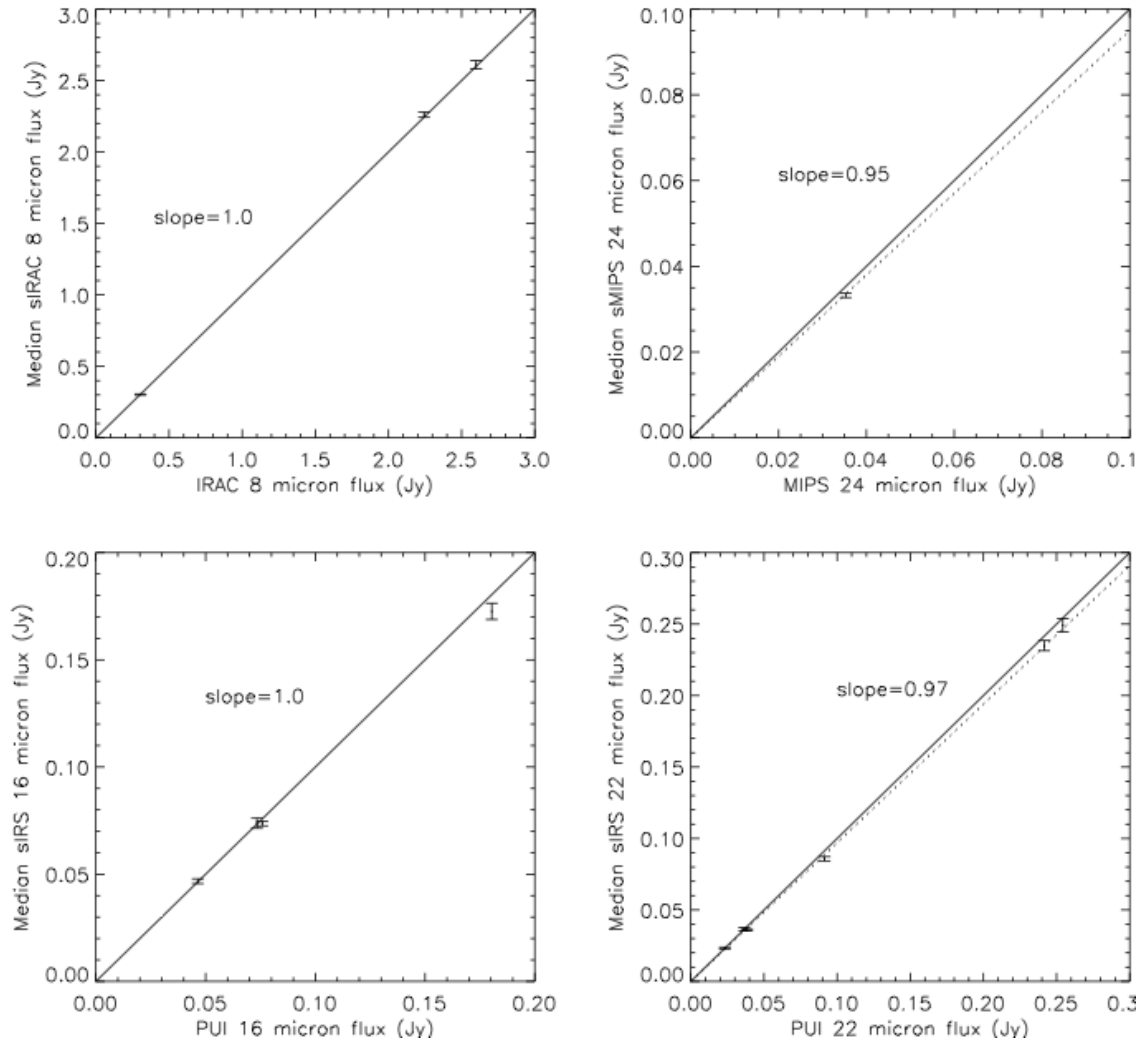
Figure 9.2 - Comparison of median synthetic photometry of IRS flux standard stars with actual IRAC 8, MIPS 24, PU 16, and PU 22 measurements of these same stars. These stars were observed many times by Spitzer IRS. The vertical error bars represent the standard deviation of the mean over all visits for the IRS spectrophotometry. The slopes of the best-fit (dotted) lines give an indication of how well the synthetic photometry compares to the integrated light measurements of the same stars. Unity slopes are indicated by the solid lines.

9.3.3 Source Colors (keywords: mips24_irac8, mips24_irs16, irs16_irac8, iras25_iras12)

Four source colors (MIPS 24/IRAC 8, MIPS 24/IRS 16, IRS 16/IRAC 8, and IRAS 25/ IRAS 12) are computed from the ratios of synthetic fluxes in five of the photometric bands. The distribution of MIPS 24 versus IRAC 8 fluxes is shown in Figure 9.3. The locus of stars with Rayleigh-Jeans spectra stands out with a MIPS 24/IRAC 8 flux density ratio of ~0.2. Star-forming galaxies typically have MIPS 24/IRAC 8 colors in the range 1-10.
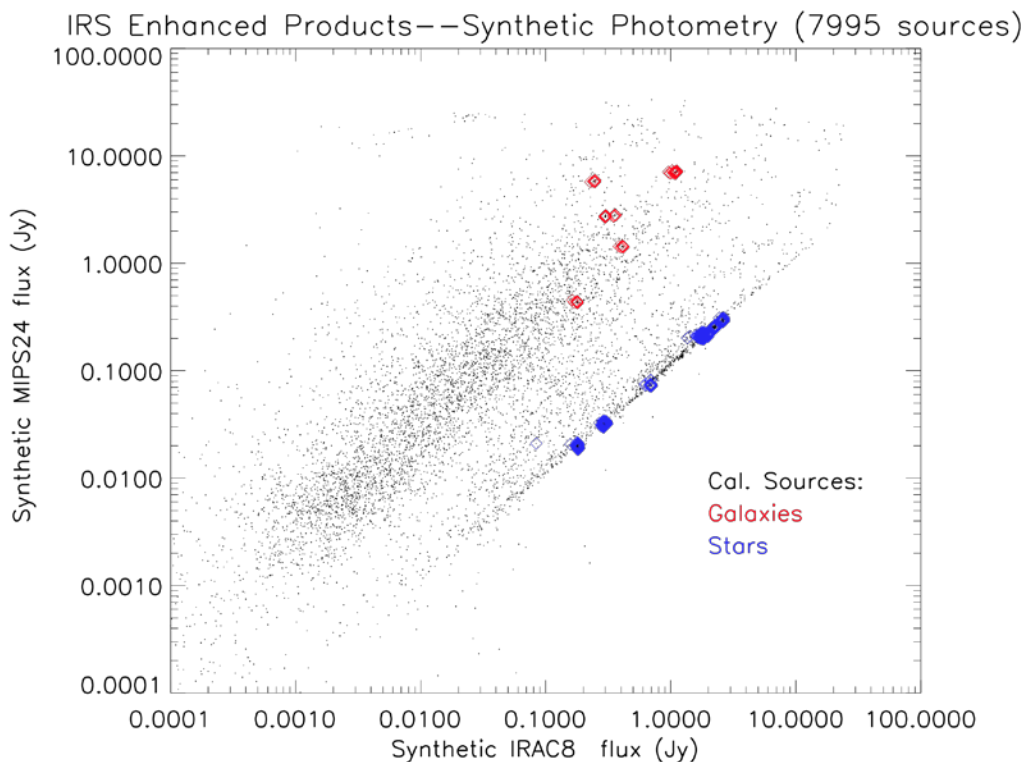
Figure 9.3 - MIPS 24 versus IRAC 8 synthetic IRS spectrophotometry. A narrow locus of stars with blue (Rayleigh-Jeans) MIPS 24/IRAC 8 colors of ~0.2 and a broader band of galaxies with red colors in the range of 1-10 are both apparent. IRS calibration stars (blue diamonds) and galaxies and AGNs (red diamonds) are shown for reference.

9.3.4 Extracted Source Positions (keywords: RA, DEC, RA_SL, DEC_SL, RA_LL, DEC_LL)

Source positions in each slit were computed from the location of the source along the slit determined from the spectral trace ('ridge') measured by the SSC pipeline, compared to the slit center position, as recorded in the FITS header for each exposure (see Section 5.7.2 in the IRS Instrument Handbook). This computation interpolated between the "_FOV" and "_SLT" coordinates given in the header of the bksub.tbl files. If SL is available, the reported right ascension and declination (RA, DEC) is for the

average of all SL exposures and nods. If SL is not available, then LL is used. The position angles (PA_SL and PA_LL) are the same as PA_FOV in the bksub.tbl files.

A plot of extracted minus requested positions for calibration targets (Fig. 9.4) gives an indication of positional uncertainty, for observations using high-accuracy blue peak-up. Location in this plot will depend upon the accuracy of the requested position and peak-up accuracy, as well as the intrinsic pointing accuracy of the telescope. Circles drawn in Figure 9.4 show the 68%, 95%, and 99% error circles for positional accuracy. The radii of these circles are 0.36", 0.62", and 1.35", respectively, after deleting 12 deviant points from Campaign 7 (3 of which are plotted; 9 fall off the plot), when there was some difficulty pointing the telescope. For all other campaigns, the 1σ uncertainty on the extracted IRS source positions is 0.36".
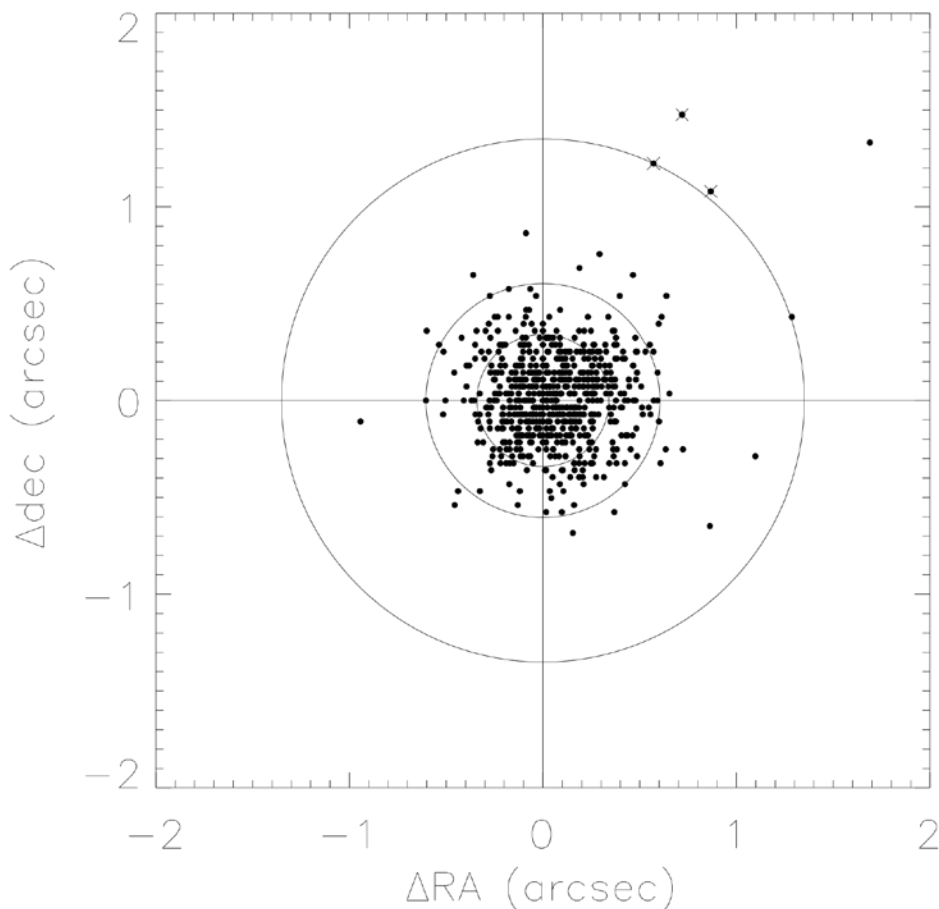
Figure 9.4 - Distribution of IRS position measurements for IRS calibration sources, relative to requested position. Circles with radii of 0.36", 0.62", and 1.35" enclose 68%, 95%, and 99% of the measurements, respectively. The three X's mark observations taken during Campaign 7, when

observations were affected by known telescope pointing issues. (Nine additional deviant observations from this campaign fall off of the plot.)

9.3.5 *Spatial Profile Widths (keywords: WIDTH_SL2, WIDTH_SL1, WIDTH_LL2, WIDTH_LL1)*

Spatial profiles are generated for each background-subtracted spectrum as part of the standard SSC pipeline. The computation of these profiles is described in section 5.7.1 of the IRS Instrument Handbook. The FWHM (") of these profiles are reported in the Catalog for each observed spectral order. The FWHM is found by first finding the maximum flux in the profile. Starting at this maximum point, the profile is searched on the left and right side for the first flux value less than half of the maximum flux. The adopted width is the distance between the left point and the right point. A profile FWHM value is not considered reliable if the SNR ("SNR_*" keyword) is less than 5.0. In this case the WIDTH value is set to -99.0.

The distribution of profile widths is shown in Table 9.3 and Figure 9.5. The distribution of profile widths for IRS calibration stars has 95.4 percentile widths in SL2, SL1, LL2, and LL1 of 2.56", 2.68", 6.97", and 8.34", respectively (Table 9.3). Source profile widths may be compared to these values to determine whether a source may potentially be extended. However, these fiducial values are strictly only valid for a source with a stellar (Rayleigh-Jeans) spectrum. For sources with redder spectral slopes, we have separated blue and red sources based on a MIPS 24/IRAC 8 flux ratio of 1.0, which roughly divides stars from galaxies in Figure 9.3. The 95.4 percentile widths for blue sources range from 2.88"-22.62", going from SL2 to LL1 (Table 9.3). The 95.4 percentile widths for red sources range from 5.54"-27.69". Red sources generally have larger profile widths in a given order because their spatial profiles are weighted more heavily towards the red end of the spectrum, which is broader in our diffraction-limited data, and because (red) galaxies are more likely to be spatially resolved than (blue) stars.

Table 9.3 - Distribution of spatial profile widths:

Category	68.2% FWHM(")	95.4% FWHM (")	99.7% FWHM (")
SL2 Cal Stars	2.51	2.56	9.90
SL2 Blue	2.51	2.88	13.82
SL2 Red	2.66	5.54	15.28
SL2 All	2.56	5.53	15.28
SL1 Cal Stars	2.60	2.68	2.76
SL1 Blue	2.65	3.36	16.24
SL1 Red	2.96	7.12	17.61

SL1 All	2.85	6.75	18.07
LL2 Cal Stars	6.05	6.97	8.93
LL2 Blue	6.38	11.26	60.26
LL2 Red	7.22	18.62	55.27
LL2 All	6.89	17.47	56.28
LL1 Cal Stars	8.15	8.34	8.68
LL1 Blue	8.34	22.62	65.52
LL1 Red	9.24	27.69	61.49
LL1 All	8.90	27.19	61.49
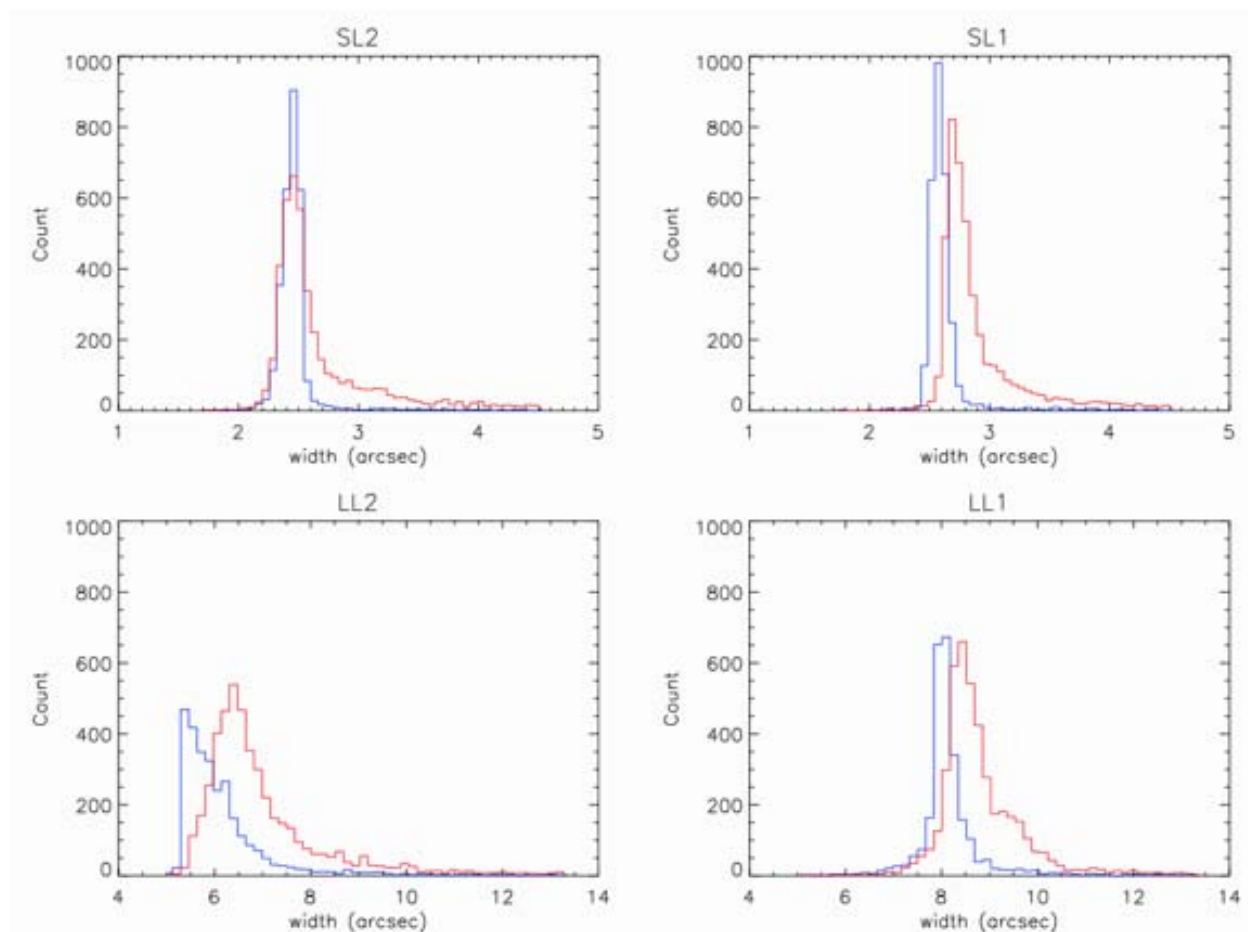
Figure 9.5 - Distributions of IRS spatial profile widths for the SL2, SL1, LL2, and LL1 orders. The profile widths generally increase going from short to long wavelengths, reflecting the spatial resolution of the telescope and instrument. Distributions are shown for blue sources (blue lines) and red sources (red lines), separated at a MIPS 24/IRAC 8 flux density ratio ratio of 1 (Fig. 9.3). Calibration stars (not shown) follow a distribution similar to that of the blue sources. Galaxies tend to be red sources with MIPS/IRAC8>1.

9.3.6 Order Ratios (keywords: RATIO_SL2_SL1, RATIO_Sl1_LL2, RATIO_LL1_LL2)

Each of these values is the ratio of the mean flux density at the edges of two neighboring orders. If a ratio differs significantly from unity, it could indicate any of the following. (1) The observed position falls away from the intended source, which misses or is offset perpendicular to one of the slits. (2) The observations are pointed at different sources. (3) The source is extended. A RATIO_SL1_LL2 of less than unity may indicate an extended source, where the larger LL slit admits more flux than the smaller SL slit. (4) There are strong spectral features near the order edges.

Order ratios are calculated as follows:

RATIO_SL2_SL1 = EDG_SL2_HI / EDG_SL1_LO

RATIO_SL1_LL2 = EDG_SL1_HI / EDG_LL2_LO

RATIO_LL2_LL1 = EDG_LL2_HI / EDG_LL1_LO

The edges of orders are in the ranges shown in Table 9.4.

Table 9.4 - Orders and wavelengths in a Merged Spectrum file:

Order	Module	"LO" edge (micron)	"HI" edge (micron)
1	SL2	--------------	7.25 - 7.56
2	SL1	7.57 - 8.15	13.60 - 14.28
3	LL2	14.29 - 15.05	19.80 - 20.66
4	LL1	20.68 – 22.30	----------------

9.4 Description of Catalog Data

Table 9.5 - Columns in the Catalog :

NOTES: All of the flux densities, flux density uncertainties, and flux density ratios in the Catalog are synthetic values measured with Spitzer IRS. All right ascension and declination values are J2000.

N	Name	Format	Nulls	Units	Description
0	reqkey	8d	n		Spitzer Request ID
1	tn	3d	n		Nth Target in this AOR
2	object	20s	n		Object name specified by observer
3	ra	9.5f	n	degree	Primary Extraction RA J2000.
4	dec	9.5f	n	degree	Primary Extraction DEC J2000
5	cra	12s	n		HHhMMmSS.SSs form for RA
6	cdec	12s	n		+DDdMMmSS.Ss form for DEC
7	irac8	10.3e	y	Jy	Synthetic IRAC 8 micron flux
8	irac8u	10.3e	y	Jy	Synthetic IRAC 8 micron flux uncertainty
9	iras12	10.3e	y	Jy	Synthetic IRAS 12 micron flux
10	iras12u	10.3e	y	Jy	Synthetic IRAS 12 micron flux uncertainty
11	irs16	10.3e	y	Jy	Synthetic IRS 16 micron flux
12	irs16u	10.3e	y	Jy	Synthetic IRS 16 micron flux uncertainty
13	irs22	10.3e	y	Jy	Synthetic IRS 22 micron flux

14	irs22u	10.3e	y	Jy	Synthetic IRS 22 micron flux uncertainty
15	mips24	10.3e	y	Jy	Synthetic MIPS 24 micron flux
16	mips24u	10.3e	y	Jy	Synthetic MIPS 24 micron flux uncertainty
17	iras25	10.3e	y	Jy	Synthetic IRAS 25 micron flux
18	iras25u	10.3e	y	Jy	Synthetic IRAS 25 micron flux uncertainty
19	mips24_irac8	8.4f	y		Synthetic color ratio: MIPS24 / IRAC8
20	mips24_irs16	8.4f	y		Synthetic color ratio: MIPS24 / IRS16
21	irs16_irac8	8.4f	y		Synthetic color ratio: IRS16 / IRAC8
22	iras25_iras12	8.4f	y		Synthetic color ratio: IRAS25 / IRAS12
23	ra_sl	9.5f	y	degree	Mean extraction RA for SL (orders 1&2)
24	dec_sl	9.5f	y	degree	Mean extraction DEC for SL (orders 1&2)
25	pa_sl	10.5f	y	degree	Mean FOV_PA for SL (orders 1&2)
26	ra_ll	9.5f	y	degree	Mean extraction RA for LL (orders 3&4)
27	dec_ll	9.5f	y	degree	Mean extraction DEC for LL (orders 3&4)
28	pa_ll	10.5f	y	degree	Mean FOV_PA for LL (orders 3&4)
29	date_obs	19s	n		Date/Time of first observation (UTCS)
30	campname	10s	n		Spitzer campaign name
31	bandpass	24s	n		Band pass definition
32	oflag	3d	n		Order flags, sum of: 1=SL2 2=SL1 4=LL2 8=LL1

33	ratio_sl2_sl1	5.3f	y		flux ratio SL2 / SL1
34	ratio_sl1_ll2	5.3f	y		flux ratio SL1 / LL2
35	ratio_ll2_ll1	5.3f	y		flux ratio LL2 / LL1
36	ra_rqst	9.5f	n	degree	Requested RA J2000
37	dec_rqst	9.5f	n	degree	Requested DEC J2000
38	ra_del	9.5f	n	degree	ΔRA = (RA-RQST_RA) * cos(DEC)
39	dec_del	9.5f	n	degree	ΔDEC = DEC - RQST_DEC
40	width_sl2	5.2f	y	arcsec	SL2 width of profile
41	width_sl1	5.2f	y	arcsec	SL1 width of profile
42	width_ll2	5.2f	y	arcsec	LL2 width of profile
43	width_ll1	5.2f	y	arcsec	LL1 width of profile
44	ra1	9.5f	n	degree	Primary extraction corner 1 RA J2000
45	dec1	9.5f	n	degree	Primary extraction corner 1 DEC J2000
46	ra2	9.5f	n	degree	Primary extraction corner 2 RA J2000
47	dec2	9.5f	n	degree	Primary extraction corner 2 DEC J2000
48	ra3	9.5f	n	degree	Primary extraction corner 3 RA J2000
49	dec3	9.5f	n	degree	Primary extraction corner 3 DEC J2000
50	ra4	9.5f	n	degree	Primary extraction corner 4 RA J2000
51	dec4	9.5f	n	degree	Primary extraction corner 4 DEC J2000

52	ra1_sl	9.5f	y	degree	SL extraction corner 1 RA J2000
53	dec1_sl	9.5f	y	degree	SL extraction corner 1 DEC J2000
54	ra2_sl	9.5f	y	degree	SL extraction corner 2 RA J2000
55	dec2_sl	9.5f	y	degree	SL extraction corner 2 DEC J2000
56	ra3_sl	9.5f	y	degree	SL extraction corner 3 RA J2000
57	dec3_sl	9.5f	y	degree	SL extraction corner 3 DEC J2000
58	ra4_sl	9.5f	y	degree	SL extraction corner 4 RA J2000
59	dec4_sl	9.5f	y	degree	SL extraction corner 4 DEC J2000
60	ra1_ll	9.5f	y	degree	LL extraction corner 1 RA J2000
61	dec1_ll	9.5f	y	degree	LL extraction corner 1 DEC J2000
62	ra2_ll	9.5f	y	degree	LL extraction corner 2 RA J2000
63	dec2_ll	9.5f	y	degree	LL extraction corner 2 DEC J2000
64	ra3_ll	9.5f	y	degree	LL extraction corner 3 RA J2000
65	dec3_ll	9.5f	y	degree	LL extraction corner 3 DEC J2000
66	ra4_ll	9.5f	y	degree	LL extraction corner 4 RA J2000
67	dec4_ll	9.5f	y	degree	LL extraction corner 4 DEC J2000
68	heritagefilename	80s	n		full path filename to product in SHA
69	table	134s	n		HTML link to product for Gator
70	enhid	8d	n		Spitzer database Enhanced Product ID

71	campid	5d	n		Campaign ID in Spitzer database
72	obsrvr	18s	n		Name of observer
73	progid	5d	n		Observation program ID
74	wave_min	9.5f	n	micron	wavelength of first data line
75	wave_max	9.5f	n	micron	wavelength of last data line
76	filetype	5s	n		Type of file (always "Table")
77	filedesc	20s	n		File description (always "IRS Merged Spectrum")
78	instmode	9s	n		Instrument mode (always "Irs Stare")
79	equinox	4d	n		Equinox of observation (always 2000)

9.5 Computation of IRS Synthetic Photometry

Photometry calculations are carried out in using the following definitions:

$\nu = c / \lambda$

T_ν = value in the response (transmission curve) table, interpolated for ν

$R_\nu = T_\nu$ for MIPS 24

   $= T_\nu / \nu$ for all others

f_ν = interpolated flux at ν

σ_ν = interpolated uncertainty of flux at ν

unc_{adjust} = uncertainty adjustment factor: SL2=0.011, SL1=0.011, LL2=0.016,   LL1=0.018

CC = color correction factor, 0.9679 for MIPS 24, and 1.0000 for all others.

    Computation of the MIPS 24 value is explained below.

$BB(\nu)$ = blackbody flux density at ν for a temperature of 10,000 Kelvin

Photometric flux is calculated as follows:

$FLUX = CC * \int f_\nu R_\nu \, d\nu \ / \ \int R_\nu \, d\nu$

The flux uncertainty is calculated by first integrating the input uncertainties:

$UNC_{initial} = \int \sigma_\nu R_\nu \, d\nu \ / \ \int R_\nu \, d\nu$

and then adding the uncertainty adjustment in quadrature:

$UNC_{final} = sqrt (UNC_{initial}^2 + (FLUX * unc_{adjust})^2)$

For all bands except MIPS 24, the standard reference spectrum is $f_\nu = 1/\nu$ so that the color correction factor is CC=1. For MIPS 24, a 10,000 Kelvin blackbody is used as a reference, necessitating a modest color correction factor at 24 microns. Calculation of the color correction factor CC for MIPS 24 starts with computing the effective wavelength:

$\lambda_{eff} = \int R_\lambda \, d\lambda \ / \ \int \lambda^{-1} R_\lambda \, d\lambda \ = \ 23.6749$ micron

$\nu_{eff} = c / \lambda_{eff} = \ 1.2663e+13$ Hz

$BB(\nu_{eff}) = BB(1.2663e+13) = 4.7694e-7$

Then the uncalibrated flux from the blackbody spectrum is computed:

uncalibrated_flux_bb = $\int$ BB(v) v R$_v$ dv / $\int v$ R$_v$ dv = 4.9275e-7

Finally, we get the color correction factor by dividing into blackbody flux density at the effective wavelength:

CC = BB(v_{eff}) / uncalibrated_flux_bb = 0.9679

The uncertainty adjustment factors are discussed in more detail in Section 9.3.2.

Appendix A.   Version Log

Version 5.0, December 2011:

Added Chapter 9: IRS Enhanced Spectrophotometic Products

Version 4.0, March 2011:

Updated Table 4.4 through Table 4.10**.**

Added Section 8.2.3 on Transit or Eclipse Spectra.

Revised several caveats in Chapter 7.

Added Table 6.2, which lists the number of reads per ramptime available for each module.

Version 3.0, January 2011:

Updated to describe S18.18.

Order of appendices changed to match order of references in text.

Removed references to obsolete software LEOPARD in favor or the [Spitzer Heritage Archive](#).

Added examination of correlation between 14 micron teardrop strength and source flux to Chapter 7.

Clarified which outputs described in Chapter 5 are available in the [Spitzer Heritage Archive](#), and which can be generated by running CUPID.

Version 2.0, September 2010:

Section 1.3 (IRS Essentials) has been updated to include all IRS operating modes.

Chapter 2 (Instrument Description) has been re-organized. Example IRS Data has been moved to Chapter 6 (Data Products).

Included information about signal-to-noise ratio for very long exposure times and link to Teplitz et al. 2007 paper in Section 2.10.2.

Added PSF/PRF Sections (Sections 4.2.3 and 4.2.4). This complements the new files provided in the IRS Calibration and Analysis Files section of the website.

Added a translation table between header keywords FOVID and FOVNAME in Section 6.6.4.

Moved example header from Chapter 6 to Appendix D.

Added Appendix E (a list of Figures) and 0 (a list of Tables).

Clarified several figures, including 2.2, 6.9, 6.4, 6.5.

Version 1.0, February 2009:

The first version of the IRS Instrument Handbook, which includes information from the IRS Data Handbook, the Cryogenic Spitzer Observer's Manual, the IRS Pipeline Description Document, and the Spitzer Science Center webpages. This version describes IRS pipeline version S18.7.

Appendix B.   Acronyms

ACQ

ACQuisition

AOR

Astronomical Observation Request

AOT

Astronomical Observation Template

ASCII

American Standard Code for Information Interchange

BCD

Basic Calibrated Data

DCE

Data Collection Event

DCS

Double Correlated Sampling

DN

Data Number

FITS

Flexible Image Transport System

IDL

Interactive Data Language

IRS

InfraRed Spectrograph

LH

Long-High (module)

LL

Long-Low (module)

MIPL

Multimission Image Processing Laboratory

NaN

Not-a-Number

PB

Peak-up Only Blue

PBI

Peak-up Imaging Blue

PCRS

Pointing Control Reference Sensor

PR

Peak-up Only Red

PRI

Peak-up Imaging Red

PSF

Point Spread Function

RSRF

Relative Spectral Response Function

SH

Short-High (module)

SL

Short-Low (module)

SPICE

SPitzer IRS Custom Extractor

SPOT

Spitzer Planning Observations Tool

SS

Sweet Spot

SSC

Spitzer Science Center

SUR

Sample Up the Ramp

WCS

World Coordinate System

Appendix C.   Pipeline History Log

This section describes changes to the IRS pipeline that accompany changes to the overall Spitzer pipeline. Roughly every six months, the pipeline number (the "S-number") for all new Spitzer data in the archive is increased. New data will appear in the archive with a different S-number than old data. Parallel to these changes, the IRS pipeline may be improved and those improvements are described below. However, old IRS data will not be reprocessed with new pipeline versions unless the are substantial changes in the data quality or the calibration files. Users that have already downloaded data do not need to download it again when new pipeline is released. When pipeline changes result in substantial improvements to the IRS data, all past campaigns will be reprocessed with the newest pipeline.

S18.18 (Release Date: January 2011)

  1. Outlier rejection logic improved for ramp-fitting in SLOPEFINDER. This helps to reduce noise in rare cases where there is one bad image plane.

  2. Improved and reduced pipeline uncertainty estimates. The new pipeline module SNEST_IRS2 revises the uncertainty estimate after droop correction. The biggest effect is seen for faint sources in SL, where droop is enhanced by flux from the Peakup Arrays.

  3. Uniform DCE weighting in coadd images. Previously, DCEs were flux-weighted in coadds. This caused spurious results, particularly noticeable in the SH module, including greatly enhanced noise in a fraction of AORs where spurious negative values might give rise to small or negative weights. For more details, see http://irsa.ipac.caltech.edu/data/SPITZER/docs/irs/features/#highres_coad_bug.

  4. Slightly revised LL1 wavsamp file to better follow stellar trace. A small sub-pixel shift at the blue end of LL1 results in a better fit to the position of the profile on the LL array and more recovered flux.

  5. Finer sampling of the object profile to more accurately determine the ridge location for extraction (Ncuts= 1000, 200, 1000, 200 for SL,SH,LL,LH), and to match the SPICE profile sampling.

  6. Rederived all flux calibration files, using data through the last IRS campaign.

  7. SL flux calibration split to account for IRS Campaign 33 frametable change. This results in slightly higher (<2%) SL1 fluxes and better low-resolution order matching for pre-33 data.

  8. SH and LH fluxes reduced by 2% at all wavelengths to match low-res flux calibration, based on standard star HR 7341.

  9. PUI zeropoints and aperture corrections updated using the best available observations of standard stars from all IRS campaigns.

 10. Blue and red peakup cutouts are now produced for all SL calibration data. These cutouts are calibrated and processed using the standard peakup imaging pipeline.

11. Peak-Up Acquisition images are now processed through a separate pipeline which calibrates these images and produces standard data products.

S18.7 (Release Date: May 2009)

1. The wavelength calibration files have been updated for S18.7 processed data. The primary change is to the wavsamp.tbl files for LL, SH, and LH, implementing improved wavelength calibration solutions.

2. The CDF files have also been updated for S18.7. SL and LL spectra are now divided by the height of the wavsamp extraction pseudo-rectangles, resulting in better matching orders in *extract.tbl* files.

3. The S18.7 flux calibration files (*fluxcon.tbl*, *aploss_fluxcon.tbl*) have been updated to account for the new wavelength calibration and CDF files described above. The SL, LL, SH, and post24 LH flux calibration are also refined by including additional calibration data from recent IRS campaigns.

4. The SH and LH flat-fields have been updated to account for the new wavelength calibration.

5. The bug causing duplicate and missing nods for background subtracted SL and LL staring mode data has been fixed. See IRS Important Note from 30 Jan 09.

6. The PU imaging calibration zeropoints are refined by including additional calibration data from recent IRS campaigns.

7. PU image cutouts have been created from SL observations.

9.5.1.1   S18.1 (Release Date: Aug 2008)

1. The file names of background-subtracted low resolution products (*bksub*) now include correct EXPID labels. Formerly, these labels incorrectly referred to the first EXPID in the AOR, instead of the actual EXPID.

2. Three new keywords have been added to PUI mosaics (post-BCD data): PA, PXSCAL1, and PXSCAL2. These keywords replace the CROTA2, CDELT1, and CDELT2 keywords in those data.

9.5.1.2   S18.0.1 (Release Date: Jun 2008)

1. Spectral table files are now provided also in FITS format

9.5.1.3   S17.2.0 (Release Date: Apr 2008)

1. The LH spectral extraction algorithm and corresponding flux calibration have been updated. The flux values (in e/sec) for LH delivered by the Extract module (Regular or Optimal) are now divided by the height (measured along the spectrum in pixels) of the extraction window, as set by the *wavsamp*

wavelength calibration file. This change improves the order matching in *_extract.tbl* spectra, but does not have much effect on the final, flux calibrated, *_spect.tbl* spectra delivered by Tune. These updates do not pertain to any of the other modules.

9.5.1.4   S17.0.0 (Release Date: Jan 2008)

1. Errors due to readnoise and Poisson noise are now incorporated in the pipeline uncertainties, and are propagated during slope estimation. Uncertainties are now propagated during background subtraction (*bksub*).

2. A new slope estimation module was developed. Slopes (fluxes) are now computed via linear fits to entire ramp, as opposed to individual slope fitting to consecutive samples.

3. Better treatment of ramp slopes after a radhit. The S16 pipeline discards all samples of a ramp following a radhit. This leads to improvement in the signal-to-noise for low illumination levels, but to a slight (10%) increase in noise in high resolution data, in the presence of many radhits (several hundred radhits per array). For S17, the ramp following a radhit is discarded only if the slope is <500 e-/s (before the radhit).

4. Darks are now campaign-dependent for LL, built from data taken in a symmetric moving window 5 campaigns wide. This improves the cosmetic appearance of non-background subtracted data but results in negligible differences for sky subtracted data.

5. The LL bias and temperature were changed in campaign 45 to reduce the number of rogue pixels. The decrease in gain resulting from the change is more than compensated by the reduction in rogue pixels, leading to a significant improvement in overall S/N (10-30%). New darks, nonlinearity coefficients, flats, and flux calibrations were derived for the new settings and used to process the S17 post-44 campaign LL data. Additional improvement was made in the post-44 flat-field spatial correction, leading to better nod and order matching.

6. The PU imaging mode has been recalibrated in order to reduce the zeropoint uncertainty, which is now 2%. The zeropoint is now tied to an infinitely large aperture. More details are given in the IRS Instrument Handbook (http://irsa.ipac.caltech.edu/data/SPITZER/docs/irs/irsinstrumenthandbook/)

9.5.1.5   S16.1.0 (Release Date: May 2007)

1. During slope fitting in SL, SH, and LH, all samples are discarded following a radhit. This implementation is already active for LL, since S15. The reason for this change is that the slopes of faint ramps can change by factors of 30% or more following a radhit (w.r.t. before the radhit).

2. The radhit module now allows to skip the first sample of a ramp during its detection process. Therefore the module now avoids the spurious detection of radhits in the second sample of a ramp. These spurious detections were caused by the first sample being depressed with respect to the rest of the ramp

slope, in modules such as SL. This implementation of skipping of the first sample does not apply to 4-sample ramps, because the radhit module needs a minimum of 4 samples to work.

3. All data taken from IRS campaign 40 onward (15 Apr 2007) will be processed with S16.1.0. Most previous data remain S15, with the exception of LH IRS campaigns 29 to 34 and campaign 36, as well as SL IRS campaigns 38 and 39. See the archive to Important Notes to Observers, note from 31 Jul 2007.

9.5.1.6   *S16.0.0 (Release Date: Apr 2007)*

No changes.

9.5.1.7   *S15.3.0 (Release Date: Feb 2007)*

All IRS data have been re-processed with S15.3.0 and are available for download.

Listed here are the most significant changes in this version.

1. To reflect all the pipeline changes, new flux calibration polynomials (fluxcons) were derived for all modules. Among other things, the new fluxcons corrected the 5% red tilt in LL2 present in S14 (see http://irsa.ipac.caltech.edu/data/SPITZER/docs/irs/features/, "Low-Res Nonrepeatability"). LL1 spectra now have slopes that are steeper (redder) by 3% over the spectral range, with respect to S14.

2. New flat-fields were built for all modules

a) The spatial behavior in all the flat-fields was improved. Observations in two different nods now match to better than 2%.

b) SH and LH flat-fields are now corrected using extended zodiacal light observations.

c) SL and LL interference fringes reduced to 1-2% level for sources well centered on the slit.

d) Bad regions in LH flat masked out to remove "bumps" at 20 microns.

3. Updated SH, SL, and LL *wavsamp* files

a) SH: The wavelength solution updated in all orders. The largest changes occurred at orders 19 and 20 (<0.5 pix). Spatial profiles changed in orders 11-15 only.

b) SL, LL: Updated spatial profile for all orders. The change is especially apparent in the LL2 ridge location. No wavelength changes were made, beyond very small shifts arising from the spatial profile change.

4. BCD products contain new header keywords VHELCORR and VLSRCORR to allow correction for the orbital velocity of Spitzer

The values of VHELCORR and VLSRCORR are to be added to velocities derived from IRS spectra, to obtain final velocities in the Heliocentric or LSR frames respectively. These keywords will be of interest only to observers measuring velocities with high precision from Short- High or Long-High spectra.

5. Revised uncertainty propagation

a) Suppressed propagation of the correlated component of uncertainty during residual droop correction.

b) During 2-D co-addition of BCDs (which produces the postBCD products *coa2d.fits* and *bksub.fits*), the output uncertainty (*c2unc.fits* and *bkunc.fits*) is now the root-sum-square of the input BCD uncertainties, divided by the number of co-added BCDs. Formerly (S14) the output uncertainty was the trim-standard deviation of the input BCDs.

c) The resulting uncertainties do not yet include all the systematics (photon noise per sample, readnoise, etc) associated with the processing.

6. Spectrum extraction heights and widths

a) SL and LL default extraction height changed from 1 pixel to native *wavsamp* height, to better follow spectrograph resolution.

b) SL3 default extraction aperture widened to 5.3333 pixels at 8.0 microns, to match SL2.

7. Updated SL, LL, and SH super-darks

New observations of the dark spot were obtained at times when the zodiacal emission was lowest. This change is most apparent for LL, which used to have a mixture of high and low zody data.

8. Radhit rejection in LL ramps

All samples of a ramp following a radhit are discarded during slope estimation in Long-Low data. This results in improved signal-to-noise in faint long-low data. Future pipelines will implement the rejection in other modules.

9. The calibration files for the Peak-Up Imaging mode have changed

a) Absolute calibration values and aperture corrections have been updated, which results in changes in measured photometric values of <15%.

b) New PRFs have been provided for APEX.

c) The bit masks have been updated to better interact with the mosaicker from MOPEX.

d) Fixed bug in error propagation. Users still need to remember the systematic zeropoint uncertainty for themselves.

9.5.1.8   S14.0.0 Partial Reprocessing (Release Date: Jul 2006)

All IRS data taken during or after IRS Campaign 30 (i.e., after the DATE_OBS keyword = 2006-04-16T00:00:00) have been processed with the S14.0.0 pipeline. Except for the special cases mentioned below, the pipeline is identical in every way to that of S13.2.0 and S13 versions of SPICE will work seamlessly with S14 data. (No changes have been made to fluxcon files or other SPICE related files for S14).

Special reprocessing of IRS campaigns back to IRS Campaign N2

Two targeted changes have been made to archived data for S14 which will lead to improvements in the quality of these data.

1. All IRS Long-Low (Channel 2) data, extending back to Campaign N2 in IOC, have been reprocessed through S14.0.0 to improve the linearity correction for saturating sources. The largest changes (15-20% in some cases) will be found for targets with flux densities well above 1 Jy, in regions of the spectrum where the ramps approach or exceed saturation. Targets with fluxes less than 1 Jy will, in general, be less affected unless long ramps were used leading to saturated/near saturated values. The improvements manifest themselves as smoother spectral continua in the 20-30 micron range, and reduced noise in this region. In all cases the apparent flux density in the affected region of the spectrum will go down, since the linearity correction has been reduced. Users should not be worried that they have mixed S13 and S14 data for targets involving observations with both SL and LL prior to Campaign 30. This is to be expected since the S13 and S14 pipelines are identical for SL (as they are for SH and LH).

2. All IRS Peak-up imaging AORs were reprocessed through S14.0.0 to ensure that improved 16 and 22 micron PRF files (Point-source Response Function) were correctly included with archived products. Previous versions of the pipeline had provided for the user a preliminary version of the PRF which could have led to problems with automated extraction of sources in MOPEX. The reprocessing and archive to these new PRF files ensures that the automated calibration, if run by the user, will lead to results consistent with those fluxes derived by manual extraction. Further refinements of the red PRF are underway and an even better version will be available in S15.

9.5.1.9   S13.2.0 (Release Date: Jan 2006)

All IRS data taken in Nominal Ops campaigns 1-27, and SV campaigns N2-R have been re-processed with S13 and are in [the process of being] archived. Check this page to see when your favorite campaigns have been archived and are available for download.

There are a number of significant changes to these data processed through the S13 pipeline. These are:

Wavelengths

   * Wavelength calibration updated for all Short-Hi orders.

   * Spatial centering of the wavelength solution was changed for most modules.

    - Largest LH shift is 0.5 pixels for order 11.

    - Largest SH shift is 0.3 pixels for order 20.

    - 0.68 pixel shift of LL2.

    - LL slit length was increased to 34 pixels.

   * The sampling of the LL and SL "bonus" (order 3) wavelength solution was changed to match the gridding of order 1.

   * LH wavelength samples were adjusted to ensure none fall completely off the detector array.

   * The sign of the spatial offset in the *b?_wavsamp_offset.fits* files were changed for SL, LL and SH, to properly align with the sense of the PA_SLT keyword in the FITS headers.

   * The scale of the LH *b3_wavsamp_offset.fits* file was updated to reflect the correct value of 4.5 arcseconds per pixel.

Flat Fields

Completely new (and improved) flat fields have been created for all modules, including a new flat field that applies specifically for LH data taken after the bias change to the detector at the beginning of IRS Campaign 25.

Flux Calibration

Significant refinements have been made to the Flux calibration in all modules, with new fluxcon tables for each module. As a result of the change in bias made for the LH module at the beginning of IRS Campaign 25, we now provide a different fluxcon table for data taken from Campaign 25 onwards.

As a result of improved flux calibration, we discovered a phenomenon we have called the "teardrop" effect in the SL module. The SL fluxcon tables differ from previous pipeline processing, in that the teardrop enhancement is not fitted out by the fluxcon tables. The resulting fluxcon table is much more linear over the SL1 module. Users are warned that as a result of the new fitting procedure, the teardrop effect will be more obvious than it was in past processing (previous processing partly masked the effect of the teardrop to the detriment of our flux calibration). The cause of the teardrop effect is not fully understood yet by our team.

Linearity Coefficients post LH bias-change

We have modified the linearity coefficients use to correct non-linearities in the ramps for data taken in LH after the bias change (Campaign 25 and onwards).

Browse-quality Automatic Background Subtraction for Low-res modules in Stare-mode only

We have implemented an automated background subtraction process for all low-res data taken in staring mode. The process operates only on co-added data, and subtracts adjacent nod positions. Spectra are extracted automatically from these new products. (See IRS DATA Handbook for details). We caution users that this process is not necessarily the optimal way to do background subtraction in a number of cases. Firstly if the source is extended over a significant part of the slit then obviously the automated nod subtraction will not work. Secondly, for very bright point sources, the extended PSF from one nod position could extended far enough at the long wavelength end of the spectrum to compromise the background subtraction. The greatest benefit of the automated subtraction will be for faint point-sources with no other confusing source in the slit. Useful filenames have the following suffixes: *bksub.tbl* (irs-tuned final nod-subtracted spectrum), *bksub_unc.fits* (uncertainty file). If you have downloaded your S13 data prior to 02 Feb 2006, it may have been missing the post-BCD background subtracted staring mode data. If this is the case, and these data are needed, you should download the files again.

Coordinates and *wavsamp_offset* files

S13 SPICE has the capability to view the coordinates of sources which are within the slit. For this purpose, it utilizes the *b?_wavsamp_offset.fits* and *b?_wavsamp_omask.fits* cal files. The cal files, specifically the *b?_wavsamp_offset.fits* files, which you get when downloading your pipeline processed data from the archive have the incorrect sign convention which will result in the coordinates being incorrect. Therefore, S13 SPICE should only be used with the cal files which come with the SPICE release rather than the archived cal files.

Row-Droop Correction Applied to SL module

As discussed in detail in the notes for the S12.0 pipeline release (below) we were not correcting fully for the effects of row-droop. This problem has been fixed in S13. The correction is only applied to SL because of the high charge loading on the SL peak-up arrays. In the other modules, no correction is necessary.

Browse-quality IRS Peak-up Imaging through the MOPEX image mapper

Unlike S12, we now pass data that was obtained under IRS Peak-up Imaging mode through the MOPEX mosaicking software and generate browse-quality peak-up images. The files are named with the following suffixes: *b_mos.fits* and *r_mos.fits* (blue and red peak-up mosaics), *b_unc.fits* and *r_unc.fits* (uncertainty files) and *b_cov.fits* and *rr_cov.fits* (coverage maps).

9.5.1.10 S12.0 (Release Date: Jun 2005)

All IRS data taken in Nominal Ops campaigns 1-20, and SV campaigns N-R have been re-processed with S12 and are in the process of being archived. Check on this page to see when your favorite campaigns have been archived and are available for download.

Memo on IRS uncertainties (October 2005)

There are three significant changes to the data processing for S12. These are:

   1. Wavelengths: The wavelength solutions (*wavsamp* files) for all modules have been changed. This was primarily to correct some inter-order offsets that were apparent in the S11 data. These changes include wavelength shifts (e.g. for SL1) and changes to the dispersion (e.g., for SH, LH LL and SL2). Lines will shift (from their S11 positions) by 0.01-0.14 microns, depending upon wavelength and module.

   2. Flux calibration: Small changes to the Short-High and Long-High flux calibration (fluxcon files) were made in accordance with the wavelength changes described above. These should reduce order to order variations seen in some S11 data.

   3. Short-Low stray light: The correction for stray light in the Short-Low module (see the Observers Manual and Pipeline Handbook) has been modified to include only an exponential fall-off from the Peak-up arrays for S12. Previously, this stray-light correction also included a small "pedestal" term in addition to the exponential. The removal of this pedestal occasionally caused unwanted horizontal striping in Short-Low data. These stripes should not be present in your S12 data. Observers should be aware that although the net effect of this modification is positive (data processed through the S12 are of generally superior quality to S11), the fact that we no longer remove a "pedestal" means that a minor effect called "row droop" will be present in the final spectra. As we discuss below, this will have almost no impact on users if they perform a background subtraction of SL data (this is highly recommended in most observing strategies). However, in the unlikely event that background subtraction is not performed, observers should be aware of the possible consequences of uncorrected row-droop.

"Row-droop" is an additive (pedestal-like) signal which can affect all the ramps along a given row of an image by a constant factor which is proportional to the total charge seen on that row of the detector. The Short-low module is the most likely detector affected by the problem because the peak-up arrays can contain a significant signal--and this signal can cause an increase in the flux seen along that entire row-- especially when observing medium and high background scenes. Because we are no longer removing a pedestal from SL data in the stray-light correction, row-droop will be present in your S12 Short-Low BCD data at some level of significance. It will manifest itself as an apparent increase in the flux in SL2 and SL1 in regions where the peak-up arrays affect those rows. In contrast, the pedestal will NOT BE present in rows between the two peak-up arrays--an effect that could cause the observer to think they had faint absorption there. The spectral region that might show an apparent flux deficit is between 5.5-5.9 microns and 11.2-11.8 microns--the wavelength regions corresponding to the rows in SL2 and SL1 that are between the peakup arrays. Sky subtraction will remove this effect. However, observers of extended sources should take care in interpreting low-level spectral variations at these wavelengths in their Short-Low S12 data if no appropriate sky subtraction is performed. We will characterize and remove this pedestal in future pipeline releases. Observers are encouraged to compare their SL data before and after sky subtraction to gauge the relevance of this effect on their science.

9.5.1.11 S11.4.0 (Release Date: Feb 2005)

Most of the changes were uplink-related (e.g., Spot-related) and thus do not affect the data. However, the LH dark calibration files (which are updated every campaign) have changed and so depending on whether or not you have data from the IRS LH module, you might have updated dark files.

9.5.1.12 S11.0.2 (Release Date: Dec 2004)

Complete reprocessing of IRS campaigns using S11.0.2 software. Modifications include:

1. Completely revised Droop Coefficients for all modules.

2. Completely revised linearity corrections for all modules.

3. Newly derived Flatfields/2dspectral response correction (Flats).

4. Newly derived Fluxcon tables (Flux conversion for 1-d spectral extraction).

5. All LH data are now processed with campaign derived darks (to partially mitigate against time-variable warm pixels).

6. Fix to stray-light correction algorithm and operation of module that was causing problems "banding" across spectral orders.

7. Fix to "bright source drop-out" problem that cause trouble with 4-sample ramps of very bright sources. This problem caused sources which were only measured with two independent samples to have spectra whose fluxes were lower than they should have been. this problem was fixed in this release.

8. Fix to "*_spec2.tbl files not being archived" problem.

9.5.1.13 S11.0 (Release Date: Nov 2004)

Complete reprocessing of IRS campaigns using S11 software. Modifications include:

1. Addition of new Peak-up mapping pipeline to support GO2 Peak-up mapping capability.

2. Fix to "high-flux drop out" problem seen in 4-sample spectral observations in which the 3rd and 4th samples are saturated because the target is so bright. RADHIT and IMAGEST modules can now handle a single-slope measurement required to capture information from the unsaturated samples. This problem ONLY affects 6-s RAW data on extremely bright sources.

3. All S11 data incorporates newly measured "Droop" coefficients and refined and improved non-linearity corrections for all 4 modules.

4. As a result of 3, new flat field/spectral response corrections and flux conversion tables are also applied.

9.5.1.14 S10.5 (Release Date: Sep 2004)

A complete reprocessing of IRS campaigns using the existing S10 pipeline but with the following change resulting from new calibration products:

1. Improved performance of pipeline slope estimates in regions close to A/D saturation.

9.5.1.15 S10.5 (Release Date: 8 Aug 2004)

A complete reprocessing of IRS campaigns incorporating the following changes:

1. Fix to ramp timing problem for slope estimates for spectral data.

2. New higher-quality "flat-fields" (i.e. spatial flats/2-d RSRFs)-- improvement mainly in spatial quality along the slit.

3. New associated fluxcon tables.

9.5.1.16 S10.0 (Release Date: 14 Apr 2004)

Complete processing of IRS campaigns using best available calibration products available at that time.

1. Nod to nod variations in flat fields no better than 7-10%.

2. Problem with spectral data slope estimatation especially for very short ramps. This problem was fixed in S10.5.

9.5.1.17 S9.5 (Release Date: 20 Feb 2004)

1. Incrementally improved calibration products after analysis of post-launch solar-flare activity and in-flight performance.

Appendix D.   Example IRS BCD File Header

```
SIMPLE  =                    T / Fits standard
BITPIX  =                  -32 / FOUR-BYTE SINGLE PRECISION FLOATING POINT
NAXIS   =                    2 / STANDARD FITS FORMAT
NAXIS1  =                  128 /
NAXIS2  =                  128 /
ORIGIN  = 'Spitzer Science Center' / Organization generating this FITS file
CREATOR = 'S18.18.0'           / SW version used to create this FITS file
TELESCOP= 'Spitzer '
INSTRUME= 'IRSX    '
CAL_SET = 'C18.18POST44.A'     / ID for the set of CAL files used
CHNLNUM =                    2 / 0=SL, 1=SH, 2=LL, 3=LH
FILENAME= 'IRSX.2.0029037824.0006.0000.01.mipl.fits' / File name
FILETYPE= 'fits-irs2d-flux'
EXPTYPE = 'sp      '           / Exposure Type
REQTYPE = 'AOR     '           / Request type (AOR,IER, or SER)
AOT_TYPE= 'IrsStare'           / Observation Template Type
AORLABEL= 'IRSS-chalo-0001'    / AOR Label
FOVID   =                   44 / Field of View ID
FOVNAME = 'IRS_Long-Lo_2nd_Order_1st_Position' / Field of View Name
READMODE= 'RAW     '           / Readout Mode

        / PROPOSAL INFORMATION

OBSRVR  = 'Greg Sloan'         / Observer Name
OBSRVRID=                  121 / Observer ID of Principal Investigator
PROCYCL =                    8 / Proposal Cycle
PROGID  =                50835 / Program ID
PROTITLE= 'Carbon stars in the Galactic Halo' / Program Title
PROGCAT =                   29 / Program Category

        / TIME AND EXPOSURE INFORMATION

DATE_OBS= '2009-04-11T16:06:20.459' / Date & time (UTC) at DCE start
MJD_OBS =         54932.6710701 / [days] MJD in UTC at DCE start (JD-2400000.5)
UTCS_OBS=         292737980.459 / [sec] DCE start time from noon Jan 1, 2000 UTC
SCLK_OBS=         923933419.849 / [sec] SCLK time (since 1/1/1980) at DCE start
SAMPTIME=                1.0486 / [sec] Sample integration time
REQMODE =                    5 / ID for mode or type of request
EXPSTRTC=            923933412 / Exposure Start Timestamp Coarse
EXPSTRTF=                32104 / Exposure Start Timestamp Fine
GRPARVTC=            923933427 / [sec] Coarse Spacecraft Group Time
GRPARVTF=                    0 / [sec] Fine Spacecraft Group Time
AIRSCMDN=                    3 / Commanded number of DCEs for IRS
AIRS_DET=                    2 / Selected IRS detector for exposure command
AIRSEXPM=                    1 / Current Mode of the IRS Exp Manager
GRPTIME =                2.0972 / [sec] Group (w/ spin) integration time
DEADTIME=                6.2916 / [sec] Reset + boost(s) time
RAMPTIME=                14.68 / [sec] Ramp (total DCE) integration time
EXPTOT_T=                44.04 / [sec] Integr. time for all DCEs in exposure
AIRSERCT=                    0 / Number of IRS exposure errors

        / TARGET AND POINTING INFORMATION

OBJECT  = 'CHALO TI13'         / Target Name
OBJTYPE = 'TargetFixedSingle'  / Target Type
RA_HMS  = '04h21m29.1s'        / [hh:mm:ss.s] RA_SLT or CRVAL1 in sexagesimal
DEC_DMS = '+01d29m17s'         / [dd:mm:ss] DEC_SLT or CRVAL2 in sexagesimal
RA_RQST =      65.3637500000001 / [deg] Commanded RA referenced to commanded FOV
DEC_RQST=      1.48705555555556 / [deg] Commanded Dec referenced to commanded FOV
PA_RQST =      262.356928767253 / [deg] Requested pos. angle of axis 2 (E of N)
```

```
PM_RA    =                         0. / [arcsec/yr] Proper Motion in RA (J2000)
PM_DEC   =                         0. / [arcsec/yr] Proper Motion in Dec (J2000)
CRDER1   = 0.000302498507801645 / [deg] Uncertainty in RA of SI boresight
CRDER2   = 0.000302461340759974 / [deg] Uncertainty in DEC of SI boresight
SIGRA    =    0.0176762389149214 / [arcsec] RMS dispersion of RA over DCE
SIGDEC   =    0.0316553090927486 / [arcsec] RMS dispersion of DEC over DCE
SIGPA    =     0.188770005148309 / [arcsec] RMS dispersion of PA over DCE
PTGDIFF  =     0.422257353245084 / [arcsec] offset btwn actual and rqsted pntng
PTGDIFFX =     0.400841625846125 / [arcsec] requested - actual pntg along axis 1
PTGDIFFY =    -0.132764960894904 / [arcsec] requested - actual pntg along axis 2
RA_REF   =      65.3637500000001 / [deg] Commanded RA (J2000) of ref. position
DEC_REF  =      1.48705555555556 / [deg] Commanded Dec (J2000) of ref. position
USEDBPHF =                      T / T if Boresight Pointing History File was used.
RMS_JIT  =    0.0226969447120985 / [arcsec] RMS jitter during DCE
RMS_JITY =    0.0146893379764364 / [arcsec] RMS jitter during DCE along Y
RMS_JITZ =    0.0173024463321832 / [arcsec] RMS jitter during DCE along Z
RA_FOV   =      65.3638565378498 / [deg] RA at FOVID averaged over DCE
DEC_FOV  =      1.48710469910878 / [deg] DEC at FOVID averaged over DCE
PA_FOV   =     -96.4445028752934 / [deg] PA at FOVID averaged over DCE
RA_SLT   =      65.3714256313725 / [deg] RA at slit center averaged over DCE
DEC_SLT  =      1.48795931158312 / [deg] DEC at slit center averaged over DCE
PA_SLT   =     -96.4443064690493 / [deg] PA at slit center averaged over DCE
RA_XSLT  =      65.4243298797844 / [deg] RA at center of non-targeted slit
DEC_XSLT =      1.49389479890495 / [deg] DEC at center of non-targeted slit
PA_XSLT  =     -96.4429326690905 / [deg] PA at center of non-targeted slit
CSDRADEC = 7.5491397168745E-06 / [deg] Costandard deviation in RA and Dec
CSD_JTYZ =    -0.014708125573636 / [arcsec] Costandard deviation of jitter in YZ
BPHFNAME = 'BPHF.0923918400.03.pntg' / Boresight Pointing History Filename
FOVVERSN = 'BodyFrames_FTU_22b.xls' / FOV/BodyFrames file version used
VHELCORR =                  -27.8 / [km/sec] Correction to heliocentric velocity
VLSRCORR =                  -43.2 / [km/sec] Correction to local standard of rest
SPTZR_X  =    -141084631.827707 / [km] Heliocentric x position
SPTZR_Y  =      47361201.45924 / [km] Heliocentric y position
SPTZR_Z  =      19225916.467843 / [km] Heliocentric z position
SPTZR_VX =           -10.22257 / [km/sec] Heliocentric x velocity
SPTZR_VY =          -25.563618 / [km/sec] Heliocentric y velocity
SPTZR_VZ =          -11.674611 / [km/sec] Heliocentric z velocity
ET_OBS   =      292738046.645 / [sec] DCE start time (TDB seconds past J2000)
HMJD_OBS =      54932.6704811 / Corresponding Heliocen. Mod. Julian Date


        / PHOTOMETRY (IRS IMAGING)


BUNIT    = 'e-/sec  '            / Units of image data

        / SPECTROPHOTOMETRY IRS SL, LL (CHNLNUM 0, 2)


FLXCON01 =        3753.664062 / [electrons/sec/Jy] Flux conversion Order 1
FLXERR01 =              124.5 / Flux conversion uncertainties Order 1
FLXCON02 =        3893.388672 / [electrons/sec/Jy] Flux conversion Order 2
FLXERR02 =              124.5 / Flux conversion uncertainties Order 2
FLXCON03 =        3760.086914 / [electrons/sec/Jy] Flux conversion Bonus Order
FLXERR03 =              124.5 / Flux conversion uncertainties Order 3

        / GENERAL MAPPING KEYWORDS


DBEXPOID =          10636652 / Current Exposure ID

        / IRS PEAKUP KEYWORDS


PKUPMODE = 'IRS     '          / Peakup mode (none, IRS, or PCRS)
PKUPACCU = 'High    '          / Peakup Accuracy (high, moderate,low)
PKUPFILT = 'BLUE    '          / Peakup filter (blue or red)
```

```
PKUPFLUX=                       27. / Flux density of peakup target for IRS [mJy] or
PKUPXTND=                        F / Extended source (T/F)
ISPUPOS =                        T / PU target given in absolute positions (T) or re
PKUPRA  =       65.6815416666667 / [deg] RA peakup position
PKUPDEC =       1.49736111111111 / [deg] Dec peakup position
PM_PKRA =                    0.008 / [''/yr]Proper motion for RA peakup position
PM_PKDEC=                   -0.035 / [''/yr]Proper motion for Dec peakup position
HP_CENQ =                        0 / Peakup centroid quality code
APKUPCEN=                        1 / Status of the peakup centroid
AXCNTRD1=                    10796 / [centipixels] X value of the brightest centroid
AYCNTRD1=                     2799 / [centipixels] Y value of the brightest centroid
AXCNTRD2=                     9603 / [centipixels] X value of the second brightest c
AYCNTRD2=                     2214 / [centipixels] Y value of the second brightest c
AINTENS1=                   134686 / [counts] Intensity value of the brightest centr
AINTENS2=                    29297 / [counts] Intensity value of the second brightes
APKUPXCE=                    10796 / [centipixels] X value of the centroid to be ret
APKUPYCE=                     2799 / [centipixels] Y value of the centroid to be ret


           / DATA FLOW KEYWORDS

DATE    = '2010-09-18T00:10:01' / [YYYY-MM-DDThh:mm:ss UTC] file creation date
AORKEY  = '29037824'            / AOR or EIR key. Astrnmy Obs Req/Instr Eng Req
EXPID   =                        6 / Exposure ID (0-9999)
DCENUM  =                        0 / DCE number (0-9999)
TLMGRPS =                        8 / Number of expected telemetry groups
FILE_VER=                        1 / Version of the raw file made by SIS
RAWNAME = 'IRSX.2.0029037824.0006.0000.01.mipl.fits' / Raw data file name
SIS_SVER= 'J5.3    '             / SIS SW VERsion
CPT_VER = '3.1.11  '             / Channel Param Table FOS version
CTD_VER = '3.0.94S '             / Cmded telemetry data version
EXPDFLAG=                        F / (T/F) expedited DCE
MISS_LCT=                        0 / Total Missed Line Cnt in this FITS
MANCPKT =                        F / T if this FITS is Missing Ancillary Data
MISSDATA=                        F / T if this FITS is Missing Image Data
PAONUM  =                     3410 / PAO Number
CAMPAIGN= 'IRSX011100'           / Campaign
DCEID   =                118724600 / Data-Collection-Event ID
DCEINSID=                 24611816 / DCE Instance ID
DPID    =                326654834 / Data Product Instance ID
PIPENUM =                      201 / Pipeline Script Number
SOS_VER =                       1. / Data-Product Version
PLVID   =                       10 / Pipeline Version ID
CALID   =                        4 / CalTrans Version ID
ORIGIN0 = 'JPL_FOS '             / site where RAW FITS files was written
CREATOR0= 'J5.3    '             / SW system that created RAW FITS

GAIN1   =                      4.6 / e/DN conversion (readout channel 1)
GAIN2   =                      4.6 / e/DN conversion (readout channel 2)
GAIN3   =                      4.6 / e/DN conversion (readout channel 3)
GAIN4   =                      4.6 / e/DN conversion (readout channel 4)
BASECH1 =                 37215.08 / Trimmed mean channel 1 signal in reference unil
BASECH2 =                 39129.25 / Trimmed mean channel 2 signal in reference unil
BASECH3 =                 37441.98 / Trimmed mean channel 3 signal in reference unil
BASECH4 =                 34813.46 / Trimmed mean channel 4 signal in reference unil

HISTORY *0 (imported)
HISTORY job.c ver: 1.50
HISTORY TRANHEAD               v.          13.1, ran Fri Sep 17 17:08:54 2010
HISTORY CALTRANS               v.           4.0, ran Fri Sep 17 17:09:03 2010
HISTORY cvti2r4          v.  1.31 A61025, generated  9/17/10 at 17:09:11
HISTORY DNTOFLUX               v.           4.2, ran Fri Sep 17 17:09:20 2010
HISTORY imagest          v.  1.80 A61012, generated  9/17/10 at 17:09:29
```

```
HISTORY   input: cvte.fits
HISTORY   unc.: cvte_unc.fits
HISTORY DROOPOP                v.       3.700000, ran Fri Sep 17 17:09:33 2010
HISTORY DARKBASE               v.       2.200000, ran Fri Sep 17 17:09:43 2010
HISTORY CUBESUB                v.       3.200000, ran Fri Sep 17 17:09:46 2010
HISTORY lineariz        v.  1.39 A40318, generated  9/17/10 at 17:09:50
HISTORY   input: cubesub.fits
HISTORY   model: ./cal/lincal.fits
HISTORY DARKDRIFT              v.            4.1, ran Fri Sep 17 17:10:01 2010
HISTORY DROOPRES               v.       2.200000, ran Fri Sep 17 17:10:08 2010
HISTORY FLATAP                 v. 1.500   Fri Sep 17 17:10:13 2010
HISTORY CALTRANS               v.            4.0, ran Fri Sep 17 17:19:12 2010
HISTORY PTNTRAN                v.            1.4, ran Fri Sep 17 17:19:16 2010
HISTORY PTNTRAN                v.            1.4, ran Fri Sep 17 17:19:16 2010
HISTORY PTNTRAN                v.            1.4, ran Fri Sep 17 17:19:17 2010
HISTORY FPGen                  v.           1.26, ran Fri Sep 17 17:19:19 2010
FBIDDARK=            1177
FBIDFLAT=             763
FBIDLNCR=              24
FBIDLNMD=             765
FBIDOMSK=              31
FBIDPMSK=             762
FBIDWSMP=            1208
FBIDUMSK=              68
FBIDWSOF=            1209
FBIDWSOM=            1210
FBIDWSWA=            1207
FBIDFLXC=            1204
FBIDFMSK=              73
FBIDCALS=            1215
FBIDLNSC=             766
HISTORY CALTRANS               v.            4.0, ran Fri Sep 17 17:34:53 2010
END
```

Appendix E.   List of Figures

Appendix F.   List of Tables